University Library

A gateway to Melbourne's research publications

Minerva Access is the Institutional Repository of The University of Melbourne

Author/s:
Beauchamp, Leah Catherine

Title:
Investigating olfactory deficits as a preclinical marker of Parkinson's disease

Date:
2020

Persistent Link:
https://hdl.handle.net/11343/253862

Terms and Conditions:
Terms and Conditions: Copyright in works deposited in Minerva Access is retained by the copyright owner. The work may not be altered without permission from the copyright owner. Readers may only download, print and save electronic copies of whole works for their own personal non-commercial use. Any use that exceeds these limits requires permission from the copyright owner. Attribution is essential when quoting or paraphrasing from these works.

Investigating olfactory deficits as a preclinical marker of Parkinson's disease

Leah Catherine Beauchamp

A thesis submitted in total fulfilment of the requirements of the degree

Doctor of Philosophy

University of Melbourne

Faculty of Medicine, Dentistry and Health Sciences

Department of Pharmacology and Therapeutics

The Florey Institute of Neuroscience and Mental Health

August 2020

ORCID identifier: 0000-0002-4896-279X

Parkinson's disease is the fastest growing neurological condition in the world, expected to affect more than 12 million people globally by 2040. Despite centuries of ground-breaking research, the diagnosis of Parkinson's disease is unreliable and there are no disease-modifying therapeutics. This may be attributable to a focus on the movement disorders associated with disease, which present only after substantial neurodegeneration has occurred. This results in a late, inaccurate diagnosis which is problematic for the development and utilisation of neuroprotective therapies which need to be administered early. Although there has been recognition of non-motor aspects of Parkinson's disease as early as 1817 by James Parkinson himself, there is no standardised utility of non-motor symptoms in the identification and monitoring of disease. The concurrence of non-motor symptoms in early Parkinson's disease has great promise in identifying people at risk of developing the clinical disease, especially in those with REM sleep behaviour disorder, however these assays still require further development. The most prevalent non-motor symptom is a loss in the sense of smell (hyposmia) and understanding the pathobiology underlying this phenomenon may help to inform future diagnostic approaches through the development of novel biomarkers of disease. As such, the aim of this thesis was to test the utility of concurrent non-motor symptoms in a clinical setting, as well as investigate the underlying biology of the olfactory system in Parkinson's disease using *post-mortem* human olfactory bulbs and tau knockout mice.

The concurrence of non-motor symptoms was investigated in a cohort of participants presenting with multiple non-motor symptoms, including REM sleep behaviour disorder, hyposmia, and anxiety. Upon positron emission tomography scanning, it was demonstrated that the participants with concurrent non-motor symptoms had reduced vesicular monoamine transporter 2 binding in the caudate nucleus and the putamen in a degenerative pattern like that of Parkinson's disease. Although these findings demonstrate the utility of non-motor symptoms to identify people with early nigrostriatal degeneration, understanding the underlying pathological changes will allow the development of more sensitive diagnostic tools.

As such, human *post-mortem* olfactory bulbs from subjects with pathologically confirmed Parkinson's disease and neurological controls were examined for changes in systems associated with Parkinson's disease, including protein clearance, the dopaminergic system, and metal homeostasis. The accumulation of monomeric α-synuclein was observed within the bulbs as determined by immunoblot and there were protein changes indicative of an environment under oxidative stress. Characterisation of the dopaminergic system demonstrated perturbations in catechol-O-methyltransferase-mediated dopamine breakdown. Finally, there was a loss of metal homeostasis as demonstrated by an accumulation of key metals, including iron, sodium, zinc, and lead. These findings warranted further investigation in an *in vivo* model.

Tau knockout mice have been reported as an age-dependent model of Parkinson's disease, and the next study of this thesis demonstrated that these mice develop an olfactory impairment at seven months of age, approximately five months before they develop a motor impairment, aligned with the presentation of symptoms in Parkinson's disease. The mechanism(s) underlying the olfactory deficits of these animals was characterised to determine the congruency between the mice and the *post-mortem* tissue. Firstly, it was found that this olfactory deficit correlates with an accumulation of α-synuclein and autophagic impairment, in the olfactory bulb. Similar to the human bulbs, young tau knockout mice appear to have a deficit in catechol-*O*-methyltransferase dopamine breakdown as well as an accumulation of bulbar metals. These findings were further implicated in the functional olfactory deficit as treatment with the dopamine 2 receptor antagonist haloperidol, and the iron/copper chelator PBT434, resulted in a rescue of the hyposmic phenotype in young tau knockout mice. These findings implicate a loss of tau function as a contributor to disease pathways. This was further investigated using the mutant tau overexpressing mice, the rTg4510s, and like the tau knockout mice these animals demonstrate an age-dependent hyposmia.

Together these studies have enabled the identification of potential mechanisms of olfactory impairment in Parkinson's disease that warrant further scrutiny, including dopamine mis-metabolism and metal accumulation. Findings in the tau knockout mice add face validity to the model and support the utility of this animal in non-motor studies. These findings may help aid in the development of novel diagnostic approaches, as well as patient stratification strategies to overcome the current hurdles in clinical trials of neuroprotective therapies in Parkinson's disease.

Declaration

This is to certify that:

(i) This thesis comprises only my original work towards the PhD except where indicated in the preface

(ii) Due acknowledgement has been made in the text to all other material used

(iii) This thesis is less than 100,000 words in length, exclusive of tables, maps, bibliographies and appendices

Leah Catherine Beauchamp

Barnham Neurotherapeutics Laboratory

The Florey Institute of Neuroscience and Mental Health

Department of Pharmacology and Therapeutics

The University of Melbourne

Parkville, Victoria 3010 Australia

I acknowledge that specific contributions to the experiments carried out in this thesis were performed by others:

- Dopamine and metabolite analysis via high-pressure liquid chromatography in Chapters 3 and 4 was performed by Dr. Cameron Hunt of the Parish Lab
- Metal concentrations in Chapters 3 and 6 using the inductively coupled plasma mass-spectrometry performed by Irene Volitakis and Celeste Mawal
- Primary cortical neuron exosome isolation experiments in Chapter 4 performed by Dr. Bradley Coleman and Dr. Lin Hung
- Primary cortical neuron, Wortmannin treatment and immunofluorescence analysis in Chapter 4 performed by Dr. Benjamin Padman and Dr. Xiang Liu
- Dosing of *S*-adenosylmethionine in Chapter 7 was performed with the assistance of Dr. Xiang Liu, cutting of the brains for histology performed by Mirjana Bogeski, and staining and stereology performed with the assistance of Amelia Sedjahtera
- Patient recruitment, clinical assessment, PET imaging, and analysis of PET scans in Chapter 8 was performed by Dr. Victor Villemagne, Dr. Vincent Doré, and Prof. Christopher Rowe

I would like to highlight the impact of COVID19 on some of the studies in this thesis. There are some readouts that are still underway and will not be included in this thesis due to the high level of restrictions imposed in Melbourne beginning in March 2020. I recognise there are gaps in the research and have plans to continue studies as soon as possible.

Acknowledgements

This thesis is bound by my love and appreciation for all of those around me and is written with memories of my wonderful grandparents Margaret, Shirley, and Darryl.

First and foremost, my utmost gratitude to Kevin Barnham, head of the Neurotherapeutics Laboratory. I entered your lab with a weight of self-doubt, but I was soon reassured and given the push I needed to prosper. There have been tough days throughout the last four years, but there hasn't been a day I haven't wanted to be a member of your group. You've always championed for my success and I can't thank you enough, Boss. I am indebted to Laura Vella, head of the Extracellular Vesicles Laboratory. Laura, you have an incredible ability to make people feel worthy of your time and you have a leadership style that is nothing short of admirable. I look forward to transitioning from student to colleague and following in your footsteps as a supportive and empowered woman in science.

I wish to thank all of the people whose assistance was a milestone in the completion of this doctorate, including my co-supervisor Ashley Bush, and my committee members David Finkelstein, Sarah Stephenson, and Peter Crack. Particularly, thank you to all the members of the Barnham group, both past and present, for making the lab such an enjoyable environment and putting up with my need to blast ABBA on the communal radio. I would also be remised if I didn't acknowledge the generosity of the brain donors and their families, as well as the ultimate sacrifice made by my research animals.

To my non-academic family - I would like to thank my grandfather, James Dwyer (poppa), for his endless support of my education and I would like to assure him that I am still enjoying myself (because that's what matters most). Thanks to my parents, Cathy and Shayne, who remain confused about how they managed to raise a neuroscientist, but supportive all the same. I've always considered myself lucky to have three big brothers and I have to thank Jon, Darren, and Cameron for pushing me out of that small town to pursue something so much greater. Over the last decade, I have created my own little family and I thank them all for their support, including Amy, Kieran, Meg, Danielle, Cynthia, Anna, Guy, and Quinn. A special mention to my favourite doctor, Alex McCutchan, for suffering through the first draft of this thesis. I couldn't ask for a more encouraging or ethanol-fuelled cheer squad.

Finally, I thank the countless number of women who have endured, overcome, and redefined the role of women in the sciences paving the way for my generation to flourish.

"I didn't succumb to the stereotype that science isn't for girls"

– Sally Ride

Abstract i
Declaration iii
Preface iv
Acknowledgements v
Table of contents vi
Abbreviations x
Figures xiv
Tables xvi
Chapter 1: An introduction to Parkinson's disease 1
1.1 The aetiology of Parkinson's disease 1
1.2 Hallmark pathology of Parkinson's disease 2
Nigrostriatal dopaminergic neurodegeneration 2
Lewy pathology 3
1.3 The pathobiology of Parkinson's disease 3
Mitochondrial dysfunction 4
Alpha-synuclein 5
Impairment in the Ubiquitin-Proteasome System 6
Impairment in the Autophagy-Lysosome Pathway 7
Neuroinflammation 9
1.4 Dopaminergic vulnerability 9
1.5 Therapeutic strategies in Parkinson's disease 10
1.6 Non-motor Parkinson's disease 12
Hyposmia in Parkinson's disease 13
1.7 The central olfactory system 13
Neuroanatomy and physiology 13
Olfactory neurobiology in Parkinson's disease 17
1.8 Animal models of Parkinson's disease 19
Genetic animal models 19
Neurotoxin-induced animal models 20
Hyposmia in mouse models of Parkinson's disease 20
1.9 Hypothesis and aims 22
Chapter 2: Materials and methods 23
2.1 Ethics 23
Human tissue 23
Animal research 23

2.2 Animals 23
2.3 Animal behaviour 24
Odour detection test 24
Locomotor Activity Test 24
Rotarod 24
Pole Test 25
Y-maze 25
2.4 Transcardial perfusion and tissue collection 26
2.5 SDS-PAGE and immunoblot analysis 26
Enhanced chemiluminescence detection 26
Fluorescence detection 27
2.6 Inductively coupled plasma mass-spectrometry 27
2.7 High pressure liquid chromatography with electrochemical detection 27
2.8 Enzyme-linked immunosorbent assays 28
S-adenosylmethionine 28
Phosphorylated tau 28
2.9 Protein phosphatase 2 activity assay 29
2.10 Parkinson's progressive markers initiative 29
2.11 Statistical analysis 30
Chapter 3: Reduced Striatal Vesicular Monoamine Transporter 2 in REM Sleep Behavior Disorder: Imaging Prodromal Parkinsonism 31
3.1 Abstract 32
3.2 Introduction 33
3.3 Methods 34
3.4 Results 36
3.4 Discussion 39
Chapter 4: Characterisation of the human Parkinson's disease post-mortem olfactory bulb: a failure of dopamine breakdown and metal homeostasis 41
4.1 Abstract 41
4.2 Introduction 42
4.3 Methods 43
4.4 Results 44
4.5 Discussion 49
Chapter 5: Ablation of tau causes an olfactory deficit in a murine model of Parkinson's disease 53
5.1 Abstract 54
5.2 Introduction 55

5.3 Methods 56
5.4 Results 61
5.5 Discussion 68
Chapter 6: Failure of extracellular dopamine clearance in the tau knockout mice is implicated in early olfactory deficits, which can be temporarily rescued by acute dopamine 2 receptor antagonism 71
6.1 Abstract 71
6.2 Introduction 72
6.3 Methods 75
6.3 Results 78
5.5 Discussion 85
Chapter 7: Metal dyshomeostasis contributes to the olfactory and motor deficits of tau knockout mice, which can be functionally rescued by PBT434 91
7.1 Abstract 91
7.2 Introduction 92
7.3 Methods 94
7.4 Results 97
7.4 Discussion 111
Chapter 8: An investigation of the rTg4510 animal model and supplementation of S-adenosylmethionine as a therapeutic strategy 115
Chapter 8A: S-adenosylmethionine rescues cognitive deficits in the rTg4510 animal model by stabilizing protein phosphatase 2A and reducing phosphorylated tau 116
8A.1 Abstract 117
8A.2 Introduction 118
8A.3 Methods 119
8A.4 Results 122
8A.5 Discussion 127
Chapter 8B: rTg4510 mice develop an olfactory deficit at 6 months of age 130
8B.1 Abstract 130
8B.2 Introduction 131
8B.3 Methods 132
8B.4 Results 134
8B.5 Discussion 137
Chapter 9: General Discussion 139
9.1 The utility of hyposmia in Parkinson's disease 139
The strength of hyposmia in a screening tool 139
The biological basis of hyposmia 140

9.2 The concurrence of non-motor symptoms in PD 143
9.3 Preclinical PD screening: a research tool 144
9.4 Future directions 146
Development of a screening tool for early Parkinson's disease 146
A differential diagnostic for hyposmia 147
Development of novel biomarkers in PD 147
9.5 Conclusion 147
References 148

α-syn: alpha synuclein

ACE-R: Addenbrooke's Cognitive Examination-Revised

ACh: acetylcholine

AD: Alzheimer's disease

Al: aluminium

ALP: autophagy-lysosome pathway

ANOVA: analysis of variance

AON: anterior olfactory nucleus

ATP: adenosine triphosphate

B: boron

Ba: barium

BCA: bicinchoninic acid

BHT: butylated hydroxytoluene

BSA: bovine serum albumin

Ca: calcium

cAMP: cyclic adenosine monophosphate

CBD: corticobasal degeneration

CCK: creatine kinase

Cd: cadmium

CDR: clinical dementia rating

CMA: chaperone-mediated autophagy

CNP: cyclic nucleotide-gated phosphodiesterase

CNS: central nervous system

Co: cobalt

CoD: cause of death

COMT: catechol-*O*-methyltransferase

Cr: chromium

CRF: corticotropin-releasing factor

CSF: cerebrospinal fluid

Cu: copper

D-PBS: Dulbecco's phosphate buffered saline

D_2R: dopamine 2 receptor

DA: dopamine

DAT: dopamine transporter

DD: disease duration

DLB: dementia with Lewy bodies

DNA: deoxyribonucleic acid

DOPAC: 3,4-dihydroxyphenylacetic acid

Dox: doxycycline

DTT: dithiothreitol

ECL: enhanced chemiluminescence

ELISA: enzyme-linked immunosorbent assay

EV: extracellular vesicle

F: female

Fe: iron

FTD: frontotemporal dementia

FTDP-17: frontotemporal dementia and parkinsonism linked to chromosome 17

GABA: gabba-aminobutyric acid

GAD: glutamic acid decarboxylase

GBA: glucocerebrosidase

GPCR: G-protein coupled receptor

GSH: glutathione

GWAS: genome-wide association study

H-Y: Hoehn-Yahr scale

H_2O_2: hydrogen peroxide

HADS: hospital anxiety and depression scale

HET: heterozygous

HPLC-ED: high pressure liquid chromatography with electrochemical detection

HVA: homovanillic acid

Hz: hertz

ICP-MS: inductively coupled plasma mass spectrometry

IHC: immunohistochemistry

ILBD: incidental Lewy body disease

IMSQ: informant MAYO sleep questionnaire

iNOS: inducible nitric oxide synthase

i.p.: intraperitoneal

ITI: intertrial interval

IVC: individually ventilated cage

K: potassium

KO: knockout

L-DOPA: l-3,4-dihydroxyphenylalanine

LAMP2A: lysosome-associated membrane protein 2A

LB: Lewy body

LC: locus coeruleus

LC3: microtubule-associated protein 1A/1B-light chain 3

LMA: locomotor activity

LR: likelihood ratio

LRRK2: leucine-rich repeat kinase 2

M: male

MDS: Movement Disorder Society

MDSRC-PPD: MDS research criteria – prodromal PD

Mg: magnesium

MMSE: mini mental state exam

Mn: manganese

MPP+: 1-methyl-4-phenylpyridinium

MPTP: 1-methyl-4-phenyl-1,2,3,6-tetrahydropyridine

MVB: multivesicular body

Na: sodium

NA: noradrenaline

NADPH: nicotinamide adenine dinucleotide phosphate

NC: neurological control

NeuN: neuronal nuclei

NFT: neurofibrillary tangle

Ni: nickel

NO: nitric oxide

NPY: neuropeptide Y

ns: not significant

OB: olfactory bulb

ODT: odour detection test

OE: olfactory epithelium

$OH^{\bullet}$: hydroxyl radical

$ONOO^{-}$: peroxynitrite

ORN: olfactory receptor neuron

OS: oxidative stress

P: phosphorus

PAR: population attributable risk

Pb: lead

PCR: polymerase chain reaction

PD: Parkinson's disease

PET: positron emission tomography

PFA: paraformaldehyde

PG: periglomerular

PHF: paired helical filaments

PiD: Pick's disease

PINK1: PTEN-induced kinase 1

PMD: post-mortem delay

PP2A: protein phosphatase 2A

PPMI: Parkinson's progressive markers initiative

PPMT: protein PP2A methyltransferase

PSP: progressive supranuclear palsy

Pt: plutonium

pTau: phosphorylated tau

pTH: phosphorylated TH

PTM: posttranslational modification

qPCR: quantitative polymerase chain reaction

Rb: rubidium

RBD: REM sleep behaviour disorder

REM: rapid eye movement

RIPA: radioimmuno precipitation assay

rpm: rotations per minute

ROS: reactive oxygen species

R_T: tissue ratio

RT: room temperature

SAMe: *S*-adenosylmethionine

Se: selenium

SEM: standard error of the mean

SH: sulfhydryl

SNpc: substantia nigra pars compacta

SOD: superoxide dismutase

SPECT: Single-photon emission computed tomography

Sr: strontium

SSV: standard suspension vehicle

STAI: state/trait anxiety index

$Tau^{-/-}$: tau knockout

$Tau^{+/+}$: tau wildtype

TBS: triphosphate buffered saline

TGN: trans-Golgi network

TH: tyrosine hydroxylase

Ti: titanium

Ub: ubiquitin

UCHL1: ubiquitin C-terminal hydrolase L1

$UPDRS_m$: Unified Parkinson's Disease Rating Scale (motor)

UPS: ubiquitin-proteasome system

UPSIT: University of Pennsylvania smell identification test

VIP: vasoactive intestinal polypeptide

VMAT2: vesicular monoamine transporter 2

WT: wildtype

Zn: zinc

5-HT: serotonin

6-OHDA: 6-hydroxydopamine

^{18}F-AV-133: 18F-(+)Fluropropyldihydrotetrabenazine

Figure 1.1 Nigrostriatal degeneration in Parkinson's disease. 2
Figure 1.2 Converging oxidative stress pathways in Parkinson's disease. 4
Figure 1.3 The ubiquitin-proteasome system in Parkinson's disease. 6
Figure 1.4 The autophagy-lysosome pathway in Parkinson's disease. 8
Figure 1.5 The Fenton reaction. 9
Figure 1.6 Clinical trial pipeline in Parkinson's disease. 11
Figure 1.7 Symptom onset in Parkinson's disease. 12
Figure 1.8 The olfactory receptor neuron G-protein coupled receptor. 14
Figure 1.9 The layers of the olfactory bulb. 15
Figure 2.1 The odour detection test. 24
Figure 2.2 The pole test. 25
Figure 2.3 The three-arm Y-maze of spatial memory. 25
Figure 3.1 RBD patients have reduced [18F]AV-133 binding in the caudate nuclei and putamen. 38
Figure 3.2 RBD participants from the PPMI have concurrent hyposmia and increased anxiety. 39
Figure 4.1 Increased expression of Parkinson's disease-related proteins in the human olfactory bulbs. 45
Figure 4.2 Increased tyrosine hydroxylase in Parkinson's disease olfactory bulbs. 46
Figure 4.3 Decreased homovanillic acid in Parkinson's disease olfactory bulbs. 47
Figure 4.4 Alterations of catechol-O-methyltransferase in Parkinson's disease olfactory bulbs. 47
Figure 4.5 Accumulation of metals in Parkinson's disease olfactory bulbs. 48
Figure 5.1 Olfactory deficit, motor performance, and pathological features in 7-month-old tau-/- mice. 63
Figure 5.2 Olfactory deficit, motor performance and pathological features in 15-month-old tau-/- mice. 65
Figure 5.3 Tau-/- primary cortical neurons display autophagic impairment and have an increase in the release of α-synuclein enriched exosomes. 67
Figure 6.1 Summary of dopamine synthesis and degradation. 73
Figure 6.2 Experimental timeline of mice treated with cocaine and haloperidol. 76
Figure 6.3 Experimental timeline of mice treated with S-adenosylmethionine. 77
Figure 6.4 Hyperlocomotion and increased rearing activity in young tau knockout mice. 78
Figure 6.5 Increased tyrosine hydroxylase in the tau knockout mouse olfactory bulb. 80
Figure 6.6 Reduced homovanillic acid and S-adenosylmethionine in the tau knockout mouse olfactory bulb. ... 81
Figure 6.7 Haloperidol acutely rescued the hyposmia in young tau knockout mice. 83
Figure 6.8. S-adenosylmethionine rescued the hyperlocomotion in young tau knockout mice. 84
Figure 6.9 A summary of the bulbar dopaminergic pathway alterations in tau knockout mice. 85
Figure 7.1 Experimental timeline of mice treated with PBT434. 95
Figure 7.2 Experimental timeline of mice treated with Cu(GTSM). 96
Figure 7.3 Accumulated metals in the olfactory bulb of young tau knockout mice. 97
Figure 7.4 Accumulated metals in the substantia nigra pars compacta of aged tau knockout mice. 98
Figure 7.5 Reduced metal levels in the caudate putamen of aged tau knockout mice. 99
Figure 7.6 Hyperlocomotion in aged tau knockout mice. 100
Figure 7.7 Motor impairment in aged tau knockout mice. 101
Figure 7.8 Cognitive deficit in aged tau knockout mice. 101
Figure 7.9 PBT434 rescued the hyposmia in young tau knockout mice. 102
Figure 7.10 PBT434 reduced metals and increased neuronal markers in the olfactory bulb of young tau knockout mice. 103
Figure 7.11. PBT434 rescued the motor deficit in aged tau knockout mice. 104
Figure 7.12 PBT434 had no overt effect on locomotion or exploratory behaviour in aged tau knockout mice. . 105
Figure 7.13 PBT434 had no overt effect on cognitive deficits in aged tau knockout mice. 106
Figure 7.14 PBT434 altered metals and increased neuronal markers in the substantia nigra pars compacta of aged tau knockout mice. 107
Figure 7.15 PBT434 altered metals and increased neuronal markers in the caudate putamen of aged tau knockout mice. 108
Figure 7.16 Cu(GTSM) induced an olfactory deficit in young wildtype mice. 109
Figure 7.17 Cu(GTSM) had no overt effect on motor skills in young wildtype mice. 110
Figure 7.18 Cu(GTSM) had no overt effect on locomotion or exploratory behaviour in young wildtype mice. .. 110
Figure 7.19 Cu(GTSM) induced a cognitive deficit in young wildtype mice. 111
Figure 8A.1 Oral S-adenosylmethionine treatment increased the concentration of SAMe in the brain. 122
Figure 8A.2 Treatment with S-adenosylmethionine increases the activity of PP2A in rTg4510 mice. 124

Figure 8A.3 Treatment with S-adenosylmethionine significantly reduced the number of AT8 positive cells and the level of phosphorylated tau in the cortex but not in the hippocampus of rTg4510 mice. 126
Figure 8A.4 Treatment with S-adenosylmethionine improves the spatial recognition memory of rTg4510 mice. 127
Figure 8A.5 Disruptions in the methionine cycle in Alzheimer's disease and the effect of S-adenosylmethionine supplementation. 129
Figure 8B.1 Experimental timeline of animals treated with S-adenosylmethionine. 133
Figure 8B.2 Odour detection test of ageing rTg4510 mice. 134
Figure 8B.3 Locomotor activity of ageing rTg4510 mice. 135
Figure 8B.4 Odour detection test of S-adenosylmethionine treated rTg4510 mice. 136
Figure 8B.5. Locomotor activity of S-adenosylmethionine treated rTg4510 mice. 137
Figure 9.1. Reported pathology within the human Parkinson's disease olfactory bulb. 142
Figure 9.2 Non-motor concurrence in the PPMI cohort. 144
Figure 9.3 Schematic of a process to screen and identify individuals at risk of developing clinical PD in a population-based study. 146

Table 1.1 Neuronal subpopulations of the central olfactory system *16*
Table 1.2 Hyposmia in murine models of Parkinson's disease *21*
Table 2.1 Rotarod protocol *25*
Table 2.2 Antibody list *27*
Table 3.1. Patient demographic and clinical data *37*
Table 3.2 Regional R_T Values for [^{18}F]AV-133 PET *39*
Table 4.1 Demographics of olfactory bulb tissue donors *44*
Table 4.2 Metal analysis of Parkinson's disease olfactory bulbs *48*
Table 8B.1 Findings from the odour detection test of young rTg4510 mice *134*
Table 9.1 Prevalence and association of PD-related non-motor symptoms in neurological conditions *143*
Table 9.2 Diagnostic accuracy studies of cohorts assessed with the MDSDC-PPD *145*

Chapter 1: An introduction to Parkinson's disease

"With advances in knowledge, disease boundaries may change. Occasionally, these changes are of such a magnitude that they require redefinition of the disease." [1]

Parkinson's disease (PD) is the fastest-growing neurological disorder in prevalence, disability, and death[2]. In 2016, there were an estimated 6.1 million individuals living with PD globally, compared to 2.5 million in 1990; representing an age-standardised prevalence rate increase of 21.7% in the last 30 years[3]. This number is expected to grow to a staggering 12.9 million by 2040, and the hunt for a disease-modifying therapeutic has become more critical than ever before. The first clinical description of *paralysis agitans* was published in 1817 by British apothecary James Parkinson[4]. In the publication, entitled 'Essay on the Shaking Palsy', Parkinson described the common symptoms of six individuals suffering from an undefined shaking palsy. The importance of this work was realised in 1861 when Jean-Martin Charcot reproduced the work of Parkinson in French and renamed the condition *Maladie de Parkinson* (Parkinson's disease)[5]. In these works, Charcot defined the 'key features' of the disease as rigidity, tremor, and slowness of movement.

Today, Parkinson's disease is said to have four cardinal features that are grouped under the acronym TRAP: *T*remor at rest, *R*igidity, *A*kinesia (bradykinesia), and *P*ostural instability. Tremor is by far the most widely recognised symptom of PD; it presents at 4-6 Hz and is unilateral at the onset of motor disease. Importantly, this tremor is only present at rest and it disappears during action and sleep. Bradykinesia is the slowing of movement and is a hallmark feature of diseases with basal ganglia disruptions. Bradykinesia presents as slowing of movement, due to difficulty in initiating and executing movements. Self-described, rigidity refers to limb stiffness, characterised by increased resistance with passive movement. Finally, there is a characteristic 'slumped' posture of PD patients (anterocollis), however, this posture is usually more prevalent in advanced disease. Although these symptoms are still heavily relied upon for diagnosis, it is now widely recognised that PD is aligned with many non-motor symptoms that occur up to a decade *before* the onset of these movement symptoms[6]. Despite the early recognition and description of the clinical disease, the underlying pathology was not described for almost a century, and to this day the aetiology of the disease remains enigmatic.

1.1 The aetiology of Parkinson's disease

In general, there are two forms of PD recognised - genetic and idiopathic. Genetic PD arises from known mutations in the *SNCA*[7], *Parkin*[8], *UCHL1*[9], *PINK1*[10], *DJ1*[11], *GBA*[12], *and LRRK2*[13] genes, among other more rare mutations[14]. These genes encode for proteins involved with synaptic function, mitochondria, the ubiquitin-proteasome system (UPS), and the autophagy-lysosomal pathway (ALP), and mutations are known to induce pathology that underlies PD. Although only 10% of PD is linked to

these genetic mutations, the study of the resulting cellular disruptions has informed the potential pathways involved in idiopathic PD. The trigger of idiopathic PD is unknown and has been theorised to be a combination of genetic susceptibility and environmental toxin exposure[15]. Although ageing remains the single highest risk factor for PD[16], an extensive genome-wide association study (GWAS) identified key genetic risk factors for the development of idiopathic PD[17].

The strongest association signal found in the GWAS was variants in *SNCA*, which encodes for the protein α-synuclein (α-syn). The loci variant with the second most significant effect size was found on the gene *MAPT*, which encodes for the protein tau. Tau is a microtubule stabilising protein that is known to dissociate from the microtubule via phosphorylation, and hyperphosphorylation leads to the instability of microtubules[18, 19]. There have been some reports of aggregated tau filaments in PD, especially in those suffering cognitive impairment[20-22]. *In vitro* tau has been demonstrated to co-aggregate with α-syn in Lewy pathology[23, 24], and tau aggregation has been found in some mutant α-syn animal models[25], but the functional role tau plays in PD is unknown. To date, the best evidence of tau loss of function being a crucial mechanism of PD development comes from the tau knockout (tau$^{-/-}$) animal model, characterised at the Florey Institute of Neuroscience and Mental Health (FINMH)[26]. This animal demonstrates age-dependent parkinsonism, which is mediated by dopaminergic neurodegeneration and iron accumulation in the midbrain, synonymous with the hallmark pathology of the human condition.

1.2 Hallmark pathology of Parkinson's disease

The *sine qua non* criteria for definitive diagnosis of PD are a loss of nigrostriatal dopamine neurons, and the presence of intraneuronal proteinaceous cytoplasmic inclusions referred to as "Lewy bodies" (LBs) in some of the surviving dopaminergic neurons.

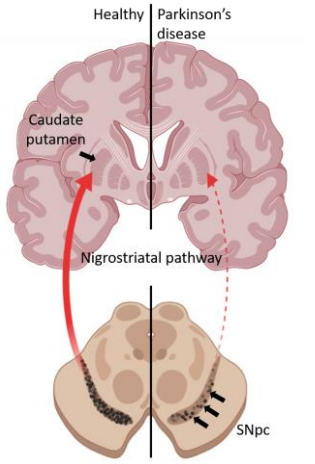

Figure 1.1 Nigrostriatal degeneration in Parkinson's disease.

Nigrostriatal dopaminergic neurodegeneration

In 1960 Ehringer and Hornykiewicz reported a dopaminergic reduction in the brains of PD patients[27]. The cell bodies of nigrostriatal dopaminergic neurons are located in the substantia nigra pars compacta (SNpc), and project axons and nerve terminals to the striatum (Figure 1.1). An interference in dopamine delivery to the striatum leads to the motor impairments seen in PD, resulting from loss of synapses and neurodegeneration. It is unknown what the initiating event of this neurodegeneration is, or why the dopaminergic system appears to be vulnerable, but there is a cascade of molecular events that lead to the demise of the affected neurons.

Lewy pathology

Intraneuronal LBs were first observed in 1912 by Fritz Jakob Heinrich Lewy and in 1919 were named 'corps de Lewy' (Lewy bodies) by Konstantin Tretiakoff. LBs are cytoplasmic protein aggregates of about 15µm diameter composed of many proteins, including (but not limited to) α-syn[28], ubiquitin (Ub)[29], neurofilament[30], and parkin[31]. LBs have a core of α-syn filament comprised of five β-strands and are primarily post-translationally modified via phosphorylation of the Ser129 residue, which results in the α-syn filaments becoming ubiquitinated[32]. These LBs are found predominantly in some of the remaining dopaminergic neurons of the SNpc, however, they have also been located in the locus coeruleus, the brain stem, thalamic nuclei, and anterior olfactory nucleus (AON) of PD patients. Although LBs are found in affected brain regions in PD, they are also present in dementia with Lewy bodies (DLB), Alzheimer's disease (AD), and incidental Lewy body disease (ILBD) in otherwise healthy individuals of advanced age, demonstrating that they are not exclusively a PD phenomenon[33]. Due in part to this, it is greatly debated whether LBs are causative, protective, or simply a consequence of the disease process in PD[34]. The precise mechanism of neurodegeneration in PD remains a contentious issue. *In vitro* and *in vivo* models of PD, as well as studies from familial genes have provided some insight into the molecular pathways involved in the formation of LBs and the nigrostriatal dopaminergic loss.

1.3 The pathobiology of Parkinson's disease

Oxidative stress is a central mechanism of the cellular pathways implicated in PD and it may be considered a unifying factor for the diverse pathogenic mechanisms (Figure 1.2). Furthermore, PD is progressive, so it is unlikely that an acute insult causes neuronal death, it is more likely the result of a persistent process such as oxidation that gradually drives dysfunction and eventually neuronal death. Regardless of the triggering event, there is sound evidence to suggest that oxidative stress-related injury is a primary mechanism of cellular dysfunction in PD.

Reactive oxygen species (ROS) are produced in the cell during oxidation-reduction (redox) reactions and in the mitochondrial electron transfer chain. This is a system with very intricate biochemistry that is unable to be explored thoroughly here - please see Dickinson and Chang[35] for a complex review of the topic. Briefly, toxic ROS are produced by reactions that utilise oxygen, which are plentiful in oxygen-based biological systems. The ROS produced in these processes are regulated by antioxidants such as superoxide dismutase (SOD) and glutathione (GSH). Failure of the physiological antioxidant system, as is seen in ageing, leads to oxidative stress which can damage cell components and lead to cell death[36-38]. If ROS are increased to levels that overwhelm the physiological antioxidant system it will also lead to oxidative stress, and in PD many pathological changes increase ROS production.

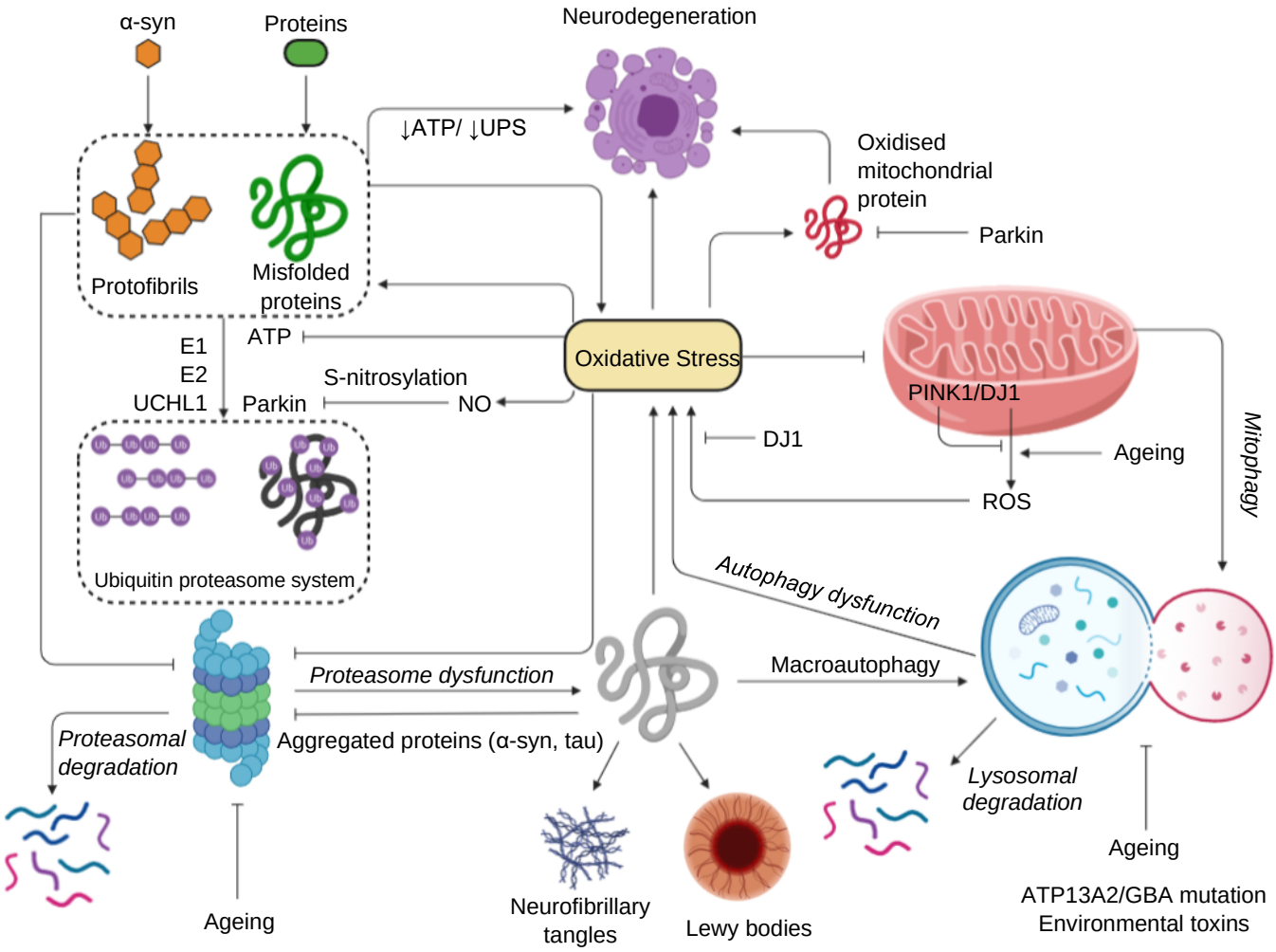

Figure 1.2 Converging oxidative stress pathways in Parkinson's disease. The intricate convergent pathways that involve failure of the ubiquitin-proteasome system and the autophagy-lysosome pathway, misfolded proteins, and mitochondrial dysfunction that both feed into, and are the result of, oxidative stress phenomenon that lead to eventual cell death. Abbreviations: α-syn, alpha-synuclein; ATP, adenosine triphosphate; GBA, glucocerebrosidase; NO, nitric oxide, PINK1, PTEN-induced kinase 1; ROS, reactive oxygen species; Ub, ubiquitin; UCHL1, ubiquitin C-terminal hydrolase L1; UPS, ubiquitin-proteasome system.

Mitochondrial dysfunction

Mitochondria are a key site of ROS production as electrons are passed through the inner membrane through a series of redox reactions. These reactions are critical for energy production, in which ROS are generated as a byproduct. While the amount of ROS generated in these reactions is healthy, if there is dysfunction of the electron transport chain, mitochondria produce excessive amounts of ROS that can lead to oxidative stress[39]. For an extensive review of mitochondria and physiological ROS, please see this publication by Starkov[40].

Mitochondrial dysfunction has been implicated in PD pathogenesis since the accidental 1-methyl-4-phenyl-1,2,3,6-tetrahydropyridine (MPTP) exposure of six individuals, referred to as the "frozen addicts"[41]. MPTP is a neurotoxin that induces toxicity via its active metabolite interfering with complex I of the electron transport chain of mitochondria. This finding was linked more definitively to PD when it was found that complex I was decreased in the SNpc of PD patients[42-44]. Complex I inhibition increases free radical production (ie ROS) and oxidative stress as well as decreasing adenosine triphosphate (ATP) production. These biochemical changes cause increased intracellular calcium concentration, excitotoxicity, and nitric oxide-mediated cellular damage. Known genetic mutations linked to familial PD encode proteins that regulate mitochondrial and ROS homeostasis, including PINK1[10], Parkin[45], and DJ1[11].

PINK1 is a mitochondrial protein that co-localises with Parkin. In a healthy mitochondrion, PINK1 phosphorylates, activates, and recruits Parkin. Parkin can then ubiquitinate proteins on the mitochondrial membrane and signal the mitochondria for degradation via mitophagy. Disruptions in this process and the resulting accumulation of damaged mitochondria in neuronal axons are a source of ROS and oxidative damage[46]. Although DJ1 has no known direct link to mitochondrial function, under oxidative conditions cysteine residues are modified to cysteine-sulfinic and cysteine-sulfonic acids[47]. Through this cysteine modification, DJ1 can sense the redox state of a cell and is activated to exert a protective effect, although the exact mechanism of this protective effect remains unclear.

Further implicating mitochondrial dysfunction as a primary mechanism of PD, neurotoxins such as MPTP, rotenone, and paraquat act at the mitochondria and induce parkinsonism. MPTP is a toxin that is metabolised in astrocytes to 1-methyl-4-phenylpyridinium (MPP+), which is then able to selectively enter dopaminergic neurons via the dopamine transporter (DAT) and inhibit complex I of the electron transport chain in mitochondria[48]. Similarly, rotenone inhibits the transfer of electrons in complex I and paraquat induces ROS production, although its precise mechanism is not yet understood[49].

Alpha-synuclein

α-syn is a presynaptic neuronal protein that has been hypothesised to contribute to PD pathogenesis through the aggregation of aberrant oligomeric species (protofibrils) that are toxic and mediate disruption of cellular homeostasis and neuronal death[50]. α-syn is localised to the nerve terminals and can bind anionic lipids, suggesting it may have a role in vesicle recycling[51]. The existence of several polymorphisms in the *SNCA* gene attributing to increased risk and duplications/triplications of the gene resulting in familial PD suggest that expression levels may be a risk factor. It is clear that α-syn has a role in idiopathic PD, however, whether it is causative in all cases is contentious.

Impairment in the Ubiquitin-Proteasome System

The UPS is the essential non-lysosomal cellular pathway responsible for the degradation and removal of damaged and misfolded proteins in neurons[52]. This is achieved by a series of enzyme-mediated reactions (Figure 1.3). The first steps involve the ubiquitination of abnormal/damaged proteins to create ubiquitin-protein conjugates that can be recognised and degraded by the 26S proteasomes[53]. The 26S proteasome catalyses the conjugates into short peptide fragments for recycling and releases the polyubiquitin chain. Ubiquitin carboxy-terminal hydrolases disassemble these chains to produce monomeric ubiquitin molecules for recycling back into the UPS.

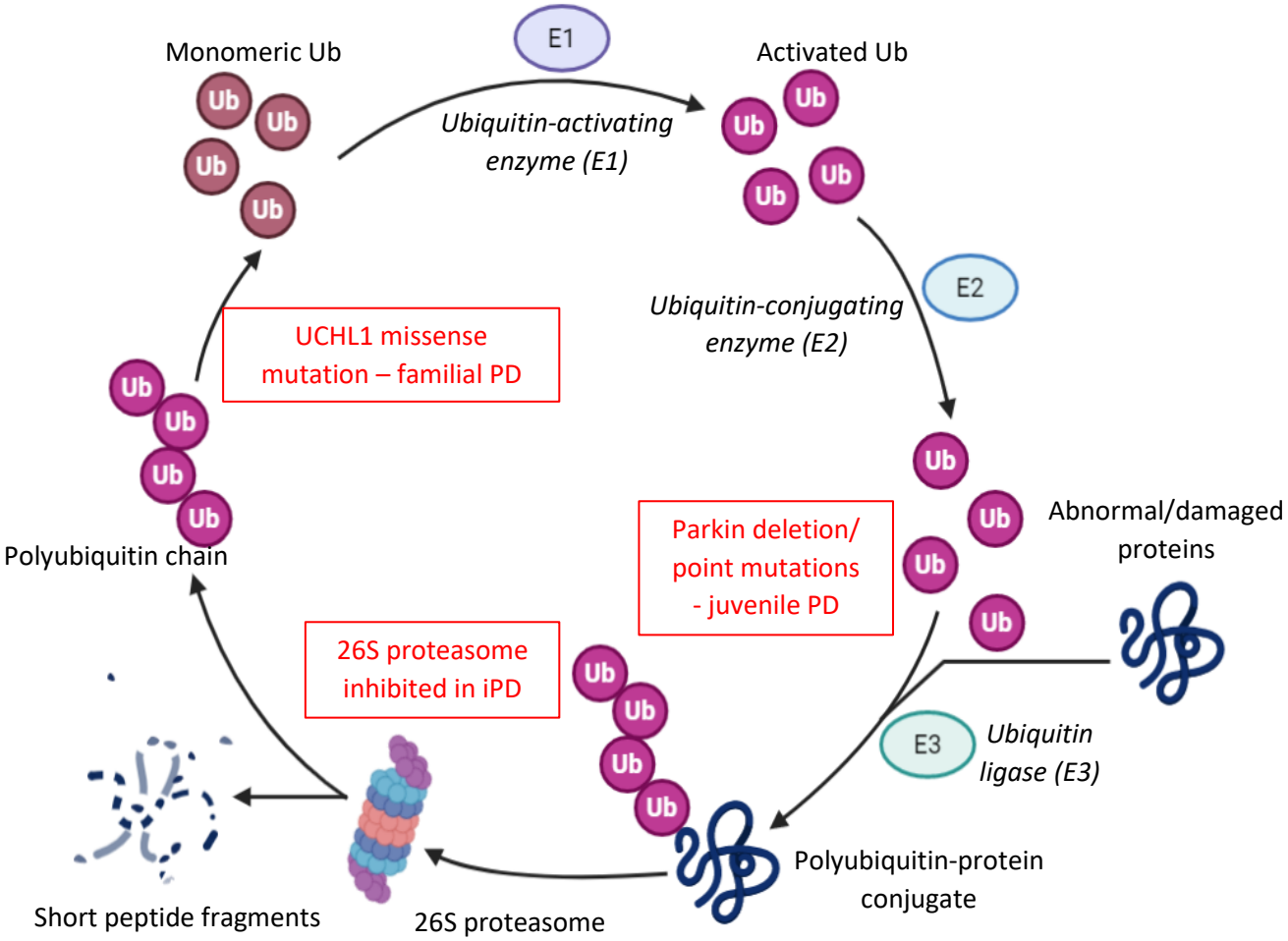

Figure 1.3 The ubiquitin-proteasome system in Parkinson's disease. Known genetic mutations in parkin and UCHL1 result in failure of the ubiquitin-proteasome system in Parkinson's disease. Abbreviations: iPD, idiopathic Parkinson's disease; UB, ubiquitin; UCHL1, ubiquitin C-terminal hydrolase L1.

Dysfunction of the UPS has been implicated in PD due to a buildup of aggregated protein products, as well as the presence of UPS-related proteins within LBs – including ubiquitin[54], parkin[55, 56], UCHL1[57], and proteasomal elements[58]. This concept has been supported by the discovery of deletion/point mutations of parkin leading to juvenile PD, and missense mutation of UCHL1 implicated in a form of

familial PD. Parkin is a ubiquitin ligase (E3) and it has been shown that ubiquitin ligase enzymatic activity is decreased in the SNpc of patients with juvenile PD[59]. A very rare missense mutation was reported in German siblings with autosomal-dominant familial PD[60], however there have been no other confirmed reports of UCHL1 mutations segregating with parkinsonism despite evidence that links UCHL1 dysfunction and neurodegeneration[61]. UCHL1 is a protein responsible for the hydrolysis of bonds between ubiquitin molecules and plays an important role in the recycling of monomeric ubiquitin needed to tag abnormal proteins. Although these mutations are only found in genetic forms of PD, it has also been shown that there are reductions in each of the three enzymatic activities of the 26S proteasome in the SNpc of patients with PD[62].

Impairment in the Autophagy-Lysosome Pathway

The ALP is the other mechanism to remove abnormal proteins in the cell. The ALP consists of three defined forms of clearance, including macroautophagy (referred to as autophagy from this point), microautophagy, and chaperone-mediated autophagy (CMA) (for the purpose of this review only autophagy and CMA will be discussed). Misfolded proteins (due to mutation, oxidative stress, or post-translational modifications) will be either refolded and repaired or undergo degradation. The first step of the degradation is through the UPS or CMA. Impairment in these degradation mechanisms, or large membrane proteins and protein complexes (including aggregates) that are too large to pass through the barrel of the proteasome are degraded by autophagy[63]. An impairment in autophagy leads to protein aggregation and deficits in ALP have been linked to multiple neurodegenerative diseases[64], including PD.

Soluble α-syn can be degraded by both the UPS and CMA[65-67], however, mutant α-syn is problematic for these systems. Fibrillar forms of α-syn become stuck in the barrel of the proteasome blocking its activity[68]. Mutant α-syn has a high affinity for the lysosomal membrane, but it cannot undergo translocation and this results in blockade of the lysosomal receptor and a failure of lysosomal translocation and degradation of other CMA substrates[67]. It has been shown that when there is reduced activity of UPS and CMA, autophagy is upregulated[69, 70]. Although this helps to maintain protein degradation, autophagy is less selective than the UPS and CMA and results in non-specific bulk degradation. Due to this phenomenon cells have reduced capacity to respond to oxidative stress and are susceptible to stressors[69].

There are many steps of autophagy and CMA where dysfunction can occur, and PD-related genes are implicated (Figure 1.4). Mitophagy is the clearance mechanism of damaged mitochondria and PINK1 and parkin have a role in the recognition, targeting, and degradation of damaged mitochondria[71]. Mutations in both PINK1 and parkin are associated with PD[8, 10] and result in disrupted mitophagy[71].

Mutations in *LRRK2* are the most common cause of genetic PD[72, 73]. Overexpression of LRRK2 and its mutant forms inhibit CMA through blockade of lysosomal receptors, much like mutant *SNCA*[74]. Furthermore, it can disrupt PINK1 and parkin-mediated mitophagy[75, 76], as well as affect lysosomal pH[77]. These mechanisms represent only a subset of proposed interactions of LRRK2 that disrupt ALP, reviewed more thoroughly in[78]. Glucocerebrosidase (*GBA*) encodes for the lysosomal enzyme GCase. As such, mutations that result in loss of function of GCase results in lysosomal dysfunction, and mutations in *GBA* are a genetic risk factor for PD. ATP13A2 is a lysosomal ATPase and *ATP13A2* mutations result in a failure of autophagy and α-syn aggregation in PD[79, 80]. Finally, ageing reduces ALP activity and age is the biggest risk factor for the development of PD[81-83]. Although the precise mechanisms of ALP disruption in PD have not been elucidated, there is a growing body of evidence that failure of macroautophagy underlies the accumulation of protein aggregation in PD.

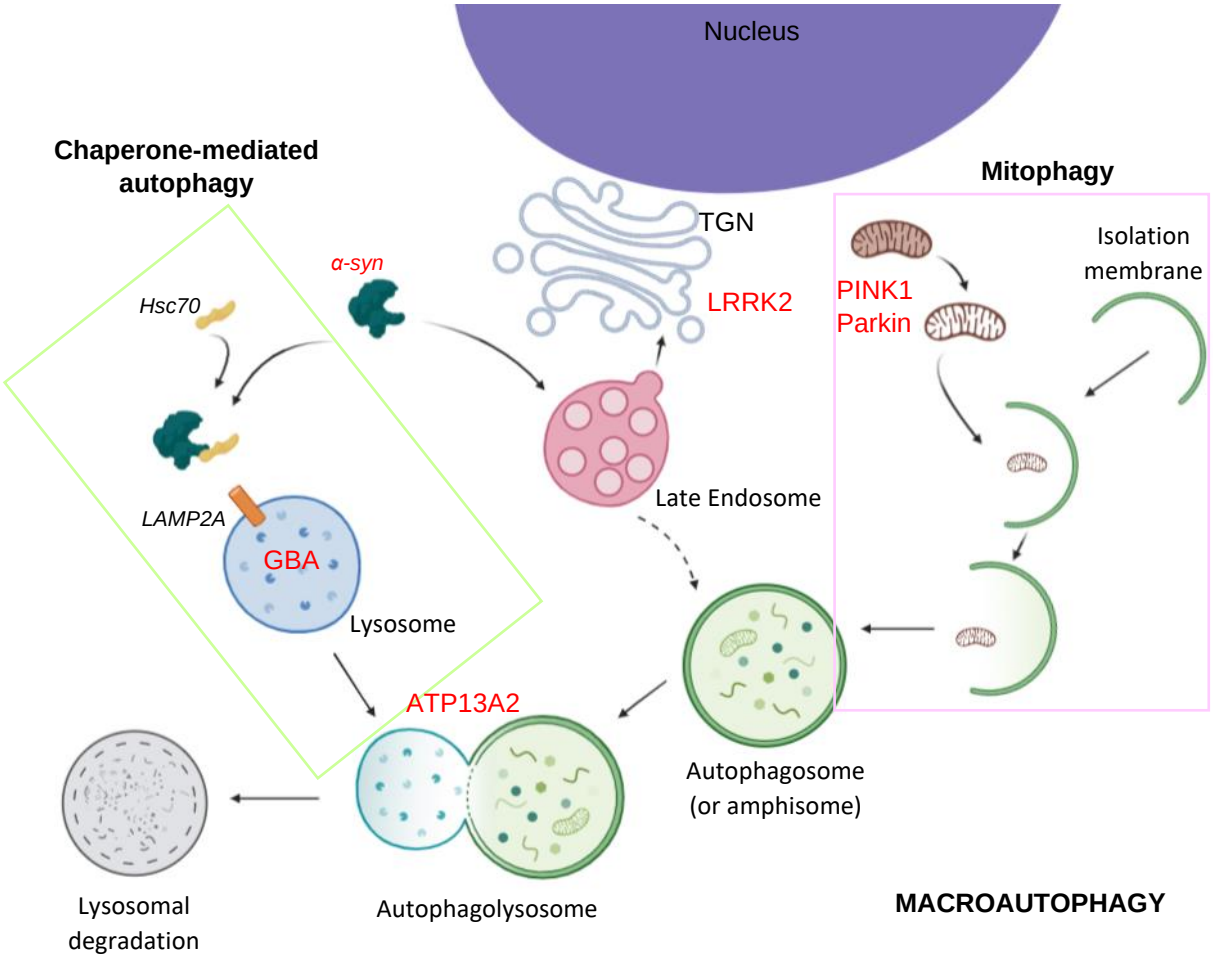

Figure 1.4 The autophagy-lysosome pathway in Parkinson's disease. Mutations in α-syn, GBA, ATP2A2, LRRK2, PINK1, and parkin are all implicated in various stages of the autophagy-lysosome pathway in Parkinson's disease. Abbreviations: GBA, glucocerebrosidase; Hsc70, heat shock cognate 71; LAMP2A, lysosome-associated membrane protein 2; LRRK2, leucine-rich repeat kinase 2; PINK1, PTEN-induced kinase 1; TGN, trans-Golgi network.

Neuroinflammation

The aforementioned mechanisms are specific to neurons, however, there is involvement of other cell types in PD. Neuroinflammation, and the engagement of inflammatory cells, are likely to contribute to the cascade of events leading to neurodegeneration. Under pathological conditions, microglial cells become activated, and these cells have been found in *post-mortem* SNpc of PD patients[84]. Activated microglia express inducible nitric oxide synthase (iNOS) which produce nitric oxide (NO) radicals. The presence of NO radicals upregulates the expression of nicotinamide adenine dinucleotide phosphate (NADPH) oxidase, which in turn produces O_2^- radicals. The combination of O_2^- and NO results in peroxynitrite ($ONOO^-$) which cause oxidative stress and damage to neurons. Furthermore, O_2^- radicals can be dismutated to hydrogen peroxide (H_2O_2), which in the presence of ferrous iron produces deleterious hydroxyl radicals ($OH^\bullet$) [85] (section 1.4). There are many other astrocytic- and microglial-mediated mechanisms implicated in the pathobiology of PD (reviewed in[85]), however, these neuroinflammatory processes are not PD-specific. Despite not being PD-specific, these mechanisms may be able to trigger and contribute to the disease process, however, it is likely in combination with genetic vulnerabilities that make the dopaminergic neurons more susceptible.

Oxidative stress seems to have a central role in the pathways involved in neurodegeneration, and it can be envisaged that it is a culmination of the pathobiological changes conspiring to cause selective neuronal demise in the presence of defects in either mitochondrial, α-syn, or clearance pathways. Cell death occurs at many levels across the nervous system in PD, including cholinergic neurons in the pedunculopontine nucleus and noradrenergic neurons in the locus coeruleus[86, 87]. However, the consistent feature of both idiopathic and genetic forms of PD is the selective vulnerability of the dopaminergic neurons in the SNpc.

1.4 Dopaminergic vulnerability

There are four leading hypotheses as to what makes the nigrostriatal dopaminergic neurons exceptionally vulnerable in PD. Firstly, the production of dopamine itself puts the neurons at risk. Dopamine is toxic in certain conditions, as it generates quinones during oxidation[88]. These quinones can negatively impact the mitochondrial complexes[89], promoting mitochondrial dysfunction and oxidative stress[90]. However, this alone cannot explain the selectivity, as not all dopaminergic subgroups are affected (the ventral tegmental area is preserved, for example). Secondly, iron is known to

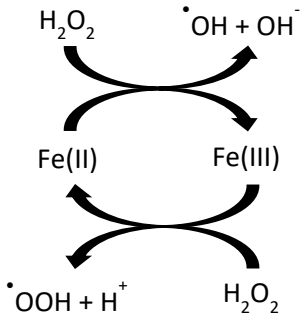

Figure 1.5 The Fenton reaction. Radicals are generated through the catalytic process that converts hydrogen peroxide (H_2O_2) into free radicals

accumulate in the SNpc with age[91, 92], and iron can generate ROS by the Fenton reaction (Figure 1.5). The combination of the mitochondrial electron transport chain requiring iron-sulfur clusters, and SNpc neurons having a high energy demand suggests that increased iron levels could contribute to the elevated and sustained mitochondrial activity, and therefore ROS production[93-95].

Thirdly, the nigrostriatal dopaminergic neurons have extensive axonal arborisation, with estimates of up to one million neurotransmitter release sites per neuron in humans[93]. These many axon terminals place a large bioenergetic burden on these cells, meaning there is little margin to cope with additional energetic stress. Finally, nigrostriatal dopaminergic neurons have autonomous pace making activity. This pace making activity requires slow oscillations in intracellular calcium levels, which can directly promote oxidative phosphorylation of the mitochondria, and result in chronically high levels of ROS production[96-98].

The underlying feature of these four hypotheses is that they suggest that vulnerability is underpinned by the fact nigrostriatal dopaminergic neurons are under intense bioenergetic, and therefore mitochondrial, demand. If there is a slight decrease in the cell's antioxidant system, such as what happens with age or specifically depletion of GSH which has been reported in PD brains[99, 100], the energy stores required to sustain neurotransmitter release will leave too little of the cell's resources to maintain other key functions. This may include the degradation of misfolded or damaged proteins[101] and may lead to a dysregulation of axon terminals, triggering a cascade of axonal retraction that eventuates in cell death[102-104]. It is clear that oxidative stress is a major contributor to the pathobiological changes in PD, and as such, current therapeutic approaches are primarily centered around the reduction of oxidative stress, as well as clearance of α-syn.

1.5 Therapeutic strategies in Parkinson's disease

The goal of a neurotherapeutic agent in PD is to generate a disease-modifying treatment that targets underlying neurodegeneration. Currently, patients are treated with dopaminergic agonists, followed by dopamine replacement therapy (L-DOPA). Dopamine replacement therapy is effective only in the short term (as long as there are functional dopaminergic neurons present), it has substantial side effect profiles, and most importantly, it doesn't halt the underlying neurodegeneration. Large-scale studies are currently testing several potential disease-modifying therapies, targeting OS, lipid metabolism, α-syn levels, and metabolic processes (Figure 1.6).

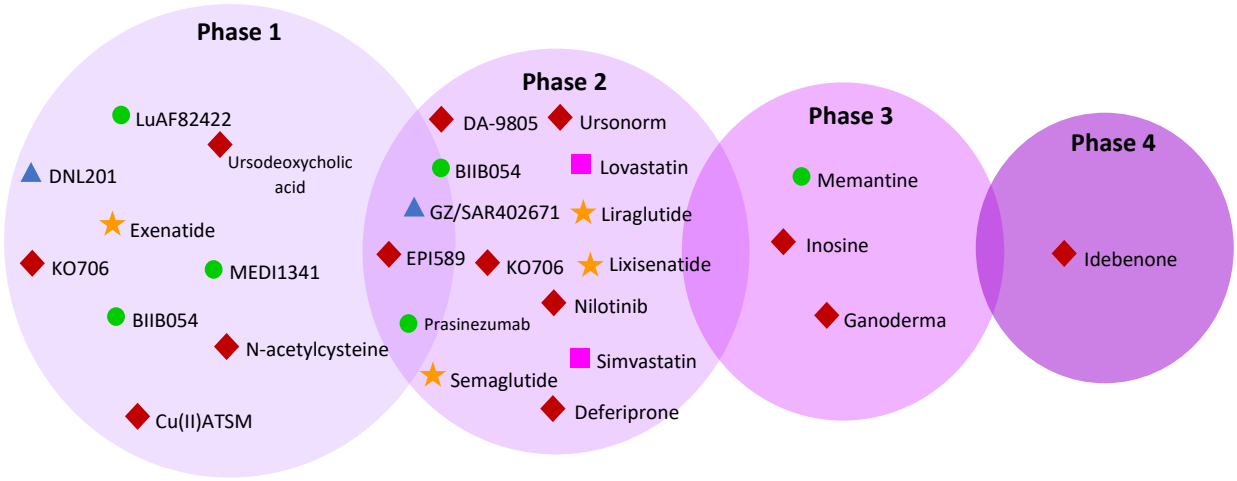

Figure 1.6 Clinical trial pipeline in Parkinson's disease. Compounds in clinical trial for Parkinson's disease as of June 2019. Drugs are separated into the phases (1-4) and categorised according to the therapeutic target; green symbol: α-synuclein, red symbol: oxidative stress, pink symbol: lipids, orange symbol: metabolic, blue symbol: other.

Despite several promising candidates, there are no approved disease-modifying drugs for PD, and pharmaceutical companies are less inclined to run PD clinical trials. This may be due to several reasons – firstly, as described above, the pathophysiology of PD is multifactorial and not completely understood. Secondly, there are no biomarkers that reflect the progression of the disease that are needed to test the efficacy of a compound on the underlying pathological process. Thirdly, PD is a very slow disease and decline is not linear in nature[105], therefore the relatively short time periods utilised in clinical trials are likely not long enough to see any significant effects on disease progression. Finally, the stratification of patients for PD clinical trials is sub-optimal, both in that patients who are recruited have a clinical diagnosis based on motor impairment – reflective of advanced disease[106, 107], and that the diagnosis of PD is sub-optimal. PD is grossly over-diagnosed and pathological confirmation has indicated that only 80% of people who have a clinical diagnosis meet the neuropathological criteria for PD[108].

PD is aligned with substantial non-motor features, which with greater understanding will provide an opportunity to better identify and target PD. Understanding the biological basis of these symptoms may help to address some of the current clinical trial design weaknesses, in both a potential pool of novel biomarkers and the ability to stratify and recruit patients in the preclinical phase. This will allow for disease-modifying neuroprotective agents to be tested in patients who still have healthy neurons to protect. Furthermore, the identification of multiple symptoms will help to increase the sensitivity of clinical diagnosis ensuring the recruitment of a reliable cohort of patients.

1.6 Non-motor Parkinson's disease

Though widely still considered a movement disorder, there is a paradigm shift beginning in the recognition of PD as a syndrome associated with a broad spectrum of both motor, and non-motor impairments. James Parkinson described prominent non-motor symptoms present in the patients with 'shaking palsy', including soft speech, dysphagia, sleep disturbances, constipation, and urinary dysfunction. Despite this early recognition of non-motor PD, the movement disorders community has focused research and energy on the motor aspects of the disease, resulting in the absolute reliance of movement as clinical trial endpoints and diagnostic criteria. Of the broad spectrum of non-motor symptoms, many have been identified as an early phenomenon in PD and understanding the presentation and molecular pathways involved in the dysfunction of these pathways may prove fruitful in the quest for diagnostic biomarkers. Several studies have suggested that at least four distinct non-motor symptoms of PD (hyposmia, sleep disorder, constipation, and depression/anxiety) predate the clinical motor signs defined in the diagnostic criteria (Figure 1.7).

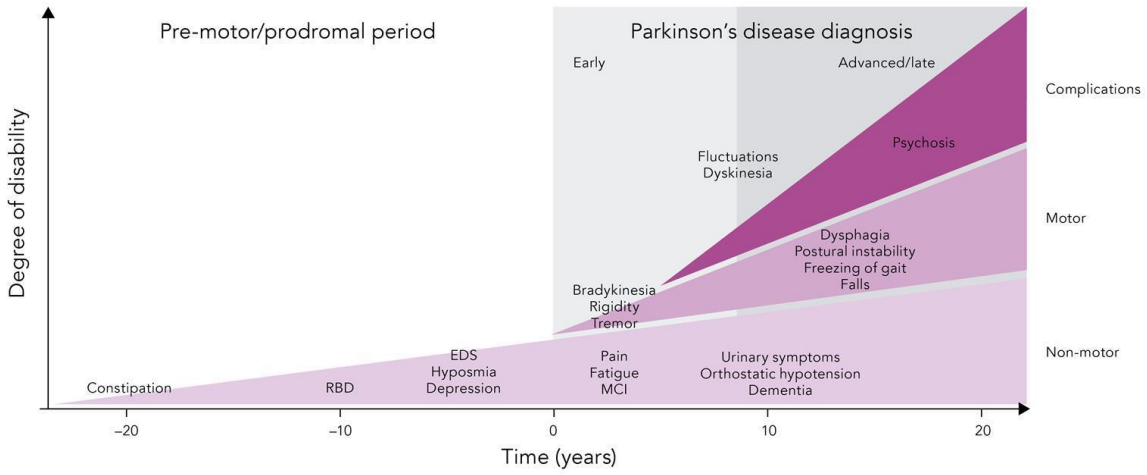

Figure 1.7 Symptom onset in Parkinson's disease. Figure adapted from[109]. The left side represents the prodromal period of Parkinson's disease, before clinical diagnosis. Abbreviations: EDS, excessive daytime somnolence; MCI, mild cognitive impairment; RBD, rapid eye movement sleep behaviour disorder.

Constipation is the second most prevalent preclinical symptom of PD, behind only hyposmia, and present in as many as 50% of diagnosed PD cases[110]. PD-related constipation is thought to be the result of autonomic dysfunction and presents as early as 10 years before the onset of clinically overt motor impairment[111]. The relative risk associated with constipation is from 2-2.5[112], however, the prevalence of constipation in the general population is high (15-20%)[113], resulting in low specificity. Depression and anxiety are often comorbid in PD and have been demonstrated to present 3 years before the onset of motor impairment[114, 115]. Due to the prevalence of depression and anxiety in the general

population, the relative risks associated with PD prediction are as low as a 1.5-fold increase, so the predictive value of these symptoms alone are low[116].

Rapid eye movement sleep behaviour disorder (RBD) is a form of sleep disturbance in which there is a loss of normal skeletal muscle atonia, resulting in patients 'acting out' their dreams during the normally paralytic stage of REM sleep. When confirmed by polysomnography, the predictive value of RBD is the highest of any of the preclinical symptoms of PD. RBD is reported in 40-50% of PD patients[117, 118], and several long-term studies have indicated that 65-90% of RBD patients will go on to develop a neurodegenerative disorder, including DLB and multiple system atrophy, but predominantly PD[119-121]. Due to the high sensitivity of RBD, it is a very strong predictive tool for the development of PD, however as only one-third to one-half of PD patients have RBD, it alone is not enough to identify PD patients.

Hyposmia in Parkinson's disease

Hyposmia is the most prevalent symptom, present in 80-90% of PD patients, and an understanding of the underlying pathobiology may aid in the development of a robust diagnostic tool in preclinical PD. In 1975 Ansari and Johnson were the first to report olfactory disturbances in PD[122]. Since this time, it has become evident that not only are there general disruptions in olfaction, but PD patients have deficits in odour detection, differentiation, and identification. Furthermore, olfactory deficits are one of the first symptoms of PD, reported to herald overt motor deficits by as much as a decade. As one of the more salient non-motor features of disease, in as many as 90% of PD cases, hyposmia has been phenotypically well characterised, however neurobiology underlying the symptom is still under-researched. Much of this can be attributed to the complex nature of the central olfactory system, involving many neural networks and brain structures that are not yet fully characterised.

1.7 The central olfactory system

Neuroanatomy and physiology

The central olfactory system begins in the superior section of the nasal cavity and terminates with the processing of signals in the olfactory cortex. The olfactory epithelium (OE) is specialised tissue within the nasal epithelium that contains six to ten million ciliated primary olfactory neurons[123]. The cilia are covered in mucus and have the olfactory signal transduction machinery to initiate nervous system signalling in response to chemical stimulation. The olfactory system is built to handle many odour molecules while still being precise enough to detect subtle differences in odour profiles, which it achieves by having a vast array of variable G-protein coupled receptors (GPCRs)[124].

The transmembrane regions of the GCPRs have variable sequences to recognise a large variety of odour molecules. There are reported to be 400 individual olfactory receptors in humans[125] and a single

olfactory receptor neuron will only express a single odourant receptor gene (known as the *one-cell-one-receptor rule*)[126]. There are seven hydrophobic transmembrane domains and this region of the GPCR plays a key role in forming odourant-binding pockets. Due to this physical binding pocket, the molecular structure of odour molecules is a key factor in binding, and there is a relationship between the structure of an odourant and the subjective perception of an odour[124]. This structure-odour relationship has two key features; the presence of a polar functional group, and the overall molecular shape.

An odourant binds to and activates the G-proteins of an olfactory receptor (Figure 1.8). Unlike classic GPCRs, there is no amplification of the signal. Instead, Ric-88 enhances the accumulation of $G\alpha_{olf}$ on the cell membrane, increasing coupling. Activated $G\alpha_{olf}$ stimulates adenylyl cyclase III resulting in an increase in cyclic adenosine monophosphate (cAMP) which opens up the cyclic nucleotide gated (CNG) channel leading to depolarisation of the olfactory receptor neuron. Ca^{2+} activates the Cl^- channel resulting in Cl^- efflux, and amplification of sensory depolarisation. The action potential generated is propagated along the olfactory receptor neuron axon, through the cribriform plate, and into the olfactory bulb (OB).

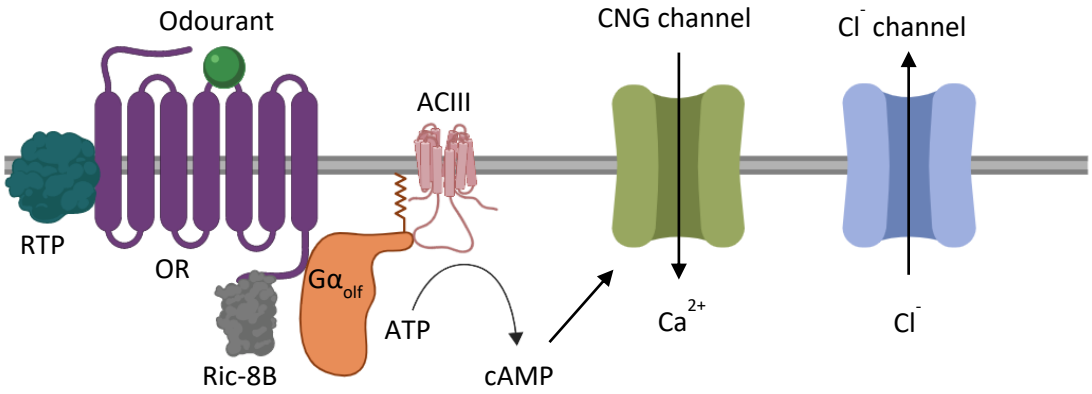

Figure 1.8 The olfactory receptor neuron G-protein coupled receptor. Abbreviations: ACIII, type III adenylyl cyclase; cAMP, cyclic adenosine monophosphate; CNP, cyclic nucleotide-gated; $G\alpha_{olf}$, stimulatory G-protein; OR, olfactory receptor; RTP, receptor transporter protein.

The Olfactory Bulbs

The OBs are located on the inferior side of the forebrain and are the first relay station of the central olfactory system[127]. The OB is organised into seven distinct layers: olfactory nerve layer, glomerular layer, external plexiform layer, mitral cell layer, internal plexiform layer, granule cell layer, and the subependymal-ependymal layer (Figure 1.9). These layers are defined by populations of neurons that process odour coding patterns and transmit codes to higher brain regions for olfactory processing[128]. Due to the conserved layering and neuronal connections of the OB, there is a sequential order to odour processing that begins in the olfactory epithelium of the nasal cavity and eventuates in the olfactory cortex.

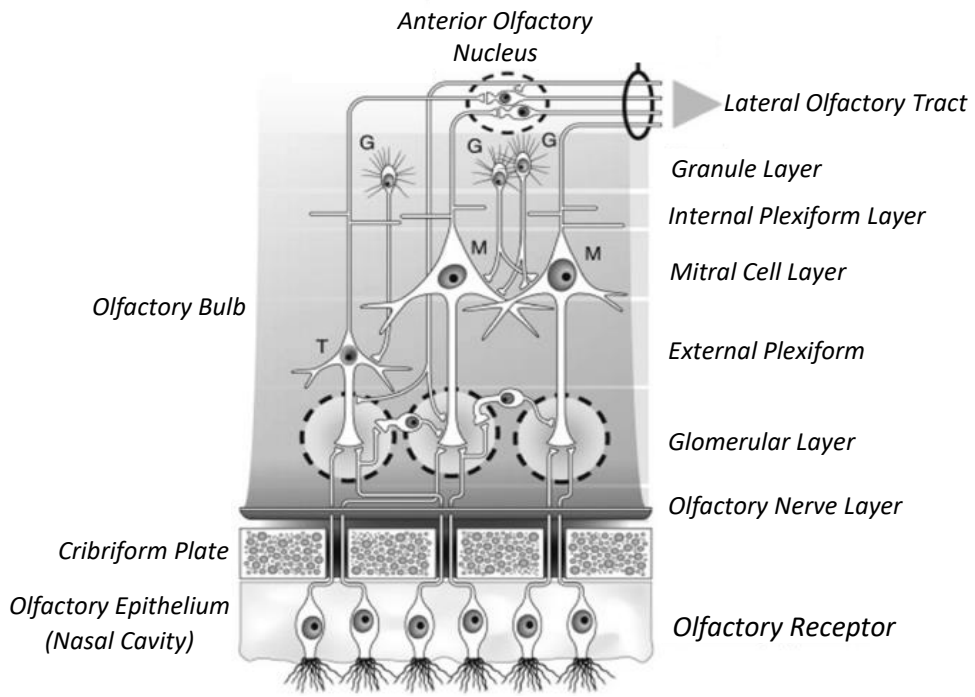

Figure 1.9 The layers of the olfactory bulb. Image modified from Doty et al. 2014[129].

The olfactory nerve layer is comprised of bundles of olfactory neuron axons (*fila olfactoria*) from the olfactory epithelium of the nasal cavity that has penetrated the cribriform plate. These bundles of neurons extend to and penetrate the glomeruli within the glomerular layer and synapse with both primary projection neurons and intrinsic local circuit neurons. The principal neurons of the olfactory system are the mitral and tufted cells. These cells are the trajectory neurons of olfactory signals to extrabulbar brain regions. Mitral and tufted cells are classified into subtypes based on the distribution of secondary dendrites and the function of the neuron (summarised in Table 1.1). Importantly, these neurons project a single primary dendrite into a single glomerulus[130].

Local circuit neurons project their axons intrabulbarly and are made up of granule cells, periglomerular cells, and short-axon cells. These neurons are considered the inhibitory neurons and regulate signal projection both directly on the primary projection neurons as well as within, and between, the glomeruli[131, 132]. Granule cells are predominantly axonless GABAergic neurons that project dendrites to the external plexiform layer. Periglomerular cells are within the juxtaglomerular regions and have been classified into two types based on immunoreactivity. PG1 cells contain gamma aminobutyric acid (GABA), tyrosine hydroxylase (TH), and glutamate decarboxylase (GAD); PG2 cells contain calbindin and calretinin. Short-axon cells are superficial neurons thought to make excitatory connections with the inhibitory periglomerular cells but are yet to be fully understood. These local circuit neurons play a key role in the regulation of signals primarily through action in the glomerular layer.

Table 1.1 Neuronal subpopulations of the central olfactory system

	Neuron type	***Subtype***	***Neuroactive substance***
Principal neurons	Mitral cell (M)	M1	Glutamate, CRF
		M2	
	Tufted cell (T)	Deep T	Glutamate, CRF
		Middle T	Glutamate, CRF
		External T	Glutamate CCK
Local circuit neurons	Periglomerular cell (PG)	PG1	GABA, GABA + DA, somatostatin, CCK, NO
		PG2	Enkephalin
	Granule cell (GR)	G1	GABA, enkephalin
		G2	
		G3	
	Short-axon cell (SA)	Deep SA	GABA, VIP, NPY, NO
		Superficial SA	GABA VIP
Afferent nerves	Olfactory nerves (ON)		Glutamate
	Centrifugal afferents	Higher olfactory cortices	Glutamate
		Nucleus of the diagonal band	ACh, GABA
		Locus coeruleus	5-HT, NA
		Raphe nuclei	

Abbreviations: 5-HT, serotonin; ACh, acetylcholine; CCK, creatine kinase; CRF, corticotropin-releasing factor; DA, dopamine; NA, noradrenaline; NPY, neuropeptide Y; VIP, vasoactive intestinal polypeptide

The Glomerulus

The individual glomeruli range from 30 to 200µm in diameter. Upon making synaptic connections in the glomerulus, olfactory neurons release glutamate and engage with post-synaptic connections that initiate neural processing of olfactory signals[130]. It is not a simple neuron to neuron connection within the glomeruli, as there is a complex circuit of synaptic connections that function within and between individual glomeruli. The glomeruli are enclosed by a layer of juxtaglomerular neurons and astrocytic cell bodies, within the periglomerular region. It is the local circuit neurons that make up this region, as well as the external tufted cells. While the periglomerular and external tufted cells send dendrites into the glomeruli, short-axon cells are only known to send dendrites within the periglomerular region.

Within the glomeruli, periglomerular cells synapse with mitral and tufted cells, as well as with the olfactory receptor neurons. The glomerulus is separated into two regions, based on the presence of the olfactory receptor neuron (ON zone and non-ON zone)[133]. The first type of periglomerular neurons, PG1, extend dendrites in both zones and receive synapses from the olfactory receptor neurons. PG2 neurons have no interaction with the olfactory receptor neurons and remain within the non-ON zone. It is thought that dopamine and GABA are released from the PG1 neurons and interact with the

olfactory receptor neuron terminals via D_2 and $GABA_B$ receptors and this represents the first inhibitory step of the olfactory system and the only point at which dopamine crucially modulates this system[134].

As the primary projection neurons, as well as the majority of the periglomerular neurons only project their dendrites to single glomerulus containing a single type of olfactory receptor neuron, the glomeruli are considered a functional module of the olfactory system. The glomerular modules are responsible for relaying odour signals throughout the olfactory bulb into higher brain regions collectively referred to as the olfactory cortex.

The Olfactory Cortex

Olfactory information needs to be transmitted from the periphery to higher cortical regions for detection and discrimination, before further processing to allow sensory consciousness and affect behaviour. Mitral and tufted neurons from the OB project axons through the olfactory tract to at least six distinct cortical regions on the surface of the ventral forebrain; anterior olfactory nucleus, piriform cortex, olfactory tubercle, anterior cortical nucleus of the amygdala, entorhinal cortex, and the accessory olfactory cortical areas[135]. Unlike other sensory cortexes, there does not appear to be topographical organisation beyond that of the olfactory bulb. There is an extensive system of intracortical connections, and these connections integrate odour information with other sensory cues and learned associations to generate a meaningful response to an odour.

Olfactory neurobiology in Parkinson's disease

One of the crucial factors to be considered with the utility of hyposmia as a diagnostic tool is that hyposmia and anosmia are not uncommon in the general population. Regardless of age, 3.8-5.8% of the general population have anosmia[136-138], 13.9% of individuals over the age of 65 are hyposmic[139], and up to 80% in people over 80[140]. It has recently been shown that people who lose their sense of smell are more likely to die in the next decade than those who don't, suggesting that olfactory function may be a valid indicator of the integrity of the ageing brain[141]. Despite this, the prevalence and early onset of olfactory dysfunction in PD suggest that there may be disease-related phenomena contributing to hyposmia, and it is different from age-related decline.

Neurotransmitter alterations

The nucleus basalis (cholinergic) has projections to olfaction-related brain regions and is significantly damaged in PD, with cell numbers decreased from 54-77%[142, 143]. A positron emission tomography (PET) study using [^{11}C] methyl-4-piperidinyl propionate acetylcholinesterase ligand demonstrated a correlation between University of Pennsylvania Smell Identification Test (UPSIT) scores and the *in vivo* activity of the ligand in PD patients[144]. Another affected brain region is the locus coeruleus (LC) which

is the source of noradrenergic projections to the OB. In fact, it has been demonstrated that the loss of neurons in the LC is more severe than the loss of neurons in the SNpc in PD[145]. However, it is also established that noradrenaline has a fundamental role in olfactory learning, not odour detection – suggesting that noradrenaline perturbations are unlikely to have a functional role in PD-related hyposmia[146, 147]. This is further supported by the fact PD patients with dopamine β-hydroxylase deficiency (who don't synthesise noradrenaline) have normal smell function[148].

While serotonin has no direct role in the OB, one study has suggested that there is a marked loss of serotonergic neurons in the dorsal raphe nuclei in PD[149], an area that is also associated with Lewy pathology. It is known that activation of brainstem serotonergic neurons activate subsets of periglomerular cells in the OB, which results in reduced amplitude of olfactory output[150]. In this hypothesis, while hyposmia may be promoted by serotonergic changes upstream, the olfactory effect is mediated via dopamine in the OB. Degeneration of dopaminergic neurons occurs within the melanin-containing cells of the ventral tegmentum[151], the major source of dopaminergic projections into the olfactory tubercle. Unlike the nigrostriatal system, hyposmia is not directly caused by a reduction in dopamine levels, as dopaminergic replenishment therapy has no effect on olfactory test scores[152-154]. Counterintuitively, although PD involves substantial neurodegeneration in the midbrain dopaminergic structures, the expression of TH is increased in the periglomerular cells of the OB in PD patients[155], and this increase is associated with a gain in the number of dopaminergic periglomerular cells[156], although the implications of this increase have not yet been characterised.

Pathology within the olfactory system

While olfactory receptor neurons contain features reported to make them susceptible to PD pathology - long, unmyelinated axons and contain α-syn - they do not contain abnormal α-syn deposits or Lewy pathology in PD. Indeed, the amount of α-syn in the olfactory mucosa is not different from healthy older controls[157]. Moving along the central olfactory system, the myelinated mitral and tufted projection neurons contain Lewy pathology, as do the unmyelinated granule and periglomerular cells[158]. By far the most damage to the olfactory system is found within the AON, where there is substantial neurodegeneration and LB pathology that correlates with disease duration[159, 160]. In a later paper, Tsuboi et al. postulated that it was the tau pathology within the AON that correlated with Lewy pathology in the amygdala and cortex, and proposed that these AON tau inclusions were driving the olfactory deficit[161]. This is supported by the findings that diseases associated with hyposmias, such as PD, AD, and DLB, have tau inclusions in the AON – whereas diseases where olfactory functions are spared, such as progressive supranuclear palsy (PSP) and corticobasal degeneration (CBD), do not[161].

Xenobiotics

Exposure to environmental toxins is a known risk factor for the development of sporadic PD. Toxins may come in the form of ionised metals, solvents, pesticides, herbicides, and viruses. Whilst environmental toxins are not likely to be the sole contributor to PD, there is sound evidence that a route of entry into the brain may be via inhalation and penetration of the olfactory mucosa[162]. In theory, xenobiotics could induce hyposmia by simply causing damage to the olfactory receptor neurons within the nasal epithelium. Alternatively, the agent could be transported into the OB where it can interrupt cellular function and initiate a pathological cascade, as is seen in manganese exposure which leads to parkinsonism[163].

Above are many proposed mechanisms of olfactory dysfunction in PD, however many of these studies have not been reproduced and propose untested hypotheses for olfactory dysfunction. In order to do a mechanistic interrogation of the features mentioned above, it is vital to utilise animal models of disease.

1.8 Animal models of Parkinson's disease

Animal models of PD are considered difficult to obtain due to the complex nature of the disease. An ideal animal model will have key features that recapitulate the clinical and neuropathological signs of disease. These features include: 1) age-dependence, since degeneration is associated with increased age, (2) progressive loss of nigrostriatal dopaminergic terminals resulting in motor dysfunction that is responsive to dopamine replacement therapy, and (3) the accumulation and aggregation of α-syn and Ub into Lewy pathology-like inclusions. The multifactorial nature of disease means one animal cannot recapitulate all of the pathobiology, and models are generally either genetic or neurotoxic.

Genetic animal models

As highlighted earlier, there are a number of key genetic modifications that have been linked to PD, as well as some that have been implicated as risk factors for idiopathic PD. Many of these genes have been modified or knocked out (KO) of animals in order to understand the disease-related implications of loss of function. There are several α-syn transgenic mice, including α-syn KO[164], and mice who overexpress human α-syn in its wildtype (WT) form[165], or with disease-associated A53T and A30P mutations[166]. These mice have been reported to have a loss of dopaminergic neurons; however, the loss is not progressive and there is no overt degenerative pathology found in the neurons. Despite this, there are functional abnormalities seen in the nigrostriatal system and this results in a motor phenotype[167]. LRRK2 R1441G BAC mice have a progressive, age-dependent motor phenotype that is responsive to levodopa, even in the absence of dopaminergic neurodegeneration[168]. More recently, tau$^{-/-}$ mice have been proposed as a model of PD, due to an age-related motor deficit and progressive

loss of nigrostriatal dopaminergic neurons[26]. Parkin, PINK1, and DJ1 KO animals have no substantial dopaminergic neurodegeneration or behavioural abnormalities[169-171]. Importantly, while some of these mice present with dopamine neurodegeneration, none of these animals develop Lewy-body-like inclusions, despite the extensive accumulation of α-syn.

Neurotoxin-induced animal models

6-hydroxydopamine (6-OHDA) is a neurotoxin most commonly used in rats to model striatal dopaminergic depletion. Often administered with a noradrenergic reuptake inhibitor, 6-OHDA can selectively induce cell death in dopaminergic neurons via the production of ROS and therefore triggering catastrophic oxidative stress. This model is most helpful in trials of dopamine replacement (such as stem cell therapy), as there is approximately a 90% reduction of dopaminergic neurons in the region injected within days to weeks. As such, this is not a model of disease progression.

MPTP is the most commonly used neurotoxin to induce PD-related mechanisms of cell death in mice. As briefly discussed earlier, MPTP is a protoxin that is able to cross the blood-brain barrier, where it is converted to the toxin MPP+. MPP+ impairs mitochondrial respiration by inhibiting complex I of the electron transport chain. This results in a decrease in ATP, an increase in ROS production, and the release of dopamine from vesicles which can further increase ROS production. MPTP-injected mice demonstrate robust motor impairments, correlated with the magnitude of the nigrostriatal lesion.

This is by no means an exhaustive list of the animal models produced for PD research. There are many other species including *Caenorhabditis elegans*, zebrafish, *drosophila melanogaster,* and non-human primates utilised. Furthermore, although the current models of disease have been well-characterised for dopaminergic neurodegeneration and the accompanying motor impairments, there is a shifting interest in looking at non-motor behavioural phenotypes in these animals, as well as an early presentation of these symptoms that mimic the human condition.

Hyposmia in mouse models of Parkinson's disease

Due to the high prevalence of early olfactory deficits in PD, animal models of progressive PD pathology would ideally present with hyposmia before the onset of motor impairment. As hyposmia is easily tested in mice, several studies have been undertaken to measure a loss of function of the olfactory system in models of PD (Table 1.2), primarily those models reported to be progressive.

Table 1.2 Hyposmia in murine models of Parkinson's disease

Animal model	*Model information*	*Hyposmia*	*Ref*
MPTP (mouse)	Intraperitoneal (15mg/kg, 4 doses)	-	[172]
MPTP (mouse)	Intranasal (0.5mg)	+	[172]
MPTP (human)	Intravenous	-	
Thy1-αSyn	Overexpressing WT human α-syn	+ (mild)	[173]
A53T	Express mutated α-syn (A53T)	+	[174]
BAsyn	Express mutated human α-syn (A30P and A53T)	-	[172]
THsyn	Express mutated human α-syn in dopaminergic neurons (A30P and A53T)	-	[172]
THsyn & Dox	Express mutated human α-syn in dopaminergic neurons (A30P and A53T) and have doxycycline-inducible depletion of dopaminergic glutathione	-	[175]

Further characterisation and interrogation of the olfactory system are needed to further our understanding of hyposmia in PD and utilise it as a valuable diagnostic tool. This includes an in-depth characterisation of changes in the human olfactory bulb, and the recapitulation of these features in an age-dependent, progressive model of PD.

1.9 Hypothesis and aims

The aim of this thesis was to identify key cellular changes in the *ex vivo* olfactory bulb from PD patients and investigate the presence of these findings in an age-dependent mouse model of PD. Beyond this, it was aimed to pharmacologically modulate key cellular pathways that were awry in the animal model, and test the effect on the olfactory system to understand which of the cellular changes are fundamental to the olfactory phenotype. Finally, it was aimed to test the clinical utility of hyposmia to identify prodromal Parkinson's disease.

Chapter 1. This chapter provides a literature review of hyposmia in PD

Chapter 2. This chapter provides a detailed description of materials and methods used in this thesis

Chapter 3. This chapter aimed to use PET imaging in patients with multiple preclinical PD symptoms to investigate levels of nigrostriatal VMAT2 positive terminals for neurodegeneration. This chapter includes the publication *'Reduced Striatal Vesicular Monoamine Transporter 2 in REM Sleep Behaviour Disorder: Imaging Prodromal Parkinsonism'* by Beauchamp *et al.* **Scientific Reports**, 2020

Chapter 4. This chapter aimed to characterise post-mortem olfactory bulbs from PD and neurological controls with a focus on the dopaminergic system, known PD-related proteins, and metals

Chapter 5. This chapter aimed to characterise the olfactory capacity of the tau$^{-/-}$ animal model, as well as investigate PD-related cellular changes in olfactory bulb and midbrain. This chapter includes the publication *'Ablation of tau causes an olfactory deficit in a murine model of Parkinson's disease'* by Beauchamp *et al.* **Acta Neuropathological Communications**, 2018

Chapter 6. This chapter aimed to characterise the dopaminergic pathway, and to test the functional effects of dopaminergic modulation on olfaction in tau$^{-/-}$ and healthy animals

Chapter 7. This chapter aimed to measure metal concentrations, and to test the therapeutic effect of metal modulation on olfactory and motor impairment in the tau$^{-/-}$ mice.

Chapter 8. This chapter aimed to characterise the olfactory capacity of the rTg4510 tau overexpressing mice and test the therapeutic effect of *S*-adenosylmethionine supplementation. This chapter includes the publication *'S-adenosylmethionine rescues cognitive deficits in the rTg4510 animal model by stabilizing protein phosphatase 2A and reducing phosphorylated tau'* by Beauchamp *et al.* **Journal of Alzheimer's disease**, 2020

Chapter 9. This concluding chapter provides a summary of the research, highlights the significance of findings, and details the future research required to translate this work into a clinical setting.

Chapter 2: Materials and methods

2.1 Ethics

Human tissue

Human *post-mortem* tissue was acquired through the New South Wales Brain Bank under the ethics to work on human tissue from University of Melbourne (HREC: 1750801).

Animal research

All experimentation was performed in accordance with the Prevention of Cruelty to Animals Act (2004), under the guidelines of the National Health and Medical Research Council Code of Practice for the Care and Use of Animals for Experimental Purposes in Australia (2013) and approved by The Florey Animal Ethics Committee (AEC number: 15-092 and 19-052). All efforts were made to minimise animal suffering

2.2 Animals

Mice were housed in transparent, individually ventilated cages (IVCs) (29.5 x 16 x 13 cm) under a 12-hour light/dark cycle (lights on at 0700 h). Rodent chow and water were available *ad libitum*. Tau KO ($tau^{-/-}$) or WT ($tau^{+/+}$) mice used in experimentation are initially described by Dawson *et al.*[176] were line bred in house. Mice bred on the Sv129BL/6 background were used for the studies described in this research. All mice were genotyped using a standardised polymerase chain reaction (PCR) assay for DNA (Transnetyx Inc.; USA).

rTg4510 mice kindly provided by Prof. Paul Adlard and A/Prof. Laura Jacobson. Mice were bred in house as previously described[177, 178]. Mice bred on the C57BL/6 background were used for the studies described in this research. All mice were genotyped using a standardised PCR assay for DNA (Transnetyx Inc.; USA).

2.3 Animal behaviour

Odour detection test

The Odour Detection Test (ODT) was adapted from a previously described protocol[179]. Mice were habituated to vehicle canisters for 3 days prior to testing. The test day (day 4) comprised of three 5-minute trials (1 hour inter-trial interval (ITI)) performed in the home cage in which the mice were exposed to two visually identical canisters; one vehicle (400 µL, MilliQ water + 0.1% Tween20) and one novel odour canister of either 0 (vehicle), 1:10^6, or 1:10^4 dilutions (400 µL, MilliQ water + 0.1% Tween20 + orange, peppermint, or juniper berry essential oil (In Essence; Aus)) (Figure 2.1). Animals were filmed and videos were manually scored (the scorer was blinded to experimental conditions) and the percentage of investigation time was calculated based on: *(time spent investigating novel odour canister ÷ time spent investigating both canisters) X 100.* Normal mice will spend more time investigating a novel odour; as such this test determines the concentration at which mice can detect a novel odour by comparing the time spent investigating the two canisters.

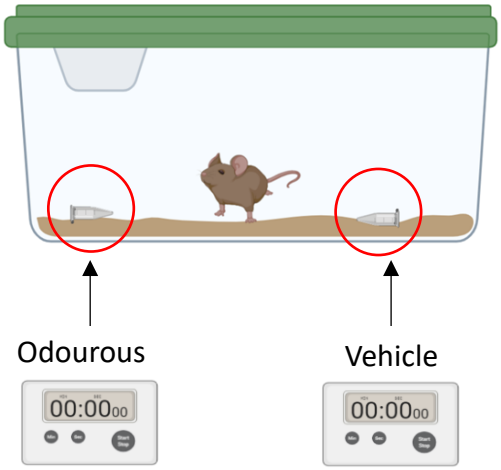

Figure 2.1 The odour detection test. Animals are placed in the home cage with two canisters, one of which contains a novel odour, and exploration time is measured.

Locomotor Activity Test

The locomotor activity test (LMA) was used to assess exploratory behavior and locomotor habituation. Mice were placed in a locomotor cell (27.3 x 27.3 x 20 cm) for a total of 1 hour. Distance traveled, velocity, and thigmotaxis was monitored by infrared beams and the data were analysed using Activity Monitor Version 6.02 software (Med Associates, Inc.; USA).

Rotarod

Motor coordination and ataxia were assessed in mice via the rotarod test[180]. Mice were trained on the rotarod (Panlab; Spain) 25 hours prior to testing according to Table 2.1. During training, if the mouse fell off the rotarod it was placed back on the rod until 2 minutes had lapsed. On the test day the rotarod was set to accelerating mode, increasing from 4-40 rotations per minute (rpm) over a 5-minute trial. Mice were allowed three atempts and the average time of latency to fall was recorded.

Table 2.1 Rotarod protocol

Protocol	***Mode; speed***	***Duration***
Training 1	Set speed; 4 rpm	2 minutes
Training 2	Set speed; 4 rpm	2 minutes
Training 3	Accelerating; 4-40 rpm	2 minutes
Test (3 attempts)	Accelerating; 4-40 rpm	Max 5 minutes

Pole Test

Motor coordination was assessed using the pole test[181]. Mice were loosely scruffed and placed vertically (nose up) on a pole (50 cm) that was wrapped in a self-adhesive bandage (NexCare; Aus) (Figure 2.2). There was a squash ball placed on top of the pole to prevent animals climbing and sitting on the top. Two lines were drawn on the pole to delineate a 40 cm segment of pole. One day prior to testing, animals were habituated to the pole and successfully completed five trials. On the day of testing, animals were allowed three consecutive attempts which were recorded. Time to turn (animal to complete a 180° rotation) and time to descend (time from beginning of turn to crossing the distal line) was recorded.

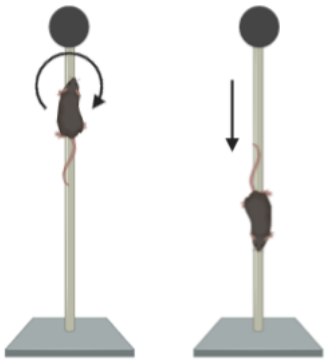

Figure 2.2 The pole test. Time to turn (T_{TURN}) and time to descend (T_{TOTAL}) are measured to assess motor coordination in mice.

Y-maze

Spatial recognition memory was investigated in a 2-trial Y-maze task. Three identical arms (starting arm, familiar arm, novel arm) of the Y-maze (arms: 59.5 (L) x 7.5 (W) x 15.5 (H) cm; radially arranged) were randomly assigned a visual cue mounted at the distal end of the arm (Figure 2.3). Mice were placed in the Y-shaped maze for 2 trials (1-hour ITI). In the first trial (acquisition) mice were able to explore the start arm and the familiar arm for 10 minutes. For the second trial (retention) mice were able to explore all 3 arms for 5 minutes. Exploratory behavior was recorded by an overhead video and analysed using the TopScan system (CleverSys Inc.; USA). Videos were analysed for the time spent in each arm and the duration of novel arm exploration generated based on: *(time spent in novel arm ÷ 5 minutes) X 100.* Furthermore, relative distance traveled in the individual arms was generated based on: *(distance traveled in X arm ÷ total distance traveled) X 100.* Normal mice will spend more time investigating a novel arm as they will remember having explored the start and

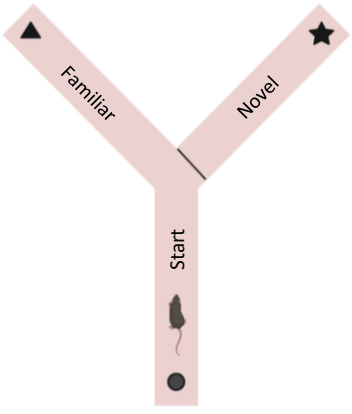

Figure 2.3 The three-arm Y-maze of spatial memory. Exploration time and entry bouts into each arm is measured.

familiar arm previously. An arm entry was defined as the whole body, excluding the tail, entering the arm.

2.4 Transcardial perfusion and tissue collection

At the conclusion of behavioural analysis, animals were terminally anaesthetised using 100 mg/kg intraperitoneal pentobarbitone (Virbac; Aus) injection and transcardially perfused with Dulbecco's phosphate buffered saline (D-PBS) (Gibco; Aus) containing 55.6 mg/L heparin (Sigma Aldrich; Aus) with approximately 3 times their blood volume (7% of body weight). Brains were extracted and micro-dissected into olfactory bulb, caudate putamen, substantia nigra, and cortex. Due to the difficulty of precise microdissection, tissue labelled 'SNpc' in the following studies may have small amounts of neighbouring brain tissue including other sections of the ventral midbrain. Regions were frozen on dry ice and stored at -80°C.

2.5 SDS-PAGE and immunoblot analysis

Samples were thawed on ice and homogenised in radioimmunoprecipitation assay (RIPA) lysis buffer (150 mM NaCl, 1% NP-40, 0.5% deoxycholic acid, 50 mM Tris) with protease and phosphatase inhibitors (Complete Mini Protease Inhibitor Cocktail and PhosSTOP Phosphatase Inhibitor Cocktail, Roche Diagnostic; Aus) and butylated hydroxytoluene (BHT) (buffer volume (µl) determined by 9 X sample weight (mg)) using a probe sonicator (Digital Sonifier, Branson; USA) for 20 seconds. Homogenate was spun at 10000 X *g* at 4°C for 20 minutes and the clarified supernatant collected. The total protein concentrations were determined using the bicinchoninic acid (BCA) assay (Pierce; USA) according to the manufacturer's directions and protein concentrations were normalised in RIPA lysis buffer. Samples were mixed with 4 X sample buffer (0.25 M Tris, 8% SDS, 20% glycerol, 0.4% bromophenol blue) containing 10% 1M dithiothreitol (DTT), boiled for 5 minutes, and centrifuged at 10000 X *g* for 5 minutes. Protein was electrophoresed at 270 V for 25 minutes on 4-20% polyacrylamide gels (BioRad; Aus).

Enhanced chemiluminescence detection

Membranes (0.45 µm nitrocellulose, BioRad; USA) were blocked in tris-buffered saline with 0.05% Tween20 (TBS-T; 6.05 g Tris, 8.76 g NaCl per litre) containing either 5% low-fat milk powder (Diploma; Aus) or bovine serum albumin (BSA) (Sigma Aldrich; Aus) for 1 hour at room temperature (RT). All antibodies were diluted in TBS-T. Primary antibody incubation overnight at 4°C and secondary antibody incubation for 2 hours at RT. Membranes were washed in TBS-T for 21 minutes (3 X 7 minutes) before and after incubation with secondary antibodies. Proteins were detected using enhanced chemiluminescence (ECL) (BioRad; Aus) and visualised with the ChemiDoc (BioRad; USA)

and analysed via densitometry (ImageLab 5.2.1, BioRad; USA). Samples normalised to total protein analysis performed on ChemiDoc.

Fluorescence detection

Membranes were blocked in Blocker™ FL Fluorescent Blocking Buffer (ThermoFischer; Aus) for 1 hour at RT. All antibodies (Table 2.2) were diluted in TBS-T. Membranes were washed in TBS-T for 21 minutes (3 X 7 minutes) before and after incubation with fluorescent secondary antibodies (Licor; Aus). Proteins were visualised with the Licor Odyssey fc system (Licor; Aus) and analysed via signal intensities (ImageStudio 5.2, Licor; Aus). Samples normalised to β-actin.

Table 2.2 Antibody list

Antibody	***Dilution***	***Company***	***Code***
Tyrosine hydroxylase	1:5000	CST	2792S
pSer40 tyrosine hydroxylase	1:1000	AbCam	Ab51206
Synaptophysin	1:5000	CST	46329S
NeuN	1:5000	CST	12943S
α-synuclein	1:5000	BD Biosciences	610786
p62	1:2000	Novus Biologicals	3868
LC3(D11)-XP	1:2000	CST	3868S
β-actin	1:10000	Invitrogen	AM4302
Tau (human)	1:10000	DAKO	A0024
PP2A(A)	1:2000	CST	2041P
PP2A(B)	1:2000	CST	2290P
PP2A(C)	1:2000	CST	2259T

2.6 Inductively coupled plasma mass-spectrometry

Inductively coupled plasma mass-spectrometry (ICP-MS) was performed as previously reported[182], and conducted by Irene Volitakis and Celeste Mawal (FINMH). Briefly, samples were lyophilised and nitric acid (65% Suprapur, Merck; USA) was added for a 6-hour digestion at room temperature. Samples were heated at 90°C for 20 minutes followed by the addition of hydrogen peroxide (30% Aristart, BDH; UAE). Samples were left at room temperature for 30 minutes before heating again for a further 15 minutes at 70°C. The average reduced volume was determined, and the samples were further diluted with 1% HNO_3 diluent. Measurements were made using an Agilent 7700 series ICP-MS instrument under routine multi-element operating conditions using a Helium Reaction Gas Cell. The instrument was calibrated using 0, 5, 10, 50, 100, and 500 ppb of certified multi-element ICP-MS standard calibration solutions (ICP-MS-CAL2-1, ICP-MS-CAL-3, and ICP-MS-CAL-4, Accustandard; USA) for a range of elements. Certified internal standard solutions containing 20 ppb of Yttrium (Y89) as an internal control (ICP-MS-IS-MIX1-1, Accustandard; USA) was used.

2.7 High pressure liquid chromatography with electrochemical detection

High pressure liquid chromatography with electrochemical detection (HPLC-ED) was performed by Cameron Hunt in the Parish Lab (FINMH). Dopamine, 3,4-Dihydroxyphenylacetic acid (DOPAC) and homovanillic acid (HVA) levels were measured as previously described[183]. Human and mouse olfactory bulbs were dissected, weighed, and placed in 200 µl 0.4 M perchloric acid ($HClO_4$) containing 0.05% sodium metabisulphate ($Na_2S_2O_5$) and 0.01% disodium EDTA. The tissue was sonicated, centrifuged at 10,500 *g* for 10 minutes and filtered through MiniSpin filters (POCD Scientific; Aus) for 3 minutes at 10,000 rpm before being injected into the HPLC.

2.8 Enzyme-linked immunosorbent assays

S-adenosylmethionine

S-adenosylmethionine (SAMe) levels were analysed using a commercially available ELISA combo kit (Cell Biolabs Inc.; USA) according to manufacturer's instructions. Briefly, the provided 96-well Protein Binding Plate was coated with 100 µl SAMe conjugate at 4°C overnight. The next day, the plate was washed (PBS), and blocked with provided Assay Diluent for 1 hour at RT. Samples were prepared by sonication in PBS, followed by centrifugation at 10,000 *g* for 15 minutes at 4°C. The total protein concentrations were determined using the BCA assay (Pierce; USA) according to the manufacturer's directions and protein concentrations were normalised to 4 µg/µl in PBS. 50 µl of samples and standards were loaded into wells and incubated for 1 hour at RT on an orbital shaker. Plates were washed and 100 µl of secondary antibody HRP-conjugate was loaded into wells and incubated 1 hour at RT on an orbital shaker. Following one final wash 100 µl of Substrate Solution was incubated at RT for 30 minutes. The reaction was stopped with 100 µl of Stop Solution and the absorbance was read on a spectrophotometer at 450 nm.

Phosphorylated tau

AT8 pTau protein levels were analysed using an AT8 ELISA kit developed in-house by Celeste Mawal and Krista Dent (FINMH). Tissue was sonicated in D-PBS with phosphatase (Roche Diagnostics; Aus) and protease inhibitors (Roche Diagnostics; Aus). Protein concentrations were quantified with the BCA Protein Assay Kit (Pierce, USA). An ELISA plate (Thermofisher; Aus) was precoated with carbonate coating buffer (made using carbonate-buicarbonate buffer capsules, Sigma Aldrich; Aus) containing 1:1000 anti-human Tau polyclonal antibody (Dako; USA) overnight at 4˚C. The next day the plate was blocked with SuperBlockTM T20 (TBS) blocking buffer (ThermoFisher; Aus). The plate was washed in TBS-T and allowed to air dry (2 hours, RT), then 1.5 µg of sample was added to each well for incubation (2 hours, RT). The plate was then washed thoroughly and incubated in 1:2000 AT8 antibody (ThermoFisher; Aus) (2 hours, RT). Finally, samples were incubated in 1:500 secondary antibody (1 hour, RT) and detected using the QuantaBluTM Fluorogenic Peroxidase Substrate Kit (ThermoFisher;

Aus). Excitation was induced at 325nm and emission was detected at 420nm immediately following the addition of stop solution using a microplate reader.

2.9 Protein phosphatase 2 activity assay

PP2A activity was measure using a commercially available PP2A Immunoprecipitation Phosphatase Assay Kit (Millipore; USA). Briefly, tissue was homogenised in 20 mM Imidazole-HCl, 2 mM EDTA, 2 mM EGTA, pH 7.0 with 10 µg/mL aprotinin leupeptin, 10 µg/mL pepstatin, 1 mM benzamidine, and 1 mM PMSF. Following sonication, homogenate was centrifuged at 2,000 *g* for 5 minutes at 4°C. The total protein concentrations were determined using the BCA assay (Pierce; USA) according to the manufacturer's directions and protein concentrations were normalised to 1 µg/µl in homogenisation buffer. 4 µg of anti-PP2A C subunit antibody, 25 µL of Protein A agarose slurry were added to 20 µL of normalised sample. Mixture was brought to 500 µL with pNNP Ser/Thr Assay Buffer and incubated for 1 hour at 4°C with constant rocking. Beads washed in TBS (3 times), and in pNNP Ser/Thr Assay Buffer once. 60 µL of 750 µM phosphopeptide and 20 µL pNNP Ser/Thr Assay Buffer added and incubated fir 10 minutes at 30°C shaking. After a short centrifugation, 25 µL of sample loaded into ½ volume microtiter plate with 100 µL Malachite Green Phosphate Detection Solution. Colour developed for 15 minutes at RT and absorbance read on a spectrophotometer at 65nM.

2.10 Real time quantitative reverse transcription polymerase chain reaction analysis of gene expression

RNA was isolated using the RNeasy purification kit (Qiagen; USA) according to manufacturer's instructions. The concentration of RNA was determined by spectrophotometry (Nanodrop 100, Thermo Scientific). cDNA was synthesised from 1µg of RNA using a High-Capacity RNA-to-cDNA Reverse Transcription Kit (Applied Biosystems; USA) as per manufactures guidelines. Predesigned TaqMan Gene Expression Assays (Applied Biosystems; USA) were used to determine the gene expression of TH. Each sample was analysed in triplicate with GAPDH used as an endogenous control gene for normalisation across samples. Data were analysed using the ΔΔCT method via QuantStudio™ Real-Time PCR Software (ThermoScientific; Aus). No-template control (no cDNA), no enzyme control (no reverse transcriptase) and water were used as controls for the qPCR experiment.

2.11 Parkinson's progressive markers initiative

The PPMI is an observational multicentre study including clinical assessments of olfaction using the University of Pennsylvania Smell Identification Test (UPSIT) (Sensonics; USA), anxiety using the State-Trait Anxiety Inventory (STAI), and rapid eye movement behaviour sleep disorder (RBD) assessment using the MAYO sleep questionnaire. Participating PPMI sites received approval from an ethical standards committee and written informed consent was obtained from all participants.

2.12 Statistical analysis

For all statistical analyses the software package GraphPad Prism (version 6.05 for Windows) was used. Data represented by bar charts are presented as mean ± standard error of the mean (SEM), and data presented by box and whisker plots display whiskers representing min-max. Detail including statistical test, replicate number, experimental repeats, and significance are reported in the Figure Legends. ANOVA p values reported are from post-hoc comparisons generated only when ANOVA terms were significant. One sample t-tests were also performed for ODT to determine if the animals could detect odours at specified concentrations (independent of genotype), as evidenced by spending significantly more than 50% of the investigation time with an odourous canister.

Chapter 3: Reduced Striatal Vesicular Monoamine Transporter 2 in REM Sleep Behavior Disorder: Imaging Prodromal Parkinsonism

Leah C. Beauchamp[1,2], MC-BMEDSC; Victor L. Villemagne[3,4], MD; David I. Finkelstein[1], PhD; Vincent Doré[3,5], PhD, Ashley I. Bush[1,6], MD, PhD; *Kevin J. Barnham[1,2,6], PhD; Christopher C. Rowe[3,4,6], MD

[1]The Florey Institute of Neuroscience and Mental Health, The University of Melbourne, Melbourne, Australia
[2]The Department of Pharmacology and Therapeutics, The University of Melbourne, Melbourne, Australia
[3]Department of Molecular Imaging & Therapy, Austin Health, Melbourne, Australia
[4]Department of Medicine, The University of Melbourne, Melbourne, Australia
[5]The Australian e-Health Research Centre, CSIRO Health & Biosecurity, Melbourne, Australia
[6]Melbourne Dementia Research Centre, The University of Melbourne, Parkville, Australia

This Chapter includes the published manuscript entitled *Reduced Striatal Vesicular Monoamine Transporter 2 in REM Sleep Behaviour Disorder: Imaging Prodromal Parkinsonism*. **Beauchamp, L**, Villemagne, V, Finkelstein, D, Doré, V, Bush, A, Barnham, K, and Rowe, C. Scientific Reports, 2020.

The candidate was involved in the analysis, and interpretation of the data. The drafting and writing of the first draft and revised manuscripts thereafter were performed by candidate. Overall, the candidate contributed to approximately 60% to the work for this paper.

Acknowledgments

We acknowledge participants and organisers of the PPMI. PPMI is funded by The Michael J. Fox Foundation for Parkinson's Research and funding partners including Abbott, Biogen Idec, F. Hoffman-La Roche Ltd., GE Healthcare, Genentech, Pfizer Inc., Meso Scale Diagnostics and Life Molecular Imaging (formerly Piramal). J.Q.T. is supported, in part, by P50 NS053488 University of Pennsylvania.

3.1 Abstract

Motor deficits in parkinsonism are caused by degeneration of dopaminergic nigral neurons. The success of disease-modifying therapies relies on early detection of the underlying pathological process, leading to early interventions in the disease phenotype. Healthy (n=16), REM sleep behaviour disorder (RBD) (n=14), dementia with Lewy bodies (n=10), and Parkinson's disease (PD) (n=20) participants underwent 18F-AV133 vesicular monoamine transporter type-2 (VMAT2) PET to determine the integrity of the nigrostriatal pathway. Clinical, neurophysiological and neuropsychological testing was conducted to assess parkinsonian symptoms. There was reduced VMAT2 levels in RBD participants in the caudate and putamen, indicating nigrostriatal degeneration. RBD patients also presented with hyposmia and anxiety, non-motor symptoms associated with parkinsonism. 18F-AV133 VMAT2 PET allows identification of underlying nigrostriatal degeneration in RBD patients. These findings align with observations of concurrent non-motor symptoms in PD and RBD participants of the Parkinson's Progression Markers Initiative. Together, these findings suggest that RBD subjects have prodromal parkinsonism supporting the concept of conducting neuroprotective therapeutic trials in RBD-enriched cohorts. Ongoing longitudinal follow-up of these subjects will allow us to determine the time-window of clinical progression.

3.2 Introduction

Parkinson's disease (PD) is associated with a period of latency in which dopaminergic neurodegeneration is occurring, yet no overt signs of parkinsonism are evident. Preservation of nigro-striatal neurons is paramount to delaying the progression of motor impairment. To date, there has been a failure of translation of neuroprotective drugs from preclinical research and there is no approved therapeutic that halt or modify the progression of the disease. Much of this failure can be attributed to an inability to identify at-risk patients in a preclinical/prodromal phase, where neuroprotective agents would be most efficacious. Currently, diagnosis of PD is based on clinical assessment and relies heavily upon the presentation of movement dysfunction. At this stage, it is estimated that there is already an irreversible loss of 50-70% of dopaminergic terminals in the putamen, based on post-mortem studies[106] and *in vivo* neuroimaging of patients in the early stages of unilateral motor impairment[107]. This substantial neurodegeneration occurs *before* clinical diagnosis, significantly narrowing the optimal window for treatment. Hence, there is a critical need to develop preclinical/prodromal markers to identify individuals at-risk that can then be enrolled in early neuroprotective clinical trials.

PD is associated with preclinical non-motor symptoms, including REM sleep behavior disorder (RBD), hyposmia, and anxiety[184]. These symptoms are often reported concurrently and together increase the likelihood of identification of preclinical/prodromal PD[1]. RBD is a form of parasomnia in which people 'act out their dreams' during the normally paralytic stage of REM sleep. RBD is reported in 40-50% of PD patients[117, 118], and a number of long-term studies have reported that 65-90% of RBD patients will go on to develop a neurodegenerative disorder, predominantly PD, but also dementia with Lewy bodies (DLB) and multiple system atrophy[119-121].

Between the extensive neurodegeneration that occurs before the onset of motor symptoms and the high likelihood of progression from RBD to PD, neuroimaging assessment of the presynaptic nigro-striatal pathway in RBD patients may help the early identification of patients that are likely to progress to PD and provide a clinical marker for enrolment into preclinical trials. A number of previous studies have demonstrated striatal dopaminergic neurodegeneration in RBD patients using presynaptic dopamine transporter (DAT) neuroimaging. An early study by Eisensehr et al. using [123I]IPT-single photon emission computerized tomography (SPECT) on 5 patients with chronic RBD demonstrated a reduced DAT density in the putamen[185]. More recently, Kim et al. reported abnormal DAT imaging using [123I]FP-CIT in the putamen of three out of 14 RBD patients[186], and Iranzo et al. demonstrated similar DAT findings in the striatum of 14 out of 43 RBD subjects[187]. These previous finding using DAT SPECT demonstrate a loss of integrity of dopamine circuits in the basal ganglia in RBD patients. Compared to DAT SPECT, VMAT2 PET imaging has improved image quality and quantification[188], as

such, we sought to investigate the dopamine system in RBD patients using the high affinity [18F]AV-133 PET tracer which selectively binds to VMAT2.

3.3 Methods

Participants

Fourteen patients with clinically diagnosed RBD, along with 10 DLB, 20 PD, and 16 healthy controls (HC) were included in the study. Written informed consent was obtained from all participants, and from a legal guardian of the participants with DLB and PD. The RBD group were referred to the study with a clinical RBD diagnosis, which was the only inclusion criteria for RBD subject recruitment. The RBD group were referred to the study with a clinical diagnosis, and the participants' bed partners completed the Informant Mayo Sleep Questionnaire (IMSQ). The core question (Q1) on the IMSQ has a sensitivity of 100% and a specificity of 95% in detecting RBD[189]. Data from the DLB and PD patients has been previously published[190]. Approval for the study was obtained from the Austin Health Research Ethics Committee. With regards to dopaminergic medications, 15 patients with PD were receiving carbidopa-levodopa; two selegiline; two, levodopa and benserazide and one, pramipexole. Three DLB patients were receiving carbidopa-levodopa and two, levodopa and benserazide.

Clinical data

The neurological evaluation of participants included duration of disease and/or symptoms, the Hoehn-Yahr score (H-Y), the motor subscale (Section III) of the Unified Parkinson's Disease Rating Scale ($UPDRS_m$) both on and off medication (medication stopped 24 hours prior to examination, and resumed just before the PET scan). The neuropsychological evaluation included the Mini-Mental State Examination (MMSE), Clinical Dementia Rating scale (CDR), and Hospital Anxiety and Depression Scale (HADS) for all groups. HC and RBD participants underwent Trail Making Test, Grooved Pegboard assessment, Addenbrook's Cognitive Assessment (ACE-R), Sniffin' Sticks *(MediSense, Netherlands)* and participants bed partners completed the Informant Mayo Sleep Questionnaire.

Imaging procedures

^{18}F-(+)Fluropropyldihydrotetrabenazine (^{18}F-AV-133) was synthesized using previously described methods [191]. Each participant underwent a 20-min static acquisition (4x5 minute frames) at 120-140 min after injection of ~250 MBq of [^{18}F]AV-133. The sorted sinograms were reconstructed using a 3D RAMLA algorithm. As described earlier[190], volumes of interest (VOIs) were placed over the standard space MRI over the caudate nucleus, anterior and posterior putamen, midbrain and primary visual cortex by an operator blind to clinical diagnosis. Volumes of interest were then transferred onto the individual [18F]AV-133 PET images

Image analysis

Tissue ratios (R_T) of the caudate, anterior and posterior putamen and the anterior midbrain were generated using the primary visual cortex, a region relatively devoid of monoaminergic terminals, as reference region [192].

Parkinson's Progressive Marker Initiative (PPMI) analysis

The PPMI is an observational multicentre study including clinical assessments of olfaction using the University of Pennsylvania Smell Identification Test (UPSIT), and anxiety using the State-Trait Anxiety Inventory (STAI). For the purposes of the data presented in this paper, only a subset of the entire PPMI cohort were analysed including HC, diagnosed iPD, and participants recruited with prodromal RBD. Participating PPMI sites received approval from an ethical standards committee and written informed consent was obtained from all participants.

Statistical analysis

Statistical comparison of normal data between HC and the three disease groups was performed using a Dunnet test. Non-normal data were analyzed using the Kruskal-Wallis one-way ANOVA. Statistical comparison between HC and RBD groups only was conducted using an unpaired Student's T test. PPMI data were analysed using a Kruskal-Wallis one-way ANOVA, significance refers to a difference to the HC group. Data were corrected for age-differences. Statistical analysis was performed using GraphPad Prism version 8.0.0 for Windows and significance for each analysis was defined as $P<0.05$. Data are presented as mean [SD].

3.4 Results

Patient demographics and clinical data are summarized in Table 3.1. There was a higher proportion of men in all clinical groups compared with HC, and the RBD patients were younger than HC (63.5 [9.9] vs. 72.9 [5.1] years, *P*=0.02). As expected, severe cognitive impairment was present in patients with DLB, as well as motor impairment in the DLB and PD groups compared to HC. There were no differences in dementia, cognitive, or motor scores between HC and RBD patients.

Patients with RBD and DLB had a higher anxiety score than HC (6.9 [3.3] and 7.8 [4.1] vs. 3.4 [2.6], *P*=0.02, respectively). Further motor, cognitive, olfactory, and sleep examinations were conducted in the HC and RBD groups only. There was no difference between HC and RBD patients in cognition (ACE-R and Trail Making Test), or motor function (Grooved Pegboard), but RBD patients demonstrated impaired olfaction on the Sniffin' Sticks (8.2 [2.7] vs. 9.9 [1.5], *P*=0.035). Using an informant-based Mayo sleep questionnaire, *none* of the HC informants responded affirmatively to Q1 (n=16) (Q1: have you ever seen the patient appear to "act out his/her dream" while sleeping?), and *all* of the RBD informants responded affirmatively (n=14). Furthermore, RBD patients had decreased alertness, reflected by a decrease in the general alertness score (7.50 [1.3] vs. 9.33 [1.3], *P*=0.0007, for RBD and HC, respectively) (Table 3.1).

Visual inspection showed lower [^{18}F]AV-133 binding in RBD, DLB, and PD patients (Figure 3.1A). There was a significantly lower R_T in all groups compared to HC in the left caudate nuclei, right caudate nuclei, left anterior putamen, right anterior putamen, left posterior putamen, and right posterior putamen (Figure 3.1B). There was no significant difference in the anterior midbrain between HC and RBD, however, there was a significant reduction of midbrain R_T in the DLB and PD patients. PD patients had significantly lower [^{18}F]AV-133 binding compared to RBD patients in all brain regions. (Table 3.2). There were three RBD participants who had [18F]AV-133 binding within the normal range (HC mean±SD).

The presence of both hyposmia and anxiety in the RBD group from this study is aligned with observations from the large PPMI dataset. The PPMI data, including participants with iPD (n=492, 55.1% female) and RBD (n=37, 14.9% female) were compared with HCs (n=197, 56.0% female). The RBD group was significantly older (70.2±6.4 years) than the iPD and the HC groups (61.7±9.9 years, P<0.0001; 60.8±11.2 years, P<0.0001; respectively). There was hyposmia and increased anxiety in the iPD (UPSIT: 23.57 [8.5], P<0.0001; STAIstate: 33.20 [10.1], P<0.0001; STAItrait: 32.66 [9.5], P<0.0001) and prodromal RBD groups (UPSIT: 18.30 [7.0], P<0.0001; STAIstate: 36.00 [9.3], P<0.0001; STAItriat: 34.67 [9.1], P=0.001) compared to HC (UPSIT: 33.87 [5.1], STAIstate: 28.09 [7.9]; STAItrait: 29.15 [7.5]) (Figure 3.2).

Table 3.1. Patient demographic and clinical data

Mean (SD)

	HC	***RBD***	***DLB***	***PD***
Sample size	16	14	9	20
Demographics				
Age, years	72.9 (5.1)	**63.5 (9.9)***	68.9 (7.9)	67.0 (9.1)
Sex (M/F), no.	9/7	13/1	7/2	18/2
Education, years	14.75 (3.4)	12.08 (4.0)	12.67 (2.6)	14.00 (4.3)
Symptom onset	-	7.6 (4.7)	3.03 (1.9)	6.11 (4.4)
Disease duration	-	-	0.87 (1.9)	4.18 (4.0)
Neurophysiology				
$UPDRS_m$ $score_{ON}$	-	-	**11.7 (5.4)***	**13.9 (7.4)***
$UPDRS_m$ $score_{OFF}$	1.1 (1.1)	1.5 (1.7)	-	**18.1 (9.2)***
$UPDRS_m$ subscale				
Bradykinesia	0	0	**0.9 (0.9)***	**2.1 (0.9)***
Rigitidity	0	0	**1.0 (0.5)***	**1.8 (0.6)***
H-Y $score_{ON}$	-	-	**1.93 (0.9)***	**1.60 (0.06)***
H-Y $score_{OFF}$	0.1 (0.3)	0.2 (0.4)	-	**1.63 (0.6)***
Neuropsychology				
MMSE	29.0 (1.0)	29.3 (1.0)	**24.4 (2.9)***	29.0 (1.2)
CDR	0	0.1 (0.2)	**0.7 (0.4)***	0.2 (0.5)
HADS				
Anxiety	3.4 (2.6)	**6.9 (3.3)***	**7.8 (4.1)***	5.1 (3.3)
Depression	2.3 (2.9)	4.1 (2.3)	**6.0 (3.5)***	**5.1 (2.4)***
ACE-R	91.88 (4.9)	92.07 (5.4)	-	-
Trail Making Test				
Trail A	35.00 (12.8)	32.29 (12.6)	-	-
Trail B	79.44 (27.7)	71.23 (29.0)	-	-
Grooved Pegboard				
Dominant	80.6 (12.5)	83.71 (13.7)	-	-
Non-dominant	95.27 (19.7)	98.93 (30.0)	-	-
Sniffin' Sticks	9.9 (1.5)	**8.2 (2.7)***	-	-
Mayo sleep Questionnaire				
Q1 response (Y/N)	0/16	14/0	-	-
General alertness rating	9.33 (1.3)	**7.50 (1.3)***	-	-

*Significantly different from HC *(P<0.05)*

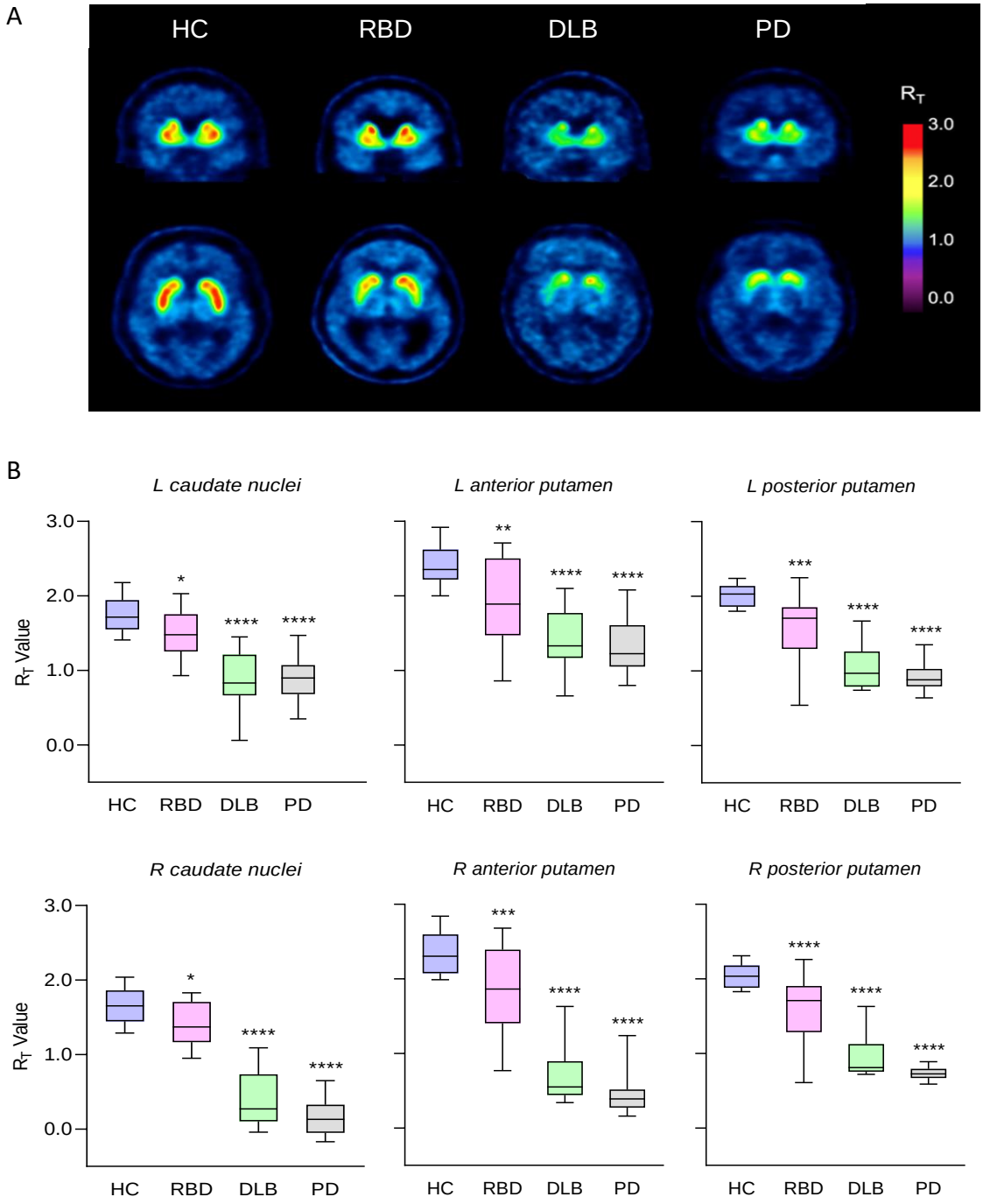

Figure 3.1 RBD patients have reduced [18F]AV-133 binding in the caudate nuclei and putamen. **A)** representative [^{18}F]AV-133 tissue ratio (R_T) positron emission tomography images. **B)** [^{18}F]AV-133 positron emission tomography R_T values from volumes of interest analysis. Box lines represent median and interquartile range, whiskers represent minimum and maximum values. *Significantly different from HC. **P<0.05, **P<0.01, ***P<0.005, ****P<0.0001*.

Table 3.2 Regional R_T Values for [^{18}F]AV-133 PET

	HC	***RBD***	***P (vs. HC)***	***P (vs. PD)***	***DLB***	***P (vs. HC)***	***PD***	***P (vs. HC)***
	Mean (SD)							
L caudate nuclei	**1.76** (0.2)	**1.47** (0.3)	0.01	<0.0001	**0.87** (0.4)	<0.0001	**0.88** (0.3)	<0.0001
R caudate nuclei	**1.66** (0.2)	**1.39** (0.3)	0.01	<0.0001	**0.39** (0.4)	<0.0001	**0.16** (0.2)	<0.0001
L anterior putamen	**2.40** (0.3)	**1.90** (0.6)	0.004	0.0011	**1.39** (0.4)	<0.0001	**1.33** (0.4)	<0.0001
R anterior putamen	**2.34** (0.3)	**1.82** (0.6)	0.005	<0.0001	**0.71** (0.4)	<0.0001	**0.45** (0.3)	<0.0001
L posterior putamen	**2.02** (0.1)	**1.56** (0.5)	0.0006	<0.0001	**1.04** (0.3)	<0.0001	**0.93** (0.2)	<0.0001
R posterior putamen	**2.04** (0.2)	**1.56** (0.5)	0.0006	<0.0001	**0.95** (0.3)	<0.0001	**0.73** (0.1)	<0.0001
Anterior midbrain	**0.74** (0.1)	**0.61** (0.1)	0.12	<0.0001	**0.34** (0.3)	<0.0001	**0.33** (0.2)	<0.0001

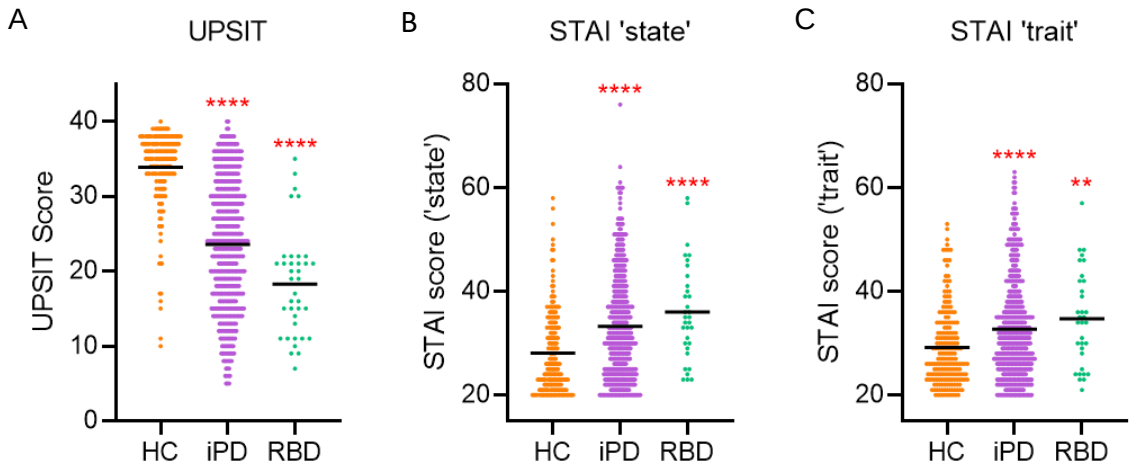

Figure 3.2 RBD participants from the PPMI have concurrent hyposmia and increased anxiety. **A)** olfactory data of HC (n=197), iPD (n=492), and RBD (n=37). **B)** 'state' anxiety of HC (n=200), iPD (493), and RBD (n=33). **C)** 'trait' anxiety data of HC (n=200), iPD (n=493), and RBD (n=33). *Significantly different from HC. ***P<0.01, ****P<0.0001*.

3.4 Discussion

This study demonstrates the utility of ^{18}F-AV133 VMAT2 PET to indicate the loss of integrity of the nigrostriatal pathway in the striatum of RBD patients in the absence of a classical Parkinson's motor phenotype. All of the RBD participants held a clinical diagnosis of RBD plus had a positive response to

the core Q1 on the Mayo Sleep Questionnaire, which has a sensitivity of 100% and a specificity of 95% in detecting RBD [189]. Furthermore, these patients have anxiety and olfactory deficits, which are recognized symptoms associated with PD [184]. It has been previously shown that there is more severe degeneration in the posterior putamen, followed by the anterior putamen and the caudate nucleus in PD [190], and this pattern is observed in the RBD patients reported here. Lower VMAT2 levels in the striatum is concordant with findings from a smaller previous study using [^{11}C]dihydrotetrabenazine [193], and these findings recapitulate reduced presynaptic dopamine transporter (DAT) levels using single-photon emission computed tomography in RBD populations [194]. The advantage of assessing VMAT2 over DAT is that while both reflect nigrostriatal degeneration, VMAT2 is less susceptible than DAT to pharmacological challenges and compensatory changes associated with the loss of dopaminergic neurons [195].

This study demonstrates the concurrence of three prevalent non-motor symptoms with clear reduced VMAT2 levels in disease-associated brain regions, suggesting an increased likelihood that these patients have preclinical/prodromal PD. To confirm the concurrence of non-motor symptoms was not an artifact of this study, we analysed olfactory and anxiety scores in the large PPMI dataset and confirmed the presence of anxiety and hyposmia in both iPD and prodromal RBD groups.

Attempts at developing disease-modifying therapies have ended in failure, attributable to the substantial loss of axons/synapses at the time of clinical diagnosis. Testing protective treatments where advanced neuronal loss has already occurred dooms these approaches to failure. Ideal subjects are those where nigrostriatal degeneration has begun but not progressed to the point of irreversible damage and profound motor impairments (prodromal PD). Well characterized RBD patients represent ideal candidates for recruitment into clinical trials for neuroprotective/disease-modifying drugs due to early nigrostriatal neurodegeneration and their increased likelihood of developing clinical PD. Our results suggest that these RBD subjects have prodromal PD and support the concept that trials of neuroprotective treatments need to be tested in RBD-enriched cohorts.

The main limitations of the present study are the relatively small number of participants and the lack of polysomnography to confirm the extent of RBD. It is also important to note that [^{18}F]AV-133 VMAT2 PET may not be reflective of the true extent of nigro-striatal degeneration, as mechanisms such as sprouting of terminals may be compensating for the progressive neuronal/terminal loss [196, 197]. ^{18}F-AV133 VMAT2 PET allows identification of underlying nigrostriatal degeneration in RBD patients. Ongoing longitudinal follow-up of these subjects will allow to determine the time-window of clinical progression.

Chapter 4: Characterisation of the human Parkinson's disease post-mortem olfactory bulb: a failure of dopamine breakdown and metal homeostasis

4.1 Abstract

Hyposmia is the most prevalent non-motor symptom in Parkinson's disease, occurring up to a decade before motor impairment. Understanding the pathobiology of the olfactory dysfunction may provide insight into the mechanisms of Parkinson's disease that lead to the inevitable neurodegeneration of midbrain dopamine neurons. Furthermore, understanding hyposmia may strengthen and inform future diagnostic tools and provide a novel source for biomarker research. To date, there have been few characterisations of the Parkinson's disease olfactory bulb, resulting in a poor understanding of bulbar changes. This study sought to investigate Parkinson's disease-related molecular changes in the olfactory system, although this is limited in *post-mortem* tissue due to it being from subjects with end-stage disease. Due to the early and persistent nature of hyposmia, it was hypothesised that unlike the midbrain, dopamine reduction does not underlie functional olfactory deficits. It was demonstrated that there is an increase in α-synuclein, DJ1, and p62 in the bulbs, consistent with existing knowledge about midbrain pathobiology. Interestingly, there was a reduction of catechol-*O*-methyltransferase mediated breakdown of dopamine to homovanillic acid, which may reflect altered dynamics of dopamine in the synapse. Finally, an accumulation of iron, zinc, sodium, and lead was demonstrated in the bulbs, implicating metal dishomeostasis in this brain region in Parkinson's disease. Whilst findings from this *post-mortem* analysis do not elucidate early disease mechanisms *per se*, they provide a blueprint to be modeled and followed up *in vivo*. Understanding the functional effect of reduced dopamine breakdown and metal dishomeostasis will help to further understand the role these changes play, if any, in functional olfactory deficits in Parkinson's disease.

4.2 Introduction

Parkinson's disease (PD) is the fastest growing neurological disorder in the world, predicted to affect 12 million people globally by 2040[198]. Although much of this predicted increase in prevalence is due to a global ageing population, there is also indication that environmental toxin exposure and living in an increasingly industrialised society is having long-term impacts on prevalence[199]. Currently, outcomes for patients are poor – there are no disease-modifying therapies, symptomatic treatments are not efficacious for the duration of the disease, and diagnosis is sub-par[108, 200]. The field relies on the motor impairments in PD as the sole means of diagnosis, and unfortunately it is now clear that overt motor impairments are reflective of advanced neurodegeneration[52, 107]. Dopaminergic neurodegeneration and aggregated α-synuclein (α-syn) are the hallmark features of disease, however they represent the end stage of what is likely a long pathological process[201]. It is crucial to understand the mechanisms that lead to these features in order to intervene in the disease process. While the focus on the underlying pathophysiology within the midbrain has been fruitful for scientific discoveries, these findings have not translated to better therapies. It is time to reassess the approach to PD research, and one potential avenue of discovery is through investigation of non-motor symptoms, many of which occur years *before* motor impairments and are reflective of a changing brain[6].

Findings from Chapter 3 demonstrate that it is possible to identify probable early PD patients in a research setting using non-motor symptoms. In order to develop more sensitive diagnostic tools and translate these findings to the clinic, it is imperative there is further research into the underlying biology driving these non-motor symptoms. A decline in the sense of smell (hyposmia) is the most prevalent non-motor symptom of PD, estimated to affect more than 90% of people, occurring as many as ten years before the onset of motor impairment[202, 203]. While the cause of this hyposmia is unknown, the olfactory bulbs (OBs) have been an area of interest for some time due to the unique nature of the olfactory receptor neurons and the proposed "dual-hit hypothesis"[204]. The bipolar olfactory receptor neurons project directly down from the brain, through the cribriform plate and into the nasal epithelium. The nature of these projections means the neurons are not protected by the blood-brain barrier, and they are exposed to the external environment, therefore vulnerable to environmental insults[205]. The "dual-hit hypothesis" proposes that a neurotropic pathogen enters the brain through the nasal epithelium, where it is able to trigger PD-pathology[204]. This theory is supported by reports from Braak *et al.* who suggest the OB is the first region of the brain to accumulate α-syn[206]. It is not known whether the aggregated α-syn is causing dysfunction, or if it is a feature that reflects poor neuronal health driven by other mechanisms. Regardless, the presence of PD-related pathology in this

brain region, as well as functional olfactory deficits, make it a region worthy of investigation in the quest to understand the disease process.

Dopamine plays a crucial role in olfaction, and the dopamine-mediated glomeruli are the first transmission relay point in the consciousness of smell[207, 208]. Dopamine is the inhibitory neurotransmitter of the glomerular layer, and unlike the midbrain dopaminergic degeneration is unlikely to underlie hyposmia, as it is not influenced by dopamine replacement therapy[152]. There are known pathophysiologies that occur in the midbrain and are thought to promote an oxidative stress environment and subsequent dopaminergic neurodegeneration – including disrupted protein clearance and metal dishomeostasis, so it is of interest to investigate these mechanisms in the olfactory system.

One can foresee many benefits to understanding the pathobiology of the OBs in PD. Firstly, it could inform future diagnostics and help to address the known mis-diagnosis rate in PD. Secondly, it may assist in biomarker development which will help in diagnostics and drug efficacy readouts. Thirdly, it will help to ascertain face validity of proposed animal models of early, non-motor PD and finally it may help to understand the mechanisms and origins of disease, specifically the role of environmental exposure. As such, this study resolved to test the hypothesis that unlike the midbrain, there is an underlying pathobiology in the olfactory system that is not due to a loss of dopamine. The first aim of this work was to analyse common proteins associated with PD pathophysiology - including mitochondria, autophagy, and α-syn. Secondly, it aimed to measure key components of dopamine synthesis and metabolism, followed by an analysis of metal levels.

4.3 Methods

Post-mortem tissue

Both olfactory bulbs (OBs) were collected from ten neuropathologically confirmed Parkinson's disease (PD) and ten neurological controls (NC) and tissue was acquired through the New South Wales Brain Bank under the ethics to work on human tissue from University of Melbourne (HREC: 1750801). One bulb was snap frozen and stored at -80°C, and the contralateral bulb was formalin fixed. For the following study, only data generated on the frozen tissue is presented as the immunohistochemical studies on the formalin fixed tissue is still ongoing (delayed due to COVID-19). Tissue information is presented in table 4.1.

Tissue analysis

Details of tissue analysis, including SDS page and immunoblots, high-pressure liquid chromatography with electrochemical detection (HPLC-ED), enzyme-linked immunosorbent assays (ELISA; catechol-O-

methyltransferase, *S*-adenosylmethionine, and *S*-adenosylhomocysteine), and inductively coupled plasma mass spectrometry (ICP-MS) were all performed according to protocols laid out in Chapter 2.

Table 4.1 Demographics of olfactory bulb tissue donors

Group	*Age*	*Sex*	*PMD (hours)*	*CoD*	*DD (years)*	*Tissue pH*
PD	84	M	5	Cholangiocarcinoma	12	6.4
	82	M	19	Cardiorespiratory failure	22	6.4
	81	F	29	Cardiorespiratory failure	22	6.4
	71	M	25	Hypertensive heart disease	15	6.5
	82	F	9	Pneumonia	8	6.1
	92	M	46	Cardiorespiratory failure	8	6.1
	93	F	9	Cardiorespiratory failure	32	6.1
	78	M	26	Cardiorespiratory failure	18	5.6
	80	F	21	Cardiorespiratory failure	7	6.0
	88	F	21	Cardiorespiratory failure	16	6.3
NC	79	M	8	Pulmonary embolism		7.5
	89	F	23	Metastatic adenocarcinoma		6.0
	88	F	31	Congestive cardiac failure		6.2
	84	M	22	Cardiorespiratory failure		5.8
	84	M	36	Severe pulmonary hypertension		6.4
	80	F	29	Cardiorespiratory failure		6.3
	73	M	39	Cardiorespiratory failure		6.3
	88	M	9	Cardiorespiratory failure		6.4
	85	F	10	Cardiorespiratory failure		6.6
	86	F	4	Cardiorespiratory failure		6.4

Abbreviations: CoD, cause of death; DD, disease duration; F, female; NC, neurological control; M, male; PD, Parkinson's disease; PMD, post-mortem delay.

Statistical Analysis

For all statistical analyses, the software package GraphPad Prism (version 6.05 for Windows) was used. Data are presented as mean ± standard error of the mean (SEM). Detail including statistical test, replicate number, experimental repeats, and significance are reported in Figure Legends. For all analyses, $p<0.05$ was considered statistically significant.

4.4 Results

Indication of protein accumulation, autophagy deficits, and an oxidative stress environment in the olfactory bulbs from Parkinson's disease patients

In order to ascertain if there were protein alterations in the olfactory bulb (OB) that align with the previously reported pathobiology of the midbrain in Parkinson's disease (PD), an analysis of protein expression was conducted on human *post-mortem* tissue. There was no difference in the average age or *post-mortem* delay of PD subjects (83.1±2.1 years, 21.0±3.8 hours; respectively) compared to NC (83.6±1.6 years, 21.1±4.0 hours; respectively). α-synuclein (α-syn), p62, and DJ1 are proteins associated with Lewy pathology, autophagy, and mitochondrial dysfunction respectively. There was an increase of 38.9% in the expression of α-syn (*P*=0.048; Figure 4.1A and B). While the expression

levels of p62 did not reach significance (*P*=0.07; Figure 4.1A and C) the mean expression level was 27.1% higher in PD cases and a post-hoc analysis suggests that increasing the sample size to n=13 in both groups would be required to detect and effect size of 25% or greater. Finally, there was a 136.4% increase in DJ1 (*P*=0.0001; Figure 4.1A and D) in PD OB tissue relative to NC.

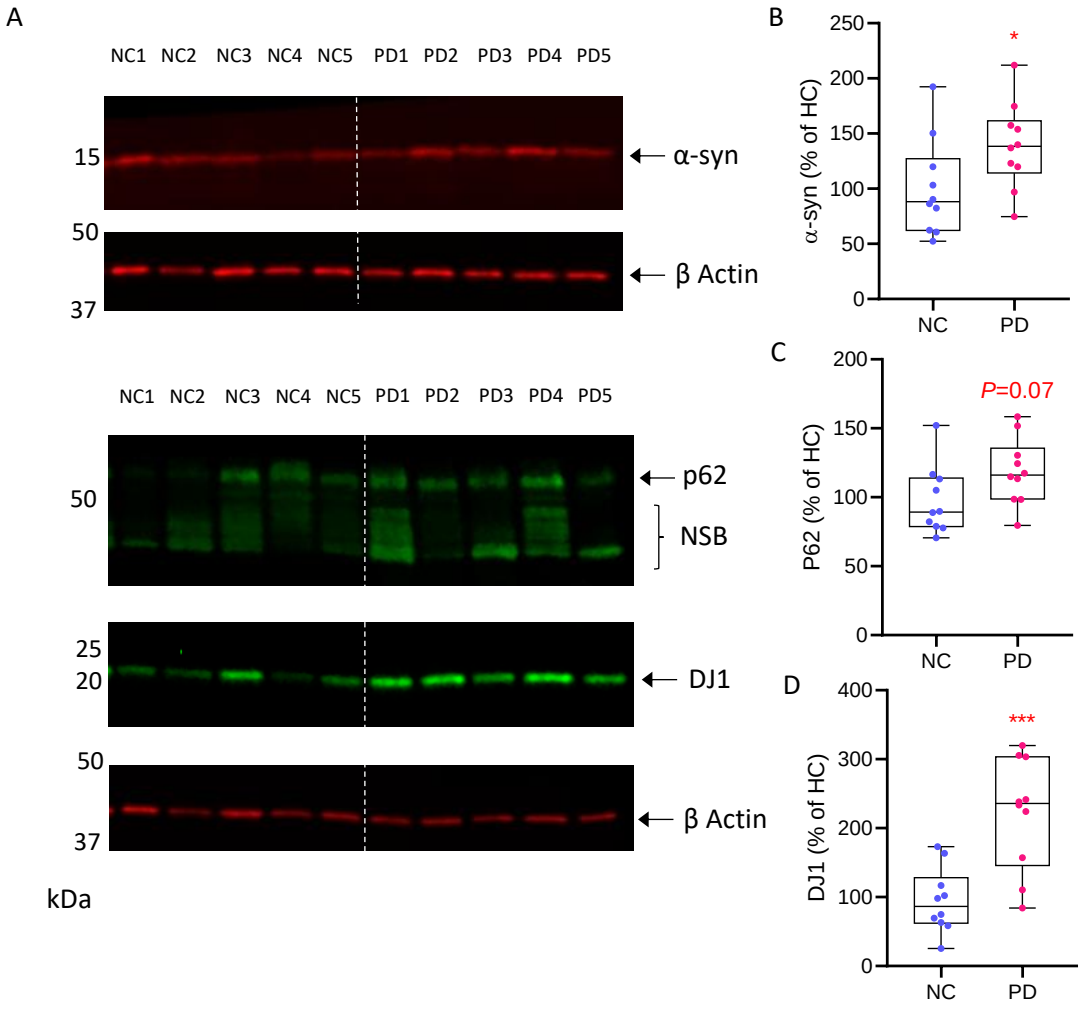

Figure 4.1 Increased expression of Parkinson's disease-related proteins in the human olfactory bulbs. **A)** Representative western blots of olfactory bulb homogenate from neurological control (n=10) and PD (n=10) probed for α-synuclein, p62, and DJ1. **B)** Quantification of western blot fluorescence presented as % of α-syn relative to HC. **C)** Quantification of western blot fluorescence presented as % of p62 relative to HC, NSB: non-specific bands. **D)** Quantification of western blot fluorescence presented as % of DJ1 relative to NC. Samples for western blots normalised to fluorescence of housekeeping protein β-actin, then to HC average. Western blot analysed by unpaired two-sided t-test from 3 independent repeats. **P*<0.05, ****P*<0.001

Reduction of catechol-O-methyltransferase activity in the olfactory bulbs from Parkinson's disease subjects

Due to the prominence of dopamine degeneration in PD and the importance of dopamine in odour signalling processing, it was then of interest to investigate potential alterations in dopamine synthesis and metabolism. Analysis of the dopamine synthesis pathway demonstrated a significant increase in the expression of the rate-limiting enzyme in dopamine synthesis, tyrosine hydroxylase (TH), in the OBs from PD subjects (*P*=0.0001; Figure 4.2A and B). TH is activated when phosphorylated at the Serine 31 residue (pTH). Despite the increase in TH, there was no significant difference in the level of activated TH, represented by the expression of pTH (Figure 4.2A and C). These changes resulted in a significant reduction in the ratio of pTH to TH in the PD bulbs relative to NC (*P*=0.002; Figure 4.2D).

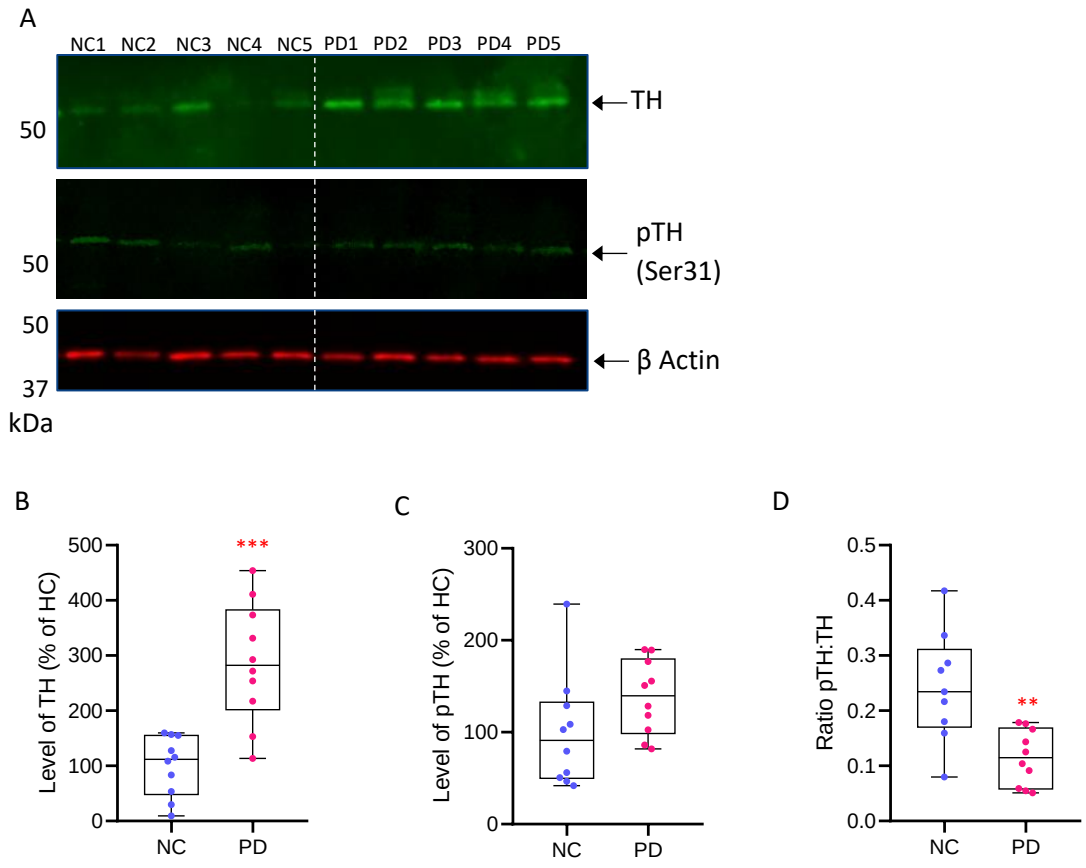

Figure 4.2 Increased tyrosine hydroxylase in Parkinson's disease olfactory bulbs. **A)** Representative western blots of olfactory bulb homogenate from neurological control (n=10) and PD (n=10) probed for tyrosine hydroxylase and phosphoSerine 31 tyrosine hydroxylase. **B)** Quantification of western blot fluorescence presented as % of TH relative to HC. **C)** Quantification of western blot fluorescence presented as % pTH relative to NC. **D)** Ratio of pTH to TH densitometry. Individual homogenate for western blots normalised to fluorescence of housekeeping protein β-actin, then to NC average. Western blot analysed by unpaired two-sided t-test from 3 independent repeats. ***P*<0.01, ****P*<0.001.

Increased TH suggests alterations in the dopamine synthesis pathway in the OB tissue in PD. As such, it was then of interest to analyse the metabolism of dopamine. In line with there being no change in the expression of pTH, there was no significant increase in the concentration of dopamine in the tissue in PD as determined by high-pressure liquid chromatography (HPLC) (Figure 4.3A). Looking at the metabolites of dopamine, there was no change in the concentration of 3,4-Dihydroxyphenylacetic acid (DOPAC) (Figure 4.3B), however there was a significant reduction in the level of homovanillic acid (HVA) in PD relative to NC, suggesting an impairment in catechol-*O*-methyltransferase (COMT)-mediated breakdown of dopamine in PD (*P*=0.01; Figure 4.3C).

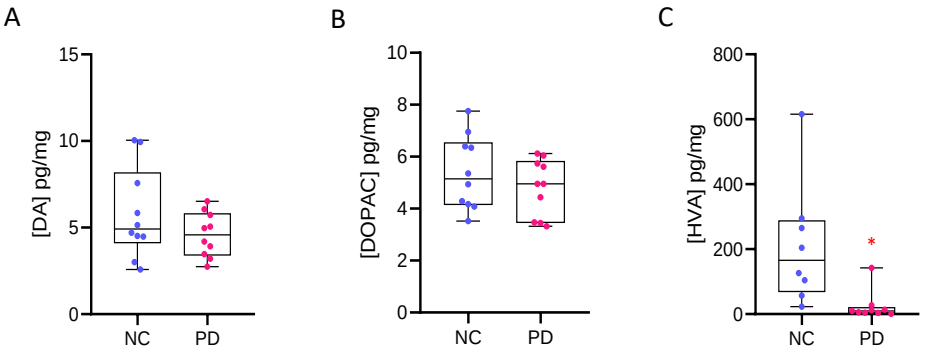

Figure 4.3 Decreased homovanillic acid in Parkinson's disease olfactory bulbs. Concentration of **A)** dopamine, **B)** DOPAC, and **C)** HVA in HC (n=10) and PD (n=10) olfactory bulb tissue, determined by HPLC-ED. Analysed by unpaired Students' T test. **P*<0.05.

The primary mechanism of dopamine breakdown to HVA is through COMT, which is an enzyme that requires three binding events: 1) *S*-adenosylmethionine (SAMe), 2) magnesium (Mg), and 3) catechol (dopamine or DOPAC); we therefore investigated these three events in the OBs. Analysing COMT and its co-factors show that there is a significant increase in the protein expression of COMT (*P*=0.02; Figure 3.4A), a significant decrease in SAMe (*P*=0.0009; Figure 3.4B), and a significant increase in Mg (*P*=0.03; Figure 3.4C) in PD relative to NC tissue. The increase in COMT and Mg in PD may reflect a compensatory mechanism due to the reduction in COMT activity.

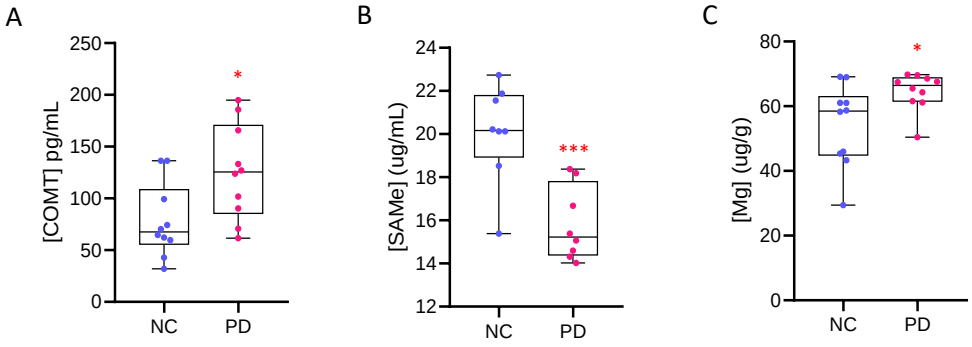

Figure 4.4 Alterations of catechol-O-methyltransferase in Parkinson's disease olfactory bulbs. **A)** concentration of catechol-*O*-methyltransferase **B)** concentration of *S*-adenosylmethionine **C)** level of magnesium in HC (n=10) and PD (n=10) olfactory bulb tissue. Analysed by unpaired Students' T test. **P*<0.05, ****P*<0.001.

Metal dyshomeostasis in the olfactory bulbs from Parkinson's disease patients

Another prominent feature of PD pathobiology in the midbrain is the accumulation of iron (Fe), and the dyshomeostasis of metals. As such, this study went on to analyse metal levels in the *post-mortem* OB tissue. Inductively coupled plasma mass spectrometry (ICP-MS) analysis demonstrated a significant increase in sodium (Na) (↑31.5%, *P*=0.007), zinc (Zn) (↑39.0%, *P*=0.04), and lead (Pb) (↑400.0%, *P*=0.0002) (Table 4.2 and Figure 4.5) in PD tissue relative to NC. There was also a 25% increase in Fe in PD however this did not reach significance (↑22.8%, *P*=0.07).

Table 4.2 Metal analysis of Parkinson's disease olfactory bulbs

Metal	***NC***	***PD***	***P***	***Metal***	***NC***	***PD***	***P***
B	0.16±0.02	0.13±0.02	0.37	Co	0.002±0.0005	0.002±0.001	0.70
Na	**1675±142.5**	**2202±88.5**	**0.007**	Ni	0.03±0.007	0.02±0.002	0.20
Mg	54.12±4.0	64.3±2.0	0.04	Cu	1.36±0.2	1.49±0.3	0.73
Al	23.43±6.3	19.33±5.6	0.64	**Zn**	**7.41±0.6**	**10.3±1.2**	**0.04**
P	1132±94.7	1243±63.5	0.35	Se	0.14±0.01	0.1±0.02	0.08
K	2090±550.2	1174±75.6	0.14	Rb	1.0±0.14	1.04±0.1	0.83
Ca	232.7±44.3	361.0±109.6	0.28	Sr	0.09±0.01	0.13±0.04	0.30
Ti	0.1±0.01	0.11±0.01	0.55	Cd	0.04±0.01	0.04±0.009	0.89
Cr	0.040.009	0.03±0.008	0.63	Ba	0.01±0.003	0.02±0.004	0.64
Mn	0.15±0.02	0.16±0.01	0.35	Pt	0.01±0.002	0.01±0.003	0.91
Fe	**17.89±1.5**	**21.96±1.5**	**0.07**	**Pb**	**0.01±0.001**	**0.04±0.005**	**0.0002**

Abbreviations: Al, aluminium; B, boron; Ba, barium; Ca, calcium; Cd, cadmium; Co, cobalt; Cr, chromium; Cu, copper; Fe, iron; K, potassium; Mg, magnesium; Mn, manganese; Na, sodium; NC, neurological control; Ni, nickel; P, phosphorus; Pb, lead; PD, Parkinson's disease; Pt, plutonium; Rb, rubidium; Se, selenium; Sr, strontium; Ti, titanium; Zn, zinc.

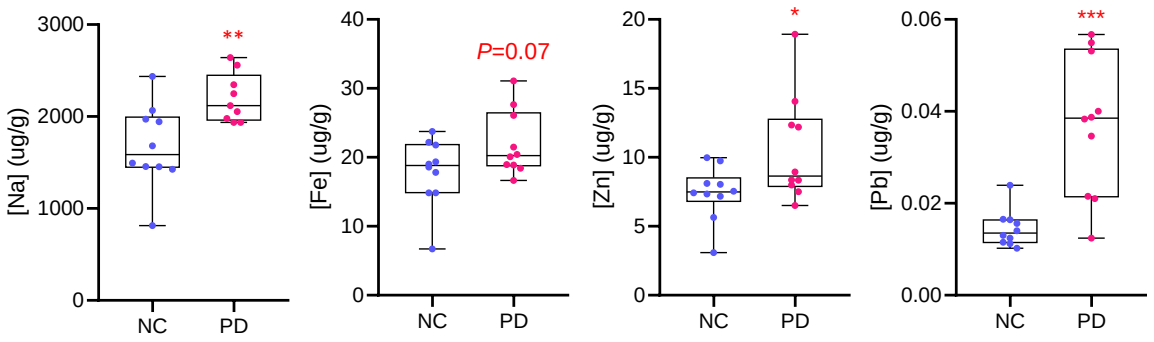

Figure 4.5 Accumulation of metals in Parkinson's disease olfactory bulbs. Sodium, iron, zinc, and lead. NC (n=10) and PD (n=10) olfactory bulb tissue. Analysed by unpaired Students' T test. **P*<0.05, ***P*<0.01, ****P*<0.001.

4.5 Discussion

Understanding the pathobiology of hyposmia in Parkinson's disease (PD) will help to inform future diagnostic approaches through the development of novel biomarkers of disease. To date, there have been few studies characterising the PD-like pathobiology within the olfactory bulbs (OBs) and understanding how this may relate to a functional decline beyond an analysis of Lewy pathology[155, 156, 161, 209]. As such, this study aimed to characterise within the OB, some of the fundamental PD-related changes that have been observed in other brain regions. Initially, an accumulation of monomeric α-synuclein (α-syn) was observed within the bulbs of PD tissue. It was also demonstrated that there is an increase in DJ1 and p62, which may suggest an environment under oxidative stress and potential impairments in autophagy, respectively. Secondly, the characterisation of dopamine synthesis and breakdown demonstrated a significant increase in the level of non-active tyrosine hydroxylase (TH), and perturbations in catechol-*O*-methyltransferase (COMT)-mediated dopamine breakdown. Finally, this study demonstrated a loss of metal homeostasis highlighted by an accumulation of iron (Fe), sodium (Na), and zinc (Zn), as well as an accumulation of the toxic environmental metal lead (Pb).

PD-related proteins

An increase in the level of α-syn is consistent with previous findings and supports the fact that the OB tissue from this study aligns well with previous characterisations of PD bulbs[159, 160]. The OB is one of the first regions of the brain to accumulate α-syn and is reported to be the most commonly affected region with α-syn pathology in the brain[206]. Furthermore, an aggregated form of α-syn (Lewy pathology) is found throughout the bulb and into the higher bulbar regions (the anterior olfactory nucleus) in which neurodegeneration is reported[160]. Similarly, DJ1 plays a critical role in the mitochondria-related oxidative stress response and increases in DJ1 have been found in the brain and the cerebrospinal fluid (CSF) of PD patients, suggestive of a cellular attempt to mitigate an oxidative environment[210]. *In vivo*, oxidised DJ1 was increased in the OBs of mice treated with the neurotoxin 1-methyl-4-phenyl-1,2,3,6-tetrahydropyridine (MPTP)[211], however this is the first report of DJ1 increases in *post-mortem* PD OBs. Finally, increases in the level of p62 are suggestive of autophagy changes, another key phenomenon linked to PD[212, 213]. Due to limited tissue, levels of insoluble α-syn, oxidative stress (via measurement of oxidised DJ1, lipid peroxidation, and protein nitration) and autophagy (via analysis of microtubule-associated protein 1A/1B-light chain 3 (LC3)) will be further investigated using immunohistochemical methods.

Dopamine metabolism

TH has been previously reported to be increased in the OB of PD patients[155], aligning with findings from this study. In the study by Huisman *et al.* authors demonstrated a 100% increase in the number

of TH-containing neurons in the glomerular layer of PD OBs, and concluded that dopamine overdose may be responsible for the olfactory dysfunction in PD. To date we do not know why TH expression is increased. As the OB is one of the few regions of the adult-mammalian brain that undergoes neurogenesis throughout life, there is debate as to whether this increase is due to an increase in the number of new neurons, or an increase in the protein expression of TH in already integrated neurons.

A compensatory increase in the number of dopamine expressing neurons from the rostral telencephalon may be the result of neuronal death in the substantia nigra pars compacta (SNpc)[214]. A compensatory mechanism has been demonstrated previously in dopaminergic cells of the striatum, which may be analogous with the changes reported here[215, 216]. One other explanation may be an increase in TH mRNA expression, as is seen in the A10 group of dopaminergic cells of the medial and ventral tegmentum in response to the degeneration of nigral dopaminergic neurons[151]. Finally, it is possible that there is a failure of TH turnover and clearance in the OB, which is mediated by ubiquitin-proteasomal system (UPS)– known to be dysfunctional in PD (reviewed in section 1.3). What is driving this increase in TH protein expression requires further investigation, however, regardless of what is causing this increase, the data presented in this study does not support the hypothesis by Huisman *et al.* that it is dopamine overdose causing olfactory deficits, as there is no change in the concentration of dopamine in the tissue.

After dopamine synthesis, it is packaged into vesicles for release as part of neurotransmission. Once it is released into the synaptic cleft, dopamine binds to post-synaptic dopamine receptors (D_2R in the olfactory system), as well as auto-receptors on the pre-synaptic neuron (reviewed in[208]). Due to the reactive nature of dopamine, it is rapidly cleared from the cleft via one of two mechanisms. In the OB, this is predominantly enzymatic breakdown of dopamine by COMT to homovanillic acid (HVA)[217] and the secondary mechanism is through reuptake via the dopamine transporter (DAT) for transmitter recycling. Compared with the striatum, the OB has a higher number of dopaminergic terminals, and contains approximately 50% more COMT per unit of tissue. Furthermore, there is substantially less DAT in the OB compared to the striatum, suggesting that COMT-mediated enzymatic breakdown is the predominant mechanism of dopamine clearance in the bulbs[217].

This study has demonstrated that HVA levels are significantly reduced in the PD tissue, suggesting that COMT-mediated breakdown may be affected. COMT activation occurs via a 3-step binding process, whereby the protein must first bind its co-factor *S*-adenosylmethionine (SAMe), followed by the binding of a magnesium (Mg) ion, then the catechol (dopamine or 3,4-Dihydroxyphenylacetic acid (DOPAC)). These binding events must occur in this order for the enzyme to become active. Interestingly, although the protein expression of COMT and the concentration of Mg is increased in

this tissue, the first co-factor of SAMe is significantly reduced and together with the reduction in HVA suggests that COMT activity is reduced in this tissue. Supportive of this finding are reports that SAMe is decreased in plasma levels in PD patients[218].

As COMT is the primary mechanism of dopamine clearance in the olfactory bulb, reduction in COMT-mediated breakdown would change the dynamics of dopamine clearance, resulting in increased residence time in the synapse with the capability of binding D_2Rs and potentially inducing inhibition of olfactory signals. Interestingly, a dysfunction in the recycling of dopamine, whether it be due to DAT ablation or a reduction in COMT activity, may impair D_2 auto-receptor function, which would increase demand on the periglomerular dopaminergic neurons resulting in increased TH levels[219]. These data are of interest, because they demonstrate that it may be a failure of clearance, as opposed to a dopamine overdose proposed in the literature, that contributes to inhibition of olfaction in PD.

Metals in the OB

Elevated Na and Fe in the PD tissue is in line with a recent paper by Gardner *et al.* who demonstrated a 57% increase in Na, and a 25% increase in Fe in the OB[209], comparable to the 32% increase in Na and the 21% increase in Fe in this study. As both Fe and Na are increased in other neurodegenerative diseases, including Alzheimer's disease[220-222], Huntington's disease[223, 224], and multiple sclerosis[225, 226], it is not known if they are general markers of neurodegeneration, they contribute to functional olfactory deficits, or both. The present study also demonstrated an increase in bulbar Zn, and although there was no bulbar increase in Zn in the Gardner study, they did demonstrate an increase of Zn in the higher up in the anterior olfactory nucleus (AON). The olfactory receptor neurons are a unique feature of the nervous system, in that they are not protected by the blood brain barrier and are susceptible to the uptake of environmental toxins, such as metals[162, 227, 228]. Fe and Zn have been demonstrated to be taken up into the OB following intranasal exposure in rodents[229-231]. A small study has associated the accumulation of Fe in humans with hyposmia[232], and intranasal Zn leads to olfactory deficits in both humans and rodents[233-236]. Na plays a fundamental role in voltage-gated Na channels required for odour perception[237]. The exact mechanisms of these metals in functional deficits and whether metal chelation is a viable strategy to alleviate hyposmia requires further investigation.

The increase in the level of Pb remains one of the more intriguing findings of this study, as Pb does not have a biological role and is therefore representative of an environmental insult. Pb is a ubiquitous heavy metal used in the production of goods, including fuel additives, batteries, and electronics[238]. Human exposure to Pb is through our environment, whether that be trace amounts in food, water, soil, or air; or high doses through occupational exposure[238]. Importantly, exposure to Pb proposes an increased risk of PD development, and there is elevated Pb in the bones of PD patients[239, 240]. The

vulnerability of the OB to the uptake of environmental toxins, including heavy metals such as trace Pb is a risk in all people, however the accumulation of Pb in PD patients as seen in these studies may reflect a failure in the ability to metabolise this insult. Pb is a thiol-binding metal, and it is predominantly detoxified by conjugating to glutathione (GSH) and forming a thioether. Mis-metabolism of GSH has been implicated in PD and the level of GSH is reduced in the SNpc[100, 241]. The correlation between reductions in GSH and Pb accumulation represents a hypothesis worthy of further research.

The OB from PD patients appears to have similar mechanisms to the pathobiology reported in the midbrain, including increased expression of α-syn, DJ1, and p62. Unlike the midbrain, there is no decrease in the level of dopamine, however COMT-mediated dopamine breakdown appears to be reduced. Finally, there is an increase in the biological metals Fe, Zn, and Na, and the heavy metal Pb. These findings suggest that there are alignments in the pathological features found in the midbrain and the OBs, however due to the unique nature of dopaminergic neurons in the olfactory system there is likely a different mechanism that underlies functional deficits. Further experimentation into the midbrain from these subjects would be of benefit to correlate the two brain regions, however this tissue was not able to be obtained. Whilst the findings in post-mortem tissue provide insight into potential mechanisms of dysfunction, it is important to keep in mind that this is tissue from end-stage disease and may not reflect some of the earlier changes occurring in the bulb. Furthermore, these findings do not elucidate mechanisms *per se*, but they provide a blueprint to be further explored *in vivo*. Understanding the functional effect of reduced dopamine breakdown and metal dishomeostasis will help to further understand the role these changes play, if any, in functional olfactory deficits in PD.

Chapter 5: Ablation of tau causes an olfactory deficit in a murine model of Parkinson's disease

Leah C. Beauchamp[1,2], Jacky Chan[1], Lin W. Hung[1], Benjamin S. Padman[3], Laura J. Vella[1], Xiang M. Liu[1], Bradley Coleman[4], Ashley I. Bush[1], Michael Lazarou[3], Andrew F. Hill[4,5], Laura Jacobson[1,2], Kevin J. Barnham[1,2,*]

[1]The Florey Institute of Neuroscience and Mental Health, The University of Melbourne, Parkville, VIC 3010, Australia

[2]The Department of Pharmacology and Therapeutics, The University of Melbourne, Parkville, VIC 3010, Australia

[3]Monash Biomedicine Discovery Institute, Monash University, Clayton, VIC 3800, Australia

[4]The Department of Biochemistry and Molecular Biology, Bio21 Institute, The University of Melbourne, Parkville, VIC 3010, Australia

[5]The Department of Biochemistry and Genetics, La Trobe Institute for Molecular Science, La Trobe University, Bundoora, VIC 3083, Australia

This Chapter includes the published manuscript entitled *Ablation of tau causes an olfactory deficit in a murine model of Parkinson's disease.* **Beauchamp, L**, Chan, J, Hung, L, Padman, B, Vella, L, Liu, X, Coleman, B, Bush, A, Lazarou, M, Hill, A, Jacobson, L, and Barnham, K. Acta Neuropathologica Communications, 2018.

The candidate was involved in the conception and design of the work as well as acquisition, analysis, and interpretation of the data. The drafting and writing of the first draft and revised manuscripts thereafter were performed by candidate. Overall, the candidate contributed to approximately 70% to the work for this paper.

5.1 Abstract

Parkinson's disease is diagnosed upon the presentation of motor symptoms, resulting from substantial degeneration of dopaminergic neurons in the midbrain. Prior to diagnosis, there is a lengthy prodromal stage in which non-motor symptoms, including olfactory deficits (hyposmia), develop. There is limited information about non-motor impairments and there is a need for directed research into these early pathogenic cellular pathways that precede extensive dopaminergic death in the midbrain. The protein tau has been identified as a genetic risk factor in the development of sporadic PD. Tau knockout mice have been reported as an age-dependent model of PD, and this study has demonstrated that they develop motor deficits at 15-months-old. We have shown that at 7-month-old tau knockout mice present with an overt hyposmic phenotype. This olfactory deficit correlates with an accumulation of α-synuclein, as well as autophagic impairment, in the olfactory bulb. This pathological feature becomes apparent in the striatum and substantia nigra of 15-month-old tau knockout mice, suggesting the potential for a spread of disease. Initial primary cell culture experiments have demonstrated that ablation of tau results in the release of α-synuclein enriched exosomes, providing a potential mechanism for disease spread. These alterations in α-synuclein level as well as a marked autophagy impairment in the tau knockout primary cells recapitulate results seen in the animal model. These data implicate a pathological role for tau in early Parkinson's disease.

5.2 Introduction

Parkinson's disease (PD) is a neurodegenerative disease primarily associated with neuronal degeneration of the Substantia Nigra pars compacta (SNpc). The disease results in severe motor deficits, as the degenerating neurons cannot provide sufficient dopamine, a neurotransmitter that helps control movement, to the axonal terminals located in the striatum. It is established that in addition to the overt motor deficits PD is associated with significant non-motor disturbances, including psychiatric symptoms, dementia, rapid eye movement (REM) sleep behaviour disorder, constipation and a reduced ability to smell odours (hyposmia) [242]. Hyposmia occurs in the prodromal phase of disease and is highly prevalent in both idiopathic and familial PD [243]. Although hyposmia is reported in as many as 90% of idiopathic PD cases [244], little is known about the underlying pathogenesis.

By virtue of its sporadic occurrence, the precise cause(s) of PD is unknown, however a range of genetic and environmental factors that increase the risk of PD developing have been identified. The dominant risk factor that relates to onset of PD is age [16]. The genetic risk factor with the highest population attributable risk (PAR) percent is the *SNCA* gene (12%) encoding the protein α-synuclein (α-syn) [245]. α-syn is the major constituent of Lewy bodies, an evident histopathological feature of PD, and as a result there is a large body of research dedicated to understanding its role in PD. Pathological staging by Braak *et al*. demonstrates that α-syn accumulation begins in the brainstem and the olfactory system (stage I), before following a topographical spread across the brain, reaching the nigrostriatal system in stage III [206].

The gene with the second highest PAR (8%) is *MAPT*, which encodes for the microtubule-associated protein, tau [245]. Tau has been implicated as a major contributor to disease pathogenesis in a number of neurodegenerative diseases including Alzheimer's disease where the presence of neurofibrillary tangles (NFTs) consisting of hyper-phosphorylated tau is a defining characteristic. NFTs are also a feature of PD brain, a finding first reported by Lewy himself (reviewed in [33]), and since reproduced a number of times [20, 21]. Despite the genetic and histopathological indications, the role tau plays in PD pathogenesis has not been well characterized.

One of the established biological functions of tau is promotion of the assembly of tubulin into microtubules, thereby stabilising the microtubule structure [246]. Tau has an intrinsically disordered structure that is subject to a number of post-translational modifications (PTMs) [247]. It has been demonstrated that the microtubule assembly role of tau is regulated by phosphorylation, and hyperphosphorylation leads to suppression of this function [18, 19]. It has been hypothesized that abnormal PTMs are a mechanism by which the function of tau is altered, resulting in loss of function, potentially via microtubule destabilisation [248].

The first line of tau$^{-/-}$ mice were generated by Harada *et al.* and although these animals were shown to have defective microtubule stability and organisation, they were viable and appeared macroscopically normal [249]. However, it has since been demonstrated that behavioural and motor impairments developed in these animals in an age-dependent manner. Lei *et al.* performed extensive behavioural and neurological investigations into tau$^{-/-}$ animals and showed that these mice display multiple features congruent with PD including an age-dependent motor and cognitive phenotype, iron accumulation and dopaminergic neurodegeneration of the SNpc [26, 250]. The findings in this study suggest dysfunction of tau is a key pathological event that eventuates in the hallmark pathological feature reported in the PD brain.

The appearance of motor symptoms associated with PD is reflective of advanced disease, as 50-70% of the dopaminergic neurons in the SNpc have perished by this stage [251, 252]. The advanced disease state currently aligned with diagnosis is a hindrance to the development of neuroprotective drugs and there is a need to develop methods to detect and diagnose patients much earlier in the prodromal phase of disease. As hyposmia is among the first symptoms to appear at the beginning of the prodromal phase, it follows that neuropathology in the olfactory system is an important feature of disease.

Studying olfactory deficits in animal models of PD is valuable in enhancing the understanding of the various mechanisms that may be contributing to PD-related hyposmia. Many animal models have been tested for a hyposmic phenotype [253, 254], and mice overexpressing human α-syn have demonstrated an age-dependent odour detection deficit [174]. Due to the age-dependent nature of the behavioural phenotype in the tau$^{-/-}$ mice, we sought to determine if hyposmia, an early process in the pathogenic pathway of PD, is associated with loss of tau function, using the tau$^{-/-}$ mice as a model.

5.3 Methods

Mice

Animals were housed according to standard animal care protocols. Rodent chow and water were available *ad libitum*. Mice were kept on a 12:12 hour light dark cycle and all testing was performed during the light phase of the circadian cycle. Sv129B/6 tau$^{-/-}$ mice were bred in house. Wild type (WT) littermate controls were used in this study. All studies were conducted in a blinded fashion. All methods conformed to the Australian National Health and Medical Research Council published code of practice for animal research and all experimentation was approved by The Florey Animal Ethics Committee (AEC number: 12-094 and 15-092). Animals were genotyped as part of the breeding strategy and confirmation of tau ablation was performed on tissue via western blot.

Odour Detection Test

The Odour Detection Test (ODT) was adapted from [255]. Mice were habituated to vehicle canisters in their home cage for 3 days prior to testing (day 1: single vehicle cannisters; day 2: two vehicle cannisters; day 3: two vehicle cannisters). The test (day 4) was comprised of four 5-min trials (1 hr inter-trial interval (ITI)) performed in the home cage in which the mice were exposed to two canisters per trial; one vehicle (400 µL, MilliQ water + 0.1% Tween20) and one novel odour of either 0 (vehicle), $1:10^8$, $1:10^6$ or $1:10^4$ dilutions (400 µL, MilliQ water + 0.1% Tween20 + orange essential oil (In Essence, Australia)). Animals were videoed, and videos manually scored (the scorer was blinded to the experimental conditions) and percentage investigation time was calculated based on the equation: (time spent with novel odour/combined time investigating either canister) X 100. An animal was deemed to be 'smelling' if their nose was within a 1-2 cm proximity to the either end of the cannister and appeared to be investigating the cannister (neck extended, whiskers forward). Normal mice will spend more time investigating a novel odour; as such this test determines the concentration at which can detect a novel odour by comparing time spent investigating the two canisters.

Rotarod

Mice were trained for three sessions on the rotarod (Panlab, Spain) 24 hrs prior to testing. Session 1 was set speed (4 rpm/2 mins), session 2 was set speed (4 rpm/2 mins) and session 3 was accelerating (4-40 rpm/2 mins). During training if the mouse fell off the rotarod it was placed back on until 2 minutes had lapsed. On the test day the rotarod was set to accelerating mode (4-40 rpm) over a 5 min trial. Mice were allowed three attempts and the average time of latency to fall was recorded.

Pole Test

Mice were placed vertically (nose up) on a pole (45 cm) that was wrapped in self-adhesive bandage (NexCare, Australia) with a squash ball placed on top to prevent animals climbing and sitting on the top of the pole. Two lines were drawn on the pole to identify a segment of set length (22 cm). One day prior to testing animals were habituated to the pole and allowed five consecutive trials. On the day of testing animals were allowed a further five consecutive attempts which were recorded. Time to turn (animal to complete a 180° rotation) and time to complete were recorded. A successful pole test was defined by an animal's ability to complete a full 360-degree rotation and descend the pole nose first using their limbs to 'walk' (animals failed if they slid or jumped down the pole).

Tissue Preparation

Animals were euthanized with a lethal dose of sodium pentobarbitone (100 mg/kg, Lethobarb, Jurox, Rutherford, NSW, Australia), and transcardially perfused with cold 0.1 M phosphate-buffered saline (PBS) (Sigma-Aldrich, St. Louis, Missouri, MO, USA), pH 7.4.

The left-brain hemisphere was dissected for regions containing the striatum (caudate nucleus and putamen (CPU)), substantia nigra par compacta (SNpc) and olfactory bulbs (OB). These fractions were homogenized using a probe sonicator (10 sec) in radioimmunoprecipitation assay (RIPA) lysis buffer (150 mM NaCl, 1% nonyl phenoxypolyethoxylethanol (NP-40), 0.5% sodium deoxycholate (DOC), 50 mM Tris (pH 8.0) + protease and phosphatase inhibitors (Complete Mini Protease Inhibitor Cocktail and PhosSTOP Phosphatase Inhibitor Cocktail, Roche Diagnostic)) and butylated hydroxytoluene (BHT) (1:5; tissue weight (mg): buffer volume (µL)). Homogenates were then centrifuged at 10,000 *g* for 20 min at 4°C. The clarified supernatant was collected (cell lysate) and total protein concentrations were determined using the bicinchoninic acid (BCA) assay (Pierce; Rockford, USA) according to the manufacturer's directions and made to 2 µg/µl aliquots and used for western Blots.

Western Blotting

Samples were mixed with 4X sample buffer (25 M Tris (pH 6.8), 20% SDS, Glycerol, 100 mg Bromo Blue) containing 100 mM dithiothreitol (DTT), boiled for 5 min and centrifuged at 10000 *g* for 5 mins. Protein was electrophoresed at 270 V for 25 minutes on 4-20% polyacrylamide gels (BioRad; USA) and transferred on to 0.45 µm (pore-size) nitrocellulose membranes (BioRad; USA). Membranes were blocked in tris-buffered saline with 0.05% Tween20 (TBS-T) containing 5% low-fat milk powder (Diploma, Australia) for 1 hour at room temperature, incubated with primary antibodies overnight at 4°C, and incubated with secondary antibodies for 2 hours at room temp. All antibodies (BD Biosciences anti- α-syn, catalogue number: 610786, dilution 1:5000; Novus Biological anti-p62/SQSTM1, catalogue number: 3868, dilution 1:2000; Cell Signalling Technology anti-LC3B(D11)-XP, catalogue number: H00008878-MO1, dilution 1:2000) were diluted in TBS-T containing 5% low-fat milk powder. Membranes were washed in TBS-T for 21 min (3 X 7 min) before and after incubation with secondary antibodies. Proteins were detected using enhanced chemiluminescence (ECL) (BioRad) and visualised with the ChemiDoc (BioRad; USA) and analysed via densitometry (ImageLab 5.2.1, BioRad; USA). Cell lysates were normalised to automated total protein measurement via ChemiDoc stain-free detection software.

Primary cortical neuron preparation

Primary cortical neurons were isolated from embryonic brain cortices harvested from tau$^{-/-}$ and wildtype (WT) pregnant mice at 14 days of gestation. The neurons were plated in T75 flasks at a density of 150,000 cells/cm^2 in Neurobasal Medium (cat# 21103049; Life Technologies), and supplement with B-27 serum-free supplement (cat# 10889038; Life Technologies), Glutamax supplement (cat# 35050061; Life Technologies), gentamicin (cat# 15710072; Life Technologies) and incubated at (humidified, 37 ˚C, 5% CO_2) for 6 days.

Exosome isolation

Exosomes were isolated from cell culture media by differential ultracentrifugation. Culture supernatants were collected, and cellular debris was removed by centrifugation at 2000 *g* for 10 min. The supernatant was then centrifuged at 10,000 *g*, for 30 min at 4°C. The supernatant was collected and centrifuged 100,000 *g* for 1 hour at 4°C to pellet exosomes. The supernatant was discarded and exosome containing pellets resuspended in filtered PBS and re-centrifuged at 100,000 *g* for 1 hour at 4°C to pellet exosomes. The pellet was resuspended in 50 µl PBS.

Electron Microscopy

Exosomes were fixed with 2% glutaraldehyde/PBS, for 30 min at room temperature. 6 µl was applied to a glow-discharged 200 mesh copper grid coated with carbon-Formvar film (ProSciTech, QLD, Australia) and allowed to absorb for 5 min. Grids were washed 2 × with milliQ water and contrasted with 1.5% uranyl acetate. Transmission electron microscopy (TEM) was performed on a Tecnai G^2 F30 (FEI, Eindhoven, NL) transmission electron microscope operating at 300 kV (Bio21 Molecular Science and Biotechnology Institute, Parkville, VIC, Australia) across 15,000× – 36,000× magnification. Electron micrographs were captured with a Gatan UltraScan® 1000 2k × 2k CCD camera (Gatan, Inc., Pleasanton, CA, USA)

Immunofluorescence confocal microscopy

Cells were cultured on Laminin/Poly-D-Lysine coated glass coverslips for 9 days before experimental treatment. Samples were fixed with 4% (w/v) paraformaldehyde (PFA) in 0.1 M phosphate buffer (15 min), rinsed three times with PBS, permeabilized with 0.1% (v/v) Triton X-100 in PBS (10 min) then blocked with 3% (v/v) goat serum in 0.1% (v/v) Triton X-100/PBS (10 min). The samples were incubated with a rabbit monoclonal LC3B antibody (Cell Signaling Technologies) diluted in 3% (v/v) goat serum in 0.1% (v/v) Triton X-100/PBS for 2 h at room temperature, rinsed three times with PBS, then incubated at room temperature for 2 h with secondary antibodies conjugated to Alexa-Fluor-555

(ThermoFisher). The coverslips were then incubated 0.1% (v/v) Triton X-100/PBS containing 1 µM Hoechst 33342 (ThermoFisher) and 1µM DiO (Sigma Aldrich) for 15 minutes to visualise the cells independently of LC3B staining. The samples were three times with PBS, then mounted using a TRIS buffered DABCO-glycerol mounting medium. All samples were imaged in 3D by optical sectioning using an inverted Leica SP8 confocal laser scanning microscope equipped with an 63x/1.40NA objective (Oil immersion, HC PLAPO, CS2; Leica microsystems), using a z-stack range of 4.8 µm and a voxel size of 180 nm laterally (x,y) and 300 nm axially (z). All figure images were acquired at ambient room temperature using a Leica HyD Hybrid Detector (Leica Microsystems) and the Leica Application Suite X (LASX v2.0.1). All images are displayed as z-stack maximum projections.

Confocal image analysis

3D image data were processed and analysed using automated image segmentation in Imaris (V8.0; Bitplane). Autophagic vacuole volume was normalized to the cellular volume rather than number of nuclei, as the number of nuclei did not provide a robust measure of cells per image. For volumetric quantification of LC3B positive autophagic vacuoles, images were segmented using 1 µm diameter background subtraction, 150 nm surface smoothing, a manual intensity threshold of 12 (arbitrary), and seeded region growing segmentation (1 µm diameter seed). Cellular volume was quantified by segmentation of DiO staining, using 360 nm surface smoothing and a manual intensity threshold of 10 (arbitrary). Segmented structures smaller than 10 voxels were excluded to remove shot noise.

Statistical Analysis

All data are presented as the means ± S.E.M., and statistical differences evaluated by Student's *t* test for two sample testing. Odour detection tests were evaluated using a Two-way ANOVA test with repeated measures (one factor repetition) with Fisher LSD post-hoc comparisons for multiple testing, details of ANOVAs and testing of parametric assumptions. For all analyses, $P<0.05$ was considered to be statistically significant

5.4 Results

7-month-old tau$^{-/-}$ mice have an olfactory deficit that is accompanied by autophagic impairment and accumulation of α-synuclein in the olfactory bulb.

In order to test whether a loss of tau can impair olfactory capability, 7-month-old tau$^{-/-}$ mice and their wildtype (WT) littermates underwent an odour detection test (ODT) (Figure 5.1A). This test showed that 7-month-old tau$^{-/-}$ mice showed no preference for investigating the canister containing the novel odour, unlike their WT littermates who showed a significant preference for the novel odour (main effect of genotype *P*=0.003). At the strongest odour concentration (1:10^4), a one sample t test with a hypothetical mean of 50% (chance) demonstrated that WT animals were performing significantly above chance, whereas tau$^{-/-}$ animals were not (WT p=0.0001, tau$^{-/-}$ *P*=0.32) (data not shown). The inability of tau$^{-/-}$ mice to differentiate between a novel odour and a vehicle canister is evidence of a hyposmic phenotype in these animals. In PD, hyposmia occurs prior to the onset of motor deficits. In order to ascertain whether the hyposmia observed in these mice similarly occurs prior to the onset of motor deficits that have previously been reported for these animals, the 7-month-old tau$^{-/-}$ mice underwent motor testing (Figure 5.1B). At 7-months-old no difference in motor function was observed between tau$^{-/-}$ and WT mice on either the rotarod (*P*=0.15) or pole test (time to turn *P*=0.76; time to complete *P*=0.88).

Accumulation and aggregation of protein is a characteristic feature of neurodegenerative diseases and may be the result of impaired clearance mechanisms in affected neurons. Macroautophagy, a major pathway for degradation and recycling of cellular material has been reported to be impaired in PD[213] and implicated in the accumulation of α-synuclein (α-syn) that is a characteristic feature of the disease [256-259]. Microtubules, which are reported to be stabilised by tau, play a key role in the endo-lysosomal trafficking process required for autophagic degradation[260, 261]. Autophagosome lysosome fusion is mediated by a number of factors including SNARE Stx17, the HOPS complex and mammalian Atg8 family proteins[262-266]. Atg8 family members are conjugated to phosphatidylethanoamine on autophagosomal membrane during autophagosome biogenesis, and degraded upon lysosomal fusion with the autophagosome [267]. When analysed by SDS-PAGE, the lapidated form of the LC3B (LC3-II) migrates faster than the cleaved precursor form (LC3-I). As such, an increase in the ratio of LC3-II/LC3-I is often used as a marker of compromised autophagy-mediated degradation[268].

We therefore used LC3B levels to monitor autophagy in tau$^{-/-}$ OB tissue and determine if ablation of tau resulted in alterations to autophagy. A significant increase in LC3-II/I ratio (*P*=0.01) was detected in the OB of 7-month old tau$^{-/-}$ mice compared to WT mice (Figure 5.1D). This increase in the ratio of LC3-II/I was accompanied by a significant 50% increase in the level of p62 (an autophagy receptor that

is basally turned over via autophagy) in tau$^{-/-}$ mice (*P*=0.003) (Figure 5.1D) further suggesting 7 mo tau$^{-/-}$ animals have an impairment in the autophagy pathway.

Hyposmia as seen in the human condition has been correlated with an accumulation of aggregated α-syn within Lewy bodies, as demonstrated in Braak staging[206]. Given the suggested autophagy impairment in the tau$^{-/-}$ mice it was of interest to probe the OB for protein accumulation. Consistent with a PD-like phenotype there was an increase of α-syn in the OB at 7-months-old (*P*=0.03) (Figure 5.1D).

The midbrain (CPU and SNpc) of these animals was also analysed for LC3B, p62 and α-syn. In line with there being no overt motor deficit, there were no detectable differences in the aforementioned protein levels evident in these brain regions (Figure 5.1D). CPU: p62 *P*=0.65, LC3-II/I *P*=0.40, α-syn *P*=0.60; SN: p62 P=0.89, LC3-II/I P=0.19, α-syn P=0.83.

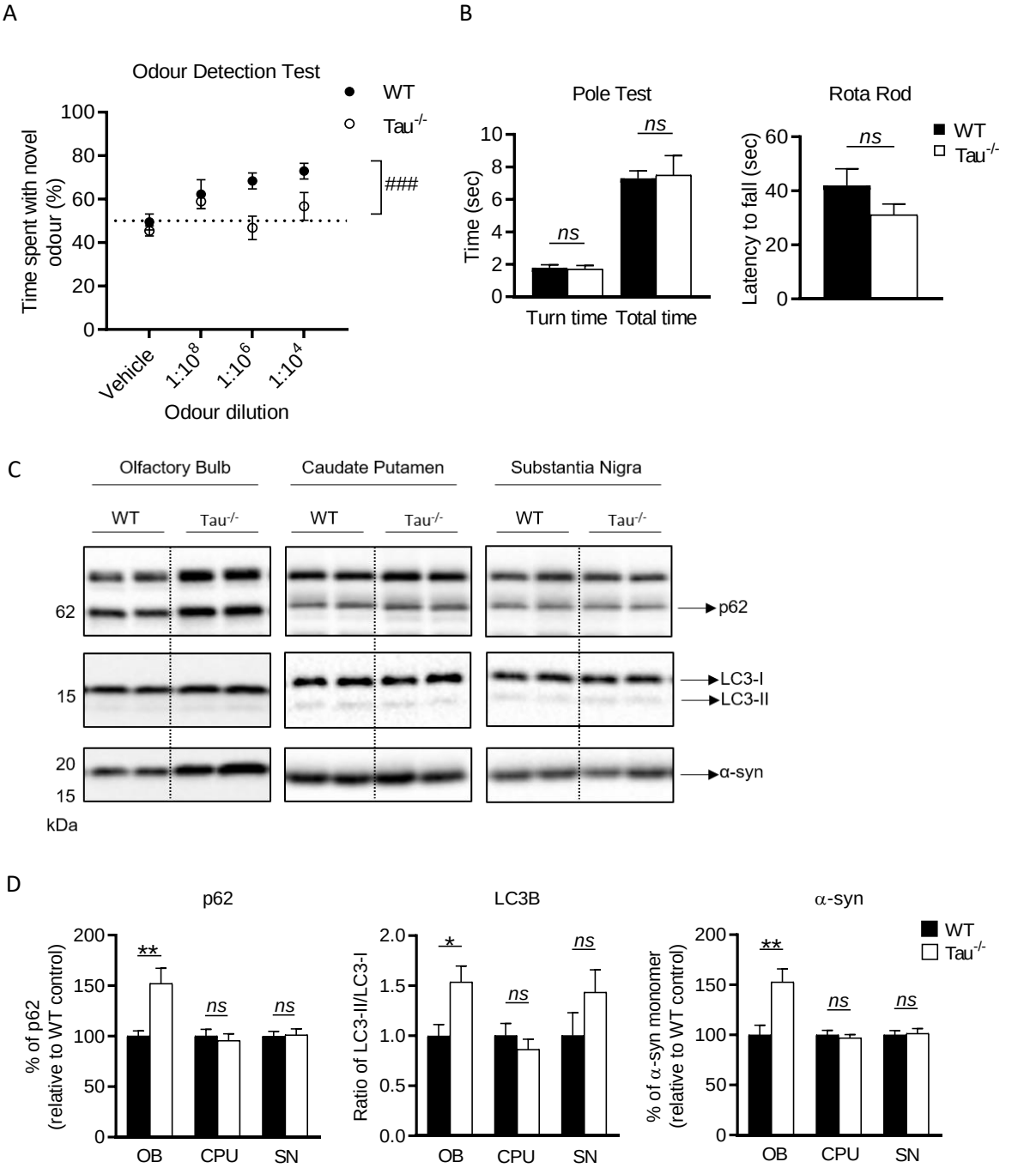

Figure 5.1 Olfactory deficit, motor performance, and pathological features in 7-month-old tau-/- mice. **A)** Odour detection test performed on 7-month-old tau$^{-/-}$ (n=10-11) and littermate WT controls (n=10-12). **B)** Motor evaluation of 7-month-old tau$^{-/-}$ (n=10) and littermate WT control (n=11), including rotarod and pole test performance. **C)** Representative western blots of cell lysate from olfactory bulb, caudate putamen and substantia nigra from 7-month-old tau$^{-/-}$ (n=6) and littermate WT controls (n=6) immunoblotted for p62, LC3B and α-syn. **D)** Quantification of western blot densitometry presented as % of p62 relative to WT control, ratio of LC3-II/I relative to WT control and % of α-syn relative to WT control. Cell lysate for western blots normalised to automated total protein measurement via ChemiDoc stain-free detection software. ODT analysed by two-way repeated measures ANOVA (one factor repetition) with Fisher LSD post-hoc comparisons. # represents significant main effect of genotype, ### P<0.001. Motor tests analysed by unpaired two-sided t test. Western blot analysed by unpaired two-sided t test from 3 independent repeats, *P<0.05, **P< 0.01, *ns*: not significant.

15-month-old tau$^{-/-}$ mice have a motor deficit that is accompanied by autophagic impairment and accumulation of α-synuclein in the midbrain.

At 15 months old tau$^{-/-}$ mice continued to display an odour detection deficiency, however WT mice were also displaying a hyposmic phenotype at this age, as demonstrated by a there being no main effect of genotype of *P*=0.54 (Figure 5.2A) when compared to tau$^{-/-}$ mice and no significant difference to a hypothetical mean of 50% at any of the odour concentrations. The onset of motor impairment in these mice is reported to occur at 12 months, and is accompanied by dopaminergic neuronal degeneration in the SNpc and iron accumulation in dopaminergic neurons[26]. Based on this data we examined 12-month-old tau$^{-/-}$ mice and found no significant difference in motor performance compared to WT controls, however there was still a robust olfactory deficit in tau$^{-/-}$ mice (*data not shown*). As such, mice were further aged to 15-months-old and at this point tau$^{-/-}$ performed significantly different on both the rotarod (*P*<0.0001) and pole test (time to turn *P*=0.004, total time *P*=0.03) than WT controls (Figure 5.2B).

Based on this behavioural deficit, we examined the autophagic markers and α-syn levels in the OB, CPU and SNpc of animals at 15-months-old. At this age the is no detectable difference in the OB between tau$^{-/-}$ and WT mice (p62 *P*=0.13, LC3-II/I *P*=0.47, α-syn *P*=0.73) (Figure 5.2D)**.** Although there was no difference in the level of p62 in either the CPU (*P*=0.15) or the SN (*P*=0.91), tau$^{-/-}$ mice had a significant increase in the ratio of LC3-II/I in both brain regions (CPU *P*=0.04, SN *P*=0.03), indicative of impaired autophagy (Figure 5.2D). In line with the early pathological features demonstrated in the OB of young animals, there was a congruent increase in α-syn in the CPU of older tau$^{-/-}$ mice (*P*=0.02) (Figure 5.2D).

Overall these data suggest that in this animal model there are changes in protein levels that align with a behavioural phenotype in the olfactory system that eventually present in the midbrain alongside a motor deficit.

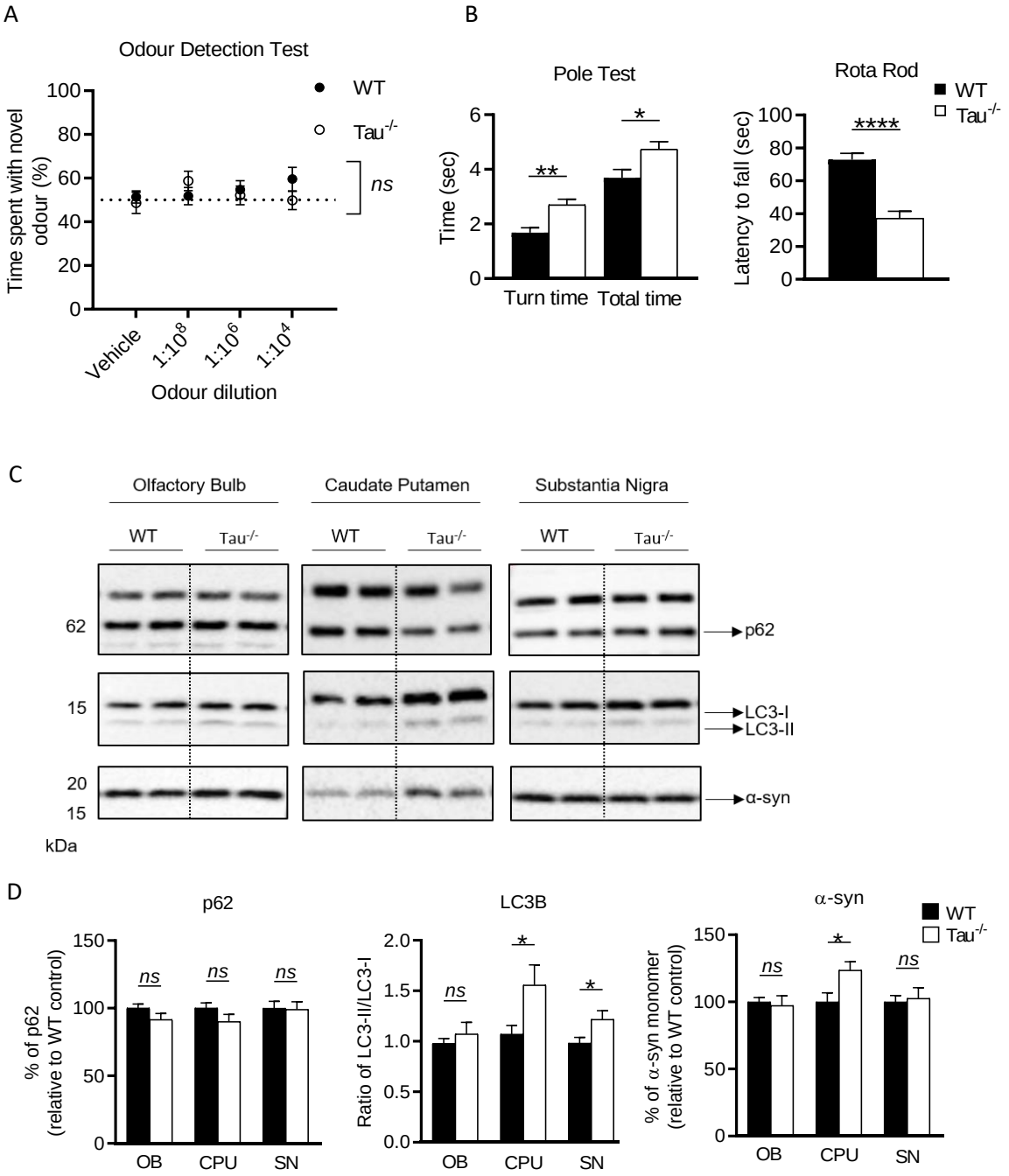

Figure 5.2 Olfactory deficit, motor performance and pathological features in 15-month-old tau-/- mice. **A)** Odour detection test performed on 15-month-old tau$^{-/-}$ (n=13) and littermate WT controls (n=8). **B)** Motor evaluation of 15-month-old tau$^{-/-}$ (n=11) and littermate WT control (n=8), including rotarod and pole test performance. **C)** Representative western blots of cell lysate from olfactory bulb, caudate putamen and substantia nigra from 15-month-old tau$^{-/-}$ (n=6) and littermate WT controls (n=6) immunoblotted for p62, LC3B and α-syn. **D)** Quantification of western blot densitometry presented as % of p62 relative to WT control, ratio of LC3-II/I relative to WT control and % of α-syn relative to WT control. Cell lysate for western blots normalised to automated total protein measurement via ChemiDoc stain-free detection software. ODT analysed by two-way repeated measures ANOVA (one factor repetition) with Fisher LSD post-hoc comparisons. Motor tests analysed by unpaired two-sided t test. Western blot analysed by unpaired two-sided t test from 3 independent repeats, **P*<0.05, ***P*<0.01, *****P*<0.0001, *ns*: not significant.

Tau disruption and impaired autophagic clearance promotes the release of α-syn in association with exosomes.

To further investigate whether a loss of tau can cause an impairment in autophagy, we harvested primary cortical neurons from tau$^{-/-}$ mice and their WT littermates and compared their autophagic flux. As we observed in the mouse tissue, there was a significant increase (*P*=0.04) in the LC3-II/I ratio in the tau$^{-/-}$ neurons as compared with WT neurons (Figure 5.3A). Immunocytochemistry was also used to assess autophagosome number in WT and tau$^{-/-}$ neurons (Figure 5.3B). Quantitation of LC3B positive structures using semi-automated 3D image analysis revealed a significant increase in autophagosome number in tau$^{-/-}$ neurons under basal conditions (*P*=0.04) (Figure 5.3C). Treatment with the autophagosome biogenesis inhibitor wortmannin resulted in no significant difference in the number of LC3B structures between WT and tau$^{-/-}$, and an overall decrease of LC3B structures supporting that the structures represent autophagosomes. The data suggest that either there was a decrease in the lysosomal turnover of autophagosomes in tau$^{-/-}$, or an increase in the amount of autophagy under basal conditions.

Impairment of autophagosome maturation or fusion with a lysosome has been suggested to result in fusion of autophagosomes to multivesicular bodies (MVBs) [269]. Once formed, MVBs can fuse with the plasma membrane to release their intraluminal vesicles as exosomes into the extracellular space. Exosomes are small vesicles released by cells and are major regulators of cell-to-cell communication in both pathological and normal conditions [270, 271]. Exosomes have been implicated in prion disease progression by promoting the cell-to-cell spread of pathological forms of the prion protein [272, 273]. The temporal displacement in the onset of disease relevant symptoms in the tau$^{-/-}$ mice suggests a phenotype that is present at an earlier age in the OB spreads to the CPU/SNpc at an older age. Could this disease spread be facilitated through an exosome mediated mechanism? To test if loss of tau function could possibly contribute to exosome mediated disease spread, we compared exosomes released into media from tau$^{-/-}$ and WT mouse primary cortical cell cultures. Tau deletion resulted in an increase in the number of exosomes released into the media (*P*<0.0001) (Figure 5.3D) and an increase in the enrichment of α-syn within these exosomes (*P*=0.049) (Figure 5.3E). Isolated extracellular vesicles were verified as exosomes using a number of positive and negative exosome markers (*data not shown*).

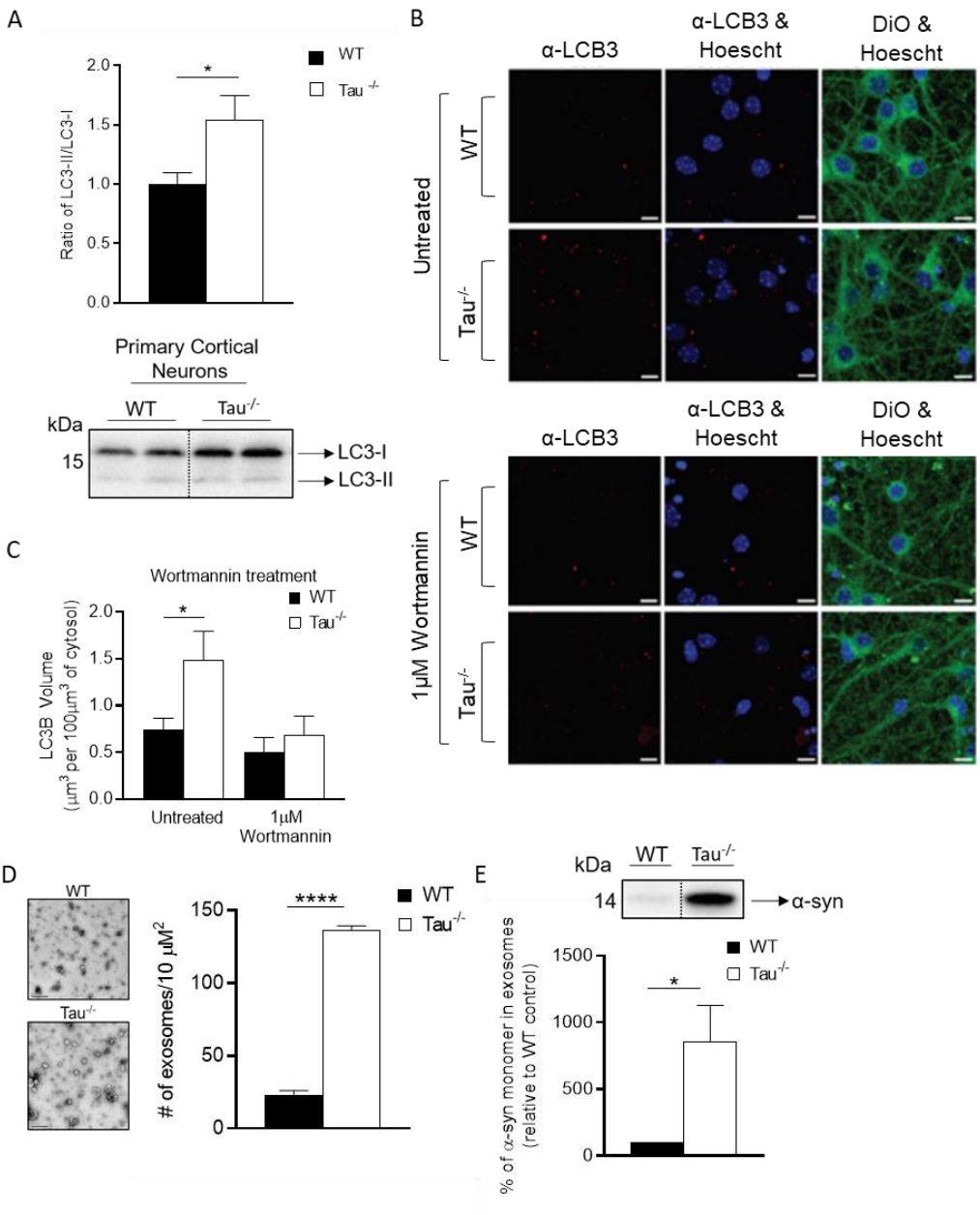

Figure 5.3 Tau-/- primary cortical neurons display autophagic impairment and have an increase in the release of α-synuclein enriched exosomes. **A)** Quantification of western blot densitometry presented as ratio of LC3-II/I of tau$^{-/-}$ primary cortical neurons (n=5) and WT primary cortical neurons (n=5). **B)** Representative images of tau$^{-/-}$ and WT primary cortical neurons immunostained for LC3B and post-stained with DiO and Hoechst 33342 after incubation with either culture medium (untreated) or 1 μM Wortmannin for 8 hours, scale bars: 10 μm. **C)** Quantification of the number of LCB3 positive autophagosomes per 100 μm^3 of DiO stained cytosol, in untreated and Wortmannin treated WT (n=5) and tau$^{-/-}$ (n=5) primary cortical neurons. **D)** Representative electron micrograph images of tau$^{-/-}$ (n=3) and WT (n=3) exosome enriched cell culture media (scale bars: 200 μm) with quantitation of number of exosomes per 10 μM^2. **E)** Quantification of western blot densitometry from exosomes isolated from tau$^{-/-}$ (n=2) and WT (n=2) primary cortical neurons, presented as % of α-syn relative to WT control and representative western blot. Cell lysate for western blots normalised to automated total protein measurement via ChemiDoc stain-free detection software. Immunocytochemistry data analysed by one-way ANOVA. Western blot analysed by unpaired two-sided t test from 3 independent repeats, **P*<0.05, *****P*<0.0001, *ns*: not significant.

5.5 Discussion

Variants of *MAPT* represent a risk factor in idiopathic Parkinson's disease (PD) and hyper-phosphorylation of tau is a consistent feature of many neurodegenerative diseases. Despite this evidence, the role tau plays in pathogenesis of PD has not been well characterised. Similarly, accumulation and aggregation of α-synuclein (α-syn) are histopathological hallmarks of PD brain and follow a defined pattern of spread with disease progression[206], however the mechanism(s) of protein aggregation and spread remain elusive. Our study demonstrates that a loss of the protein tau, via genetic knock out, resulted in a functional olfactory deficit coinciding with α-syn accumulation and autophagic impairments that began in the olfactory bulb and appeared in the midbrain 8 months later. These finding suggest that dysfunction of tau is an early pathological event in the neurodegenerative cascade associated with PD.

In this study, odour detection tests revealed an inability of 7-month-old tau$^{-/-}$ mice to detect a novel odour. There have been numerous studies interrogating the tau$^{-/-}$ mouse as potential model of PD[26, 176, 250, 274-277]. Although there have been no published investigations into the olfactory capacity of tau$^{-/-}$ mice to date, two tau-overexpressing models have reported olfactory dysfunction. Tα1-3RT tau transgenic mice that overexpress human tau and P301S tau mice that overexpress human mutant tau both demonstrate functional olfactory deficits[278, 279]. Although the exact cause of hyposmia has not been determined, there appeared to be a relationship between Lewy pathology and olfactory function[280, 281]. The delayed onset of motor impairment in this study (15-months-old) compared to published findings in this animal model (12-months-old) may be the result of genetic modifiers, as there have been differing results between models on different background strains in tau$^{-/-}$ animals[250, 276]. This is one factor that may also explain a lack of olfactory capacity in WT controls at 15-months-old on this background strain and requires further investigation. Protein aggregates appear across multiple levels of the olfactory system[282] and both tau and α-syn are known to accumulate in neurodegenerative disease[161, 206]. Braak staging references an initial increase of α-syn in the anterior olfactory nucleus in human tissue, and in this study, there was an accumulation of α-syn in the olfactory bulb of hyposmic tau$^{-/-}$ mice before midbrain pathological features appeared.

One explanation of the accumulation of α-syn in the tau$^{-/-}$ mice may be disrupted clearance. The autophagy-lysosome pathway (ALP) is a fundamental mechanism used to remove misfolded and aggregated proteins[283, 284]. Defects in the ALP have been linked to PD[285, 286] and other neurodegenerative disorders (for review see: [287]). Increasing evidence suggests that dysregulation of autophagy results in the accumulation of abnormal proteins and/or damaged organelles, and impairments in the autophagy pathway have been implicated as a pathogenic feature of PD, as observed in PD brains as well as in animal models of PD[288-290]. Data from this study suggests there was

impairment in autophagy in the olfactory bulb of 7-month-old tau$^{-/-}$ mice, a deficit that appears in the midbrain in 15-month-old animals, correlating with motor deficits and α-syn accumulation in these brain regions. Although there is evidence of disrupted autophagic flux in 15-month-old animals, as demonstrated by an increase in the LC3II-I ratio, there was no notable change in p62 levels in the midbrain. While this was initially surprising, Sahani *et al*. have demonstrated *in vivo* that in distressed cells, there is an initial decrease in p62, but the cells were able to restore the level of p62 to basal levels[291]. Authors demonstrate that there are three major factors that control the expression level: autophagic degradation, transcriptional upregulation and availability of lysosomal-derived amino acids. Based on this, it is concluded that expression level of p62 does not always inversely correlate with autophagic activity and should only be taken in conjunction with other autophagic markers.

Many of the steps involved in autophagy require a functional cytoskeletal network. Disruption of dynein function leads to the accumulation of autophagosomes, suggesting that impairments to microtubule transport disrupt autophagosome-lysosome fusion[292, 293]. Tau is a microtubule-associated protein with a proposed role in microtubule stability; therefore, microtubule destabilisation following tau dysfunction is a potential mechanism of autophagy disruption. Data from this study demonstrates that ablation of tau *in vivo* lead to increases in the autophagy marker LC3B, suggestive of autophagy deficits that may lead to protein accumulation. It appears that although there is an increase in α-syn levels in the caudate putamen (CPU) at 15 months of age, the substantia nigra pars compacta (SNpc) has no detectable difference between the WT and tau$^{-/-}$ animals. Shimozawa et al. have investigated the distribution and spread of α-syn and they demonstrated a retrograde spread of pathology from the CPU to the SNpc[294]. It is possible that in this study the tissue has been collected at a time point that is reflective of the beginning of pathological pathways in the midbrain, reflected by the accumulation of α-syn only in the CPU. Autophagy deficits were confirmed in primary cortical neurons of tau$^{-/-}$ neurons, supporting the principle that tau disruption results in altered autophagy.

α-syn aggregates are a histopathological hallmark of PD brain and follow a defined pattern of spread across the brain with disease progression. It was recently demonstrated that injection of exogenous α-syn into the brains of healthy animals could induce α-syn propagation in a “prion-like” manner and induce a PD phenotype[295, 296]. The specific mechanisms underlying the propagation of α-syn across the brain have however remained elusive.

Recent studies have shown that α-syn can be secreted via exosomes[297-299], although non-exosomal release of α-syn has also been described [299, 300]. Exosomes are the released form of intraluminal vesicles that are generated from invaginated membranes of multivesicular bodies (MVB) (reviewed in[301]). Exosome release is enhanced by impaired autophagosome-lysosome fusion, a key step in

autophagy, as illustrated by genetic and pharmacological manipulations[259, 302]. The mechanism of this effect is not clear, although it has been proposed that autophagosomes may fuse with MVBs to subsequently effect fusion with the plasma membrane and release[257, 259, 299, 302]. Our study indicates that disruption of tau lead to autophagic impairment appearing initially in the olfactory bulb and later in the midbrain. Defective autophagy results in an accumulation of α-syn and in combination with autophagic impairments may drive the release of α-syn enriched exosomes, which may be an important mediator of α-syn spread.

This study has demonstrated a link between tau ablation and autophagic disruption that coincides with α-syn accumulation and related behavioural deficits beginning in the olfactory system and eventuating in the midbrain. This implicates dysfunction of tau as an early pathological event in PD and signifies the value of $tau^{-/-}$ mice as an age-dependent model of both prodromal and clinically overt Parkinson's disease.

Chapter 6: Failure of extracellular dopamine clearance in the tau knockout mice is implicated in early olfactory deficits, which can be temporarily rescued by acute dopamine 2 receptor antagonism

6.1 Abstract

Dopaminergic neurodegeneration is a hallmark feature of Parkinson's disease, and *post-mortem* analysis of the bulbar dopaminergic system in this thesis needs to be further investigated in an *in* vivo model. Tau knockout mice are a model of Parkinson's disease due to their age-dependent behavioural phenotype; including an early olfactory deficit followed by a motor impairment that coincides with a loss of nigrostriatal dopaminergic neurons. Understanding the pathobiology of the early olfactory dysfunction may provide insight into the early pathways involved in the human condition, which will inform future diagnostic techniques of preclinical Parkinson's disease. Due to its neuronal vulnerability and selective degeneration, the dopamine system is of interest in models of Parkinson's disease. It was hypothesized that disruptions in dopamine homeostasis underlie hyposmia in young tau$^{-/-}$ mice. 7-month-old hyposmic tau knockout mice were analysed for locomotion and exploratory behaviour, as a reflection of changes in a system that is dopamine-mediated. Olfactory bulbs of tau knockout and wildtype mice were extracted and analysed for dopamine and metabolite levels, as well as key enzyme levels in synthesis and metabolism, including tyrosine hydroxylase and catechol-*O*-methyltransferase. Furthermore, the effect of dopamine homeostasis on functional olfactory performance was tested using cocaine, haloperidol, and *S*-adenosylmethionine supplementation.

Initial characterisation demonstrated that 7-month-old tau knockout animals in this study had hyperlocomotion and increased rearing behaviour, reflective of dopamine perturbations. Although dopamine levels were not changed in the olfactory bulb, there was a significant increase in tyrosine hydroxylase, and a decrease in the dopamine breakdown product homovanillic acid, which is mediated by catechol-*O*-methyltransferase. The hyposmia present in tau knockout mice was able to be acutely rescued by the dopamine 2 receptor antagonist haloperidol. Although supplementation of *S*-adenosylmethionine (required for catechol-O-methyltransferase activation) was able to reduce the hyperlocomotive and rearing phenotype of tau$^{-/-}$ mice, it was not able to significantly rescue olfactory performance. Taken together, these results suggest that a reduction of catechol-*O*-methyltransferase-mediated dopamine clearance may be resulting in increased extracellular dopamine and activation of the bulbar dopamine 2 receptor. This is a mechanism that is similar to what is found in *post-mortem* human Parkinson's disease olfactory bulbs (Chapter 4), and further emphasises the utility of the tau knockout mice as a model of preclinical Parkinson's disease.

6.2 Introduction

Understanding the pathobiology of Parkinson's disease (PD)-related hyposmia is paramount to its utilisation as an early diagnostic tool. As a decline in smell is considered a normal part of the ageing process, differentiating age-related from disease-related loss of smell will help to identify the population at risk of developing a neurodegenerative disorder. While characterising human *post-mortem* tissue has provided valuable insight into the olfactory pathways disrupted (Chapter 4), it is an important consideration that this tissue is from late-stage PD and may not be an accurate reflection of the initial changes that are driving the early dysfunction. As such, an animal model that aligns with the human condition is a necessity to track age-dependent changes.

As presented in Chapter 5, tau knockout ($tau^{-/-}$) mice display early, pre-motor hyposmia[303]. The presentation of early olfactory deficits, as well as nigrostriatal neuronal degeneration and iron accumulation correlated with motor impairment at an advanced age, add face validity to this animal model in PD[26]. The accumulation of α-synuclein (α-syn) and autophagy deficits indicate cellular impairments within the olfactory bulb (OB)[303], however, what is driving the early olfactory dysfunction is not clear. As such this study focused on characterising a known pathological phenomenon in PD, perturbation of the dopamine pathway, as it is so strongly implicated in the human olfactory deficits (Chapter 4).

The dopaminergic system is tightly regulated, and there are several key enzymes involved in synthesis and metabolism that are known to be altered in PD[304] (Figure 6.1). Tyrosine hydroxylase (TH) is considered the principal regulator of dopamine biosynthesis, and as dopamine is the only monoamine present in the olfactory system, the status of TH is reflective of dopamine synthesis[305]. Once dopamine is released into the synapse it is rapidly cleared, as free dopamine readily interacts with metals in Fenton chemistry to produced radicals[306]. Extracellular dopamine produces its inhibitory effect via the dopamine 2 receptor (D_2R) in the OB glomerular layer and it is responsible for the depression of neural activity and transmission of signals from the olfactory receptor neurons (ORNs) to the projection neurons within the glomeruli. Changes in this tightly regulated system result in increased extracellular dopamine, which is postulated to underlie the olfactory disturbances in animal models with dopamine modifications, such as the vesicular monoamine transporter 2 $(VMAT2)^{-/-}$ and the $D_2R^{-/-}$ mice[253, 307]. As such there is ample evidence that dopamine is a critical bulbar neuromodulator.

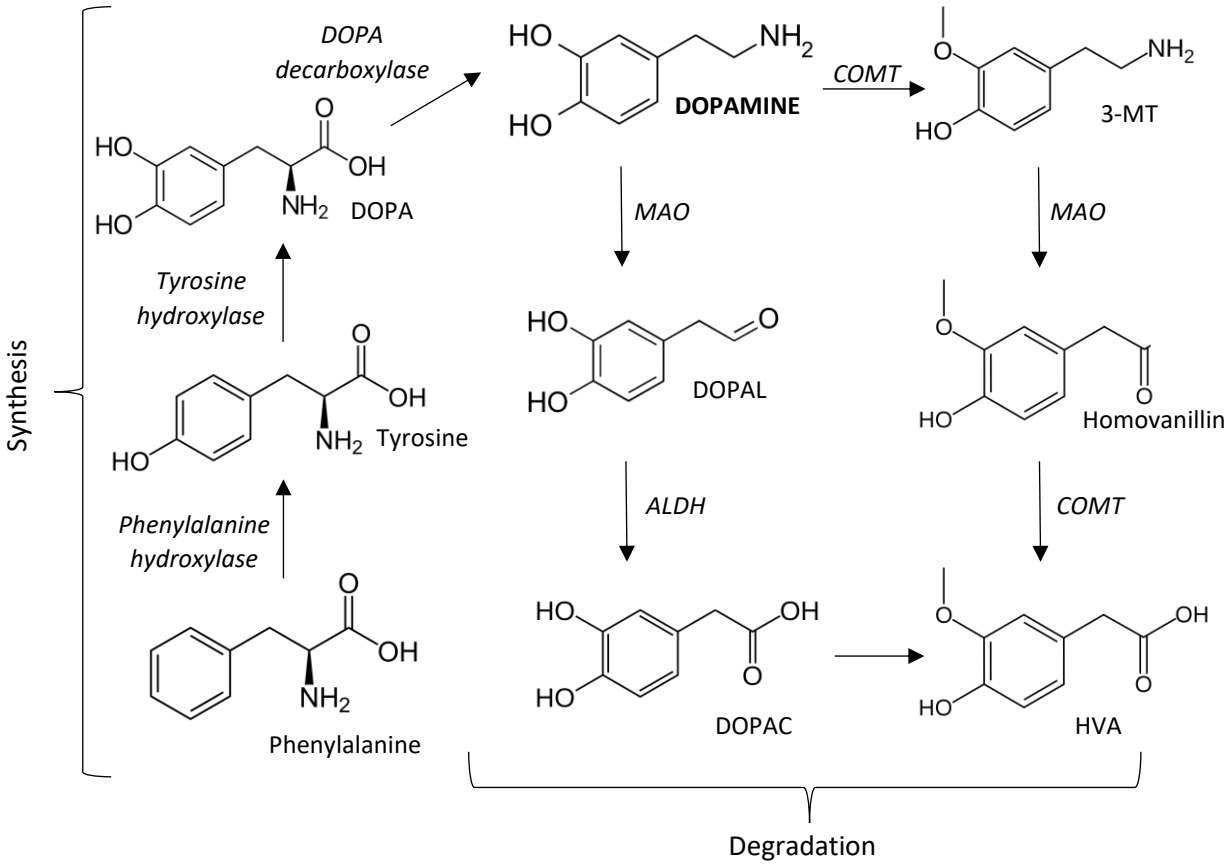

Figure 6.1 Summary of dopamine synthesis and degradation. Abbreviations: 3-MT, 3-methoxytyramine; ALDH, aldehyde dehydrogenase; COMT, catechol-*O*-methyltransferase; DOPA, dihydroxyphenylalanine; DOPAC, 3,4-dihydroxyphenylacetic acid, DOPAL, 3,4-dihydroxyphenylacetaldehyde; HVA, homovanillic acid; MAO, monoamine oxidase.

An increase in extracellular dopamine, or a reduction in the rate of clearance, will increase activation of the post-synaptic D_2R resulting in inhibition of the signal. The primary clearance mechanisms of extracellular dopamine are reuptake via the dopamine transporter, and breakdown via catechol-*O*-methyltransferase (COMT). However, it has been shown in rat OBs that COMT breakdown is the primary mechanism of dopamine clearance within the olfactory system, and knockout of the dopamine transporter (DAT) doesn't significantly alter dopamine clearance. COMT clearance is of great importance in the extracellular space as COMT can methylate dopamine and this methylation event prevents interaction with metals and subsequent ROS production[306]. Secondly, it ensures dopamine is cleared rapidly and is unable to excessively bind to and activate the D_2R. As reported in Chapter 4, there is a suggestion that COMT failure is contributing to dopaminergic changes in the *post-mortem* human OB tissue, making it an enzyme of interest in this animal model.

In light of these findings, the present study resolved to test the hypothesis that disruptions in dopamine homeostasis in the tau$^{-/-}$ animals underlie early olfactory impairments. Alterations in dopamine homeostasis may present as changes in locomotion, olfaction, and exploratory behaviour (among many others) depending on the region of the brain affected[134, 308-311]. As such, this study initially aimed to phenotype 7-month-old tau$^{-/-}$ mice for dopamine-related behavioural changes. The second aim was to characterise the dopamine synthesis and breakdown pathways within the olfactory bulb of hyposmic tau$^{-/-}$ mice. It is possible to acutely alter extracellular dopamine levels using cocaine, restrict activation of the D_2R using haloperidol, and increase COMT enzymatic activity using *S*-adenosylmethionine. Therefore, the final aim was to pharmacologically modulate the dopaminergic system and understand the contribution of dopamine disruption in non-motor hyposmia of the tau$^{-/-}$ mice.

6.3 Methods

Animals

Animals used in this study are the tau knockout ($tau^{-/-}$) mice on an Sv129/B6 background from the same colony reported in Chapter 5, initially described by Dawson *et al* [176]. Animals were derived from a HETXHET breeding strategy and were line bred for 3 generations thereafter. All mice were genotyped using a standardised polymerase chain reaction assay for tail DNA (Transnetyx Inc., USA). Mice were group-housed in standard transparent individually ventilated cages (IVC; 29.5 x 16 x 13 cm) on sawdust under a 12 h light/dark cycle (lights on at 0700 h). Rodent chow and water were available *ad libitum*. Experimentation was performed in accordance with the Prevention of Cruelty to Animals Act (2004), under the guidance of the National Health and Medical Research Council Code of Practice for the Care and Use of Animals for Experimental Purposes in Australia (2013). Individual experiments were approved by The Florey Animal Ethics Committee (AEC number: 15-092 and 19-052). All efforts were made to ensure comfort and minimise the suffering of animals throughout.

Animal behaviour

Animal behaviour, including locomotor activity and odour detection tests, presented in this chapter are described in detail in Chapter 2.

Tissue analysis

Brains were harvested according to the procedure reported in Chapter 2. Details of tissue analysis, including SDS page and immunoblots, high-pressure liquid chromatography with electrochemical detection (HPLC-ED), enzyme-linked immunosorbent assays (ELISA; catechol-O-methyltransferase, *S*-adenosylmethionine, and *S*-adenosylhomocysteine), inductively coupled plasma mass spectrometry (ICP-MS), quantitative polymerase chain reaction (qPCR) were all performed according to protocols laid out in Chapter 2.

Compounds

Cocaine (kindly provided by the laboratory of Prof. Andrew Lawrence, FINMH) was diluted in dH_2O 30 minutes before injection. Haloperidol (Sigma Aldrich, Aus) was diluted in 0.1M HCl and neutralised to pH 7.2 one hour before injection. *S*-adenosylmethionine (SAMe) (Sigma Aldrich, Aus) was stored at -80˚C and aliquots were diluted in dH_2O 30 minutes before oral gavage dosing.

Experimental timelines

Cocaine and haloperidol

7-month-old tau$^{+/+}$ (n=29) and tau$^{-/-}$ (n=31) animals underwent a baseline odour detection test (ODT) (vehicle, 1:10^6, 1:10^4, peppermint scent). One-week later animals were dosed with either cocaine (20mg/kg), haloperidol (0.33mg/kg), or dH_2O via i.p. injection. Post-injection, animals were isolated for one hour in a clean cage before undergoing an ODT with a single odour probe (diluted to 1:10^4, juniper berry scent). Animals were then monitored for two hours for safety as the compounds were metabolised. 24 hours later animals underwent a final ODT with a single odourant (diluted to 1:10^4, orange scent) to test olfactory capacity after the compounds had been metabolised. Scents were changed throughout the experiment to avoid olfactory memory confounds.

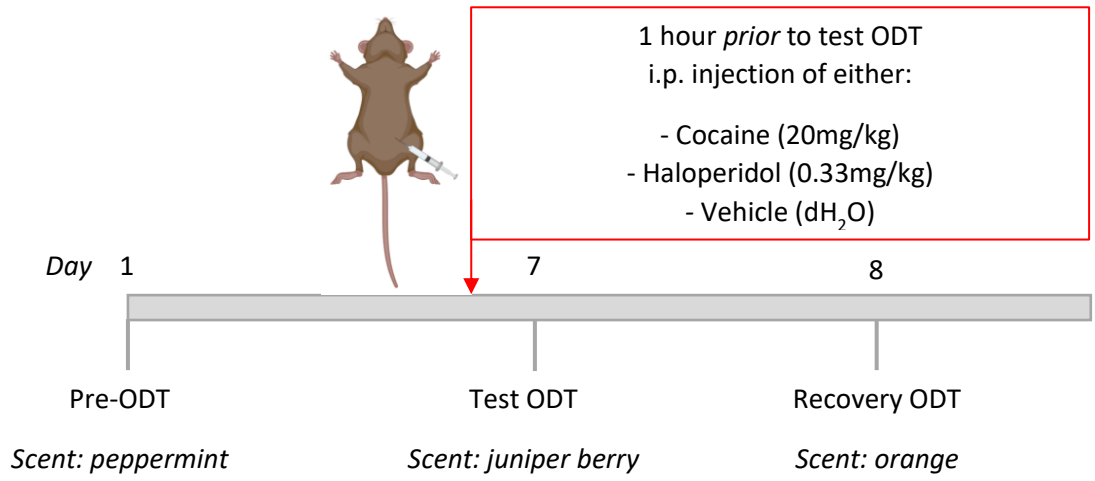

Figure 6.2 Experimental timeline of mice treated with cocaine and haloperidol. 7-month-old tau$^{-/-}$ and tau$^{+/+}$ animals underwent three olfactory tests on days 1, 7, and 8 with different odours. Animals were injected with either cocaine, haloperidol, or dH_2O one hour before the second odour detection test ('test').

S-adenosylmethionine

6.5-month-old tau$^{-/-}$ mice were allocated to either a vehicle (dH_2O; n=11) or treatment group (100 mg/kg SAMe; n=12). Animals underwent baseline locomotor activity (LMA) and ODTs in the two days before daily oral gavage treatment. Dosing was performed on the days of the test LMA and ODT *after* the behavioural tests were performed. On the final day of experimentation, animals were dosed 30 minutes before death, and animals were culled, and their brains harvested according to the protocol reported in Chapter 2.

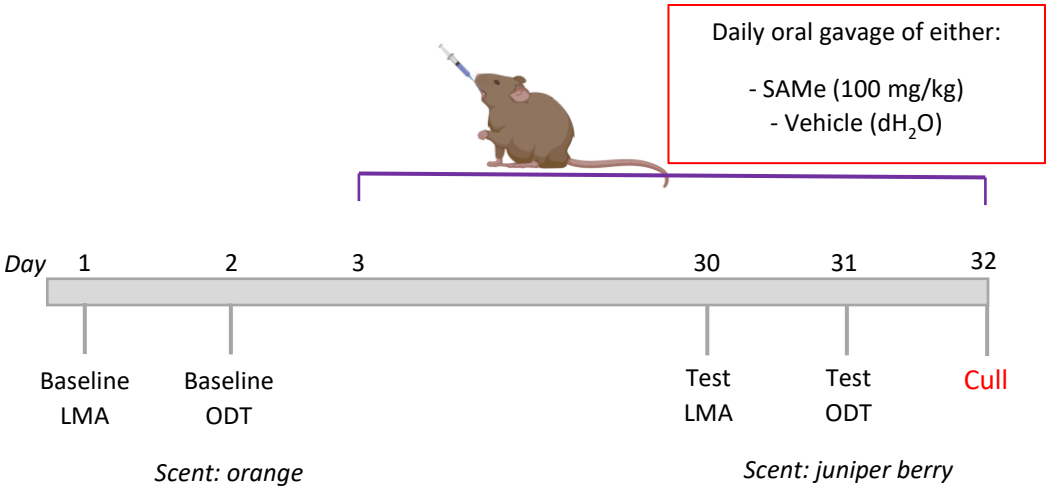

Figure 6.3 Experimental timeline of mice treated with S-adenosylmethionine. 6.5-month-old tau$^{-/-}$ mice were tested for baseline locomotor activity and odour detection, followed by daily oral gavage treatment of either *S*-adenosylmethionine or dH_2O for 29 days. On the two days before culling animals underwent a test locomotor activity and odour detection test, followed by being culled.

Statistical Analysis

For all statistical analyses, the software package GraphPad Prism (version 6.05 for Windows) was used. Data are presented as mean ± standard error of the mean (SEM). Detail including statistical test, replicate number, experimental repeats, and significance are reported in Figure Legends. ANOVA p values reported are from posthoc comparisons generated only when ANOVA terms were significant. As well as unpaired Students t-tests for comparison between groups, one-sample t-tests were also performed for ODT results to determine if the animals could detect odours at specified concentrations (independent of genotype), as evidenced by spending significantly more than 50% of the investigation time with an odourous canister. An investigation time of 50% represents chance, indicating an animal cannot differentiate between the canisters, i.e. cannot detect an odour. For all analyses, $P<0.05$ was considered statistically significant.

6.3 Results

Tau$^{-/-}$ mice have hyperlocomotion and increased rearing behaviour reflective of a hyper-dopaminergic phenotype

Changes in dopamine play an essential role in the pathobiology of Parkinson's disease (PD) and are a system of interest in animals reported to model the disease. In addition to olfactory and motor deficits, 7-month-old tau knockout (tau$^{-/-}$) mice have a hyperdopaminergic phenotype as supported by hyperlocomotion and increased rearing behaviour (Figure 6.4). Tau$^{-/-}$ mice traveled further (Figure 6.4A, C; *P*=0.006) and faster (Figure 6.4B; *P*=0.05) on the locomotor activity test (LMA). Furthermore, tau$^{-/-}$ mice had a higher number of rearing events (Figure 6.4D; *P*=0.02) and increased exploration time (Figure 6.4E; *P*=0.02).

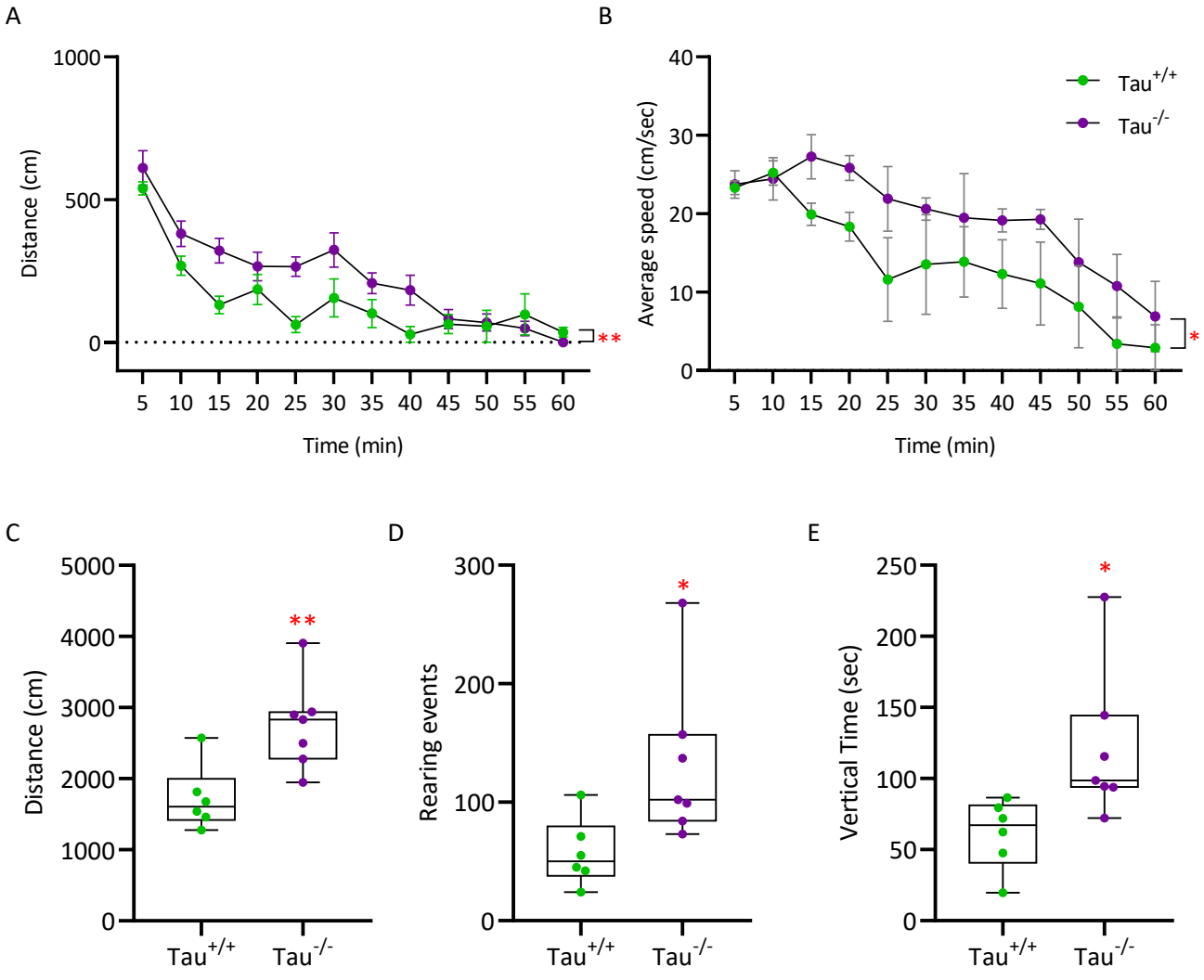

Figure 6.4 Hyperlocomotion and increased rearing activity in young tau knockout mice. **A)** Increased distance traveled and **B)** increased average speed during a 60-minute locomotor activity assessment; analysed by two-way ANOVA. **C)** Total distance traveled, **D)** total number of rearing events, and **E)** cumulative amount of exploration time during rearing behaviour during a 60-minute locomotor activity assessment; analysed by unpaired Students t-test. Tau$^{+/+}$ n=6, tau$^{-/-}$ n=7; **P*<0.05, ***P*<0.01.

Tau$^{-/-}$ mice have perturbations of the dopaminergic synthesis pathway in the olfactory bulb at 7 months of age.

Dopamine has been implicated in the perturbations of the olfactory bulb (OB) in previous publications[155, 156], as well as in Chapter 4. Tyrosine hydroxylase (TH) is the rate-limiting enzyme of dopamine synthesis and is activated when phosphorylated at the Serine 31 residue (pTH). TH and pTH levels give an indication of the number of dopamine-producing neurons, or the neuronal dopamine synthesis potential of neurons. 7-month-old tau$^{-/-}$ olfactory bulb had a significant increase in the level of TH measured via western blot (Figure 6.5B; P=0.003), however, there was no significant increase in the active form of TH, pTH (Figure 6.5B). This resulted in a significant decrease in the ratio of pTH to TH in the bulb (Figure 6.5C; P=0.02). Despite an increase in TH, in line with no increase in pTH, there was no significant increase in the amount of dopamine in the bulb as shown by high-pressure liquid chromatography (HPLC) (Figure 6.5D). The increase in TH protein expression is not a result of increased gene expression, reflected by there being no change in the gene expression measured via quantitative polymerase chain reaction (qPCR) (Figure 6.5E).

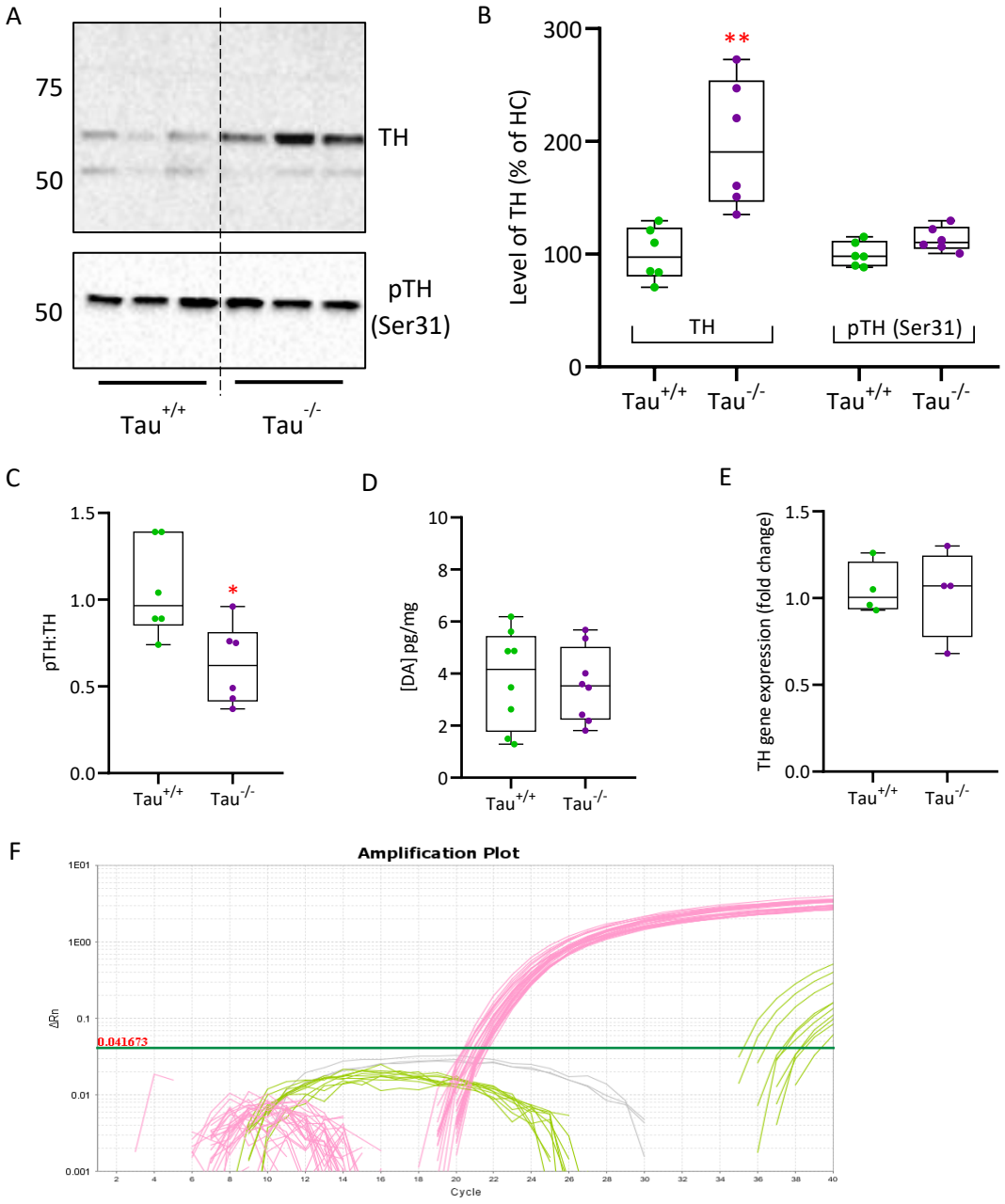

Figure 6.5 Increased tyrosine hydroxylase in the tau knockout mouse olfactory bulb. **A)** Representative western blots of olfactory bulb homogenate from 7-month-old tau$^{+/+}$ (n=6) and tau$^{-/-}$ (n=6) probed for tyrosine hydroxylase and phosphoSerine 31 tyrosine hydroxylase. **B)** Quantification of western blot densitometry presented as % of TH and pTH relative to tau$^{+/+}$ control. Homogenate for western blots normalised to automated total protein measurement via ChemiDoc stain-free detection software. **C)** The ratio of phosphoSerine31 tyrosine hydroxylase to tyrosine hydroxylase. D) The concentration of dopamine via HPLC-ED (n=8). **E)** Tyrosine hydroxylase gene expression fold change determined by qPCR (n=4/group), qPCR data produced by earlier generations of tau$^{-/-}$ and tau$^{+/+}$ animals in 2016. **F)** Amplification plot of TH qPCR. Pink lines represent TH probe, green lines represent various controls. Western blot analysed by unpaired two-sided t-test from 3 independent repeats, HPLC-ED and qPCR performed in triplicate and analysed by unpaired two-sided t-test. *P<0.05, **P<0.01.

Tau$^{-/-}$ mice have subtle changes in the dopaminergic metabolism pathway in the olfactory bulb at 7 months of age.

Due to the changes in dopamine synthesis, it was then of interest to investigate the dopamine metabolism pathway in the bulbs of tau$^{-/-}$ mice. Dopamine is broken down into the metabolites 3,4-dihydroxyphenylacetic acid (DOPAC) and homovanillic acid (HVA). DOPAC is the metabolite predominantly found intracellularly, whereas HVA is the result of the extracellular breakdown of dopamine by COMT. COMT activation is reliant on the binding of cofactors, including *S*-adenoysylmethionine (SAMe) and magneisum (Mg). DOPAC and HVA levels in the OB of tau$^{-/-}$ and tau$^{+/+}$ animals was measured by HPLC. There was no change in the level of DOPAC between tau$^{+/+}$ and tau$^{-/-}$ mice (Figure 6.6A), however, there was a reduction in the amount of HVA (Figure 6.6B, *P*=0.08). The concentration of SAMe was reduced in the tau$^{-/-}$ olfactory bulb compared to tau$^{+/+}$ controls (Figure 6.6C, *P*=0.05). There was no significant difference in the level of magnesium between groups (Figure 6.6D)

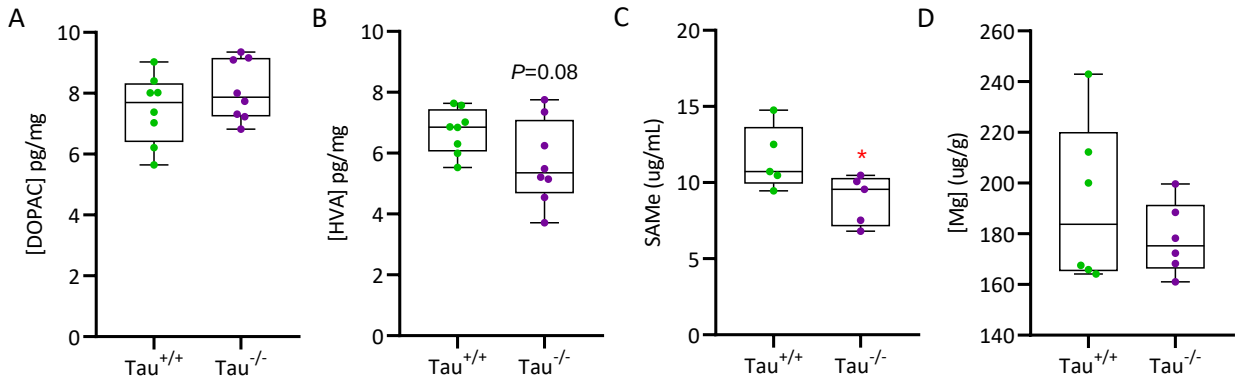

Figure 6.6 Reduced homovanillic acid and S-adenosylmethionine in the tau knockout mouse olfactory bulb. **A)** The concentration of bulbar DOPAC (n=8). **B)** The concentration of bulbar HVA (n=8). **C)** The concentration of *S*-adenosylmethionine (n=5). **D)** The concentration of magnesium. HPLC-ED performed in triplicate, SAMe ELISA and ICP-MS performed in duplicate and analysed by unpaired two-sided t-test. **P*<0.05.

Haloperidol acutely rescues the hyposmia of 7-month-old tau$^{-/-}$ mice.

Much like in the human *post-mortem* tissue analysed in Chapter 4, there appear to be perturbations in dopamine breakdown in the young tau$^{-/-}$ tissue. A decrease, or slowing, in dopamine clearance will result in increased dopamine available to bind to the dopamine 2 receptors (D_2R) in the extracellular space. To ascertain if D_2 activation contributes to hyposmia in the tau$^{-/-}$ mice, animals were injected with vehicle, 20 mg/kg cocaine, or 0.33 mg/kg haloperidol. Cocaine binds and blocks the dopamine transporter and increases the amount of dopamine able to bind to the D_2R, whereas haloperidol is a potent D_2R antagonist that physically impedes dopamine binding.

At baseline, before any pharmacological modulation, tau$^{-/-}$ mice showed no preference for canisters in the control trial and did not spend an increased amount of time investigating a novel odour compared to a control (Figure 6.7A, n=31). During the test ODT tau$^{-/-}$ mice treated with either vehicle (n=10) or cocaine (n=10) did not detect the novel odour, as demonstrated by a lack of significance in the percentage of investigation of time above chance (50%). Tau$^{-/-}$ mice treated with haloperidol (n=11) spent significantly more time investigating the novel odour compared to vehicle-treated animals (*P*=0.007) and performed significantly greater than chance (*P*=0.003). The tau$^{-/-}$ mice in the haloperidol treatment group returned to a hyposmic baseline 24 hours after treatment, demonstrated by a significant difference between 'test' and 'recovery' scores (*P*=0.03), and a loss of significance above chance.

To determine the effects of these compounds on normosmic animals, wildtype tau$^{+/+}$ animals underwent the same dosing protocol (Figure 6.7B). At baseline, animals showed no preference for either canister in the control trial and performed significantly above chance investigating a novel odour canister (*P*<0.0001). During the test ODT, vehicle-treated tau$^{+/+}$ mice (n=10) performed significantly above chance (*P*=0.0001). Tau$^{+/+}$ mice treated with cocaine (n=9) showed no preference for the odour canister as demonstrated by no significant difference to chance, and a significant reduction in investigation percentage to vehicle-treated animals (*P*=0.001). Tau$^{+/+}$ mice treated with haloperidol (n=10) performed significantly different from vehicle-treated mice (*P*=0.004), however, mice performed above chance (*P*=0.06). During the recovery ODT, tau$^{+/+}$ animals from the vehicle, cocaine, and haloperidol groups performed significantly greater than chance (*P*=0.01, *P*=0.0008, *P*=0.0004, respectively). Furthermore, animals treated with cocaine had a significantly increased investigation percentage in the recovery ODT compared to the test ODT (*P*=0.02), a significant increase also seen in the haloperidol treated animals (P=0.004).

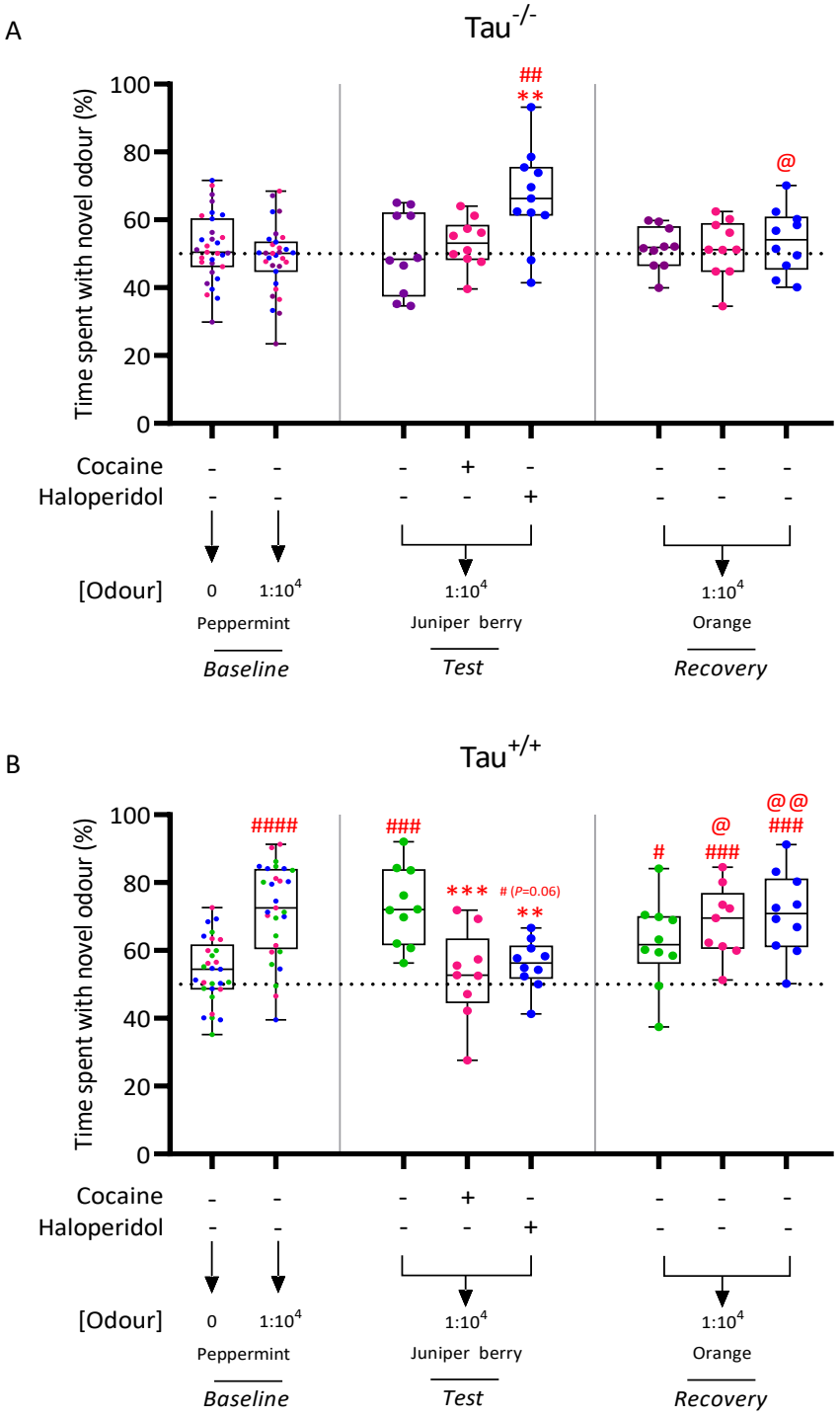

Figure 6.7 Haloperidol acutely rescued the hyposmia in young tau knockout mice. **A)** Odour detection test of tau$^{-/-}$ mice at baseline (n=31), after treatment with vehicle (n=10), 20 mg/kg cocaine (n=10), or 0.33 mg/kg haloperidol (n=11) ('test'), and after drug metabolism ('recovery') . **B)** Odour detection test of tau$^{+/+}$ mice at baseline (n=29), after treatment with vehicle (n=10), 20 mg/kg cocaine (n=9), or 0.33 mg/kg haloperidol (n=10) ('test'), and after drug metabolism ('recovery'). Data is presented as % time spent with novel odour cannisters compared to vehicle cannisters. Comparison of treatment groups performed by one-way ANOVA; ***P*<0.01, ****P*<0.001, *****P*<0.0001. Comparison of individual groups to chance (50%, dotted line) performed by one-sample T test (hypothetical mean of 50%); # *P*<0.05, ## *P*<0.01, ### *P*<0.001. Comparison of individual groups between 'test ODT' and 'recovery ODT' performed by unpaired Students T test; @ *P*<0.05, @@ *P*<0.01.

S-adenosylmethionine rescued the hyperlocomotion, but not hyposmia in tau$^{-/-}$ mice

Due to the success of D_2R antagonism to transiently rescue functional olfactory deficits, targeting and increasing COMT-mediated breakdown was of interest in this animal model. SAMe is a key co-factor for catechol-O-methyl transferase, responsible for the breakdown of released dopamine. To test the hypothesis that D_2R activation was increased due to a reduction in the breakdown of dopamine, we dosed tau$^{-/-}$ with SAMe for 4 weeks, to increase COMT activity.

Tau$^{-/-}$ mice displayed a reduced hyperlocomotion, as supported by a decrease in the distance traveled (Figure 6.8A, *P*=0.001) and the average speed (Figure 6.8B, *P*=0.0002) during the 60-minute LMA test compared to untreated tau$^{-/-}$ mice. There was also a significant reduction in the rearing behaviour of treated animals, as seen by a reduction in exploration time during rearing (Figure 6.8C, *P*=0.004) and the number of rearing events (Figure 6.8D, *P*=0.004). There was no significant reduction in odour detection observed in the treated tau$^{-/-}$ mice (Figure 6.8E).

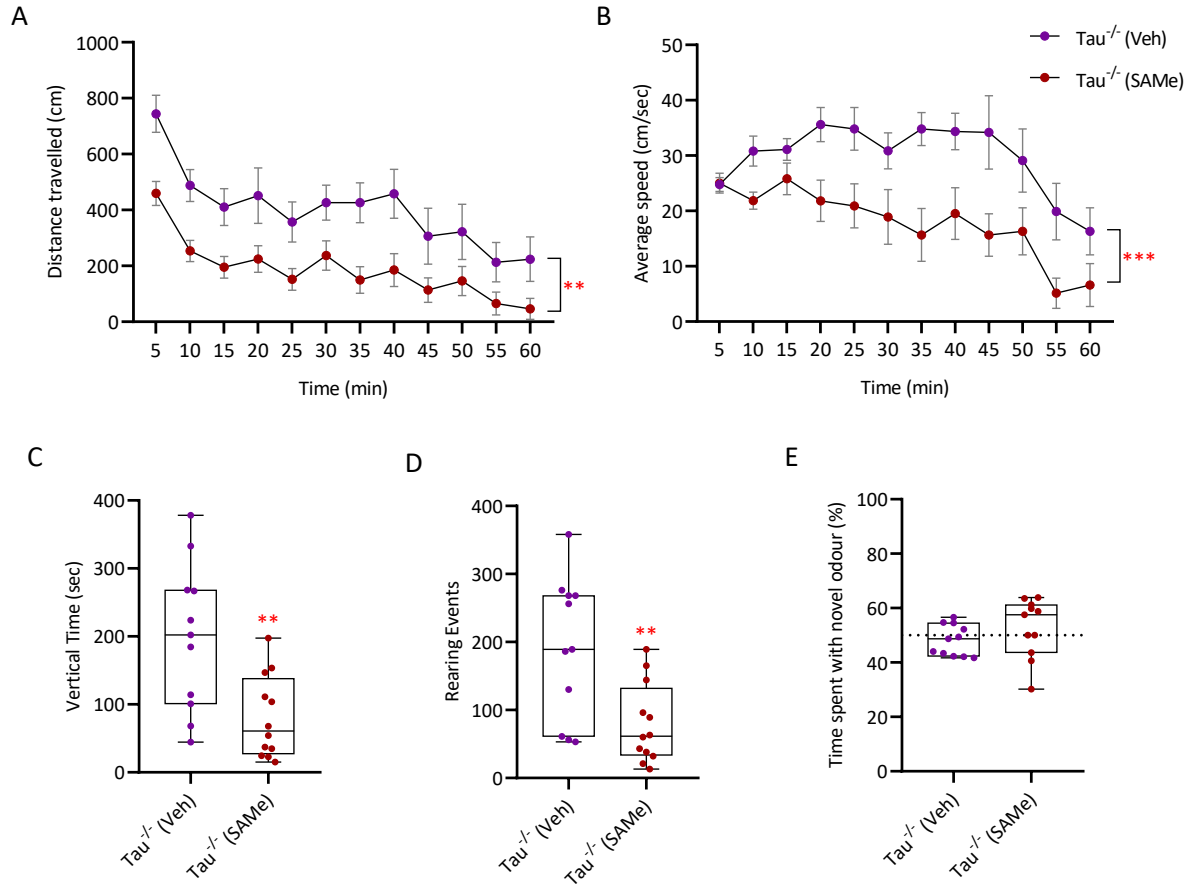

Figure 6.8. S-adenosylmethionine rescued the hyperlocomotion in young tau knockout mice. Locomotor activity and odour detection tests of 7-month-old tau$^{-/-}$ mice treated with vehicle (n=11) or SAMe (n=12). **A-B)** Distance traveled and average speed during the locomotor activity test; analysed via two-way ANOVA. **C)** Amount of exploration time during rearing behaviour, **D)** the number of rearing events, E) amount of time spent exploring a novel odour during odour detection test; analysed via unpaired Students t-test. ** *P*<0.01, *** *P*<0.001.

5.5 Discussion

The tau knockout (tau$^{-/-}$) mice have been proposed as an age-dependent model of Parkinson's disease (PD), as they have a motor impairment that is associated with degeneration of nigrostriatal dopaminergic neurons[26], a key feature of the human condition. As seen in Chapter 5, tau$^{-/-}$ animals have an olfactory impairment at 7 months of age, before the onset of the motor impairment at 15 months, modeling the timing of symptom onset in PD. To expand on these findings, this study aimed to analyse dopamine-mediated behaviours and characterise the bulbar dopaminergic system of tau$^{-/-}$ animals to understand the contribution dopamine may have to the early hyposmia. This study has demonstrated that young tau$^{-/-}$ mice have a dopaminergic phenotype, as seen by hyperlocomotion and increased rearing activity compared to their wildtype (tau$^{+/+}$) controls. Furthermore, the olfactory function in these mice may be due to changes in the dopaminergic synthesis and breakdown pathway, reflected in a significant increase in tyrosine hydroxylase (TH), and a slight reduction in homovanillic acid (HVA). This finding is supported by the acute rescue of hyposmia using a dopamine 2 receptor (D_2R) antagonist haloperidol, which was able to relieve the olfactory dysfunction of young tau$^{-/-}$ mice (Figure 6.9).

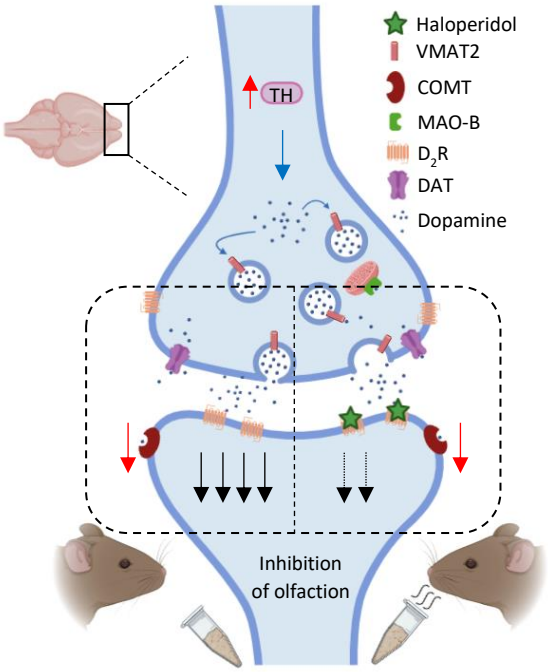

Figure 6.9 A summary of the bulbar dopaminergic pathway alterations in tau knockout mice. There is an increase in TH, and a decrease in COMT activity. D_2R antagonism by haloperidol transiently rescues hyposmia. Abbreviations: COMT, catechol-*O*-methyltransferase; D_2R, dopamine 2 receptor; DAT, dopamine transporter; MAO-B, monoamine oxidase B; TH, tyrosine hydroxylase; VMAT2, vesicular monoamine transporter 2.

Hyperlocomotion and increased rearing behaviour have been previously attributed to changes in the dopaminergic system, as systemic interventions that decrease dopaminergic activity in all brain regions produce hypoactivity. Hypoactivity can be induced in animals treated with dopamine receptor blocking drugs[312], or dopamine depleting compounds such as reserpine[313, 314]. Conversely, drugs that enhance synaptic dopaminergic transmission, such as cocaine, D-amphetamine, and l-3,4-dihydroxyphenylalanine (L-DOPA), increase locomotor activity (LMA)[315-319]. Dopamine transporter knockout mice are also hyperlocomotive, attributed to a reduction in the amount of dopamine cleared, and therefore its ability to bind the post-synaptic dopamine receptors[253]. Despite global interventions of dopamine activity inducing hypo- or hyperactivity, the exact brain regions responsible for locomotor activity are contentious.

Bilateral injections of 6-hydroxydopamine (6-OHDA) induce degeneration of dopaminergic neurons and is a useful tool to understand the behavioural changes induced by localised dopamine loss. 6-OHDA injections into the substantia nigra pars compacta (SNpc) resulted in severe hypolocomotion of rats, however, neuronal loss was extensive in this study, and likely included many non-dopaminergic regions[320]. 6-OHDA injections into the limbic terminal regions, nucleus accumbens, and olfactory tubercle decrease LMA in rodents[321, 322], implicating the dopaminergic fronto-cortical regions in control of LMA[323]. By far the most support for a brain region controlling LMA comes from the injection of dopamine and dopamine agonists into the nucleus accumbens, resulting in increased LMA in a range of studies[308-310, 324-328]. It is thought that these mesolimbic dopamine neurons are primarily involved in the increased LMA, whereas the striatal dopamine neurons are responsible for the stereotypical behaviours, such as biting and licking, that is also observed after dopamine agonist treatment[315, 316], suggesting the nucleus accumbens and striatum mediate different aspects of locomotive behaviour.

Interestingly, another genetic model of tau, the rTg4510 mouse, also demonstrates a hyperlocomotive phenotype. rTg4510 mice conditionally express mutant P301L human tau, discussed more extensively in Chapter 8. Briefly, rTg4510 mice express 13 times more human mutant tau than endogenous murine tau predominantly in the forebrain regions, including the nucleus accumbens. These animals have progressive hyperphosphorylation of tau and eventually develop neurofibrillary tangles (NFT). While it is rare for PD patients to develop NFTs, the role of tau is unknown, and it is proposed that there may be a loss of function mechanism. Hyperactivity is correlated to the level of phosphorylated P301L tau expression and was rescued by switching off transgene expression[329]. Other models of P301L mutations also display a hyperactive phenotype[330, 331], suggesting that there may be a common tau-dependent mechanism underlying the development of hyperactivity. Taken together with the results

of this study, it suggests a tau loss of function resulting in dopamine mis-homeostasis in the nucleus accumbens may be an underlying contributor to hyperlocomotion.

Much like the nucleus accumbens, the dopamine-reliant olfactory system is also vulnerable to mis-homeostasis caused by a tau loss of function. As presented in Chapter 5, tau$^{-/-}$ mice have early hyposmia, however, the contribution of dopamine to this dysfunction is unknown. Activation of the glomerular D_2Rs pre-synaptically inhibits signal transduction from the olfactory nerve terminals, causing a marked depression and even total ablation of synaptic transmission between the olfactory receptor neuron (ORN) and its synaptic target[134, 207, 311, 332]. *In vitro* blockade of baseline D_2R activation from spontaneous periglomerular cell activity enhanced the transmission of signals at ORN output synapses[333]. ORNs can directly innervate the dopaminergic periglomerular cells, which in turn can inhibit the ORN terminals to generate a tightly regulated negative feedback loop responsible for the normalisation of the degree of excitation provided to mitral and tufted cells [134, 334]. It has been reported that there is a hyposmic phenotype in the dopamine transporter (DAT)$^{-/-}$ mice[253], as well as an olfactory discrimination deficit in mice lacking the D_2R[253], suggesting that regulation of dopamine is a fundamental feature of intact olfaction. Whilst there is no change in the amount of dopamine seen in the olfactory bulb (OB) of tau$^{-/-}$ mice in this study, there are changes in both the dopamine synthesis and dopamine breakdown pathways, suggesting dopamine homeostasis may be altered. With regards to dopamine synthesis, there is a significant increase in the level of TH, the rate-limiting enzyme in dopamine synthesis. Despite an increase in TH, TH phosphorylated at the Ser31 residue is not increased, and this is the activated form of TH, explaining why gross dopamine levels remain unchanged.

The mechanism of the increase in TH protein levels has not been elucidated in this study. Based on the quantitative polymerase chain reaction (qPCR) data, it is not an increase in the gene expression of *MAPT,* therefore it is not increased production of the protein. This leads to two potential explanations, increased neurogenesis of TH-containing neurons, or decreased clearance resulting in accumulation of the protein. Although there is no increase in NeuN (data not shown), which is a marker of neurons, it does not rule out neurogenesis and a more detailed immunohistochemical stereology count is required. Decreased clearance of TH is a viable mechanism, as there are impairments in autophagy and protein accumulation in the OB of 7-month-old tau$^{-/-}$ mice, as presented in Chapter 5[303].

Once dopamine is produced, it is packaged into vesicles and released upon activation. Once in the synaptic cleft, dopamine binds to post-synaptic dopamine receptors (D_2R in the olfactory system), as well as auto-receptors on the pre-synaptic neuron. Due to its ability to contribute to reactive oxygen species (ROS) formation, dopamine is rapidly cleared from the cleft, primarily via enzymatic

breakdown by catechol-O-methyltransferase (COMT), and secondarily by reuptake from DAT. $DAT^{-/-}$ mice have hyposmia postulated to be the result of increased extracellular dopamine, and there is a similar increase in the level of TH in the OB of these animals[253]. A dysfunction in the recycling of dopamine, whether it be due to DAT ablation or a reduction in COMT activity, may impair D_2 auto-receptor function, which would increase demand on the periglomerular dopaminergic neurons resulting in increased TH levels[219].

COMT is responsible for the breakdown of dopamine to homovanillic acid (HVA). The $tau^{-/-}$ mice in this study demonstrated a reduction in the amount of HVA, although it did not reach significance. This result indicates that it may be a mechanism similar to the one reported in the *post-mortem* PD tissue in Chapter 4. To test the hypothesis that it is reduced extracellular clearance of dopamine, resulting in increased activation of the D_2Rs that may be causing inhibition of the olfactory system, animals were dosed with cocaine (to increase dopamine levels) or haloperidol (to antagonise the D_2R).

This experiment demonstrated that the modulation of dopamine availability was able to induce olfactory deficits in $tau^{+/+}$ mice by increasing the level of extracellular dopamine using cocaine. The action of cocaine is mediated through a blockade of the DAT transporter[335]. It is known that cocaine-mediated behavioural and biochemical changes are driven by its ability to increase the level of extracellular dopamine[336-338]. It has been reported that cocaine can induce reversible hyposmia and anosmia in people[339] and previous *in vivo* studies have demonstrated that D_2R agonists, such as quinpirole, reduce the odour detection performance in rats[340]. Furthermore, female mice have a surge of dopamine within the OB directly after mating that seems to disrupt the perception of odours contained within male mouse urine[341]. These data suggest that activation of the D_2R mediated olfactory disruptions, and D_2R activation-mediated hyposmia can be rescued by pre- or post-treatment with Spiperone, a potent D_2R antagonist similar to haloperidol[340].

In this study decreasing the ability of dopamine to bind to the D_2R using potent antagonist haloperidol reduced the olfactory capacity of $tau^{+/+}$ mice but did not induce anosmia. Antipsychotic drugs, such as haloperidol, are considered to block dopamine receptors resulting in an accelerated turnover of dopamine[342, 343], and the subsequential increase in metabolites[344]. Interestingly, a low dose blockade of the D_2R improves the ability of the adult rat to discriminate structurally and perceptually similar odours[345]. Although anosmia was not induced in $tau^{+/+}$, the olfactory performance was significantly decreased, however, this may be due to a relatively high dose of haloperidol that caused an acute disruption of the system, as opposed to low dose long term studies where the system was able to adapt.

With regards to the hyposmic tau$^{-/-}$ mice, increasing extracellular dopamine with cocaine did not change the olfactory dysfunction, however, treatment with haloperidol was able to temporarily rescue deficits. This result suggests that the olfactory dysfunction in the tau$^{-/-}$ animals is at least in part due to increased activation of the D_2R, and olfaction can be restored by acute antagonism. Based on this, a sustained increase in the clearance of extracellular dopamine may be a meaningful strategy to further understand the mechanisms underlying hyposmia. As discussed above, COMT is the primary mechanism of extracellular bulbar dopamine breakdown. COMT failure is attributed to hyperdopaminergia, as one-third of people with 22q11.2 deletion syndrome (the region in which the *COMT* gene is located) develop psychosis[346]. Furthermore, COMT$^{-/-}$ mice manifest higher spikes in dopamine, as they cannot rapidly clear dopamine[347]. COMT comes in both a soluble and membrane-bound form. About 70% of COMT in the brain is membrane-bound and in rat cortical neurons has been found in the cell body, axons, and dendrites[348]. Soluble COMT is primarily intracellular, and membrane-bound COMT has the C-terminal catalytic domain in the extracellular space meaning it is able to inactivate extra-synaptic dopamine on the surface of both the presynaptic and postsynaptic neurons[348].

COMT catalyses the *O*-methylation of dopamine using *S*-adenosylmethionine (SAMe) as the methyl donor. As presented in Chapter 4, SAMe is decreased in *post-mortem* human PD OBs, which may be a contributor to COMT inactivity. As such, supplementing animals with SAMe may increase the activity of COMT, therefore reducing levels of extracellular dopamine. In this study, tau$^{-/-}$ animals treated with SAMe had a significant rescue in the hyperlocomotive and exploratory phenotypes, however, there was no significant reduction in the olfactory dysfunction. This may suggest that there are regional differences in compound distribution, or other mechanisms are contributing to the olfactory deficit in the tau$^{-/-}$ mice, both of which require further investigation. Interestingly, the levels of COMT and COMT activity appear to be difficult to induce or down-regulate with compounds. Previously, it has been demonstrated that treatment with pyrogallol[349], dipyridamole[350], butylated hydroxyanisole[351], and SAMe[352] only caused very small increases in hepatic COMT activity, suggesting that supplementation of SAMe may not be enough to induce a global increase in brain COMT activity and a more direct approach is required to test the mechanism.

This study aimed to phenotype tau$^{-/-}$ mice for dopamine-mediated behavioural changes, to measure key enzymes of bulbar dopamine synthesis and breakdown pathways, and to measure the functional olfactory effects of pharmacological modulation of dopamine availability and breakdown. It was demonstrated that mice have a fronto-cortical dopaminergic phenotype and that disruptions in dopamine homeostasis likely underlie the olfactory disruption in tau$^{-/-}$ mice. Although more extensive pathway analysis is required, including target engagement of compounds and dopamine

localisation/breakdown dynamics studies, the findings from this work support the hypothesis that disruptions in dopamine homeostasis in the tau$^{-/-}$ animals contribute to early olfactory impairments. Furthermore, changes demonstrated here align with findings in the *post-mortem* human tissue, supporting the utility of the tau$^{-/-}$ mice as a model of preclinical PD.

Chapter 7: Metal dyshomeostasis contributes to the olfactory and motor deficits of tau knockout mice, which can be functionally rescued by PBT434

7.1 Abstract

Tau knockout mice are a proposed model of Parkinson's disease due to their age-dependent behavioural phenotype; including an early olfactory deficit followed by a motor impairment that coincides with a loss of nigrostriatal dopaminergic neurons. It has been previously reported that aged tau knockout mice have a dyshomeostasis of metals in the midbrain which coincides with motor impairment. It was hypothesised that there is a similar mechanism occurring in the bulbs and as such this study sought to determine the bulbar metal levels of young tau knockout mice to determine if it is a contributing factor to olfactory impairment. The brain regions of interest at these age groups were analysed along with wildtype controls for metal concentration, as well as synaptic and neuronal markers. It was found that there was an accumulation of metals in the olfactory bulb and the substantia nigra pars compacta concurrent with a loss of synaptic and neuronal health markers. As the iron/copper chelator PBT434 has demonstrable effects on the motor impairment of other *in vivo* Parkinson's disease models, both age groups were treated with the metal chelator PBT434 to test the behavioural effects in tau knockout mice. Both olfactory and motor impairments were rescued by treatment with PBT434, which reduced copper and iron, alongside and increased expression of synaptic and neuronal markers in both regions. To ascertain to what degree metals can contribute to olfactory dysfunction, young wildtype mice were dosed with the copper delivery agent Cu(GTSM) to evaluate the role of copper in functional deficits. Cu(GTSM) induced hyposmia in healthy widltype animals without affecting motor skills. These results suggest that metal homeostasis is awry in the tau knockout animal model, and metal chelation is a viable therapeutic strategy in the treatment of Parkinson's disease.

7.2 Introduction

Although once considered non-biological (ie inorganic), metal ions are crucial for structural, regulatory, and catalytic functions of enzymes, receptors, and transporters[353]. There are 12 metals with reported physiological functions, including iron (Fe), copper (Cu), and zinc (Zn)[354]. Zn is a cofactor for more than 300 enzymes and metalloproteins and is a component of many proteins involved in oxidative damage defense[355]. In health, Zn has a crucial role in antioxidant mechanisms including competing with and displacing redox active Fe and Cu, binding to sulfhydryl (SH) groups and protecting them against oxidation, increasing the activation of known antioxidants such as glutathione (GSH) and superoxide dismutase (SOD), as well as inducing the expression of cysteine-rich metallothionines that scavenge oxygen radicals (•OH ions)[356].

Cu is the third most abundant transition metal in the brain and a cofactor for many enzymes that mediate cellular processes such as neurotransmitter synthesis (dopamine β hydroxylase), generation of energy (cytochrome-*c*-oxidase), antioxidant action (SOD), and iron homeostasis (ceruloplasmin)[357]. The importance of neuronal Cu homeostasis is highlighted by the severe neurodevelopmental delays seen in infants with Menkes disease, which is caused by a cellular Cu deficiency, as well as the neurological side-effects associated with Cu accumulation in Wilson's disease[358]. The most abundant transition metal in the brain is Fe. Fe facilitates trafficking and utilisation of O_2, consistent with the high energy needs of the brain (~ 20% of the body's O_2) the neuronal demand of Fe is high. Fe is an essential component of cytochromes (a,b,c), cytochrome oxidase, and the Fe-S complexes of the oxidative chain in adenosine triphosphate (ATP) production[359]. Fe is required for many other cellular processes including DNA synthesis[360], neurotransmitter production (tyrosine hydroxylase (TH) and tryptophan hydroxylase)[361, 362], and the biosynthesis of lipids and cholesterol[363]. There is an increased potency of Fe to induce oxidative stress as it is involved in the formation of reactive hydroxyl radicals. As such, homeostasis of Fe is tightly regulated at the uptake, storage, and release levels. Perturbations in iron homeostasis has been implicated in many neurological diseases including Alzheimer's disease[364], multiple sclerosis[365], Friedereichs's ataxia[366], Huntington's disease[367], and Parkinson's disease (PD)[368].

Research into these key biometals in ageing and neurodegenerative diseases has increased steadily over the past two decades[369] and metals have been implicated in various mechanisms of PD pathogenesis. Many studies have found that Fe and Zn are elevated in the *substantia nigra pars compacta* (SNpc), in PD, whereas Cu is decreased[370]. An increase in Fe is postulated to contribute to oxidative stress and the resultant degeneration of nigral dopaminergic neurons. This hypothesis is well supported by the findings that iron chelation is shown to be protective in various animal models of PD[371-375]. These data suggest that facilitation of iron homeostasis through iron

chelation may be an advantageous strategy in PD, and indeed the iron chelator Deferiprone is able to reduce the accumulation of iron in the central nervous system (CNS) of PD subjects[376]. Whilst the contribution of metal perturbation in the SNpc has been reasonably well established, the role of metal accumulation in the olfactory system is not well understood.

The olfactory bulb (OB) is unique in that it is a brain region that is not protected by the blood brain barrier, making it particularly susceptible to the uptake of environmental toxins[227]. Among these environmental toxins are metals, which, as described above, have been implicated in PD[162, 228]. Whilst there has only been one published examination of the metal content in the human OB of PD patients, which demonstrated an increase in the levels of Fe and sodium (Na), findings from Chapter 4 demonstrated that Zn, lead (Pb), calcium (Ca), and magnesium (Mg) are also increased in the PD tissue examined for this research. It is known that metal workers and individuals with occupational exposure to metals have significantly impaired olfaction compared to the general population[163, 377]. Intracellular metals are a fundamental physiological feature of cells, and perturbations of Fe, Cu, and Zn have been implicated in functional olfactory deficits. However, whether metals have a functional role in olfaction, or if they underlie dysfunction in disease, remains unknown.

Oxidative stress and resulting neurodegeneration have been reported as a consequence of toxic exposure to metals, as well as dyshomeostasis in metal metabolism[378]. Reactive oxygen species (ROS) can be generated though many pathways in cells, including interactions between redox-active metals and oxygen species in Fenton and Haber-Weiss reactions. Metal ions, in particular Fe and Cu, that are present but not regulated by homeostatic systems readily participate in these chemical reactions within dopaminergic neurons due to the production of hydrogen peroxide (H_2O_2) during dopamine metabolism.

It has been previously demonstrated that Fe is accumulated in the SNpc of aged tau knockout ($tau^{-/-}$) mice, and that this increase aligns with dopaminergic neurodegeneration and motor impairments[26]. As such, the present study resolved to test the hypothesis that metal dyshomeostasis in the OB and the SNpc of the $tau^{-/-}$ animals contributes to functional deficits in olfaction and movement, respectively. This study initially aimed to investigate the concentrations of metals in the OB of young (7-month-old) $tau^{-/-}$ animals at the time in which olfactory impairment presents, and the concentration of metals in the SNpc and caudate putamen (CPU) of aged animals (15-months-old) aligned with the presentation of motor impairment.

Lei *et al.* have also demonstrated therapeutic benefit of Fe chelation using iodochlorhydroxyquin (clioquinol), in which there was a reduction in Fe, neurodegeneration, and a rescue of the motor impairment[182]. As such, the functional outcome of Fe/Cu chelation using the chelator PBT434 on

motor impairment was investigated in this study. Additionally, as there are similar biochemical changes in the OB and the SNpc in this animal model at different ages, this study sought to test the therapeutic benefit of chelation on olfactory impairments using PBT434. Finally, given the elevation of Cu in the OB of young animals, young wildtype ($tau^{+/+}$) were treated with the copper delivery agent Cu(GTSM) to ascertain the functional effect of increased bioavailable Cu.

7.3 Methods

Animals

Animals used in this study are the tau knockout ($tau^{-/-}$) mice on an Sv129/B6 background from the same colony reported in Chapter 5, initially described by Dawson *et al* [176]. Animals were derived from a HETXHET breeding strategy and were line bred for 3 generations thereafter. All mice were genotyped using a standardised polymerase chain reaction assay for tail DNA (Transnetyx Inc., USA). Mice were group-housed in standard transparent individually ventilated cages (IVC; 29.5 x 16 x 13 cm) on sawdust under a 12 h light/dark cycle (lights on at 0700 h). Rodent chow and water were available *ad libitum*. Experimentation was performed in accordance with the Prevention of Cruelty to Animals Act (2004), under the guidance of the National Health and Medical Research Council Code of Practice for the Care and Use of Animals for Experimental Purposes in Australia (2013). Individual experiments were approved by The Florey Animal Ethics Committee (AEC number: 15-092 and 19-052). All efforts were made to ensure comfort and minimise the suffering of animals throughout.

Animal behaviour

Animal behaviour, including odour detection test (ODT), locomotor activity (LMA), Y-maze, rotarod, and pole test presented in this chapter are described in detail in Chapter 2.

Tissue analysis

Brains were harvested according to the procedure reported in Chapter 2. Details of tissue analysis, including SDS page and immunoblots, and inductively coupled plasma mass spectrometry (ICP-MS) were all performed according to protocols laid out in Chapter 2.

Compounds

PBT434 was kindly provided by Alterity Therapeutics (formally Prana Biotechnology). PBT434 was sonicated in standard suspension vehicle (SSV) (recipe provided in Chapter 2) 30 minutes before oral gavage dosing. Glyoxalbis(thiosemicarbazone) (referred to as Cu(GTSM) from here) was synthesised and provided by the Donnelly Laboratory (University of Melbourne). Similarly, Cu(GTSM) was sonicated in SSV 30 minutes before oral gavage dosing.

Experimental timelines

PBT434

5.5-month-old tau$^{+/+}$ (n=20) and tau$^{-/-}$ (n=22) (trial 1) and 13.5-month-old tau$^{+/+}$ (n=19) and tau$^{-/-}$ (n=23) (trial 2) animals underwent six weeks (42 days) of daily oral gavage treatment of PBT434 (30mg/kg/day) or SSV control. For the subsequent 7 days animals underwent one behavioural task per day, receiving treatment immediately after completing the behavioural task each day. Behavioural tasks were performed in the order: ODT, LMA, rotarod, pole test, and Y-Maze. The following day animals were dosed 30 minutes before cull.

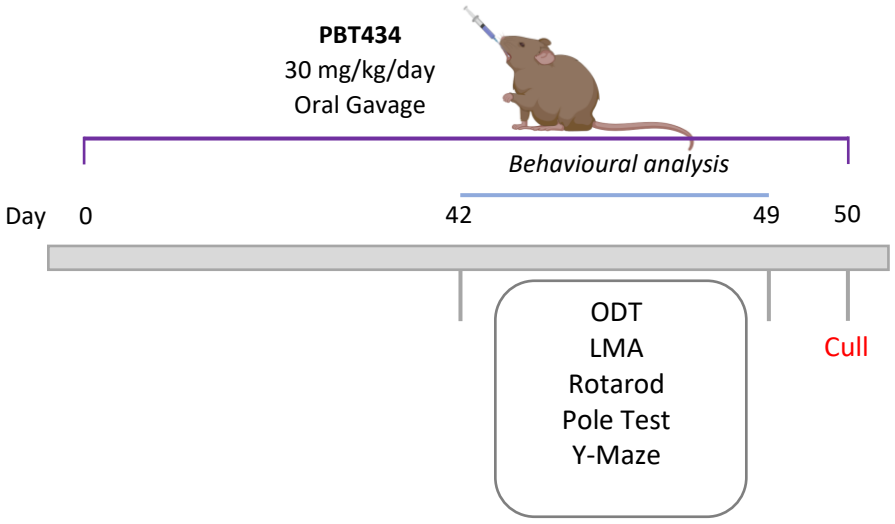

Figure 7.1 Experimental timeline of mice treated with PBT434. Tau$^{+/+}$ and tau$^{-/-}$ 5.5-month-old and 13.5-month-old mice underwent 42 days of daily oral gavage followed by 7 days of behavioural analysis. Animals were 7 (trial 1) and 15 months (trial 2) old at the time of cull on day 50.

Cu(GTSM)

6-month-old tau$^{+/+}$ (n=22) mice underwent 28 days of Cu(GTSM) treatment, broken up into two dosing schedules. For the first 7 days, animals received 1 mg/kg/day to ensure drug tolerance. For the subsequent 21 days the concentration of drug was increased to 3 mg/kg/day, a safe dosing schedule reported in[379]. Animals continued to be dosed for the 7 days of behavioural analysis, receiving treatment immediately after completing the behavioural task each day. Behavioural tasks were performed in the order: ODT, LMA, rotarod, pole test, and Y-Maze. The following day animals were dosed 30 minutes before cull.

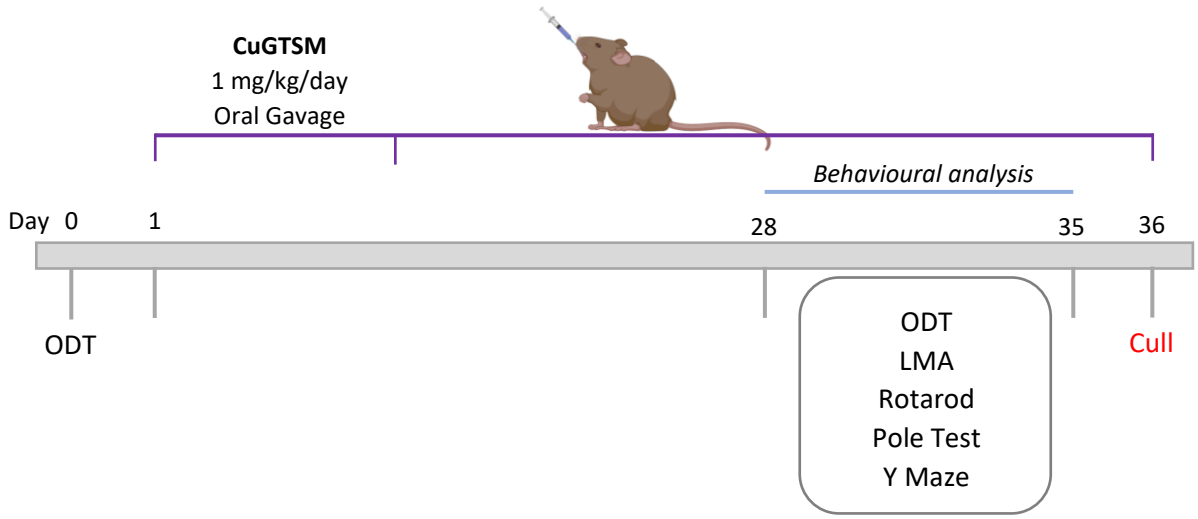

Figure 7.2 Experimental timeline of mice treated with Cu(GTSM). 6-month-old tau$^{+/+}$ underwent 7 days of 1 mg/kg daily oral gavage, followed by 28 days of 3 mg/kg daily oral gavage of which the last 7 days also included behavioural analysis.

Statistical Analysis

For all statistical analyses, the software package GraphPad Prism (version 6.05 for Windows) was used. Data are presented as mean ± standard error of the mean (SEM). Detail including statistical test, replicate number, experimental repeats, and significance are reported in Figure Legends. ANOVA p values reported are from post-hoc comparisons generated only when ANOVA terms were significant. As well as unpaired Students t-tests for comparison between groups, one-sample t-tests were also performed for ODT results to determine if the animals could detect odours at specified concentrations (independent of genotype), as evidenced by spending significantly more than 50% of the investigation time with an odourous canister. An investigation time of 50% represents chance, indicating an animal cannot differentiate between the canisters, i.e. cannot detect an odour. For all analyses, $P<0.05$ was considered statistically significant.

7.4 Results

Young tau$^{-/-}$ mice have metal accumulation in the olfactory bulb

To further test the alignment of the tau knockout (tau$^{-/-}$) mice with human *post-mortem* tissue, bulbar metal levels were compared between wildtype (tau$^{+/+}$) and tau$^{-/-}$ animals at 7-months-old, the age in which animals present with an olfactory impairment. The level of copper (Cu) (↑32.1%, *P*<0.0001), zinc (Zn) (↑31.9%, *P*=0.05), and iron (Fe) (↑11.6%, *P*=0.04) were significantly increased in tau$^{-/-}$ tissue (Figure 7.3). Lead (Pb) was also increased however this result did not reach significance (↑77.7%, *P*=0.06).

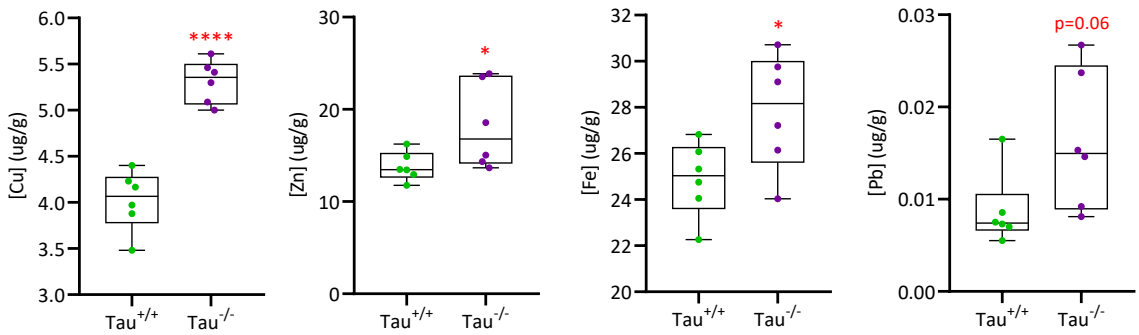

Figure 7.3 Accumulated metals in the olfactory bulb of young tau knockout mice. Increased bulbar metals as measured by inductively coupled plasma mass spectrometry, including copper, zinc, iron, rubidium, and lead. Comparison analysed by unpaired Students t-test. Tau$^{+/+}$ n=6, tau$^{-/-}$ n=6, performed in triplicate; **P*<0.05, *****P*<0.0001.

Aged tau$^{-/-}$ mice have metal accumulation in the substantia nigra pars compacta

Increases in Fe have been reported in substantia nigra pars compacta (SNpc) of Parkinson's disease (PD) patients, as well as multiple animal models of PD aligned with substantial motor deficits. The level of nigral metals was compared between 15-month-old tau$^{+/+}$ and tau$^{-/-}$ animals. Many metals were increased in the tau$^{-/-}$ SNpc, including biometals such as sodium (Na) (↑25.3%, *P*=0.009), calcium (Ca) (↑21.8%, P=0.02), and potassium (K) (↑25.7%, *P*=0.01) (Figure 7.4A). Transition metals of interest that increased are Cu (↑22.7%, *P*=0.02), Zn (↑21.6%, *P*=0.01), and Fe (↑24.2%, *P*=0.04) (Figure 7.4B).

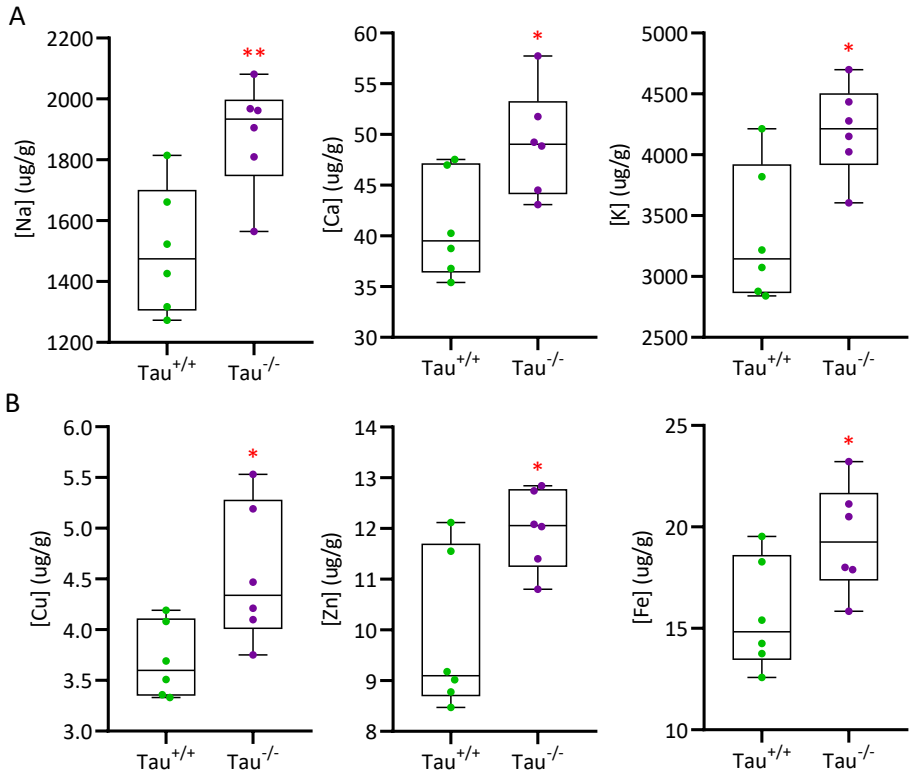

Figure 7.4 Accumulated metals in the substantia nigra pars compacta of aged tau knockout mice. Increased nigral metals as measured by inductively coupled plasma mass spectrometry. **A)** Increased signalling metals, including sodium, calcium, and potassium. **B)** Increased biometals including zinc, copper, and iron. Comparison analysed by unpaired Students t-test. $Tau^{+/+}$ n=6, $tau^{-/-}$ n=6, performed in triplicate; **P*<0.05, ***P*<0.01.

Aged $tau^{-/-}$ mice have a decrease in metals in the caudate putamen

The caudate putamen (CPU) is relatively devoid of dopamine in the later stages of dopamine reflective of synaptic degeneration. The level of putamen metals was compared between 15-month-old $tau^{+/+}$ and $tau^{-/-}$ animals. There was a significant decrease in Na (↓15.2%, *P*=0.01) and K (↓13.5%, *P*=0.01), as well as a decrease in Ca that did not reach significance (↓12.4%, *P*=0.06), possibly reflective of poor neuronal health (Figure 7.5).

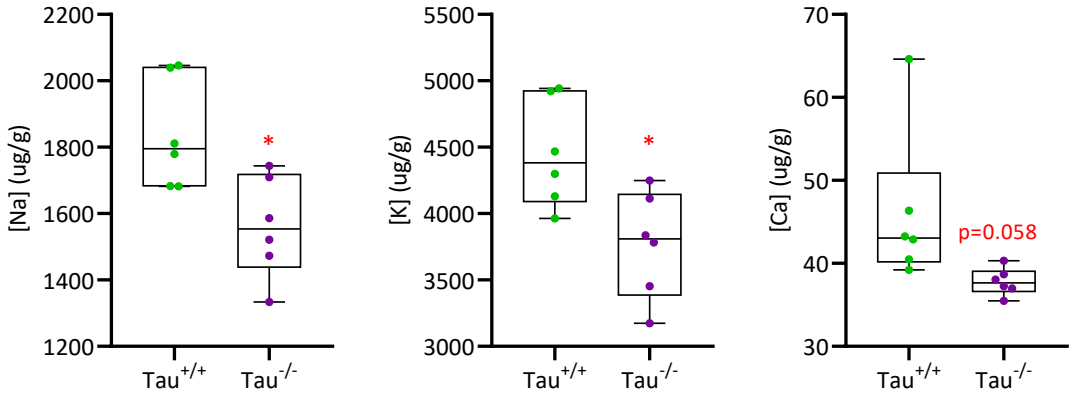

Figure 7.5 Reduced metal levels in the caudate putamen of aged tau knockout mice. Increased putamen metals as measured by inductively coupled plasma mass spectrometry including sodium, potassium, and calcium. Comparison analysed by unpaired Students t-test. $Tau^{+/+}$ n=6, $tau^{-/-}$ n=6, performed in triplicate; *P<0.05.

$Tau^{-/-}$ mice aged to 15 months have hyperlocomotion, motor impairments, and hippocampal memory deficits

Chapter 5 established that $tau^{-/-}$ mice have an olfactory impairment at 7 months of age in the absence of a motor impairment, which isn't overt until at least 15 months of age. As such, a cohort of aged animals were tested for this study to confirm the timing of motor phenotype presentation. Aligned with previous reports[250], aged $tau^{-/-}$ mice from this colony present with a hyperlocomotive phenotype as demonstrated by increased distance travelled (P=0.008; Figure 7.6A and C), increased speed (P=0.0009; Figure 7.6B), and vertical time (P=0.02; Figure 7.6D) on the locomotor activity test. There was a no significant difference in the number of rearing events (Figure 7.6E).

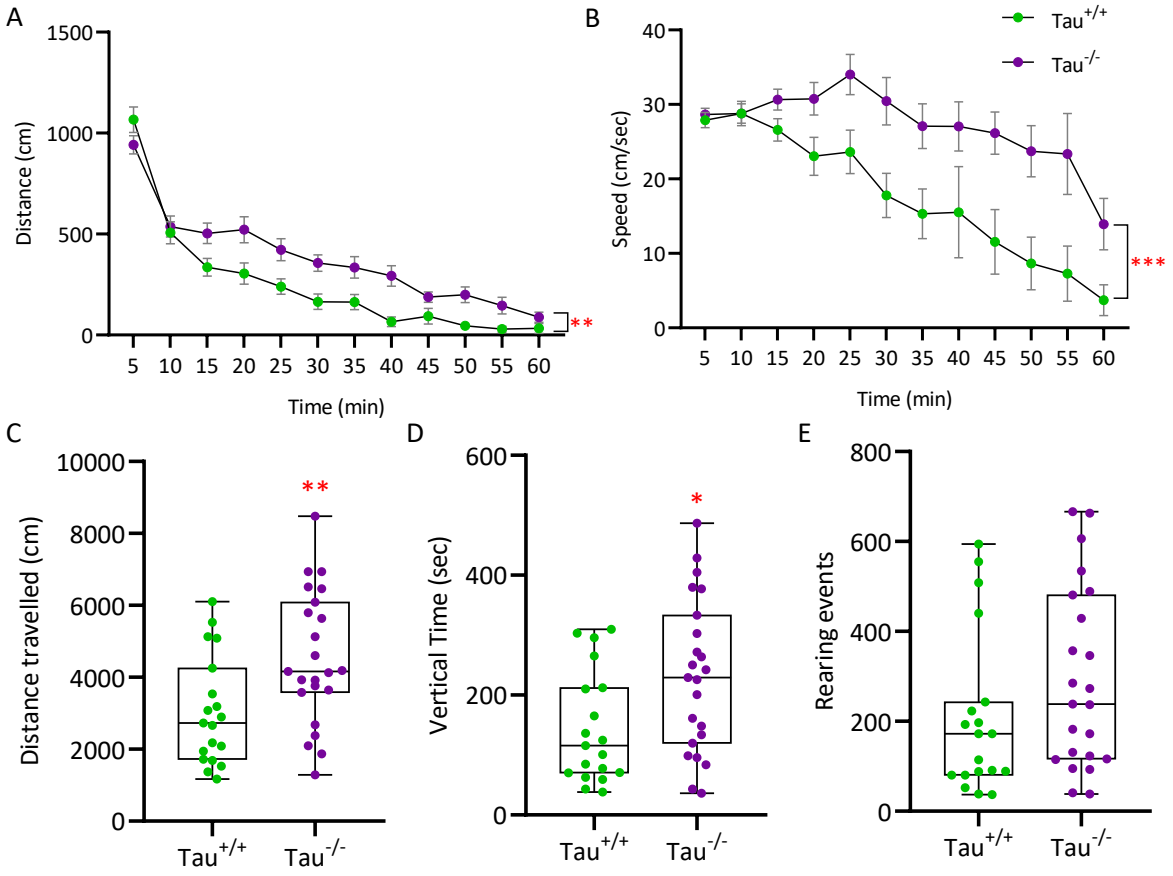

Figure 7.6 Hyperlocomotion in aged tau knockout mice. **A)** Average distance travelled over the 60-minute locomotor activity test. **B)** Average speed over the 60-minute locomotor activity test. **C)** The total distance travelled, **D)** vertical time, and **E)** number of rearing events during the locomotor activity test. $Tau^{+/+}$ (n=20) and $tau^{-/-}$ mice (n=23). Distance and speed across the 60-minute trial analysed via two-way ANOVA; all other comparisons analysed by unpaired Students T test. **P*<0.05, ***P*<0.01, ****P*<0.001.

Aged tau$^{-/-}$ mice also present with a motor impairment as indicated by a reduced latency to fall on the rotarod (*P*=0.02; Figure 7.7A) and increased total time (*P*=0.0002; Figure 7.7B) and turn time (*P*=0.001; Figure 7.7C) on the pole test.

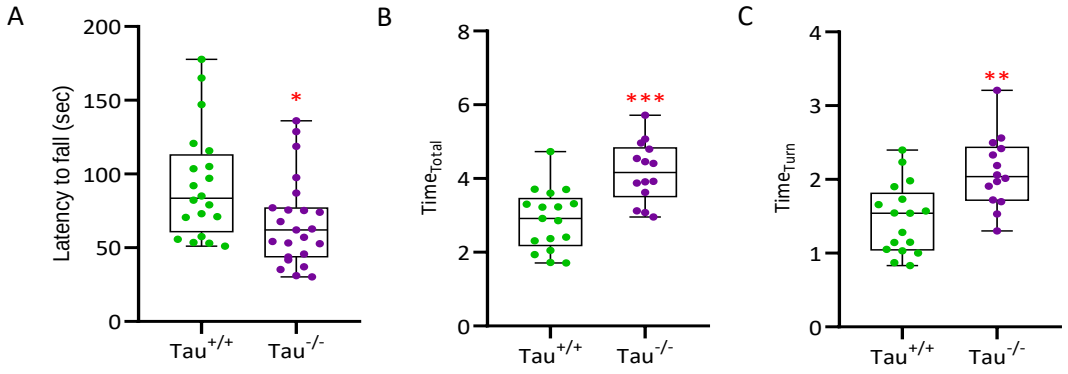

Figure 7.7 Motor impairment in aged tau knockout mice. **A)** Latency to fall on the rotarod, **B)** total time to complete the pole test, **C)** time to turn on the pole test. Tau$^{+/+}$ (n=20) and tau$^{-/-}$ mice (n=23). Comparisons analysed by unpaired Students T test. **P*<0.05, ***P*<0.01, ****P*<0.001.

Finally, tau$^{-/-}$ mice have a significantly reduced exploration time (*P*<0.0001; Figure 7.8A) and arm entry score (*P*=0.003; Figure 7.8B) of the novel arm of the Y-maze compared to tau$^{+/+}$ mice, reflective of a hippocampal memory deficit.

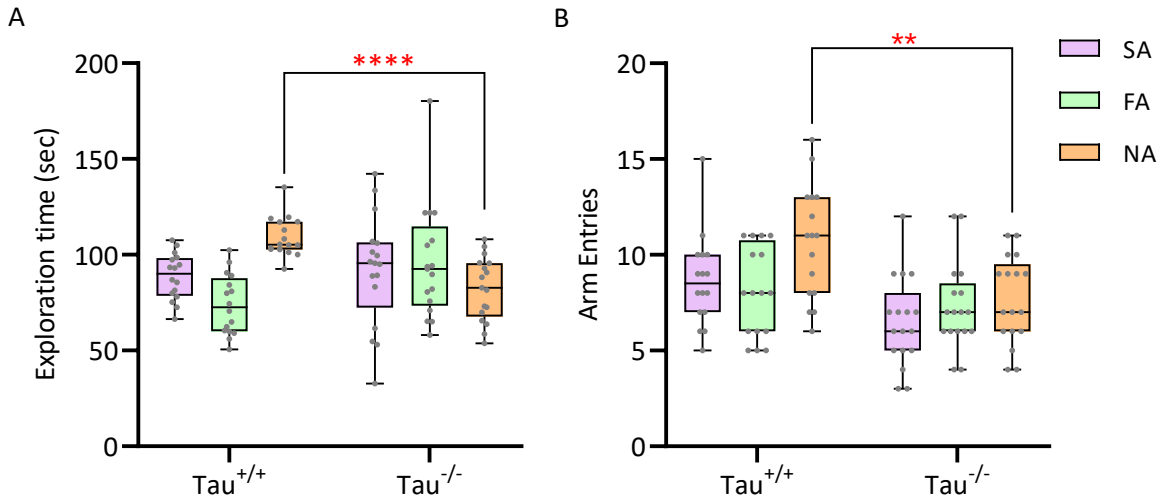

Figure 7.8 Cognitive deficit in aged tau knockout mice. **A)** Exploration time of the three-armed Y-maze, **B)** number of arm entries in the three-armed Y-maze. SA: starting arm, FA: familiar arm, NA: novel arm. Tau$^{+/+}$ (n=20) and tau$^{-/-}$ mice (n=23). Y-maze analysed by unpaired Students t-test between individual arms. ***P*<0.01, *****P*<0.0001.

Treatment with PBT434 rescues the olfactory deficit of young tau$^{-/-}$ mice

To ascertain if increased metal levels contributed to hyposmia in the 7-month-old tau$^{-/-}$ mice, 5.5-month-old tau$^{+/+}$ and tau$^{-/-}$ animals were treated with either PBT434, a Fe/Cu chelator, or SSV for 6 weeks. During the odour detection test (ODT), tau$^{+/+}$ that were treated with vehicle spent significantly more time exploring the odourous cannister compared to the control trial and compared to chance (P<0.0001, P<0.0001, respectively; Figure 7.9 (left)). Tau$^{+/+}$ animals treated with PBT434 spent significantly more time exploring the odourous cannister compared to the control trial and compared to chance (P<0.0001, P=0.0002, respectively; Figure 7.9 (left)). Tau$^{-/-}$ mice that were treated with vehicle did not detect the novel odour, as demonstrated by a lack of exploration time differing from the control trial or chance. Tau$^{-/-}$ animals treated with PBT434 spent significantly more time exploring the odourous cannister compared to the control trial and compared to chance (P<0.0001, P=0.0001, respectively; Figure 7.9 (right)).

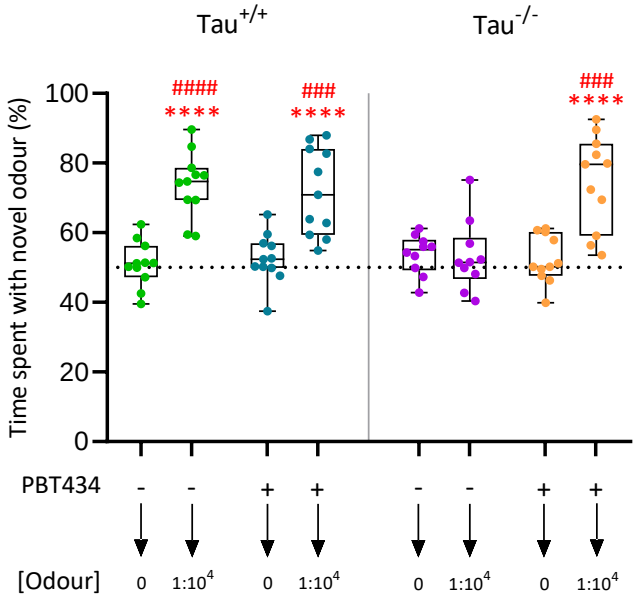

Figure 7.9 PBT434 rescued the hyposmia in young tau knockout mice. Odour detection test of tau $^{+/+}$ (n=22) and tau$^{-/-}$ (n=21) mice treated with either vehicle or PBT434. Left: tau$^{+/+}$ mice treated with vehicle (n=11) or PBT434 (n=11). Right: tau$^{-/-}$ mice treated with vehicle (n=10) or PBT434 (n=11). Data is presented as % time spent with novel odour cannisters compared to vehicle cannisters. Comparison of treatment groups performed by one-way ANOVA; **** P<0.0001. Comparison of individual groups to chance (50%, dotted line) performed by one-sample T test (hypothetical mean of 50%); #### P<0.0001.

Treatment with PBT434 lowered metal levels in the olfactory bulb of 7-month-old tau$^{-/-}$ mice

The level of bulbar metals and neuronal markers were compared between vehicle and PBT434 treated tau$^{+/+}$ and tau$^{-/-}$ animals. There was a significant increase in Cu (P=0.0005), Zn (P=0.05), Fe (P=0.04), and Pb (P=0.04) between vehicle treated tau$^{+/+}$ and tau$^{-/-}$ mice. There were no significant changes between treated and untreated tau$^{+/+}$ mice, as such, only the levels of vehicle treated animals are

presented as a relative value for comparison of tau$^{-/-}$ treatment effects. The level of Cu (↓17.9%), Zn (↓22.2%), Fe (↓9.8%), and Pb (↓56.2%) were reduced in PBT434 treated tau$^{-/-}$ animals to tau$^{+/+}$ levels (Figure 7.10A).

Synaptophysin is a membrane protein localised to synaptic vesicles, and neuronal nuclei (NeuN) is a neuron-specific nuclear protein. The level of synaptophysin is used as a semi-quantitative marker of synaptic health, as is NeuN for number of neurons. There is a significant reduction in the bulbar protein expression levels of synaptophysin between tau$^{+/+}$ and tau$^{-/-}$ (P<0.0001), which was partially rescued by treatment with PBT434 (P=0.01) (Figure 7.10B and C). Similarly, there was a significant reduction in the neuronal marker NeuN between tau$^{+/+}$ and tau$^{-/-}$ mice (P=0.0007), which was partially rescued by treatment with PBT434 (P=0.02) (Figure 7.10B and C).

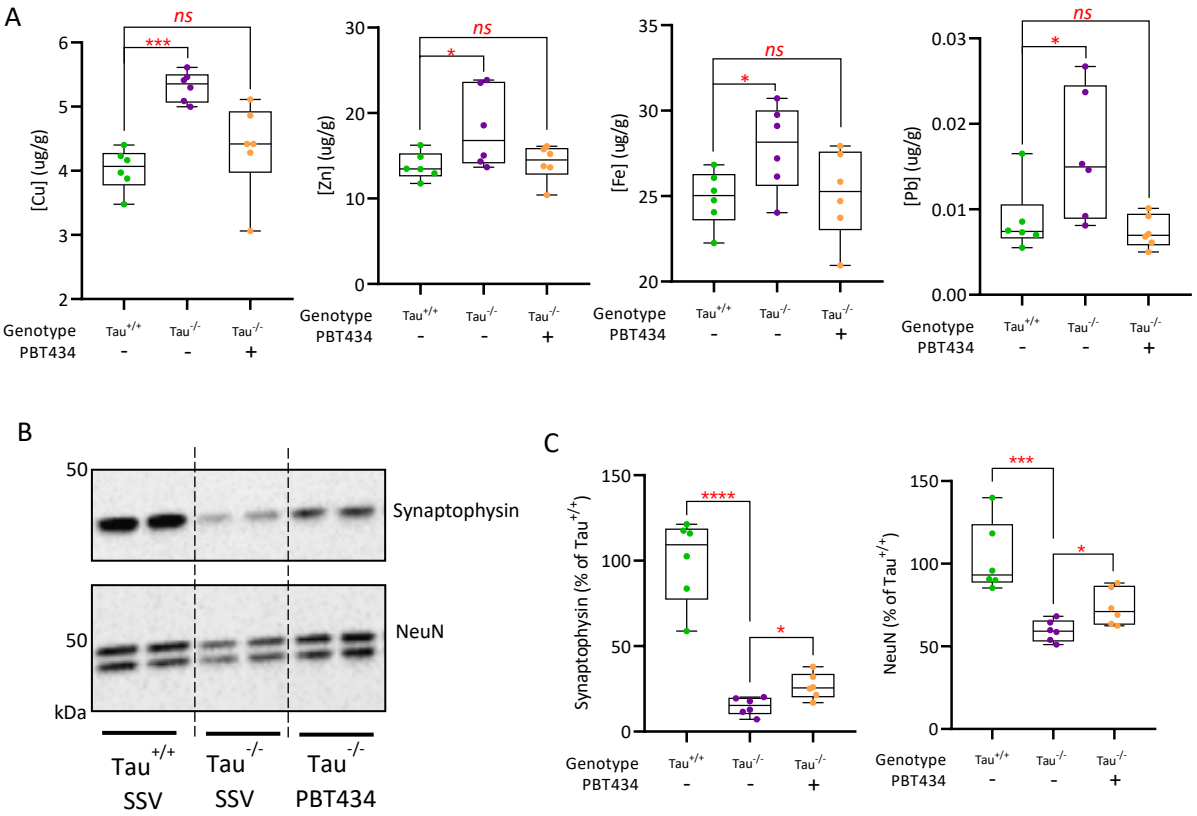

Figure 7.10 PBT434 reduced metals and increased neuronal markers in the olfactory bulb of young tau knockout mice. **A)** Reduced bulbar metals in PBT434 treated tau$^{-/-}$ mice, measured by inductively coupled plasma mass spectrometry, including copper, zinc, iron, rubidium, and lead. **B)** Representative western blots of olfactory bulb homogenate from tau$^{+/+}$ SSV treated (n=6), tau$^{-/-}$ SSV treated (n=6), and tau$^{-/-}$ PBT434 treated (n=6) probed for synaptophysin and NeuN. **C)** Quantification of western blot densitometry presented as % of synaptophysin and NeuN relative to tau$^{+/+}$ SSV treated control. Homogenate for western blots normalised to automated total protein measurement via ChemiDoc stain-free detection software. ICP-MS tau$^{+/+}$ n=6, tau$^{-/-}$ n=6, ICP-MS analysis performed in triplicate. Western blot analysed from 3 independent repeats. Comparison of treatment groups performed by one-way ANOVA; *P<0.05, **P<0.01, ***P<0.001, ****P<0.0001.

Treatment with PBT434 rescues the motor deficit of 15-month-old tau$^{-/-}$ mice

To ascertain if metal reduction was similarly able to alleviate the motor impairment in tau$^{-/-}$ animals, 13.5-month-old tau$^{+/+}$ and tau$^{-/-}$ mice were treated with either PBT434 or SSV for 6 weeks. There was a significant decrease in the latency to fall between vehicle treated tau$^{+/+}$ and tau$^{-/-}$ mice (P=0.005), and PBT434 treatment resulted in a significant increase in this latency in tau$^{-/-}$ mice (P=0.03) (Figure 7.11A). There was a significant increase in the total time on the pole test between vehicle treated tau$^{+/+}$ and tau$^{-/-}$ mice (P=0.008), which was reduced in PBT434 treated tau$^{-/-}$ mice (P=0.05) (Figure 7.11B). There was a significant increase in the turn time on the pole test between vehicle treated tau$^{+/+}$ and tau$^{-/-}$ mice (P=0.0005), which was reduced in PBT434 treated tau$^{-/-}$ mice (P=0.02) (Figure 7.11C).

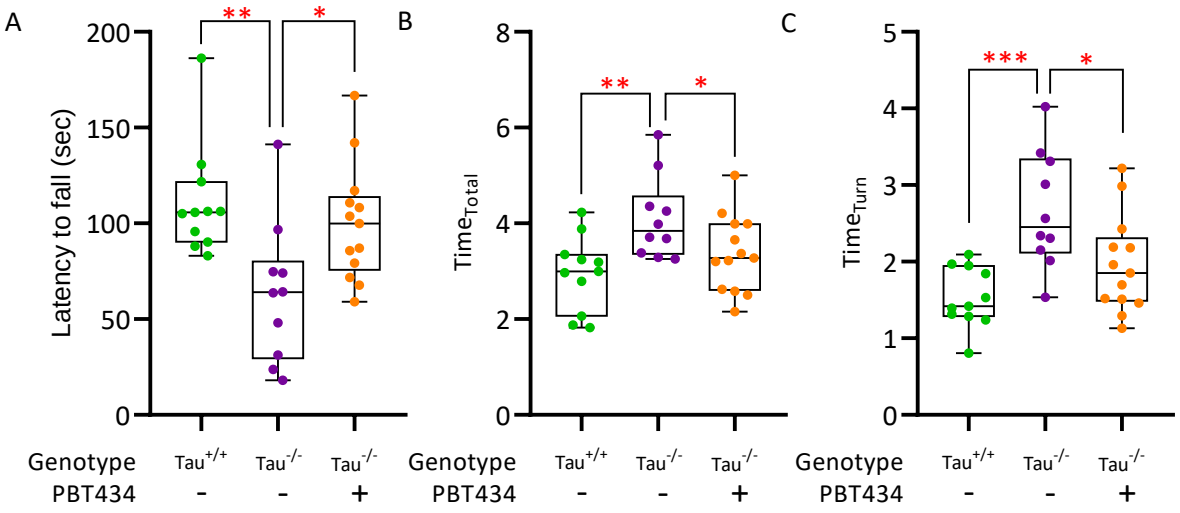

Figure 7.11. PBT434 rescued the motor deficit in aged tau knockout mice. **A)** Latency to fall off the rotarod, **B)** average total time to turn on the pole test and **C)** average time to turn on the pole test. Tau$^{+/+}$ treated with SSV (n=11), tau$^{-/-}$ treated with SSV (n=10) and tau$^{-/-}$ treated with PBT434 (n=13). Analysed by one-way ANOVA. *P<0.05, **P<0.01, ***P<0.001, ****P<0.0001.

Treatment with PBT434 had no effect on the hyperlocomotion or hippocampal memory deficit of aged tau$^{-/-}$ mice

Metal reduction was able to alleviate the motor impairment in the aged tau$^{-/-}$ animals, however there was no difference in the locomotor or y-maze performance between treated and untreated mice. Vehicle and PBT434 treated tau$^{-/-}$ mice travelled further (P=0.0005, P=0.001; Figure 7.12A and C), had increased speed (P=0.02, P=0.01; Figure 7.12B) and had increased vertical time (P=0.009, P=0.02; Figure 7.12D). There was no significant difference between vehicle and PBT434 treated tau$^{-/-}$ mice in locomotor measures.

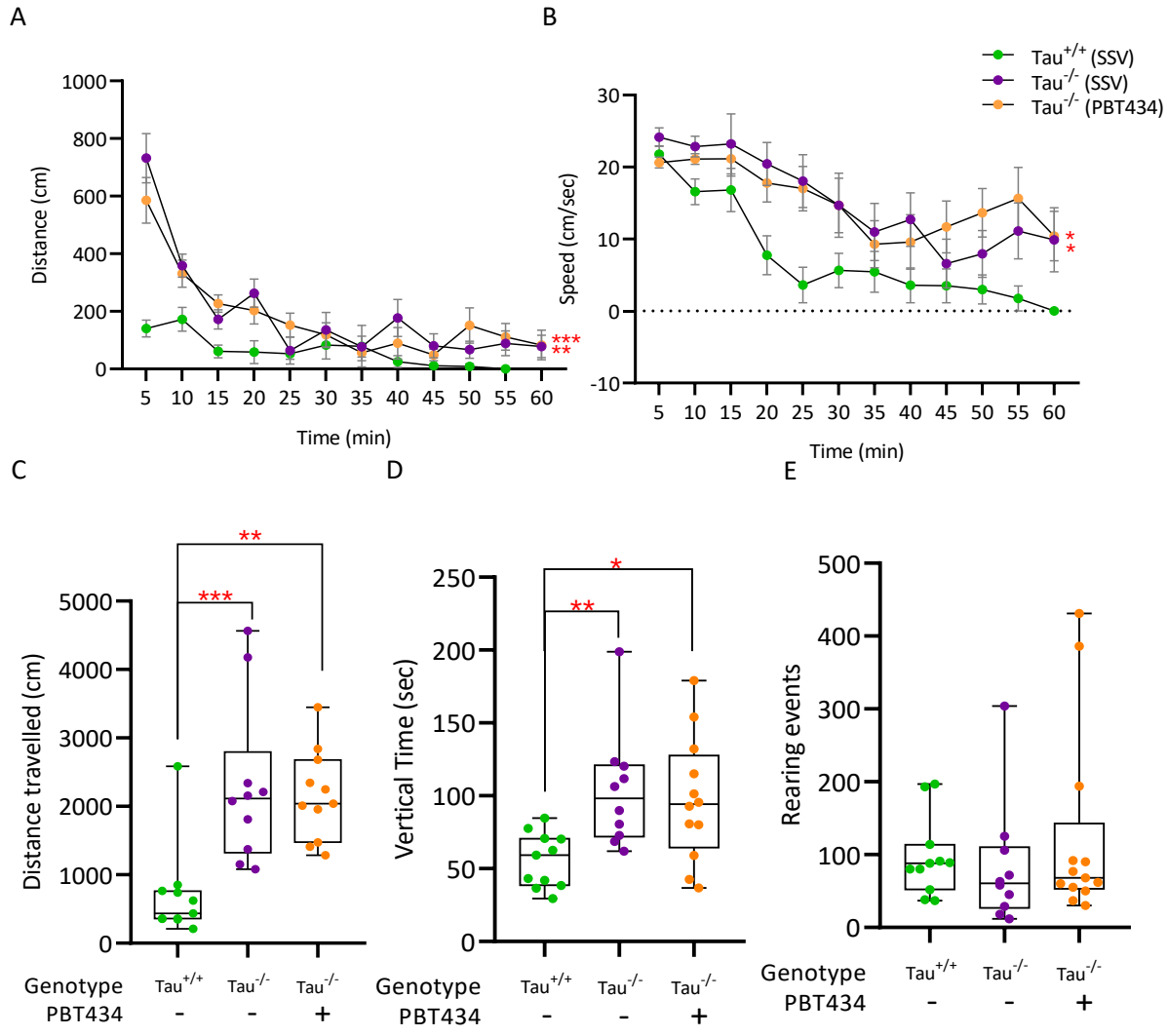

Figure 7.12 PBT434 had no overt effect on locomotion or exploratory behaviour in aged tau knockout mice. **A)** Average distance travelled over the 60-minute locomotor activity test. **B)** Average speed over the 60-minute locomotor activity test. **C)** The total distance travelled, **D)** vertical time, and **E)** number of rearing events during the locomotor activity test. Tau$^{+/+}$ treated with SSV (n=11), tau$^{-/-}$ treated with SSV (n=10) and tau$^{-/-}$ treated with PBT434 (n=13). Distance and speed across the 60-minute trial analysed via two-way ANOVA, all other comparisons analysed by one-way ANOVA. *P<0.05, **P<0.01, ***P<0.001.

There was a spatial memory deficit present in both vehicle and PBT434 treated animals demonstrated by a significant reduction in novel arm exploration time (*P*=0.01, *P*=0.002; Figure 7.13A) and novel arm entries (*P*=0.01. *P*=0.02; Figure 7.13B). There was no significant difference in either measures between vehicle and PBT434 treated tau$^{-/-}$ mice, suggesting PBT434 treatment had no effect on spatial memory deficits.

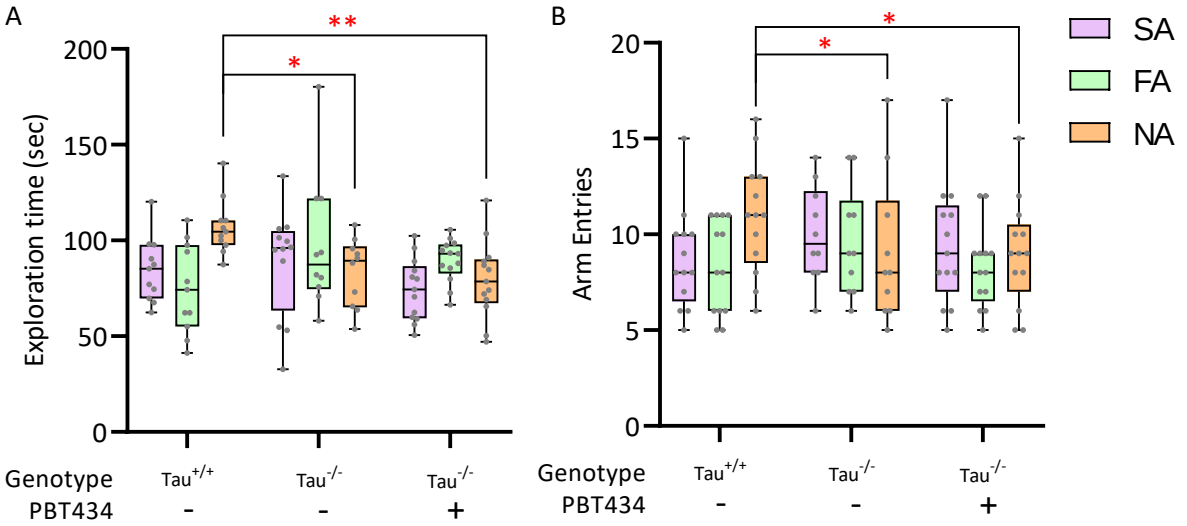

Figure 7.13 PBT434 had no overt effect on cognitive deficits in aged tau knockout mice. **A)** Exploration time of the three-armed Y-maze, **B)** number of arm entries in the three-armed Y-maze. SA: starting arm, FA: familiar arm, NA: novel arm. Tau$^{+/+}$ treated with SSV (n=11), tau$^{-/-}$ treated with SSV (n=10) and tau$^{-/-}$ treated with PBT434 (n=13). Y-maze analysed two-way ANOVA. *P<0.05, **P<0.01.

Treatment with PBT434 lowered iron in the substantia nigra pars compacta and increased sodium and potassium of 15-month-old tau$^{-/-}$ mice

The level of nigral metals was compared between vehicle and PBT434 treated tau$^{+/+}$ and tau$^{-/-}$ animals. There were no significant changes in the metal levels between treated and untreated tau$^{+/+}$ mice, as such, only the levels of untreated animals are presented as a relative value for comparison of tau$^{-/-}$ treatment effects. Iron was significantly increased (*P*=0.03) between vehicle treated tau$^{+/+}$ and tau$^{-/-}$ mice, and PBT434 treatment reduced tau$^{-/-}$ Fe (↓12.6%) back to tau$^{+/+}$ levels (Figure 7.14A). There was a significant reduction in the nigral protein expression levels of synaptophysin between tau$^{+/+}$ and tau$^{-/-}$ (*P*=0.03), which was rescued by treatment with PBT434 (*P*=0.02) (Figure 7.14B and C). Similarly, there was a significant reduction in the neuronal marker NeuN between tau$^{+/+}$ and tau$^{-/-}$ mice (*P*=0.004), which was rescued by treatment with PBT434 (*P*=0.04) (Figure 7.14B and C).

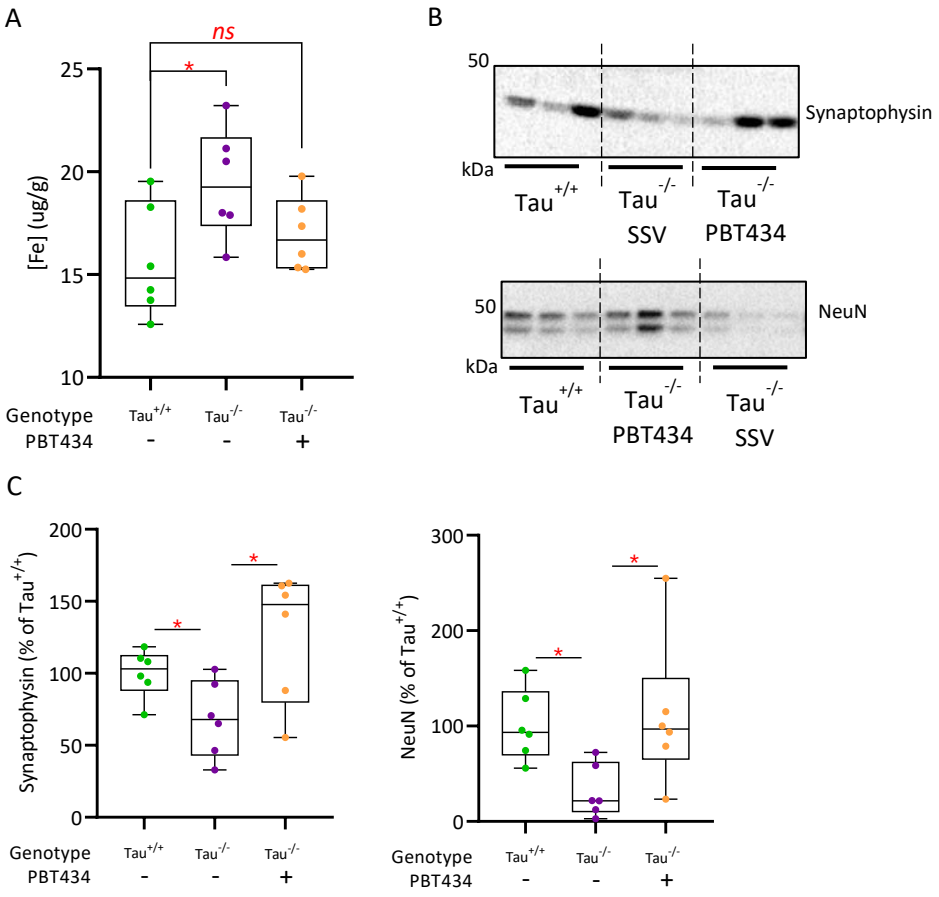

Figure 7.14 PBT434 altered metals and increased neuronal markers in the substantia nigra pars compacta of aged tau knockout mice. **A)** Reduced Fe in the SNpc as measured by ICP-MS. **B)** Representative western blots of SNpc homogenate from tau$^{+/+}$ SSV treated (n=6), tau$^{-/-}$ SSV treated (n=6), and tau$^{-/-}$ PBT434 treated (n=6) probed for synaptophysin and NeuN. **C)** Quantification of SNpc western blot densitometry presented as % of synaptophysin and NeuN relative to tau$^{+/+}$ SSV treated control. Homogenate for western blots normalised to automated total protein measurement via ChemiDoc stain-free detection software. ICP-MS tau$^{+/+}$ n=6, tau$^{-/-}$ n=6, ICP-MS analysis performed in triplicate. Western blot analysed from 3 independent repeats. Comparison of treatment groups performed by one-way ANOVA; *P<0.05, **P<0.01

The level of metals in the CPU was compared between vehicle and PBT434 treated tau$^{+/+}$ and tau$^{-/-}$ animals. There were no significant changes in the metal levels between treated and untreated tau$^{+/+}$ mice, as such, only the levels of untreated animals are presented as a relative value for comparison of tau$^{-/-}$ treatment effects. Na and K were significantly decreased (P=0.006, P=0.01) between vehicle treated tau$^{+/+}$ and tau$^{-/-}$ mice, and PBT434 treatment increased tau$^{-/-}$ Na (↑14.1%) and K (↑13.3%) back to tau$^{+/+}$ levels (Figure 7.15A).

There was a significant reduction in the CPU protein expression levels of synaptophysin between tau$^{+/+}$ and tau$^{-/-}$ (*P*=0.002), which was partially rescued by treatment with PBT434 (*P*=0.02) (Figure 7.15B and C). Similarly, there was a significant reduction in the neuronal marker NeuN between tau$^{+/+}$ and tau$^{-/-}$ mice (*P*=0.007), however this was not rescued by treatment with PBT434 (Figure 7.15B and C).

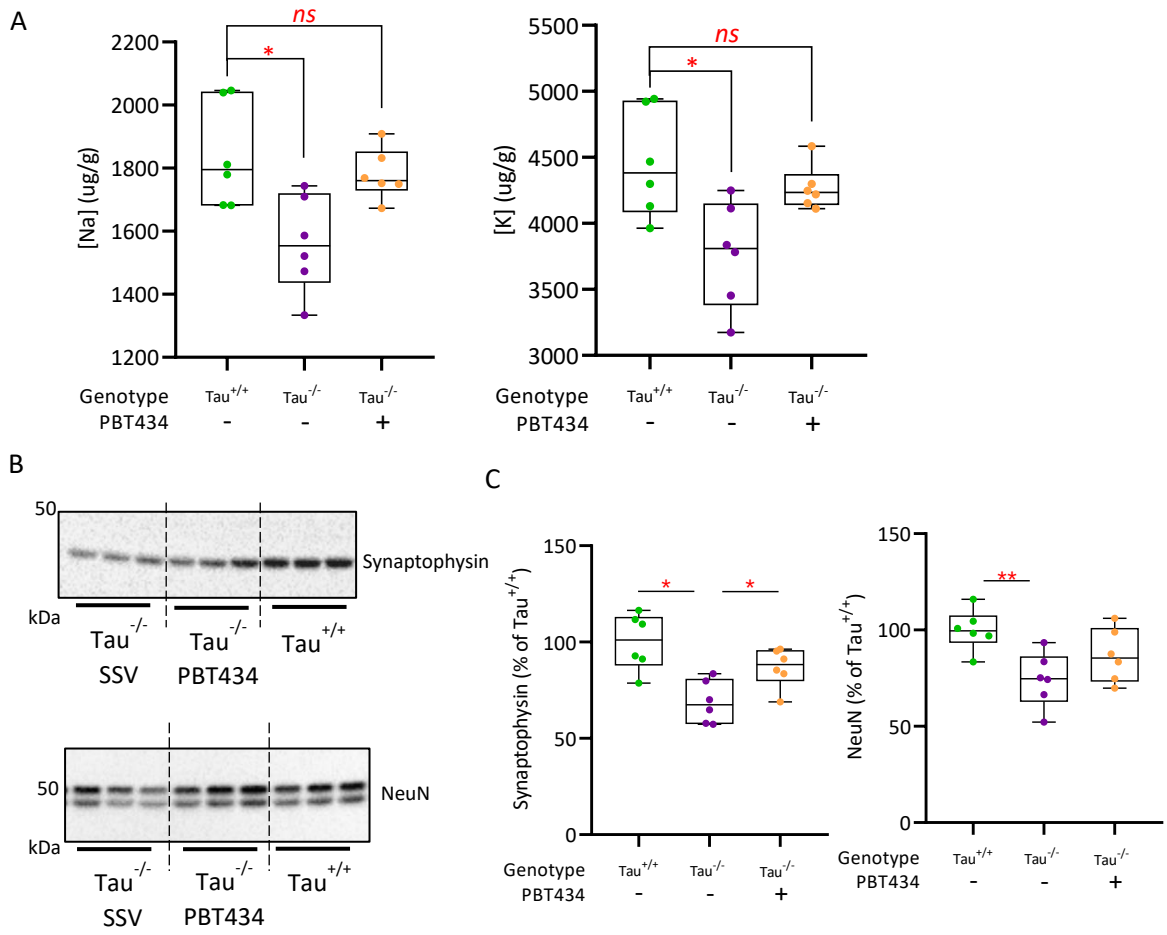

Figure 7.15 PBT434 altered metals and increased neuronal markers in the caudate putamen of aged tau knockout mice. **A)** Increased Na and K in the CPU as measured by ICP-MS. **B)** Representative western blots of CPU homogenate from tau$^{+/+}$ SSV treated (n=6), tau$^{-/-}$ SSV treated (n=6), and tau$^{-/-}$ PBT434 treated (n=6) probed for synaptophysin and NeuN. **C)** Quantification of CPU western blot densitometry presented as % of synaptophysin and NeuN relative to tau$^{+/+}$ SSV treated control. Homogenate for western blots normalised to automated total protein measurement via ChemiDoc stain-free detection software. ICP-MS tau$^{+/+}$ n=6, tau$^{-/-}$ n=6, ICP-MS analysis performed in triplicate. Western blot analysed from 3 independent repeats. Comparison of treatment groups performed by one-way ANOVA; **P*<0.05, ***P*<0.01

Treatment with Cu(GTSM) induced hyposmia in 6-month-old tau$^{+/+}$ mice

There was a significant elevation of Cu in the OB of young hyposmic tau$^{-/-}$ mice. To investigate whether increased Cu was able to contribute to dysfunctional olfaction and mimic the deficits seen in tau$^{-/-}$ mice, healthy tau$^{+/+}$ were treated with the copper delivery agent Cu(GTSM) for four weeks. Untreated animals spent significantly more time with the 1:10^6 odourous cannister compared to control trial and chance (P=0.0002; P=0.0009; respectively) and with the 1:10^4 odourous cannister compared to control trial and chance (P<0.0001; P<0.0001; respectively) (Figure 7.16). There was no significant preference for odourous canisters in the Cu(GTSM) treated mice, reflective of olfactory dysfunction (Figure 7.16).

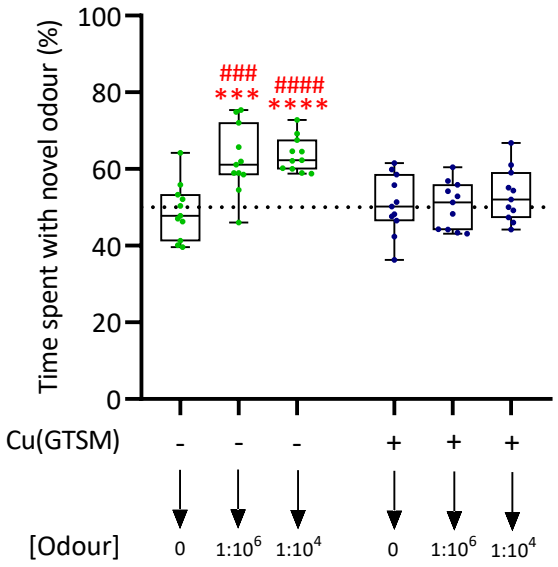

Figure 7.16 Cu(GTSM) induced an olfactory deficit in young wildtype mice. Odour detection test with multiple odour dilutions of tau$^{+/+}$ treated with SSV (n=11) and Cu(GTSM) (n=11). Data is presented as % time spent with novel odour cannisters compared to vehicle canisters. Comparison of treatment groups performed by one-way ANOVA; *** P<0.001, **** P<0.0001. Comparison of individual groups to chance (50%, dotted line) performed by one-sample T test (hypothetical mean of 50%); ### P<0.001, #### P<0.0001.

Treatment with Cu(GTSM) had no effect on motor skills of 6-month-old tau$^{+/+}$ mice

The hyposmia present in these animals was not associated with motor impairments, as treated animals performed equally to their untreated control littermates on the rotarod and pole test (Figure 7.17). Similarly, there was no change in locomotive or exploratory behaviour in treated mice (Figure 7.18)

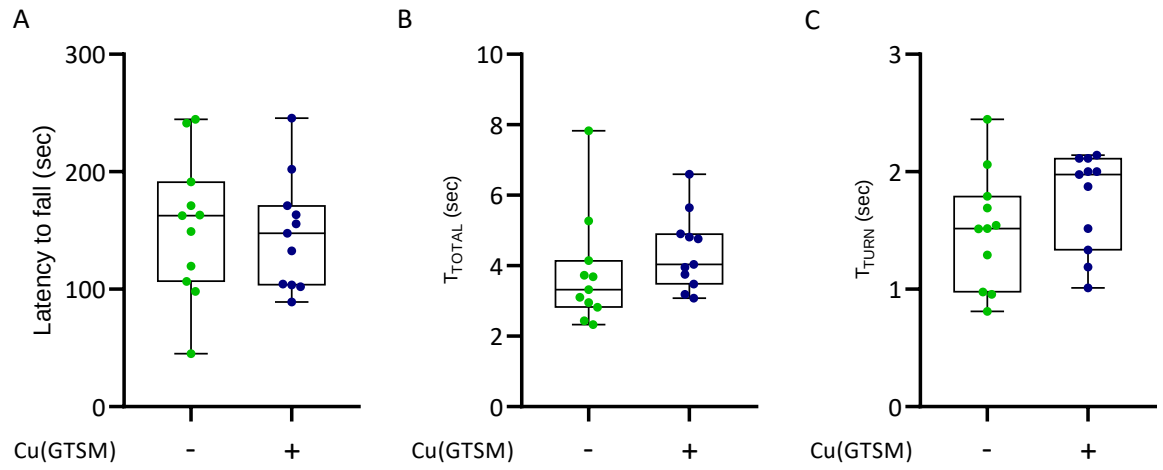

Figure 7.17 Cu(GTSM) had no overt effect on motor skills in young wildtype mice. **A)** Latency to fall off the rotarod, **B)** average total time to turn on the pole test and **C)** average time to turn on the pole test. $Tau^{-/-}$ SSV treated (n=11) $tau^{-/-}$ PBT434 treated (n=11). Analysed by unpaired Students T test.

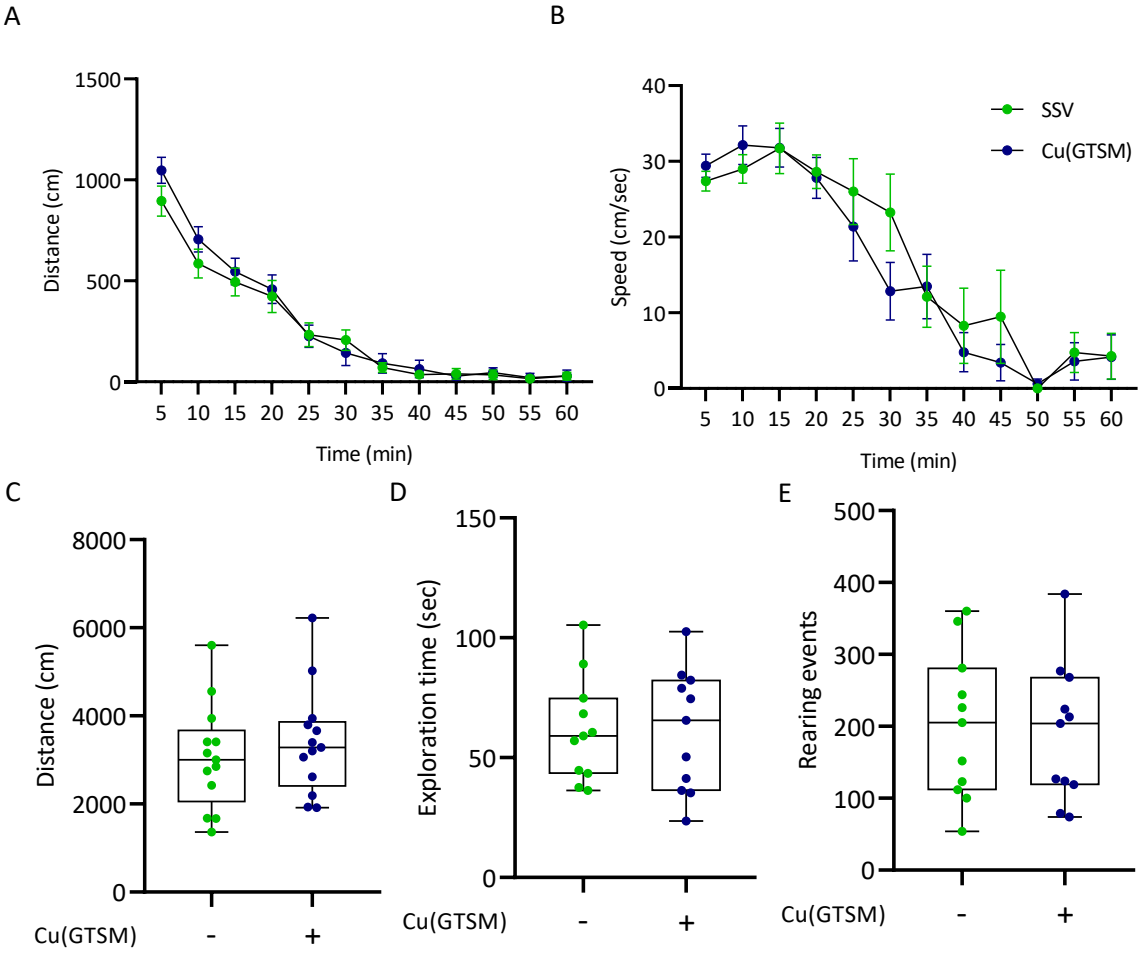

Figure 7.18 Cu(GTSM) had no overt effect on locomotion or exploratory behaviour in young wildtype mice. **A)** Average distance travelled over the 60-minute locomotor activity test. **B)** Average speed over the 60-minute locomotor activity test. **C)** The total distance travelled, **D)** vertical time, and **E)** number of rearing events during the locomotor activity test. $Tau^{+/+}$ treated with SSV (n=13) and or Cu(GTSM) (n=14). Distance and speed across the 60-minute trial analysed via two-way ANOVA, all other comparisons analysed by unpaired Students T test.

Treatment with Cu(GTSM) induced a hippocampal memory deficit in 6-month-old tau$^{+/+}$ mice

Finally, there was a significant reduction in the amount of time Cu(GTSM) treated mice spent in the novel arm of the Y-Maze (*P*=0.01; Figure 7.19A), and the number of entries into the novel arm (*P*=0.009; Figure 7.19B).

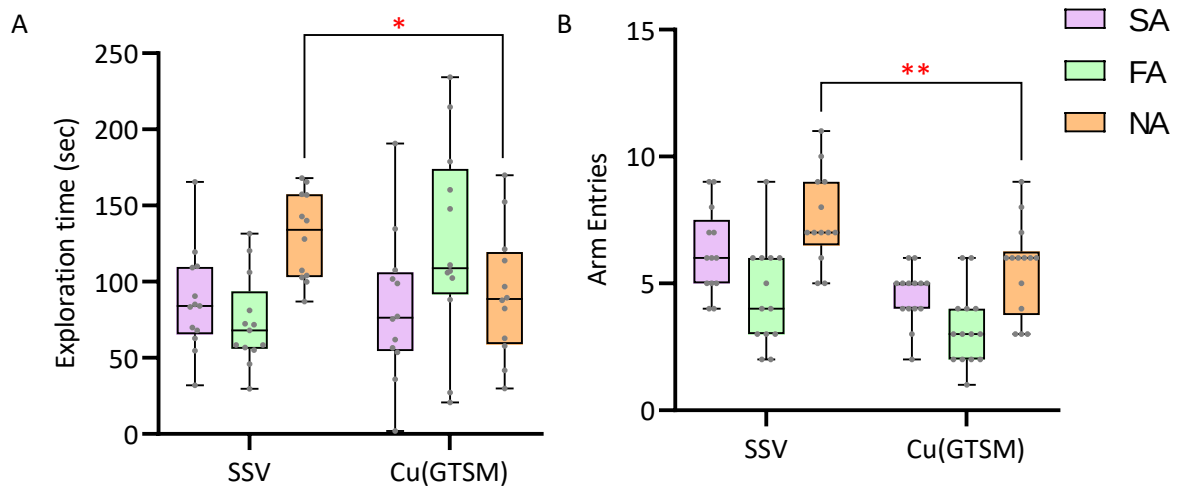

Figure 7.19 Cu(GTSM) induced a cognitive deficit in young wildtype mice. **A)** Exploration time of the three-armed Y-maze, **B)** number of arm entries in the three-armed Y-maze. NA: novel arm, FA: familiar arm, SA: starting arm. SSV treated (n=13) and Cu(GTSM) treated (n=14). Y-maze analysed by two-way ANOVA. **P*<0.05, ***P*<0.01.

7.4 Discussion

The tau knockout (tau$^{-/-}$) mice have been proposed as an age-dependent model of Parkinson's disease (PD), as they have a motor impairment that is associated with degeneration of nigrostriatal dopaminergic neurons and accumulation of nigral iron (Fe)[26], a key feature of the human condition. As reported in Chapter 5, tau$^{-/-}$ animals have an olfactory impairment at 7 months of age, before the onset of the motor impairment at 15 months, modeling the timing of symptom onset in PD. To expand on these findings, this study aimed to analyse the levels of metals in the brain regions related to both olfactory and motor impairment at the ages of symptom onset. This study has demonstrated that young tau$^{-/-}$ mice have an increase in bulbar zinc (Zn), copper (Cu), and Fe that is concurrent with olfactory impairments. Furthermore, there is an increase in nigral Zn, Cu, and Fe in the substantia nigra pars compacta (SNpc), as well as a reduction in metals in the caudate putamen (CPU), that is concurrent with motor impairments in aged animals.

The role of accumulated metals, in particular Cu and Fe, in the behavioural dysfunction in both brain regions was investigated using the Cu/Fe chelator PBT434. Young animals treated with PBT434

demonstrated a rescue in odour detection ability, which was aligned with a reduction in all three metals, as well as a significant increase in protein expression of neuronal nuclei (NeuN) and synaptophysin. Aged animals had a significant restoration of motor capacity, which was aligned with a decrease in Fe in the SNpc, as well as an increase in sodium (Na) and potassium (K) in the CPU. These findings were aligned with a significant increase in protein expression of NeuN and synaptophysin in both regions. Finally, wildtype ($tau^{+/+}$) mice treated with Cu(GTSM) had impaired olfaction and a hippocampal memory deficit in the absence of motor impairments.

Three abundant transition metals in the human brain are Fe, Zn, and Cu – all three of which are significantly increased in the $tau^{-/-}$ olfactory bulb (OB) and SNpc. Alterations in metal storage, transport, and cellular handling are of interest in many neurodegenerative diseases, and each of the aforementioned metals has been implicated in PD. The status of Zn in PD is the most ambiguous of the biometals. Zn has been reported to be *decreased* in blood[380] and serum[381], however others have reported an *increase* in Zn in the serum[382] and cerebrospinal fluid (CSF)[383] in PD samples. *In vitro* intracellular Zn accumulated in tyrosine hydroxylase (TH) positive mouse striatum primary neurons treated with either 1-methyl-4-phenylpyridinium (MPP+) or 6-hydroxydopamine (6-OHDA)[384]. This accumulation is also seen *in vivo* in 1-methyl-4-phenyl-1,2,3,6-tetrahydropyridine (MPTP) and 6-OHDA treated mice, accompanied by the death of dopaminergic neurons[384]. The increase in Zn and the decrease is synaptophysin and NeuN in the $tau^{-/-}$ animals aligns with the findings in these toxin-based models of PD.

Cu is a metal of interest in PD for a number of reasons. Firstly, Cu is found in relatively high concentrations within Lewy bodies and is effective at causing fibrillation and 'seeding' of protein aggregates[385]. In line with this is the finding that Cu is found in relatively high concentrations within Lewy bodies. Secondly, Cu is a key cofactor in cellular antioxidants known to be altered in PD[386-391]. The reliance on Cu of these key antioxidants represents an interesting duality of the metal, as free Cu ions are able to participate in Fenton-like reactions to generate reactive oxygen species, therefore causing oxidative stress and subsequent neurodegeneration, a known phenomenon in PD. It is this latter mechanism of Cu involvement that is of interest in this animal model, as the mice have concurrent Cu accumulation and reductions in NeuN and synaptophysin in the SNpc and OB.

As described earlier, an increase in Fe in the SNpc is a well-established phenomenon in PD[241, 370, 392-394]. The Fe accumulation reported seems to have regional differences, however, as there are studies that report no significant difference between PD and age-matched controls in the caudate or the putamen[241, 370, 394, 395], a pattern that is reflected in our findings in the $tau^{-/-}$ mice. Ferritin is the protein responsible for storing iron within a cell, and there are reported alterations in the distribution of

ferritin in PD[396, 397]. Inadequate storage and accumulation of Fe are postulated to contribute to oxidative stress in PD, and this animal model has demonstrated accumulation of Fe in both regions of interest.

The tau$^{-/-}$ mice have significant increases in biometals, suggesting that this animal model has dysfunctions in metal homeostasis. A previous study by Lei et al. demonstrated an accumulation of Fe in the SNpc that was correlated to neurodegeneration[26], a concurrence that can also been seen in this study based on the increased Fe and reduction in synaptic and neuronal markers in the SNpc of aged tau$^{-/-}$ mice. The reduction in metals Ca, K, and Na in the CPU at this age suggests that neuronal health is affected, and synaptic function is altered in this brain region. There was a similar increase in the levels of Zn, Cu, and Fe in the olfactory bulb of tau$^{-/-}$ mice in this study that aligned with reductions in synaptic and neuronal markers, as well as a functional olfactory impairment.

The olfactory receptor neurons are unique in that they are not protected by the blood brain barrier and as such, are susceptible to the uptake of environmental toxins, such as metals[162, 227, 228], a mechanism of interest given the increased risk of PD associated with elevated exposure to metals[398]. Fe, Cu, and Zn have been demonstrated to be taken up into the OB following intranasal exposure in rodents[229-231], however the precise role of metals in olfactory function, or dysfunction, is not well understood. A small study has associated the accumulation of Fe in humans with hyposmia[232], intranasal Zn leads to olfactory deficits in both humans and rodents[233-236], and Cu contamination has been well reported to affect the olfactory capacity of various fish species[399-401]. Interestingly, the tau$^{-/-}$ mice also have a significant increase in bulbar lead, much like the increase that is reported in the *post-mortem* human tissue in Chapter 4. Unlike Cu, Zn, and Fe – lead (Pb) is not a physiological metal and is only present in biological systems due to environmental exposure, whether that be through contaminated air, water, or food sources. Occupational exposure to lead is a risk factor for the development of PD[239], and suggests that there is a failure of lead metabolism and clearance associated with PD, which may be modelled in these animals.

In order to ascertain the functional role of accumulated metals in both the motor impairment and olfactory impairment of the tau$^{-/-}$ mice, animals underwent metal chelation therapy. Chelating agents with moderate affinity for transition metals, such as PBT434, are able to form complexes with the exchangeable pool of metals that arise as a consequence of a breakdown in metal homeostasis without affecting the high affinity bound metals found in essential enzymes and metal chaperones. PBT434 has been shown to inhibit iron-mediated redox activity and rescue motor impairments in the 6-OHDA, MPTP, and an α-synuclein (α-syn) genetic mouse model of PD previously[402]. Treatment with PBT434 in aged animals in this study resulted in reduced Fe in the SNpc, although this did not reach

significance, likely due to the experiment being under powered. There was an increase in the Na and K in the CPU, possibly reflecting a normalisation of synaptic signalling, which is further supported by the significant increase in synaptophysin and NeuN in both brain regions. These changes underlie a functional rescue of the motor impairment in the $tau^{-/-}$ mice and align well with previous reports of the effects of PBT434, and are in line with various mouse models of PD in which there were neuroprotective effects seen with iron chelators such as apomorphine, clioquinol, deferoxamine, M30, and VK-28[371, 373, 375, 403-405]. PBT434 normalised bulbar Cu, Zn, and Fe back to $tau^{+/+}$ levels. These reductions align with a significant increase in synaptophysin and NeuN, but these were not restored to $tau^{+/+}$ levels. Importantly, treatment with PBT434 restored the olfactory function in young $tau^{-/-}$ mice, and this is the first demonstration of metal chelation rescuing a premotor olfactory deficit in a mouse model of PD.

Given the significant reduction of bulbar Cu in PBT434 treated mice with restored olfaction, we sought to investigate the functional effect of increased Cu in young $tau^{+/+}$ mice. Cu(GTSM) is a Cu bis(thiosemicarbazone) complex that has been used to as a vehicle for delivery of radioactive Cu isotopes due to its ability to cross the blood brain barrier with ease.[406, 407] Once Cu(GTSM) is inside a cell, the bound Cu^{2+} is reduced to Cu^{+} dissociates from the ligand, therefore increasing the amount of bioavailable Cu[408]. Cu(GTSM) has been demonstrated to localise in the midbrain, the hippocampus, and the olfactory bulb previously[409]. Cu(GTSM) treatment induced an olfactory and hippocampal memory deficit in $tau^{+/+}$ mice, however there was no effect on movement. Chronic exposure to Cu has been reported to induce hyposmia in fish, and has been implicated in spatial (hippocampal) memory previously[410]. These findings suggest that an increase in bulbar Cu may underlie the olfactory deficit in young $tau^{-/-}$, and removing the excess Cu with PBT434 is enough to restore function.

This study aimed to measure the concentration of metals in the brain regions associated with symptoms at the time of their onset, and to investigate the therapeutic potential of metal chelation in PD. It was demonstrated that metal homeostasis is awry in both the olfactory bulb and the SNpc of animals during at the time of behavioural dysfunction associated with those brain regions. Although immunohistochemical stereology needs to be performed, these data suggest that metal chelation was able to reduce the number of neurons and synapses lost in these animals, and this resulted in a functional restoration of behaviour. Furthermore, this work highlights the necessity of research into the role of Cu in the olfactory system. The findings from this work support the hypothesis that disruption of metal homeostasis underlies impairments in this animal model, and metal chelation is a viable therapeutic strategy in PD.

Chapter 8: An investigation of the rTg4510 animal model and supplementation of S-adenosylmethionine as a therapeutic strategy

This Chapter is separated into 2 sections, 7A and 7B.

8A includes the published manuscript entitled *S-adenosylmethionine rescues cognitive deficits in the rTg4510 animal model by stabilizing protein phosphatase 2A and reducing phosphorylated tau.* **Beauchamp L**, Liu X, Sedjahtera A, Bogeski, M, Vella L, Bush A, Adlard P, Barnham K. Journal of Alzheimer's Disease, 2020.

The candidate was involved in the conception and design of the work as well as acquisition, analysis, and interpretation of the data. The drafting and writing of the first draft and revised manuscripts thereafter were performed by candidate. Overall, the candidate contributed to approximately 80% to the work for this paper.

8B includes an age-dependent behavioural analysis of the rTg4510 mice with a focus on olfactory performance, as well as functional effects of *S*-adenosylmethionine.

Chapter 8A: S-adenosylmethionine rescues cognitive deficits in the rTg4510 animal model by stabilizing protein phosphatase 2A and reducing phosphorylated tau

Leah C. Beauchamp[a,b], Xiang M. Liu[a], Amelia Sedjahtera[a], Mirjana Bogeski[a], Laura J. Vella[a,c], Ashley I. Bush[a,d], Paul A. Adlard[a,d], Kevin J. Barnham[a,b,d]

[a]Florey Institute of Neuroscience and Mental Health, The University of Melbourne, Parkville, Australia
[b]Department of Pharmacology and Therapeutics, The University of Melbourne, Parkville, Australia
[c]Department of Surgery, The University of Melbourne, The Royal Melbourne Hospital, Parkville, Australia.
[d]Melbourne Dementia Research Centre, The University of Melbourne, Parkville, Australia

Acknowledgements

The Florey Institute of Neuroscience and Mental Health acknowledges the strong support from the Victorian Government and in particular the funding from the Operational Infrastructure Support Grant. We acknowledge the assistance of A/Prof Laura Jacobson in this research, the Alzheimer's Association for a Fellowship (AARF-18-566256) to L.J.V and the Australian Research Training Scholarship for financial support of L.C.B.

8A.1 Abstract

Introduction: Alterations in the methionine cycle and abnormal tau phosphorylation are implicated in many neurodegenerative diseases, including Alzheimer's disease and Frontotemporal dementia. rTg4510 mice express mutant human P301L tau and are a model of tau hyperphosphorylation. The cognitive deficit seen in these animals correlates with a burden of hyperphosphorylated tau and is a model to test therapies aimed at lowering phosphorylated tau. This study aimed to increase protein phosphatase 2A activity through supplementation of *S*-adenosylmethionine and analyze the effect on spatial memory and tau in treated animals.

Methods: 6-month-old rTg4510 mice were treated with 100 mg/kg S adenosylmethionine by oral gavage for 3 weeks. Spatial recognition memory was tested in the Y-maze. Alterations to phosphorylated tau and protein phosphatase 2A were explored using immunohistochemistry, western blot, and enzyme-linked immunosorbent assays.

Results: Treatment with *S*-adenosylmethionine increased the Y-maze novel arm exploration time and increased both the expression and activity of protein phosphatase 2A. Furthermore, treatment reduced the number of AT8 positive neurons and reduced the expression of phosphorylated tau (Ser202/Thr205). *S*-adenosylmethionine contributes to multiple pathways in neuronal homeostasis and neurodegeneration.

Conclusion: This study shows that supplementation with *S*-adenosylmethionine stabilizes the heterotrimeric form of PP2A resulting in an increase the enzymatic activity, a reduced level of pathological tau and improved cognition.

8A.2 Introduction

Tau is a protein with many isoforms that are produced by alternative splicing of the *MAPT* gene. The most well-established physiological role for tau is as a microtubule stabilizer, and this key function of tau is regulated by its phosphorylation state [18, 412]. There is a physiological equilibrium of tau and phosphorylated tau (pTau), regulated by a balance of kinase and phosphatase activity. A disruption of this balance and the subsequent shift in the equilibrium of tau and pTau results in abnormal tau phosphorylation and is suggested to contribute to tau aggregation and the formation of tau aggregates. Tau is known to be hyperphosphorylated and aggregated into neurofibrillary tangles (NFTs) in many neurological conditions, including Alzheimer's disease (AD), frontotemporal dementia (FTD), corticobasal degeneration (CBD), Pick's disease (PiD), and progressive supranuclear palsy (PSP) [413]. Furthermore, mutations in tau are known to initiate frontotemporal dementia with parkinsonism type-17 (FTDP-17) [414]. Collectively these diseases are often referred to as the tauopathies.

Normally, tau contains 2-3 phosphate groups per molecule of protein, however, in AD there is reported to be 9-10 moles of phosphate per mole of tau [415, 416]. This abnormal level of phosphorylation is associated with a loss of normal tau function, a gain of toxic function, and aggregation into paired helical filaments (PHFs) [19, 417, 418]. This highlights the crucial role of tau dephosphorylation in modulating tau function, which is primarily regulated by protein phosphatase 2A (PP2A) in the brain [419]. PP2A is the predominant phosphatase, accounting for more than 70% of phosphatase activity in the brain, and in the AD brain PP2A activity is reduced by half [420]. PP2A exists as a heterodimer, with the structural A subunit and the catalytic C subunit; the fully active form of the enzyme is a heterotrimeric assembly, with the A/C and regulatory B subunit. The activity of PP2A is regulated by phosphorylation, methylation, and the binding of endogenous inhibitors. In the absence of a methylation event, the PP2A(A/C) subunits are unable to bind to the PP2A(B) subunit and this renders the enzyme inactive [421].

S-adenosylmethionine (SAMe) is the primary methyl donor for methyltransferase enzymes in the cell, including PP2A [422]. In AD patients SAMe levels are reduced by up to 80% in both the CSF and brain [423, 424]. It is likely that this reduction results in decreased methylation and de-activation of PP2A which in turn leads to the hyperphosphorylation of tau that occurs in disease. However, whether an increase in pTau is a contributor to disease pathogenesis, or simply a marker of the disease remains contentious. The rTg4510 mice are a transgenic model of tauopathy that express a form of mutant human tau^{P301L}, predominantly in the forebrain regions, that can be repressed by administration of doxycycline (Dox) [177, 178]. These mice have progressive hyperphosphorylation of tau and eventually develop NFTs. These mice have been previously reported to have spatial memory deficits, coinciding with reductions in PP2A [379]. Utilizing this *in vivo* model of tau hyperphosphorylation, we sought to test

the potential therapeutic benefit of SAMe supplementation, as well as the biological consequences on PP2A and tau.

8A.3 Methods

Animals

The rTg4510 (n=15; M:9, F:6) and WT control (n=23; M:10, F:13) mice are on a FVBN/129 background and were a kind gift from The Mayo Foundation for Medical Education and Research. Animals were housed in transparent, individually ventilated cages under a 12-hour light/dark cycle. Rodent chow and water were available *ad libitum*. All experimentation was approved by The Florey Animal Ethics Committee (AEC number: 15-092) and conformed to the Australia National Health and Medical Research Council published code for animal research.

Drug treatment, behavior, and tissue analysis were performed on rTg4510 and WT animals, however, there were no changes in treated WT animals, so data is not shown.

Drug administration

6-month-old rTg4510 and WT control mice were treated with either 100 mg/kg SAMe (#A7007; Sigma Aldrich, Germany) or dH_2O daily for 21 days. The drug was administered via oral gavage using a blunt 23-gauge needle. SAMe was stored in powder form at -80˚C and dissolved in dH_2O 30 mins before dosing each day. 100 mg/kg has been previously demonstrated as a safe dose that is able to cross the blood-brain barrier[425].

Y-maze

Spatial recognition memory was investigated in a two-trial Y-maze task as previously reported [426]. Briefly, three identical arms (starting arm, familiar arm, novel arm) of the Y-maze (arms: 59.5 (L) x 7.5 (W) x 15.5 (H) cm; radially arranged) were randomly assigned a visual cue mounted at the distal end of the arm. Mice were placed in the Y-shaped maze for two trials (1-hour inter-trial interval). In the first trial (acquisition) mice were able to explore the start arm and the familiar arm for 10 mins. For the second trial (retention) mice were able to explore all three arms for five mins. Exploratory behavior was recorded by an overhead video and analyzed using the TopScan system (CleverSys Inc.; USA).

Brain tissue collection and preparation

Animals were anaesthetised 30-mins post-gavage (100mg/kg intraperitoneal pentobarbitone; Virbac; Australia) and transcardially perfused with Dulbecco's phosphate-buffered saline (D-PBS) (#14190136; Gibco, Aus). Brains were then removed and the right hemisphere microdissected, frozen on dry ice and stored at -80˚C. The left hemisphere was placed in 50mL 4% paraformaldehyde for post-fixation. After 24-hours brains were transferred to 30% white sugar (CSR, Aus) solution (in D-PBS) and stored

at 4˚C overnight. Brains were then transferred to fresh 30% white sugar solution and stored at 4˚C for one week before being snap-frozen with isopentane and stored at -20˚C.

AT8 Immunohistochemistry

30µm thick sections (1:10) were processed for immunohistochemical (IHC) analysis. Sections were removed from the freezer and allowed to air dry at room temperature (RT) overnight (ON). The next day sections were heated at 62˚C for 10 mins, then microwaved in citric acid buffer (pH 6.0) for 2 mins. After cooling to RT, sections were washed in PBS and incubated in blocking solution (5 mL NGS, 1500 µL Triton X (10%), 43.5 mL PBS) for 30 mins at RT. Sections were then incubated in 1:1000 AT8 antibody (#MN1020; ThermoFisher, Aus) ON at RT. After washing with PBS, sections were incubated in biotin-labeled secondary antibodies (3 hours, RT). Sections were washed, incubated in avidin peroxidase (1 hr, RT), then incubated in 3,3'-Diaminobenzidine (DAB) (20 mins, RT). The immunoreaction was detected using 3% H_2O_2. Sections were washed, dehydrated in ethanol, immersed in xylene and coverslipped.

Stereological estimates of the number of AT8+ tau neurons were quantitated using StereoInvestigator (version 11.06.2, MBF Bioscience, USA). The whole hippocampus (including the dentate gyrus and Cornu Ammonis (CA) subfields – CA1, CA2, and CA3) and the cortex in the same sections were traced. The average volume of the hippocampus and cortex (mean±SD) for vehicle-treated animals is 1.49 x 10^6 µm^2 ± 4.99 x 10^5 µm^2 and 1.03 x 10^6 µm^2 ± 3.79 x 10^5 µm^2 respectively. The average volume of the hippocampus and cortex (mean±SD) for SAMe treated animals is 1.37 x 10^6 µm^2 ± 5.67 x 10^5 µm^2 and 1.09 x 10^6 µm^2 ± 4.66 x 10^5 µm^2 respectively. The quantitation represents the total number of positive cells counted divided by the area (the area is: total area of the region traced/area of the counting frame; where the counting frame is 30µm (X axis) by 3µm (Y axis)), normalised to average of vehicle-treated counts.

AT8 ELISA

Hippocampus and cortex tissues were sonicated in D-PBS with phosphatase (#4906837001, PhosSTOP Phosphatase Inhibitor Cocktail; Roche Diagnostics, Aus) and protease inhibitors (#4906837001, Complete Mini Protease Inhibitor Cocktail; Roche Diagnostics, Aus). Protein concentrations were quantified with the BCA Protein Assay Kit (#23225; Pierce, USA). An ELISA plate was precoated with carbonate coating buffer containing 1:1000 anti-human Tau polyclonal antibody (#A0024; Dako, USA) ON at 4˚C. The next day the plate was blocked with SuperBlock™ T20 (TBS) blocking buffer (#37515; ThermoFisher, Aus). The plate was washed in Tris-buffered saline (TBS-T) and allowed to air dry (2 hrs, RT), then 1.5 µg of sample was added to each well for incubation (2 hrs, RT). The plate was then washed thoroughly and incubated in 1:2000 AT8 antibody (#MN1020; ThermoFisher, Aus) (2 hrs, RT).

Finally, samples were incubated in 1:500 secondary antibody (1 hr, RT) and detected using the QuantaBlu™ Fluorogenic Peroxidase Substrate Kit (#15169; ThermoFisher, Aus). Excitation was induced at 325nm and emission was detected at 420nm after immediately after stop solution was added using a microplate reader.

Protein Phosphatase 2A activity

The PP2A enzyme activity assay was performed according to the manufacturer's instructions (#17-313; Millipore, Germany). Briefly, hippocampus and cortex tissues were sonicated in buffer (20 mM imidazole-HCl, 2 mM EDTA, 2 mM EGTA, 10 µg/mL aprotinin leupeptin, 10 µg/ml pepstatin, 1 mM benzamidine, and 1mM PMSF) and centrifuged at 2000 x *g* for 5 mins at 4˚C. Protein concentrations were quantified with the BCA Protein Assay Kit (#23225; Pierce, USA). Immunoprecipitation of PP2A was performed by incubating lysate containing 500 mg of protein with 4 mg of anti-PP2A(C) antibody and 40 mL of protein A-agarose slurry for 2 hrs at 4°C with constant rocking. Immunoprecipitated samples were washed in TBS and Ser/Thr buffer (50 mM Tris-HCl (pH 7.0) and 100 mM $CaCl_2$), followed by resuspension in Ser/Thr buffer. 60 µL of diluted phosphopeptide and 20 µL of Ser/Thr assay buffer were then added to beads for 10 mins at 30°C in a shaking incubator to initiate the reaction. After brief centrifugation 25 µL of lysate supernatant was transferred to a 96-well microtiter plate. The reaction was terminated by the addition of malachite green phosphate detection solution for 10 –15 mins at RT and free phosphate was quantified by measuring the absorbance at 650 nm using a microplate reader.

S-adenosylmethionine ELISA

Hippocampus and cortex tissue was sonicated in D-PBS with phosphatase and protease inhibitors. Protein concentrations were quantified with the BCA Protein Assay Kit. SAMe levels were quantified using an *S*-adenosylmethionine ELISA Kit (#STA-671-C; Cell Biolabs, USA) according to manufacturer's instructions. Briefly, a pre-coated ELISA plate was prepared by adding SAMe conjugate (1:100) to each well (ON, 4°C). The next day, the plate was blocked for 1 hour at RT, washed, then the wells were incubated with pre-prepared standards or samples (200 µg) (1 hr, RT). After washing, secondary antibody HRP conjugate was added to each well (1 hr, RT). Finally, substrate solution was added to each well (20 mins, RT). Absorbance was read at 450 nm immediately after the addition of stop enzyme.

Immunoblots

Hippocampus and cortex tissues were sonicated in D-PBS with phosphatase and protease inhibitors. Protein concentrations were quantified with the BCA Protein Assay Kit Levels of PP2A(A), PP2A(B), PP2A(C), and total tau were determined by western blotting. Equivalent amounts of proteins were

resolved on 4-20% Tris-HCl SDS-PAGE gels and transferred to nitrocellulose membranes. Membranes were blocked in 5% skim milk (Diploma, Aus) (1 hr, RT) then incubated in either PP2A(A) (1:1000, #2039; CST, USA), PP2A(B) (1:1000, #4953; CST, USA), PP2A(C) (1:1000, #2038; CST,USA) or human Tau (1:2000, #A0024; Dako, USA) ON at 4°C. Membranes were washed in PBS-T (7 mins X 3, RT), and incubated with IRDye® secondary antibody (Li-Cor, Aus) (2 hrs, RT). Visualization of bands was performed on the Odyssey® Fc system (Li-Cor, Aus).

Statistical Analysis

For all statistical analyses, the software package GraphPad Prism (version 6.05 for Windows) was used. Y-maze data are presented as mean ± standard error of the mean (SEM), all other analysis is presented by box and whisker plots with whiskers representing min-max. Detail including statistical test, replicate number, experimental repeats, and significance are reported in Figure Legends. Data were analyzed by unpaired Students t-tests for comparison between groups. $P<0.05$ was considered statistically significant.

8A.4 Results

S-adenosylmethionine levels were increased in the cortex and hippocampus of treated rTg4510 mice

The concentration of SAMe was decreased in the cortex (19.4%; $P=0.002$) and the hippocampus (21.1%; $P<0.0001$) of untreated rTg4510 mice compared to WT controls (Figure 8A.1). Oral supplementation of SAMe in the rTg4510 mice resulted in higher brain levels in both the cortex (14.8%; $P=0.04$; Figure 8A.1A and the hippocampus (21.6%; $P=0.0008$; Figure 7A.1B), indicating the molecule had reached the brain regions of interest. It was hypothesized that once in the brain, SAMe would stabilize the active heterotrimer form of PP2A.

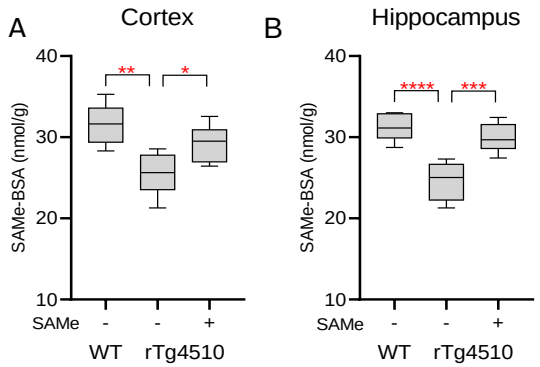

Figure 8A.1 Oral S-adenosylmethionine treatment increased the concentration of SAMe in the brain. **A)** The relative concentration of SAMe in cortical homogenate from WT, treated and untreated rTg4510 mice. **B)** The relative concentration of SAMe in hippocampal homogenate from WT, treated and untreated rTg4510 mice. Analysis by one-way ANOVA. ELISA samples performed in duplicate, N=6 per group. *$P<0.05$, **$P<0.01$, ***$P<0.001$, ****$P<0.00001$.

S-adenosylmethionine increases PP2A activity and PP2A(B) and (C) protein levels in the hippocampus and cortex of rTg4510 mice

The enzymatic activity of PP2A was measured in both cortex and hippocampal tissue and shown to be decreased in rTg4510 mice, compared to WT controls in both the cortex (17.5%; *P*=0.01) and the hippocampus (18.6%; *P*=0.03) (Figure 7A.2A and B). PP2A activity was increased by 29.6% in the cortex (*P*=0.001; Figure 7A.2A) and 31.0% in the hippocampus (*P*=0.005; Figure 8A.2B).

PP2A subunit protein levels were analysed using western blot. With respect to the cortical tissue there is a significant reduction in PP2A(A), (B), and (C) in untreated rTg4510 mice compared to WT controls (31.5% *P*=0.04; 38.1% *P*<0.0001; 22.9% *P*=0.002; respectively). There were significant increases in PP2A(B) (28.4%; *P*=0.03) and PP2A(C) (38.0%; *P*=0.0002) (Figure 8A.2D). With respect to the hippocampal tissue there is a significant reduction in PP2A(B) in untreated rTg4510 mice compared to WT controls (22.2% *P*=0.002). With respect to the hippocampal tissue, there was a non-significant 21.4% increase in the level of PP2A(A), and a significant 20.2% increase in PP2A(B) (*P*=0.02), and a 26.9% increase in PP2A(C) (*P*=0.006) (Figure 8A.2F). This increase in activity and protein subunit levels is consistent with SAMe treatment stabilizing the active PP2A complex. As PP2A is the phosphatase responsible for the dephosphorylation of tau, with an increase in PP2A activity it was hypothesised that there would be a reduction in the levels of phosphorylated tau in the cortex and the hippocampus.

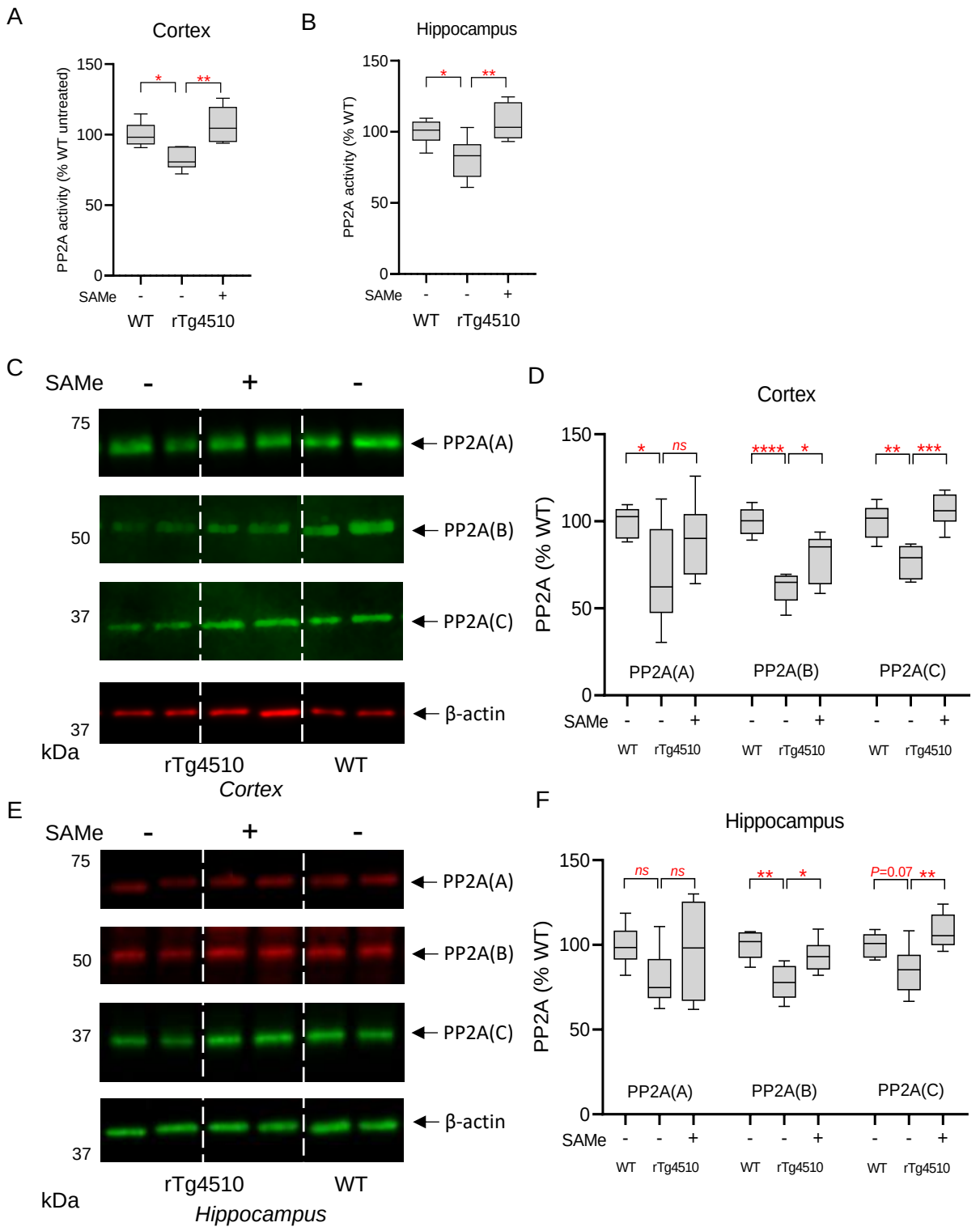

Figure 8A.2 Treatment with S-adenosylmethionine increases the activity of PP2A in rTg4510 mice. **A)** Relative PP2A activity in cortical homogenate and **B)** hippocampal homogenate from WT, treated and untreated rTg4510 mice. **C)** Representative cortical immunoblot probed for PP2A(A), PP2A(B), and PP2A(C). **D)** Quantification of cortical PP2A immunoblots, normalized to β-actin, then calculated relative to vehicle-treated. **E)** Representative hippocampal immunoblot probed for PP2A(A), PP2A(B), and PP2A(C). **F)** Quantification of hippocampal PP2A immunoblots, normalized to β-actin, then calculated relative to vehicle-treated. Analysis by one-way ANOVA. PP2A activity ELISA samples performed in triplicate, N=6 per group. Western blot analyzed by one-way ANOVA from 3 independent repeats, N=6 per group. *P<0.05, **P<0.01, ***P<0.001.

S-adenosylmethionine reduces AT8+ neurons and AT8 protein levels in the cortex of rTg4510 mice

Cortex and hippocampal tissue were analysed by IHC, WB and ELISA utilizing the AT8 antibody. This antibody recognizes a form of tau that is phosphorylated at Ser202 and Thr205 which is enriched in paired helical filaments, a precursor to the formation of NFTs. Compared to untreated mice, there was a 31.2% reduction in the number of AT8 positive neurons in the cortex of SAMe treated rTg4510 mice as visualized by IHC (*P*=0.05; Figure 8A.3A and B), and a 25.0% reduction in the hippocampus, although this was not statistically significant (*P*=0.21; Figure 8A.3A and B). Similar to the IHC results, when utilizing an ELISA for AT8 the concentration of pTau was shown to be significantly reduced by 24.1% in the cortical tissue (*P*=0.05; Figure 8A.3C), but not significantly reduced in the hippocampus (13.7%; *P*=0.49; Figure 8A.3C). There was no significant change in the level of soluble tau as determined by immunoblot, in the cortex (Figure 8A.3D and 8A.3E) or the hippocampus (Figure 8A.3F and 8A.3G).

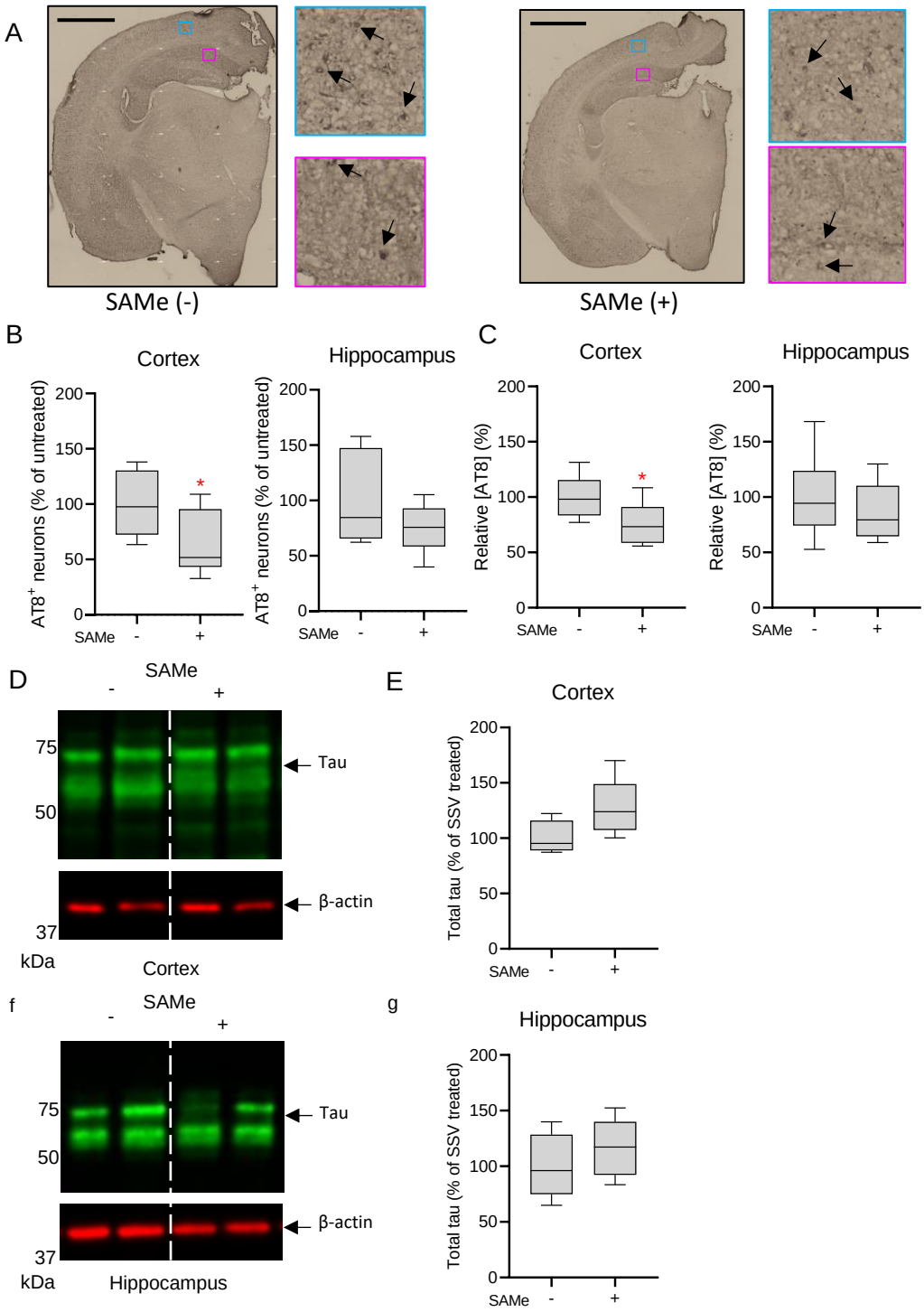

Figure 8A.3 Treatment with S-adenosylmethionine significantly reduced the number of AT8 positive cells and the level of phosphorylated tau in the cortex but not in the hippocampus of rTg4510 mice. **A)** Representative images of AT8+ stained brain sections from rTg4510 untreated and SAMe treated mice, arrows indicating AT8 positive structures. **B)** Quantification of neuronal counts from cortical and hippocampal AT8+ brain sections. **C)** Relative AT8 pTau level in cortical and hippocampal homogenate from treated and untreated rTg4510 tissue as measured by ELISA. **D)** Representative cortical immunoblot probed for soluble human tau. **E)** Quantification of cortical soluble tau western blot, normalized to β-actin, then calculated relative to vehicle-treated. **F)** Representative hippocampal immunoblot probed for soluble human tau. **G)** Quantification of hippocampal soluble tau immunoblot. Analysis by unpaired Student's t-test. Neuronal counting performed on 5 sections per animal, N=6 per group. ELISA samples performed in triplicate, N=6 per group. Western blot analyzed by unpaired t-test from 3 independent repeats, N=6 per group. *P<0.05.

S-adenosylmethionine rescues the spatial memory deficit in rTg4510 mice

SAMe was increased in the cortex and hippocampus which lead to an increase in the activity and expression of PP2A subunits, and a subsequent reduction in cortical AT8+ neurons. The level of pTau has been previously correlated with a hippocampal memory deficit in the rTg450 mice and in concordance with the literature, rTg4510 mice demonstrate an impairment in spatial recognition memory in this study, as indicated by reduced exploration time in the novel arm of the Y-maze compared to WT controls (*P*=0.01; Figure 7A.4). Treatment of rTg4510 mice with 100mg/kg of SAMe daily for three weeks resulted in a significant increase in the investigation time of the novel arm of the Y-maze (*P*=0.01; Figure 7A.4).

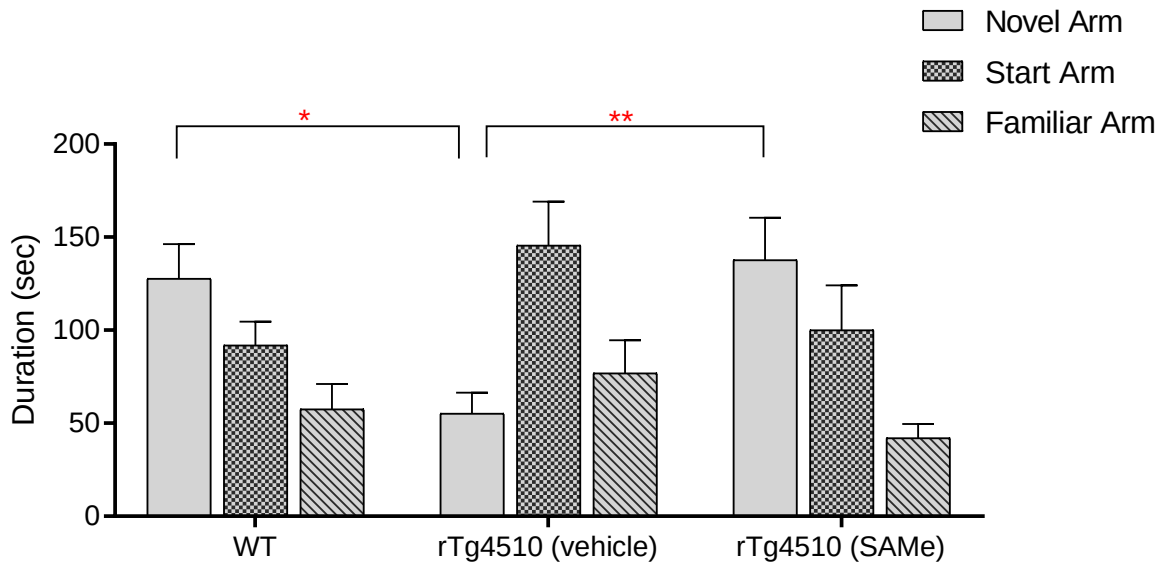

Figure 8A.4 Treatment with S-adenosylmethionine improves the spatial recognition memory of rTg4510 mice. Analysis by two-way ANOVA, with Sidak test for multiple comparisons, *P<0.05, N=12 (WT), N=7 in both rTg4510 groups.

8A.5 Discussion

The rTg450 mice conditionally express mutant human P301L tau and are used widely as a model of progressive tau dysfunction and hyperphosphorylation[178]. It has been previously demonstrated that there is a spatial memory deficit in the rTg4510 mice which is rescued by turning off Tau^{P301L} through administration of doxycycline (Dox), reducing the overall tau burden and subsequent aggregation[427]. In this study, treatment with *S*-adenosylmethionine (SAMe) improved spatial memory deficits, as measured by the Y-maze, in seven-month-old rTg4510 mice. As well as cognitive rescue there was a

significant reduction in the level of phosphorylated tau in the treated animals. As total tau levels were unchanged in the animals, it suggests that it is the AT8+ tau that underlies cognitive deficits.

The phosphorylation state of tau is tightly regulated by a balance of kinase and phosphatase activity. The phosphatase responsible for dephosphorylation of tau is protein phosphatase 2A (PP2A), which has been implicated in the pathogenesis of Alzheimer's disease (AD)[428, 429]. There was an increase in PP2A activity and PP2A(B) and (C) protein expression in SAMe treated animals in this study. The results are consistent with previous work demonstrating that modulation of PP2A with the metal-binding compounds Cu(GTSM) and PBT2 will induce a reduction in p-Tau levels and consequent cognitive rescue in rTg4510 animals[379, 430].

PP2A is a holoenzyme that exists in a heterodimeric and heterotrimeric assembly, consisting of a structural A subunit, a regulatory B subunit, and a catalytic C subunit. PP2A(A) and PP2A(C) exist in a dimeric assembly and require the methylation of the Leu-309 residue on the C terminal of PP2A(C) to enable the formation and stabilization of the heterotrimer with PP2A(B)[431]. This methylation event occurs via the action of PP2A methyltransferase (PPMT), which uses SAMe as a substrate and methyl donor[432].

SAMe is a ubiquitous methyl group donor with a role in DNA methylation, membrane stability, and synthesis of neurotransmitters[433, 434]. SAMe synthesis is part of a cycle in which methionine is converted to SAMe, which is used as a substrate for methylation reactions resulting in the degradation product *S*-adenosylhomocysteine (SAH). SAH is then hydrolyzed to homocysteine and it can then be remethylated to methionine. This re-methylation is dependent on the derivatives of folate and vitamin B_{12} as cofactors[435]. Impairments in any aspect of this methionine cycle will inhibit SAMe-dependent reactions, and it has been shown that folate deficiency induces accumulation of homocysteine resulting in decreased formation and catabolism of SAMe[436, 437]. Plasma levels of SAH are elevated in AD, and the elevation reflects an increased risk of the development of AD[438-440]. Elevated SAH results in decreased PP2A methylation, which is associated with PP2A(B) subunit downregulation, and subsequent accumulation of pTau[441], and knockout of PP2A(B) in wildtype animals results in tauopathy[442]. Furthermore, PPMT expression and PP2A methylation are both downregulated in AD[443] (Figure 8A.5A).

As seen in this study, supplementation of SAMe resulted in higher protein levels of PP2A(B) and PP2A(C) subunits, this leads to an increase in enzymatic activity of PP2A (Figure 8A.5B). This is in line with recent findings by Ma et al., who demonstrated that increasing PP2A activity and methylation of Leu-309 on the PP2A(C) subunit with Cornel Iridoid Glycoside reduced tau phosphorylation and improved memory deficits in the rTg4510 mice[410]. Dietary supplementation of SAMe delayed tau

pathology in the 3xTg-AD mice, a model that develops neurofibrillary tangles (NFTs) and extracellular Aβ plaques[444]. Furthermore, Phase I and Phase II results of a neutraceutical formulation, including SAMe, have demonstrated improved cognitive performance in individuals with AD[445-447]. The same formulation has also improved cognitive performance in people with mild cognitive impairment, and in individuals with no cognitive difficulties[448, 449].

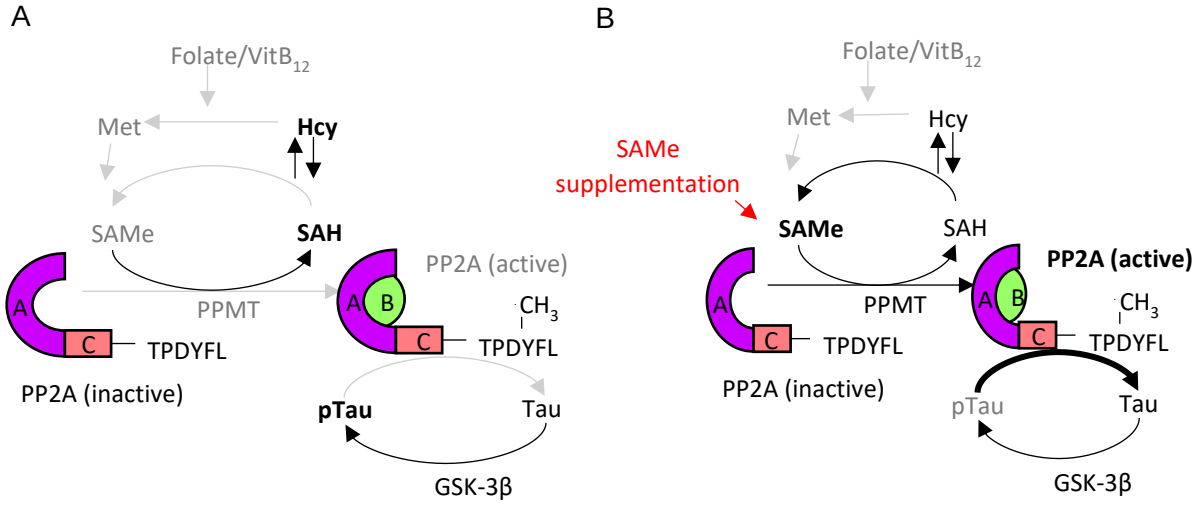

Figure 8A.5 Disruptions in the methionine cycle in Alzheimer's disease and the effect of S-adenosylmethionine supplementation. **a)** Reductions in key components of the methionine cycle (grey text) resulting in increased phosphorylated tau level. **b)** SAMe supplementation is hypothesized to increase PP2A activation by increasing methylation, leading to a reduction in pTau. Abbreviations: GSK-3β – glycogen synthase kinase 3 beta; HCY – homocysteine; Met – methionine; SAH – *S*-adenosylhomocysteine; SAMe – *S*-adenosylmethionine; PP2A – protein phosphatase 2A; PPMT – protein phosphatase 2A methylatransferase; VitB12 – Vitamin B12.

Disruptions in the methionine cycle and abnormal tau have been implicated in the pathogenesis of neurodegenerative diseases. SAMe contributes to multiple pathways in neuronal homeostasis that are directly relevant to age-related neurodegeneration. As SAMe is widely available and approved for use in humans, SAMe represents a pragmatic therapeutic option for diseases where aberrant phosphorylation of tau occurs, such as AD. This study suggests that SAMe can increase the enzymatic activity and stabilization of the heterotrimeric form of PP2A and reduce the level of pathological tau resulting in cognitive improvement, suggesting that clinical evaluation of SAMe is warranted.

Chapter 8B: rTg4510 mice develop an olfactory deficit at 6 months of age

8B.1 Abstract

rTg4510 mice are a model of tau hyperphosphorylation and an *in vivo* tool to investigate the corruption of tau metabolism and function. In light of findings from earlier chapters in the $tau^{-/-}$ mice, is study sought to ascertain which behavioural phenotypes are due to a tau loss of function, and which may be the result of a toxic gain of function. This study aimed to assess the presence of an olfactory impairment at various ages, as well as test the effect of increased protein phosphatase 2A activity through supplementation of *S*-adenosylmethionine on olfactory and locomotor phenotypes in rTg4510 mice. A cohort of rTg4510 and wildtype control mice underwent locomotor and olfactory testing at 2-, 4- and 6-months of age. Afterwards, the 6-month-old rTg4510 and wildtype mice were treated with 100 mg/kg S adenosylmethionine by oral gavage for 3 weeks. Following this treatment regimen, animals were once again tested for olfactory and locomotor phenotypes. There was no overt phenotype in the mice at either 2- or 4-months of age. At 6 months, rTg4510 mice had an olfactory impairment and hyperlocomotor activity similar to that of tau knockout animals suggesting that tau hyperphosphorylation results in tau loss of function. Treatment with *S*-adenosylmethionine resulted in a rescue of olfaction, however there was no change in the level of hyperlocomotion in the rTg4510 mice. This study solidifies the link between tau dysfunction and olfactory impairments seen in neurodegenerative conditions.

8B.2 Introduction

Tau is a microtubule-associated protein that has been linked with numerous neurodegenerative diseases. The H1 haplotype of tau has been associated with Parkinson's disease (PD)[450, 451] and the rs393152 locus on the *MAPT* gene represents a risk factor of idiopathic PD[17, 451], supporting a genetic link between tau and PD. The role of tau in disease, however, remains enigmatic. Increased levels of phosphorylated (Ser396) tau has been found in synapse-enriched fractions of PD brains[452] and as discussed extensively in previous chapters, tau ablated mice have an age-dependent Parkinson-like phenotype[26].

In health there is a physiological balance between tau and phosphorylated tau maintained by a combination of kinases and phosphatases. A disruption of this balance and the subsequent shift in the equilibrium of tau and pTau results in the dissociation of tau from microtubules and there is a subsequent loss of microtubule stability which has downstream effects on axonal transport[453]. This mechanism represents a loss of tau function and is proposed to be a contributor disease pathogenesis in PD (reviewed in[454]). Mutated tau resulted in disruption in axonal transport and subsequent dopaminergic degeneration and motor deficits in the K3 mice[455]. Furthermore, mutations in tau are known to initiate frontotemporal dementia with parkinsonism type-17 (FTDP-17)[414].

As discussed in Chapters 5-7, tau knockout ($tau^{-/-}$) mice model the olfactory deficits found in human *post-mortem* tissue. These findings suggest a loss of tau function may underlie the pathological cascades in PD that contribute to olfactory deficits. It is known that diseases with tau pathology in the anterior olfactory nucleus are aligned with hyposmia, whereas neurodegenerative diseases free from tau-pathology and impairments are not, further highlighting the potential of tau to underlie bulbar dysfunction[161]. In order to further elucidate a role of tau in hyposmia, this study sought to ascertain whether hyposmia is driven by a corruption of tau homeostasis using the rTg4510 mice.

The rTg4510 mice are a transgenic model of frontotemporal dementia that express a form of mutant human tau^{P301L}, predominantly in the forebrain regions[177, 178]. These mice have progressive hyperphosphorylation of tau and have been previously reported to have spatial memory deficits and hyperlocomotion associated with the burden of pTau[379]. It was hypothesised that the rTg4510 mice will develop an olfactory deficit and this preliminary study aimed to investigate the olfactory phenotype at increasing ages of these animals. The enzyme responsible for tau dephosphorylation, protein phosphatase 2A (PP2A) is known to be reduced in rTg4510 mice (discussed in Chapter 8A). As such, the rTg4510 mice were treated with the primary PP2A methyl donor *S*-adenosylmethionine (SAMe)[422] and it was hypothesised that supplementing PP2A activity via administration of SAMe would alleviate the olfactory deficit in this mouse model.

8B.3 Methods

Animals

Animals used in this study are rTg4510 and WT littermate control mice on the FVBN/129 background. Animals were provided by Prof. Paul Adlard and A/Prof Laura Jacobson (FINMH). All mice were genotyped using a standardised polymerase chain reaction assay for tail DNA (Transnetyx Inc., USA). Mice were group-housed in standard transparent individually ventilated cages (IVC; 29.5 x 16 x 13 cm) on sawdust under a 12 h light/dark cycle (lights on at 0700 h). Rodent chow and water were available *ad libitum*. Experimentation was performed in accordance with the Prevention of Cruelty to Animals Act (2004), under the guidance of the National Health and Medical Research Council Code of Practice for the Care and Use of Animals for Experimental Purposes in Australia (2013). Individual experiments were approved by The Florey Animal Ethics Committee (AEC number: 15-092 and 19-052). All efforts were made to ensure comfort and minimise the suffering of animals throughout.

The initial 2- and 4-month old phenotyping was performed on N=13 WT and N=10 rTg4510. In order to increase power of the drug trial, at the 6-month time point animal numbers were supplemented to N=23 WT and N=16 rTg4510.

Animal behaviour

Animals were tested at 2-, 4-, and 6-months of age to determine the onset of olfactory and locomotor phenotypes, followed by a final analysis at 7-months of age following a three-week *S*-adenosylmethionine (SAMe) dosing regimen. Animal behaviour including locomotor activity and odour detection tests presented in this chapter are described in detail in Chapter 2. Y-maze data is presented in section 8B.

Drug administration

6-month-old rTg4510 and WT control mice were treated with either 100 mg/kg SAMe (#A7007; Sigma Aldrich, Germany) or dH_2O daily for 24 days. The drug was administered via oral gavage using a blunt 23-gauge needle. SAMe was stored in powder form at -80˚C and dissolved in dH_2O 30 mins before dosing each day.

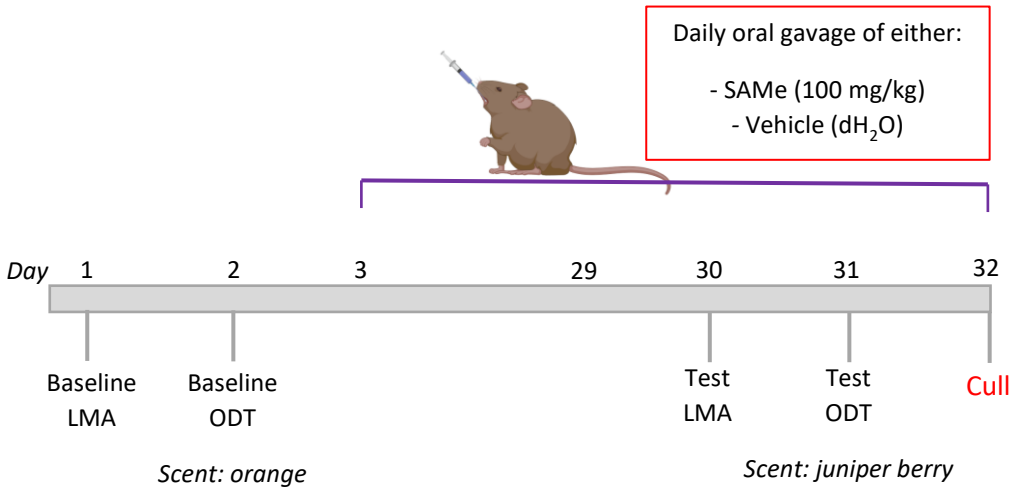

Figure 8B.1 Experimental timeline of animals treated with S-adenosylmethionine. 6-month-old WT and rTg4510 animals underwent a baseline locomotor activity and olfactory test on days 1 and 2. Animals underwent 21 days of daily oral gavage with either 100 mg/kg SAMe or vehicle before undergoing a Y-maze, LMA, and ODT.

8B.4 Results

rTg4510 mice develop hyposmia and hyperlocomotion at 6-months of age

In order to determine the age of onset of an olfactory impairment in rTg4510 mice, animals were tested and re-tested at 2-, 4-, and 6-months of age. 2- and 4-month old mice spent significantly more time exploring the odour cannister compared to vehicle canister and chance, indicative of intact olfaction (summarised in Table 8B.1, Figure 8B.2A and B)

Table 8B.1 Findings from the odour detection test of young rTg4510 mice

	WT		***rTg4510***	
Age	***Odour vs. vehicle***	***Odour vs. chance***	***Odour vs. vehicle***	***Odour vs. chance***
2-month	*P*=0.0001	*P*<0.0001	*P*<0.0001	*P*=0.0004
4-month	*P*=0.0004	*P*<0.0001	*P*=0.001	*P*=0.002

At the 6-month timepoint rTg4510 mice did not perform differently compared to either the vehicle control trial or chance, indicative of hyposmia. At this age wildtype (WT) mice spent significantly longer with the odourous canisters compared to the vehicle control and chance (*P*=0.008 and *P*=0.0001, respectively) (Figure 8A.2C).

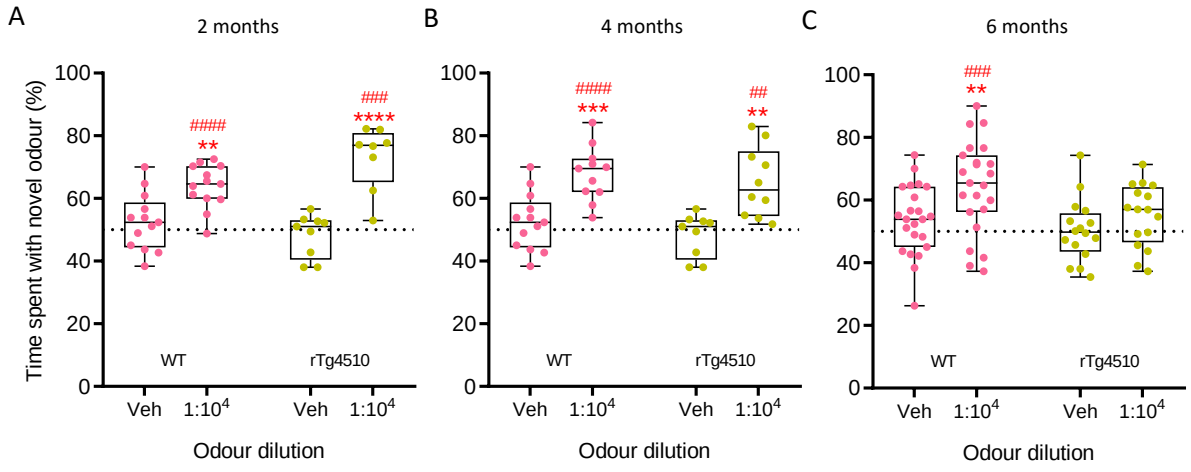

Figure 8B.2 Odour detection test of ageing rTg4510 mice. Amount of time spent exploring a novel odour during odour detection test of WT and rTg4510 mice at 2-, 4-, and 6-months of age. (A) WT n=13, rTg4510 n=9. (B) WT n=13, rTg4510 n=9. (C) WT n=24, rTg4510 n=16. Comparison of genotype within age performed by one-way ANOVA. ***P*<0.01, ****P*<0.001, *****P*<0.0001. Comparison of individual groups to chance (50%, dotted line) performed by one-sample T test (hypothetical mean of 50%); ## *P*<0.01, ### *P*<0.001, #### *P*<0.0001.

Hyperlocomotion is a known phenotype in rTg4510 mice, associated with the burden of phosphorylated tau[456]. In this study with regards to locomotor activity, there was no effect of genotype on the speed and distance travelled on the locomotor activity test at 2- or 4-months of age (Figure 8B.3A and B). At 6-months-old rTg4510 mice had an increased average speed (*P*=0.07) and distance travelled (*P*=0.01) compared to WT controls (Figure 8B.3C), indicative of hyperlocomotion.

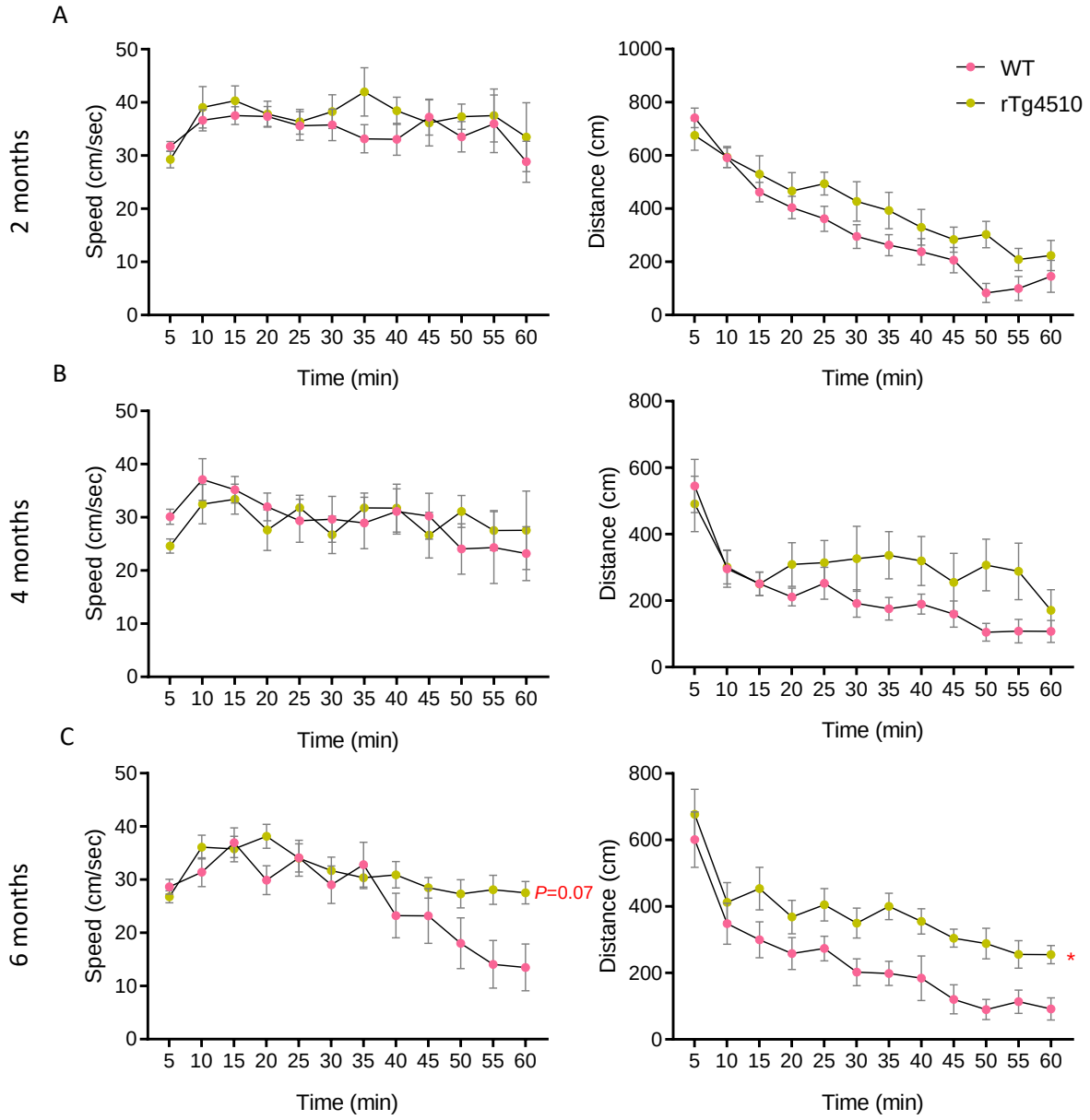

Figure 8B.3 Locomotor activity of ageing rTg4510 mice. **A)** No difference in the average speed or distance travelled between 2-month old rTg4510 and WT controls, rTg4510 n=9, WT n=13. **B)** No difference in the average speed or distance travelled between 4-month old rTg4510 and WT controls, rTg4510 n=9, WT n=13. **C)** Increased average speed and distance traveled in 6-month old rTg4510 mice rTg4510 n=16. WT n=24. Analysed by two-way ANOVA., **P*<0.05.

S-adenosylmethionine rescues the hyposmia of 7-month-old rTg4510 mice

The phosphatase responsible for tau dephosphorylation is protein phosphatase 2A (PP2A). PP2A is a methylation-dependent enzyme and as such relies upon *S*-adenosylmethionine (SAMe) for activity, as such we aimed to supplement the mice with SAMe in order to test the effect on hyposmia. Untreated WT mice had intact olfaction as expected, demonstrate by spending significantly more time exploring the novel odour compared to the vehicle control (P=0.02) and chance (P=0.0004). Treatment with 100 mg/kg *S*-adenosylmethionine had no effect on the olfaction of WT mice compared to vehicle or chance (P=0.001, P<0.0001, respectively). Untreated 7-month-old rTg4510 mice could not detect a novel odour, however mice treated with SAMe spent more time investigating the novel odour compared to vehicle control (P=0.06), and chance (P=0.02) (Figure 8B.4).

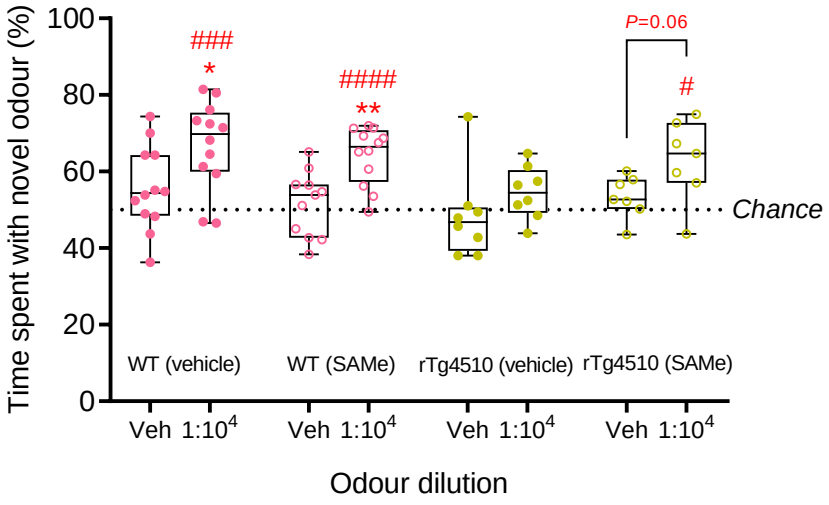

Figure 8B.4 Odour detection test of S-adenosylmethionine treated rTg4510 mice. Amount of time spent exploring a novel odour during odour detection test. WT (vehicle) n=12, WT (SAMe) n=12, rTg4510 (vehicle) n=8, rTg4510 (SAMe) n=7. Comparison of treatment groups performed by one-way ANOVA; *P<0.05, **P<0.01. Comparison of individual groups to chance (50%, dotted line) performed by one-sample T test (hypothetical mean of 50%); # P<0.05, ### P<0.001, #### P<0.0001.

S-adenosylmethionine has no effect on the hyperlocomotion of 7-month-old rTg4510 mice

There were no treatment effects on the hyperlocomotion of rTg4510 mice, and both treated and untreated animals had a significantly higher average speed (P<0.0001, P<0.0001, respectively), and travelled further during the test (P<0.0001, P<0.0001, respectively) (Figure 8B.5)

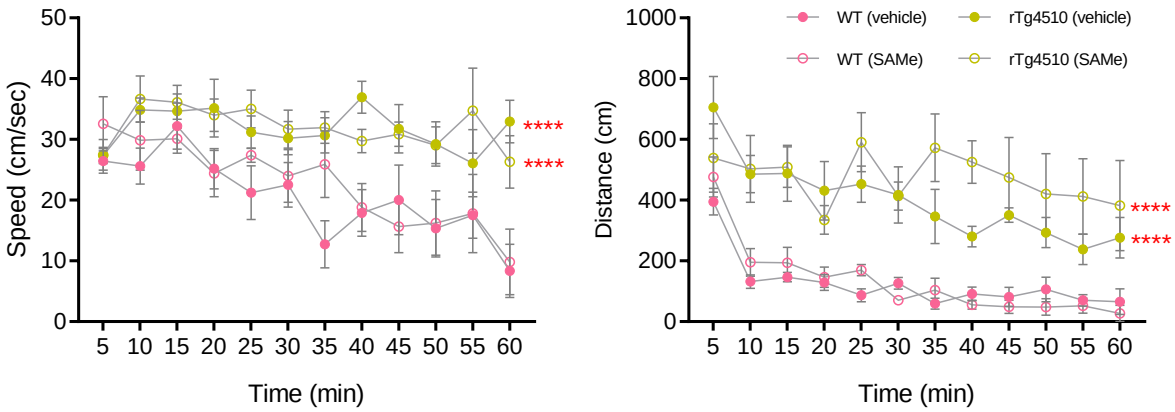

Figure 8B.5. Locomotor activity of S-adenosylmethionine treated rTg4510 mice. Increased average speed and distance traveled of rTg4510 mice treated with vehicle or SAMe during a 60-minute locomotor activity assessment. WT (vehicle) n=12, WT (SAMe) n=12, rTg4510 (vehicle) n=8, rTg4510 (SAMe) n=7. Analysed by two-way ANOVA. WT (vehicle) n=12, WT (SAMe) n=12, rTg4510 (vehicle) n=8, rTg4510 (SAMe) n=7. ****P<0.0001.

8B.5 Discussion

The rTg4510 mice are used as a model of tau hyperphosphorylation and have an age-dependent hippocampal memory deficit and hyperlocomotion. Although predominantly a model of frontotemporal dementia (FTD), the rTg4510 mice also provide a tool to study loss of tau function. Tau exists in a homeostasis of phosphorylated and non-phosphorylated species. When tau is hyperphosphorylated, like is seen in the rTg4510 mice, it disassociates from the microtubules[19]. As well as its ability to oligomerise into toxic species, this dissociation weakens microtubules and is known to disrupt axonal transport and microtubule-dependent mechanisms, representing a loss of function[457]. This study aimed to phenotype the onset of olfactory impairment to further understand the link between tau and hyposmia, as is seen in the tau knockout animals from previous chapters. There was no olfactory deficit in the mice at the 2 or 4-month time points, however at 6 months the animals had an odour detection deficit that coincided with the onset of hyperlocomotion. To understand if the hyposmia could be rescued by lessening the burden of phosphorylated tau, animals

were treated with *S*-adenosylmethionine (SAMe). A three-week supplementation of SAMe was able to rescue the olfactory deficit, however it did not affect hyperlocomotion in the mice.

Tau has been implicated in olfactory deficits due to the presence of hyposmia in tauopathies[458]. Neurodegenerative conditions that have tau aggregation in the anterior olfactory nucleus are aligned with functional olfactory deficits, whereas those with no tau burden in this region have preserved olfaction[161]. A number of tau animal models present with olfactory impairment, including the tau knockouts ($tau^{-/-}$)[303], P301L mutant tau knockin mice[459], and tau Ta1-3RT transgenic mice[278]. Interestingly, the P301S tau transgenic mice have reduced olfactory sensitivity from 3 months of age and have overt olfactory deficits at 5 months of age[279], aligned with the findings from this study in the rTg4510 mice. The rTg4510 mice have a severe age-dependent hyperlocomotion that correlate with the level of tau pathology in the brain[229]. In this study olfactory deficits presented at the same time as hyperlocomotion, suggesting olfactory deficits may also be related to tau burden, however this hypothesis requires a biochemical investigation which has been delayed due to COVID-19.

Targeting phosphorylated tau (pTau) is a therapeutic strategy that is being widely considered in neurodegenerative conditions. One of the mechanisms to reduce the level of pTau is to increase the activity of protein phosphatase 2A (PP2A), the phosphatase responsible for tau dephosphorylation. PP2A activation requires the enzyme to be methylated, which is a SAMe-dependent mechanism (discussed in detail in section 7B). Increasing the level of SAMe will increase the activity of PP2A which will reduce the level of pTau[422]. In this study, SAMe supplementation was able to rescue the olfactory deficit in the rTg4510 mice, without having an effect on hyperlocomotion. It is difficult to draw conclusions from this research in the absence of further biochemical studies, which are underway, however it is promising to see that this animal model aligns well with the olfactory deficits reported in other tau transgenic animals. These findings add weight to the hypothesis that tau dysfunction contributes to olfactory impairments in neurodegenerative conditions.

Chapter 9: General Discussion

Parkinson's disease (PD) can no longer be regarded as primarily a movement disorder. Despite 200 years of scientific discovery and technological advances, the ability to identify and intervene in the disease process is lacking. There are fundamental issues with clinical trials in PD that need to be addressed in order to develop and test disease-modifying therapies. Firstly, PD is diagnosed late, when there is a 50-70% loss of nigral dopaminergic synapses[106, 107]. Secondly, PD is grossly over-diagnosed with an accuracy of only 80%[108]. Thirdly, there are no biomarkers that can monitor disease status or report on drug efficacy, and as PD is a very slow progressing disease the time frame to detect changes in diseases are long and therefore expensive. Unfortunately, these issues act as disincentives to evaluate new treatment strategies. One promising avenue to address some of these failings is to refocus the field on the early and highly prevalent non-motor features of the disease.

9.1 The utility of hyposmia in Parkinson's disease

The strength of hyposmia in a screening tool

Hyposmia is the most prevalent non-motor symptom of PD, in as many as 90% of patients[203]. Unlike other putative biomarkers such as dopamine transporter single-photon emission computed tomography (DAT SPECT) or vesicular monoamine transporter 2 positron emission tomography (VMAT2 PET), olfactory testing is cheap and non-invasive[460]. There are a number of convincing studies that demonstrate the utility of hyposmia to identify and in some cases predict development of PD in later life. A study performed by Deeb *et al.* found that the University of Pennsylvania Smell Identification Test (UPSIT) and DAT SPECT have an equitable specificity to detect PD of 90% [460] and an analysis of motor and non-motor symptoms by Bohnen *et al.* found that olfactory testing was the best predictor of PD in patients with mild disease[461]. In the larger population-based Honolulu Ageing Study of 2267 asymptomatic men, 35 developed PD during an 8-year follow-up period and there was an odds ratio of 5.2 for developing PD in those in the lowest quartile of olfactory scores[462]. Ponsen *et al.* performed an observational study on 361 asymptomatic relatives of PD patients who underwent a baseline UPSIT and dopamine neuroimaging. After a 2-year follow up, 10% of the relatives that had hyposmia and significant reduction in ligand binding on a DAT SPECT developed PD, suggesting that hyposmia carries a risk factor of at least 10% in first degree relatives of PD patients[463]. These studies highlight the utility of hyposmia as a screening tool to detect individuals at high risk of development of PD in later life.

There is much room for improvement in our approach to PD, and the utilisation of hyposmia will strengthen with more data. Due to the presence of hyposmia in other neurodegenerative

conditions[464], as well as age-related decline in smell[465], a low specificity of hyposmia results in limited diagnostic application as a sole disease indicator. An understanding of the underlying pathobiology is the key to identifying disease-specific biomarkers and understanding of the relationship to other non-motor symptoms will increase the potential of hyposmia as a diagnostic tool. As such, this thesis explored some of underlying pathobiology of hyposmia, that has indicated pathways for future research, and may inform part of a screening strategy for early identification of PD.

The biological basis of hyposmia

To date, there have been very few examinations of the PD olfactory bulb (OB)[155, 156, 158-161, 209]. Reported pathological features have been summarized in Figure 9.1. There is a reported increase in the expression of tyrosine hydroxylase (TH) in the periglomerular cells of the OB[155], associated with an increase in the number of dopamine containing periglomerular cells[156]. Huisman *et al.* proposed that this resulted in an increase in dopamine production, which would result in inhibition of the olfactory receptor neurons in the glomeruli. Although an increase in TH was also found in human PD and tau knockout ($tau^{-/-}$) OBs in this thesis, it did not result in an increase in dopamine, therefore not supporting the hypothesis proposed by Huisman *et al.* Although a simple increase in dopamine does not appear to be the mechanism of hyposmia based on these studies, activation of the dopamine 2 receptor (D_2R) is still implicated. A more in-depth analysis of the dopaminergic pathways presented in this thesis suggests that it is a reduction in catechol-*O*-methyltransferase (COMT) metabolism of dopamine as demonstrated by reduced levels of homovanillic acid (HVA). COMT is the primary mechanism of extracellular dopamine clearance in the OB, and reductions in this enzyme will increase the amount of dopamine available to bind to post-synaptic D_2Rs and induce inhibition of the olfactory receptor neurons. This hypothesis was tested in the hyposmic $tau^{-/-}$ mice in Chapter 6 and antagonism of the D_2R using haloperidol resulted in a transient rescue of functional olfactory deficits.

The second proposed pathobiology underlying hyposmia in PD is Lewy pathology. Sengoku *et al.* performed an autopsy series investigation of 320 patients from a geriatric hospital with a focus on the prevalence of Lewy bodies (LB) in the olfactory system[158]. 102 subjects had Lewy pathology within the central nervous system (CNS) and 85 of subjects had Lewy pathology within the olfactory system. It is important to note that only 2 of the subjects had PD, and there were neurological controls with Lewy pathology within the OB. Interestingly, in *all* subjects with degeneration of the substantia nigra there were LBs found in the OB, irrespective of the presence or absence of clinical parkinsonism, suggesting a correlation between the two brain regions. Although this study suggests the presence of LB in the bulbs of PD patients, it also demonstrates the high incidence of LBs in the ageing human OB. Most interestingly, there was rarely LBs found within the dopaminergic neurons of the OB suggesting they

are independent biological changes within the OB. It is also unknown whether LBs in the OB have a detrimental effect on olfaction.

By far the most damage in the olfactory system is found within the anterior olfactory nucleus (AON), where there are substantial neurodegeneration and Lewy body pathology that correlates with disease duration[159, 160]. The AON forms part of the forebrain and distributes olfactory information to the contralateral olfactory bulb and the piriform cortex. Once odour signals have been processed in the OB, the lateral olfactory tract passes thorough the AON, however, the role the AON plays in processing of odour information is poorly understood. Although the damage is severe in the AON as reported in the Pearce *et al.* study, it is important to recall that hyposmia occurs early and does not worsen throughout the duration of the disease. Neurodegeneration of this extent is reflective of end-stage disease and if hyposmia was solely reflective of neurodegeneration, one would expect it to worsen with increasing cell death, as is seen with motor impairment and midbrain degeneration.

Interestingly, a paper by Tsuboi *et al.* later reported tau pathology within the AON that correlated well with Lewy pathology in PD tissue. The authors proposed that these AON tau inclusions were driving the olfactory deficit[161]. This is supported by findings that diseases associated with hyposmias, such as PD, AD, and DLB, have tau inclusions in the AON – whereas diseases where olfactory functions are spared, such as progressive supranuclear palsy (PSP) and corticobasal degeneration (CBD), do not[161]. Indeed, in this thesis tau was implicated in olfactory deficits as two models of tau dysfunction, the tau knockout and the rTg4510 mice, developed age-dependent olfactory deficits. Although time- and pandemic-restraints (statement provided in thesis preface) impacted the fullness of the biochemical investigations of the rTg4510 mice, the $tau^{-/-}$ mice, the data presented in this thesis aligned well with biochemical changes in the PD tissue, including impaired dopamine metabolism, autophagy impairments, α-synuclein accumulation, and a potential role for tau dysfunction in PD-related hyposmia.

The final interesting finding of the studies performed in this thesis involves a change in metal homeostasis in the OB of PD tissue and $tau^{-/-}$ mice. The role of metal accumulation in PD has been characterised with reference to the midbrain, however studies into the status of metals in olfactory system are scarce[209]. The olfactory system is an obvious region of interest when it comes to investigating a role for environmental exposure in the development of sporadic PD. The anatomical nature of olfactory receptor neurons results in a neuronal pathway that bypasses the blood brain barrier and leaves these neurons, and the OBs, vulnerable to intranasal environmental insults. An example of the capacity for agents to be transported into the OB to interrupt cellular function and initiate a pathological cascade is seen in manganese exposure, which is known to induce

parkinsonism[163]. Multiple metals, including iron, copper, and lead, were accumulated in the human and murine OBs as reported in this thesis, warranting more in-depth analysis of the biological cause and consequences going forward.

Most interesting was the success in iron (Fe) and copper (Cu) chelation in the young tau$^{-/-}$ mice. Both D_2R antagonism and chelation were viable means of restoring olfaction in the young animals, suggesting an interplay between the two that is resulting in functional deficits. Fe is an important mediator of dopamine neurotransmission[466]. Fe deficiency has been reported to both *increase* pre-synaptic dopamine activity[467] and *decrease* the number of D_2R sites in the caudate putamen[468]. It has not been established whether these changes are present in the OB, nor whether Fe accumulation has an influence on D_2R numbers, a concept that will be investigated by immunohistochemical analysis of this tissue going forward.

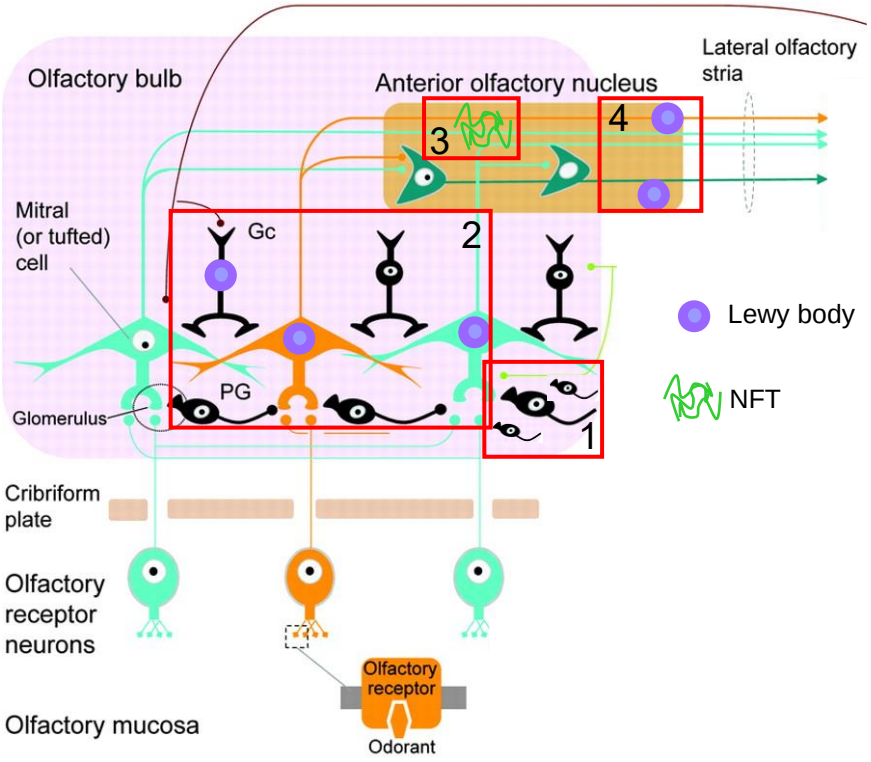

Figure 9.1. Reported pathology within the human Parkinson's disease olfactory bulb. 1. Increased dopaminergic periglomerular neurons. 2. Lewy pathology within the distal olfactory bulb including mitral, tufted, and granule cells. 3. Tau inclusion in the anterior olfactory nucleus. 4. Lewy pathology within the anterior olfactory nucleus. Abbreviations: Gc: granule cells, NFT: neurofibrillary tangles; PG: periglomerular cells. Image adapted from[469].

9.2 The concurrence of non-motor symptoms in PD

As discussed throughout this thesis, the presence of a single non-motor symptom alone is not likely to inform a diagnosis of PD. Not only are many of the defined symptoms present in the neurologically healthy ageing population but they are associated with other neurological conditions (Table 9.1). As such, the more markers present the easier it will be to predict risk. This concept is supported by a longitudinal study of non-motor features in male health professionals that demonstrated constipation, probable RBD, and hyposmia in 29.3% of PD cases, compared to only 1.1% of controls. The age-adjusted odds ratio for having these three features of disease compared to none in PD was 160. This odds ratio elevated substantially with the addition of more nonmotor features. Data from this study, as well as a number of others, suggest that there is a co-occurrence of non-motor symptoms and they cumulatively increase the likelihood of a PD diagnosis, but there is no evidence that symptoms are dependent on one another[470-473].

Table 9.1 Prevalence and association of PD-related non-motor symptoms in neurological conditions

Symptom	*Prevalence (PD)*	*Prevalence (healthy ageing)*	*Association with other neurological conditions*
Hyposmia	90.0%[203]	19.1%[474]	AD[475], HD[476], head trauma[477]
Constipation	50.0%[478]	28.0%[479]	MS[480], stroke[481]
Anxiety	61.8%[482]	16.6%[483]	MS[484], HD[485], dementia[486], CJD[487]
RBD	42.3%[117]	1.1%[488]	LBD[489], AD[490], MSA[491]
Depression	35.0%[492]	9.1%[493]	Stroke[494], dementia[495]

Abbreviations: AD, Alzheimer's disease; CJD, Creutzfeldt-Jakob disease; HD, Huntington's disease; LBD. Lewy body disease; MSA, multiple systems atrophy; MS, multiple sclerosis; RBD, rapid eye movement sleep behaviour disorder.

The Parkinson's Progressive Marker Initiative (PPMI) is an observational multicentre study including clinical assessments of olfaction using the UPSIT, RBD with the Mayo sleep questionnaire and anxiety using the State-Trait Anxiety Inventory (STAI). Analysis of the PPMI database performed for the purposes of this thesis demonstrated a similar concurrence of anxiety, hyposmia, and RBD in the idiopathic and genetic PD cohorts, as well as in the two prodromal groups (Figure 9.2). These data support the findings reported in Chapter 3 in which participants had concurrent anxiety, hyposmia, and RBD and, importantly, these patients had evidence of dopaminergic neurodegeneration in PD-related brain regions, demonstrating the utility of concurrent non-motor symptoms in identifying patients at risk of developing clinical PD.

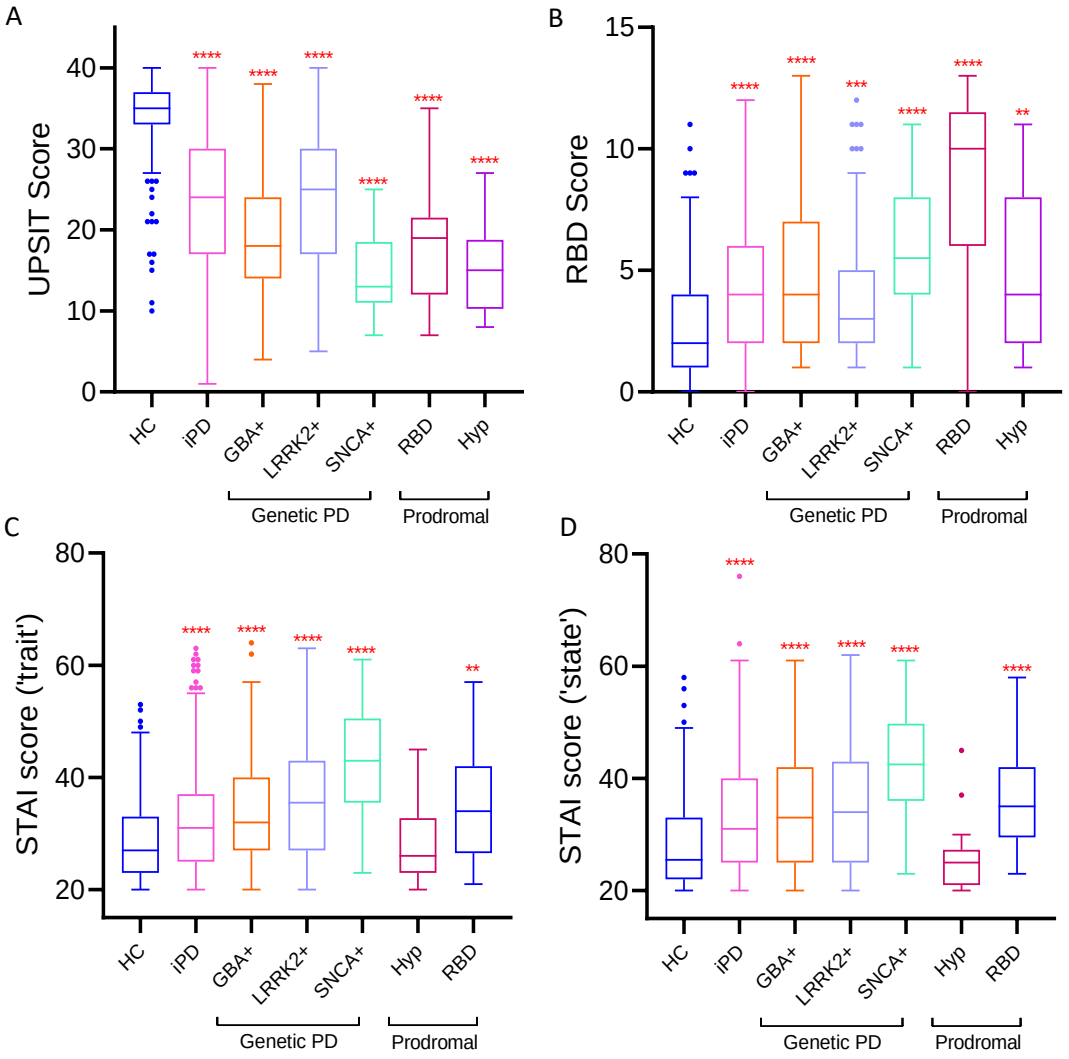

Figure 9.2 Non-motor concurrence in the PPMI cohort. **A)** Olfactory UPSIT scores between healthy controls, genetic PD and prodromal PD groups. **B)** RBD Mayo Sleep Questionnaire scores between healthy controls, genetic PD and prodromal PD groups. **C)** Trait anxiety scores between healthy controls, genetic PD and prodromal PD groups. **D)** State scores between healthy controls, genetic PD and prodromal PD groups. Data analysed by one-way ANOVA, ** *P*<0.01, *** *P*<0.001, **** *P*<0.0001. Abbreviations: HC: healthy control; hyp: hyposmia; iPD: idiopathic Parkinson's disease; RBD: rapid eye movement sleep behaviour disorder; STAI: state-trait anxiety index; UPSIT: University of Pennsylvania smell identification test.

9.3 Preclinical PD screening: a research tool

The concurrence of non-motor symptoms, and the cumulative risk associated with this, is the basis of the Movement Disorder Society (MDS) research criteria for prodromal PD. The MDS Research Criteria for prodromal PD (MDSRC-PPD) framework is the first standardised attempt to help identify patients in the prodromal stage, however this is a framework that is designed for use in a research setting. The MDSRC-PP uses a naïve Bayesian classifier methodology to combine age-dependent risk with established risk (genetics, sex etc.) and prodromal markers that are assigned a 'likelihood ratio' (LR)

reflective of the strength of a diagnostic test. To date there are few studies that have investigated the utility of the criterion, and none of these studies have followed patients through to autopsy therefore a PD diagnosis *has not* been confirmed.

The Tübingen Evaluation of Risk Factors for Early Detection of Neurodegeneration (TREND) study involved an enriched-risk cohort recruited on the presence of probable-RBD, depression and/or hyposmia or none of these at baseline. These patients were then reassessed at 2-, 4- and 6-years post-baseline. Of the 650 participants recruited, 10 converted to incidental PD and these participants had significantly higher LRs of risk *and* prodromal markers at baseline compared to the participants who didn't convert. Despite this, only a minority of these PD patients met the criteria for probable prodromal PD on the MDSRC-PPD *before* their clinical diagnosis.

A study by Fereshtehnejad et al. also included an enriched-risk cohort of polysomnographic-proven RBD at baseline. Interestingly, this study demonstrates a much higher sensitivity than the TREND study. PSG-proven idiopathic RBD has an LR^+ of 130, whereas a positive response to a screening test (interview-based) for RBD only has an LR^+ of 2.3. This means participants who self-report RBD must also have a substantial number of other risks and markers present for them to reach the >80% threshold for a categorisation of probable prodromal PD. Authors of this study suggest that this is indication for two-stage screening processes when recruiting into these studies – an initial consult with nonspecific testing to identify likely candidates followed by a more expensive high-LR^+ test for those identified.

The Prospective Evaluation of Risk Factors for Idiopathic Parkinson's Syndrome (PRIPS) cohort was a population-based study of 715 participants in which 7 converted to incident PD and much like the TREND cohort, these participants showed significantly higher LRs of risk and prodromal markers at baseline. Finally, the Bruneck study followed 574 participants 3-, 5- and 10-year post baseline. At baseline, 12 participants met the criteria for probable prodromal PD and unlike the TREND and PRIPS cohorts, this study reported a moderate to high predictive power at baseline, however this decreased with follow up.

Table 9.2 Diagnostic accuracy studies of cohorts assessed with the MDSDC-PPD

Study	*n*	*Sensitivity*	*Specificity*	*Ref*
TREND	10	30%	> 98%	[496]
PRIPS	7	14%	> 98%	[496]
Bruneck (3 years)	12	66.7%	98.8%	[497]
Bruneck (5 years)		54.6%	99.2%	
Bruneck (10 years)		35.0%		
Fereshtehnejad	48	81.3%	67.9%	[498]

Whilst these findings are certainly promising, they are designed for use in a research setting. Development of an early PD screening tool for clinical implementation is paramount to future observational studies and meaningful identification of at-risk populations.

9.4 Future directions

Development of a screening tool for early Parkinson's disease

Parkinson's disease is the fastest growing neurological disorder in the world, with a predicted prevalence of 12 million by 2040. Currently, it is not possible to identify people at risk of developing PD in the general population. This results in late and inaccurate identification of PD, with downstream implications for clinical trial outcomes. There is more need than ever to develop a screening protocol that can be used clinically to identify and monitor at-risk individuals. Due to the intrusive, timely, and expensive nature of dopamine neuroimaging, it is not possible to screen large populations of people in the community. As such, there is a requirement to 'filter' people through a series of tests in order to determine a group of people with increased risk, who can then go on to be imaged. As discussed extensively above, hyposmia is the ideal initial screening tool due to the high prevalence and convenience of olfactory testing. Around 20% of the healthy ageing population will have an olfactory impairment, which will reduce a population-based study of many thousands down by 80% for further analysis of non-motor PD (Figure 9.3). Due to a prevalence of 90% in PD, this strategy will also capture the largest number of individuals who are at risk of developing PD in later life. Once reduced to hyposmic individuals, further assessment of individual symptoms, such as RBD, anxiety, and constipation can be assessed, as well as the concurrence of symptoms. Powerfully, these assessments are questionnaire-based and can be completed using an online platform. With the help of artificial intelligence, it will be possible to build an algorithm into these programs and assign a risk-ratio to participants, and those over a certain threshold can be recommended for clinical assessment and neuroimaging.

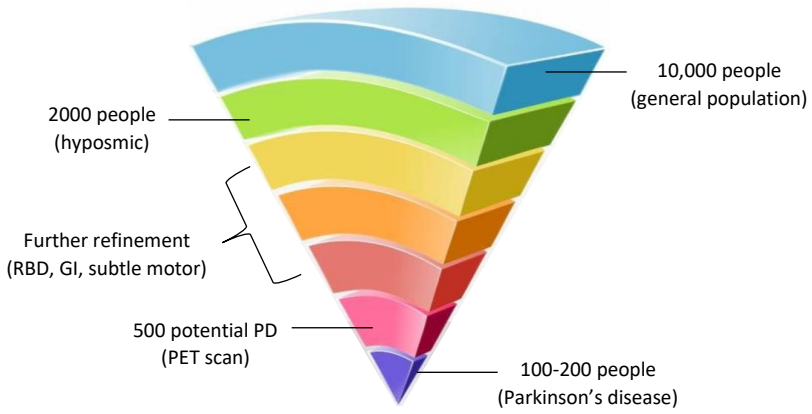

Figure 9.3 Schematic of a process to screen and identify individuals at risk of developing clinical PD in a population-based study.

A differential diagnostic for hyposmia

Whilst the presence of hyposmia is a powerful indicator of PD, it would be of great value to further refine olfactory testing in order to ascertain a potential disease-specificity to the dysfunction. Findings in this thesis have implicated the mis-metabolism of dopamine and metal dyshomeostasis, warranting future scrutiny to investigate disease-specificity. Firstly, it will important to analyse *post-mortem* olfactory bulbs from AD and LBD for pathway similarities. With regards to dopamine mis-metabolism, due to the success of short-term haloperidol in $tau^{-/-}$, it would be of interest to test the effect of intranasal D_2R antagonism on recently diagnosed drug naïve PD patients, as well as a population of neurologically healthy hyposmic patients for the potential of D_2R antagonists as a differential diagnostic tool. Iron chelating compounds such as deferiprone are already in clinical trials for PD providing an opportunity to test the effects of treatment in people. Due to the success of iron and copper chelation in young $tau^{-/-}$ animals regular olfactory testing should be included in the readouts for clinical trials going forward and may lead to the development of an important phenotypic readout.

Development of novel biomarkers in PD

The direct projection of the olfactory receptor neurons from the nasal mucosa to the OB provides a unique opportunity to sample a potential pool of CNS biomarkers. The olfactory receptor neurons are bipolar and like all neurons will secrete extracellular vesicles (EVs). EVs carry cargo from the neuron, including proteins, lipids, metabolites, and nucleic acids which provide information about the parent cell[499]. By capturing these EVs in a nasal lavage, it is possible to isolate and investigate the contents which may provide information about the state of the olfactory receptor neurons between neurologically healthy and PD patients. This hypothesis forms the basis of a pilot clinical trial designed and being run by myself in collaboration with local neurologists Dr. David Darby and Dr. Andrew Evans (University of Melbourne HREC:1852908).

9.5 Conclusion

The experiments described in this thesis above will hopefully aid in the development of improved diagnostic tools and biomarkers of disease to monitor disease progression and efficacy of disease-modifying compounds. A paradigm shift is required in the approach to PD, and a direct and concerted effort to understand the non-motor features prevalent before irreversible midbrain neurodegeneration may alleviate the suffering caused by this devastating disease. The redefinition of Parkinson's disease beyond a movement disorder is both warranted and imminent.

References

1. Berg D, Postuma RB, Adler CH, et al. MDS research criteria for prodromal Parkinson's disease. *Movement disorders : official journal of the Movement Disorder Society* 2015; **30**(12): 1600-11.
2. Group GBDNDC. Global, regional, and national burden of neurological disorders during 1990-2015: a systematic analysis for the Global Burden of Disease Study 2015. *The Lancet Neurology* 2017; **16**(11): 877-97.
3. Collaborators GBDPsD. Global, regional, and national burden of Parkinson's disease, 1990-2016: a systematic analysis for the Global Burden of Disease Study 2016. *The Lancet Neurology* 2018; **17**(11): 939-53.
4. Parkinson J. An essay on the shaking palsy. 1817. *The Journal of neuropsychiatry and clinical neurosciences* 2002; **14**(2): 223-36; discussion 2.
5. Walusinski O. Jean-Martin Charcot and Parkinson's disease: Teaching and teaching materials. *Revue neurologique* 2018; **174**(7-8): 491-505.
6. Khoo TK, Yarnall AJ, Duncan GW, et al. The spectrum of nonmotor symptoms in early Parkinson disease. *Neurology* 2013; **80**(3): 276-81.
7. Polymeropoulos MH, Lavedan C, Leroy E, et al. Mutation in the alpha-synuclein gene identified in families with Parkinson's disease. *Science* 1997; **276**(5321): 2045-7.
8. Kitada T, Asakawa S, Hattori N, et al. Mutations in the parkin gene cause autosomal recessive juvenile parkinsonism. *Nature* 1998; **392**(6676): 605-8.
9. Leroy E, Boyer R, Auburger G, et al. The ubiquitin pathway in Parkinson's disease. *Nature* 1998; **395**(6701): 451-2.
10. Valente EM, Abou-Sleiman PM, Caputo V, et al. Hereditary early-onset Parkinson's disease caused by mutations in PINK1. *Science* 2004; **304**(5674): 1158-60.
11. Bonifati V, Rizzu P, van Baren MJ, et al. Mutations in the DJ-1 gene associated with autosomal recessive early-onset parkinsonism. *Science* 2003; **299**(5604): 256-9.
12. Nichols WC, Pankratz N, Marek DK, et al. Mutations in GBA are associated with familial Parkinson disease susceptibility and age at onset. *Neurology* 2009; **72**(4): 310-6.
13. Funayama M, Hasegawa K, Kowa H, Saito M, Tsuji S, Obata F. A new locus for Parkinson's disease (PARK8) maps to chromosome 12p11.2-q13.1. *Annals of neurology* 2002; **51**(3): 296-301.
14. Dawson TM, Dawson VL. Rare genetic mutations shed light on the pathogenesis of Parkinson disease. *The Journal of clinical investigation* 2003; **111**(2): 145-51.
15. Burbulla LF, Kruger R. Converging environmental and genetic pathways in the pathogenesis of Parkinson's disease. *Journal of the neurological sciences* 2011; **306**(1-2): 1-8.
16. Reeve A, Simcox E, Turnbull D. Ageing and Parkinson's disease: why is advancing age the biggest risk factor? *Ageing research reviews* 2014; **14**: 19-30.
17. Simon-Sanchez J, Schulte C, Bras JM, et al. Genome-wide association study reveals genetic risk underlying Parkinson's disease. *Nature genetics* 2009; **41**(12): 1308-12.
18. Lindwall G, Cole RD. Phosphorylation affects the ability of tau protein to promote microtubule assembly. *The Journal of biological chemistry* 1984; **259**(8): 5301-5.
19. Alonso AC, Zaidi T, Grundke-Iqbal I, Iqbal K. Role of abnormally phosphorylated tau in the breakdown of microtubules in Alzheimer disease. *Proceedings of the National Academy of Sciences of the United States of America* 1994; **91**(12): 5562-6.
20. Bancher C, Braak H, Fischer P, Jellinger KA. Neuropathological staging of Alzheimer lesions and intellectual status in Alzheimer's and Parkinson's disease patients. *Neuroscience letters* 1993; **162**(1-2): 179-82.
21. Joachim CL, Morris JH, Kosik KS, Selkoe DJ. Tau antisera recognize neurofibrillary tangles in a range of neurodegenerative disorders. *Annals of neurology* 1987; **22**(4): 514-20.
22. Braak H, Rub U, Del Tredici K. Cognitive decline correlates with neuropathological stage in Parkinson's disease. *Journal of the neurological sciences* 2006; **248**(1-2): 255-8.

23. Arima K, Hirai S, Sunohara N, et al. Cellular co-localization of phosphorylated tau- and NACP/alpha-synuclein-epitopes in lewy bodies in sporadic Parkinson's disease and in dementia with Lewy bodies. *Brain research* 1999; **843**(1-2): 53-61.
24. Ishizawa T, Mattila P, Davies P, Wang D, Dickson DW. Colocalization of tau and alpha-synuclein epitopes in Lewy bodies. *Journal of neuropathology and experimental neurology* 2003; **62**(4): 389-97.
25. Oaks AW, Frankfurt M, Finkelstein DI, Sidhu A. Age-dependent effects of A53T alpha-synuclein on behavior and dopaminergic function. *PloS one* 2013; **8**(4): e60378.
26. Lei P, Ayton S, Finkelstein DI, et al. Tau deficiency induces parkinsonism with dementia by impairing APP-mediated iron export. *Nature medicine* 2012; **18**(2): 291-5.
27. Ehringer H, Hornykiewicz O. [Distribution of noradrenaline and dopamine (3-hydroxytyramine) in the human brain and their behavior in diseases of the extrapyramidal system]. *Klinische Wochenschrift* 1960; **38**: 1236-9.
28. Spillantini MG, Schmidt ML, Lee VM, Trojanowski JQ, Jakes R, Goedert M. Alpha-synuclein in Lewy bodies. *Nature* 1997; **388**(6645): 839-40.
29. Kuzuhara S, Mori H, Izumiyama N, Yoshimura M, Ihara Y. Lewy bodies are ubiquitinated. A light and electron microscopic immunocytochemical study. *Acta neuropathologica* 1988; **75**(4): 345-53.
30. Goldman JE, Yen SH, Chiu FC, Peress NS. Lewy bodies of Parkinson's disease contain neurofilament antigens. *Science* 1983; **221**(4615): 1082-4.
31. Schlossmacher MG, Frosch MP, Gai WP, et al. Parkin localizes to the Lewy bodies of Parkinson disease and dementia with Lewy bodies. *The American journal of pathology* 2002; **160**(5): 1655-67.
32. Anderson JP, Walker DE, Goldstein JM, et al. Phosphorylation of Ser-129 is the dominant pathological modification of alpha-synuclein in familial and sporadic Lewy body disease. *The Journal of biological chemistry* 2006; **281**(40): 29739-52.
33. Goedert M, Spillantini MG, Del Tredici K, Braak H. 100 years of Lewy pathology. *Nature reviews Neurology* 2013; **9**(1): 13-24.
34. Chartier S, Duyckaerts C. Is Lewy pathology in the human nervous system chiefly an indicator of neuronal protection or of toxicity? *Cell and tissue research* 2018; **373**(1): 149-60.
35. Dickinson BC, Chang CJ. Chemistry and biology of reactive oxygen species in signaling or stress responses. *Nature chemical biology* 2011; **7**(8): 504-11.
36. Rego AC, Oliveira CR. Mitochondrial dysfunction and reactive oxygen species in excitotoxicity and apoptosis: implications for the pathogenesis of neurodegenerative diseases. *Neurochemical research* 2003; **28**(10): 1563-74.
37. Sies H, Berndt C, Jones DP. Oxidative Stress. *Annual review of biochemistry* 2017; **86**: 715-48.
38. Wiseman H, Halliwell B. Damage to DNA by reactive oxygen and nitrogen species: role in inflammatory disease and progression to cancer. *The Biochemical journal* 1996; **313 (Pt 1)**: 17-29.
39. Liu Y, Fiskum G, Schubert D. Generation of reactive oxygen species by the mitochondrial electron transport chain. *Journal of neurochemistry* 2002; **80**(5): 780-7.
40. Starkov AA. The role of mitochondria in reactive oxygen species metabolism and signaling. *Annals of the New York Academy of Sciences* 2008; **1147**: 37-52.
41. Langston JW. The MPTP Story. *Journal of Parkinson's disease* 2017; **7**(s1): S11-S9.
42. Mizuno Y, Ohta S, Tanaka M, et al. Deficiencies in complex I subunits of the respiratory chain in Parkinson's disease. *Biochemical and biophysical research communications* 1989; **163**(3): 1450-5.
43. Parker WD, Jr., Boyson SJ, Parks JK. Abnormalities of the electron transport chain in idiopathic Parkinson's disease. *Annals of neurology* 1989; **26**(6): 719-23.
44. Schapira AH, Cooper JM, Dexter D, Jenner P, Clark JB, Marsden CD. Mitochondrial complex I deficiency in Parkinson's disease. *Lancet* 1989; **1**(8649): 1269.

45. Mouton-Liger F, Jacoupy M, Corvol JC, Corti O. PINK1/Parkin-Dependent Mitochondrial Surveillance: From Pleiotropy to Parkinson's Disease. *Frontiers in molecular neuroscience* 2017; **10**: 120.
46. Wang X, Winter D, Ashrafi G, et al. PINK1 and Parkin target Miro for phosphorylation and degradation to arrest mitochondrial motility. *Cell* 2011; **147**(4): 893-906.
47. Wilson MA. The role of cysteine oxidation in DJ-1 function and dysfunction. *Antioxidants & redox signaling* 2011; **15**(1): 111-22.
48. Przedborski S, Jackson-Lewis V, Djaldetti R, et al. The parkinsonian toxin MPTP: action and mechanism. *Restorative neurology and neuroscience* 2000; **16**(2): 135-42.
49. Tanner CM, Kamel F, Ross GW, et al. Rotenone, paraquat, and Parkinson's disease. *Environmental health perspectives* 2011; **119**(6): 866-72.
50. Lucking CB, Brice A. Alpha-synuclein and Parkinson's disease. *Cellular and molecular life sciences : CMLS* 2000; **57**(13-14): 1894-908.
51. Burre J, Sharma M, Tsetsenis T, Buchman V, Etherton MR, Sudhof TC. Alpha-synuclein promotes SNARE-complex assembly in vivo and in vitro. *Science* 2010; **329**(5999): 1663-7.
52. Sherman MY, Goldberg AL. Cellular defenses against unfolded proteins: a cell biologist thinks about neurodegenerative diseases. *Neuron* 2001; **29**(1): 15-32.
53. DeMartino GN, Slaughter CA. The proteasome, a novel protease regulated by multiple mechanisms. *The Journal of biological chemistry* 1999; **274**(32): 22123-6.
54. Forno LS. Neuropathology of Parkinson's disease. *Journal of neuropathology and experimental neurology* 1996; **55**(3): 259-72.
55. Shimura H, Hattori N, Kubo S, et al. Immunohistochemical and subcellular localization of Parkin protein: absence of protein in autosomal recessive juvenile parkinsonism patients. *Annals of neurology* 1999; **45**(5): 668-72.
56. Shimura H, Schlossmacher MG, Hattori N, et al. Ubiquitination of a new form of alpha-synuclein by parkin from human brain: implications for Parkinson's disease. *Science* 2001; **293**(5528): 263-9.
57. Lowe J, McDermott H, Landon M, Mayer RJ, Wilkinson KD. Ubiquitin carboxyl-terminal hydrolase (PGP 9.5) is selectively present in ubiquitinated inclusion bodies characteristic of human neurodegenerative diseases. *The Journal of pathology* 1990; **161**(2): 153-60.
58. Ii K, Ito H, Tanaka K, Hirano A. Immunocytochemical co-localization of the proteasome in ubiquitinated structures in neurodegenerative diseases and the elderly. *Journal of neuropathology and experimental neurology* 1997; **56**(2): 125-31.
59. Shimura H, Hattori N, Kubo S, et al. Familial Parkinson disease gene product, parkin, is a ubiquitin-protein ligase. *Nature genetics* 2000; **25**(3): 302-5.
60. Wintermeyer P, Kruger R, Kuhn W, et al. Mutation analysis and association studies of the UCHL1 gene in German Parkinson's disease patients. *Neuroreport* 2000; **11**(10): 2079-82.
61. Saigoh K, Wang YL, Suh JG, et al. Intragenic deletion in the gene encoding ubiquitin carboxy-terminal hydrolase in gad mice. *Nature genetics* 1999; **23**(1): 47-51.
62. McNaught KS, Jenner P. Proteasomal function is impaired in substantia nigra in Parkinson's disease. *Neuroscience letters* 2001; **297**(3): 191-4.
63. Klionsky DJ, Emr SD. Autophagy as a regulated pathway of cellular degradation. *Science* 2000; **290**(5497): 1717-21.
64. Martinez-Vicente M, Cuervo AM. Autophagy and neurodegeneration: when the cleaning crew goes on strike. *The Lancet Neurology* 2007; **6**(4): 352-61.
65. Webb JL, Ravikumar B, Atkins J, Skepper JN, Rubinsztein DC. Alpha-Synuclein is degraded by both autophagy and the proteasome. *The Journal of biological chemistry* 2003; **278**(27): 25009-13.
66. Betarbet R, Sherer TB, Greenamyre JT. Ubiquitin-proteasome system and Parkinson's diseases. *Experimental neurology* 2005; **191 Suppl 1**: S17-27.
67. Cuervo AM, Stefanis L, Fredenburg R, Lansbury PT, Sulzer D. Impaired degradation of mutant alpha-synuclein by chaperone-mediated autophagy. *Science* 2004; **305**(5688): 1292-5.

68. Stefanis L, Larsen KE, Rideout HJ, Sulzer D, Greene LA. Expression of A53T mutant but not wild-type alpha-synuclein in PC12 cells induces alterations of the ubiquitin-dependent degradation system, loss of dopamine release, and autophagic cell death. *The Journal of neuroscience : the official journal of the Society for Neuroscience* 2001; **21**(24): 9549-60.
69. Massey AC, Kaushik S, Sovak G, Kiffin R, Cuervo AM. Consequences of the selective blockage of chaperone-mediated autophagy. *Proceedings of the National Academy of Sciences of the United States of America* 2006; **103**(15): 5805-10.
70. Iwata A, Riley BE, Johnston JA, Kopito RR. HDAC6 and microtubules are required for autophagic degradation of aggregated huntingtin. *The Journal of biological chemistry* 2005; **280**(48): 40282-92.
71. Jin SM, Youle RJ. PINK1- and Parkin-mediated mitophagy at a glance. *Journal of cell science* 2012; **125**(4): 795-9.
72. Zimprich A, Biskup S, Leitner P, et al. Mutations in LRRK2 cause autosomal-dominant parkinsonism with pleomorphic pathology. *Neuron* 2004; **44**(4): 601-7.
73. Paisan-Ruiz C, Lang AE, Kawarai T, et al. LRRK2 gene in Parkinson disease: mutation analysis and case control association study. *Neurology* 2005; **65**(5): 696-700.
74. Orenstein SJ, Kuo SH, Tasset I, et al. Interplay of LRRK2 with chaperone-mediated autophagy. *Nature neuroscience* 2013; **16**(4): 394-406.
75. Saez-Atienzar S, Bonet-Ponce L, Blesa JR, et al. The LRRK2 inhibitor GSK2578215A induces protective autophagy in SH-SY5Y cells: involvement of Drp-1-mediated mitochondrial fission and mitochondrial-derived ROS signaling. *Cell Death Dis* 2014; **5**.
76. Bonello F, Hassoun SM, Mouton-Liger F, et al. LRRK2 impairs PINK1/Parkin-dependent mitophagy via its kinase activity: pathologic insights into Parkinson's disease. *Human molecular genetics* 2019; **28**(10): 1645-60.
77. Wallings R, Connor-Robson N, Wade-Martins R. LRRK2 interacts with the vacuolar-type H+-ATPase pump a1 subunit to regulate lysosomal function. *Human molecular genetics* 2019; **28**(16): 2696-710.
78. Albanese F, Novello S, Morari M. Autophagy and LRRK2 in the Aging Brain. *Front Neurosci* 2019; **13**: 1352.
79. Di Fonzo A, Chien HF, Socal M, et al. ATP13A2 missense mutations in juvenile parkinsonism and young onset Parkinson disease. *Neurology* 2007; **68**(19): 1557-62.
80. Ramirez A, Heimbach A, Grundemann J, et al. Hereditary parkinsonism with dementia is caused by mutations in ATP13A2, encoding a lysosomal type 5 P-type ATPase. *Nature genetics* 2006; **38**(10): 1184-91.
81. Keller JN, Dimayuga E, Chen Q, Thorpe J, Gee J, Ding Q. Autophagy, proteasomes, lipofuscin, and oxidative stress in the aging brain. *The international journal of biochemistry & cell biology* 2004; **36**(12): 2376-91.
82. Cuervo AM, Bergamini E, Brunk UT, Droge W, Ffrench M, Terman A. Autophagy and aging: the importance of maintaining "clean" cells. *Autophagy* 2005; **1**(3): 131-40.
83. Kiffin R, Kaushik S, Zeng M, et al. Altered dynamics of the lysosomal receptor for chaperone-mediated autophagy with age. *Journal of cell science* 2007; **120**(Pt 5): 782-91.
84. McGeer PL, Itagaki S, Boyes BE, McGeer EG. Reactive microglia are positive for HLA-DR in the substantia nigra of Parkinson's and Alzheimer's disease brains. *Neurology* 1988; **38**(8): 1285-91.
85. Hirsch EC, Hunot S. Neuroinflammation in Parkinson's disease: a target for neuroprotection? *The Lancet Neurology* 2009; **8**(4): 382-97.
86. Hirsch E, Graybiel AM, Agid YA. Melanized dopaminergic neurons are differentially susceptible to degeneration in Parkinson's disease. *Nature* 1988; **334**(6180): 345-8.
87. Gesi M, Soldani P, Giorgi FS, Santinami A, Bonaccorsi I, Fornai F. The role of the locus coeruleus in the development of Parkinson's disease. *Neurosci Biobehav Rev* 2000; **24**(6): 655-68.
88. Segura-Aguilar J, Paris I, Munoz P, Ferrari E, Zecca L, Zucca FA. Protective and toxic roles of dopamine in Parkinson's disease. *Journal of neurochemistry* 2014; **129**(6): 898-915.

89. Van Laar VS, Mishizen AJ, Cascio M, Hastings TG. Proteomic identification of dopamine-conjugated proteins from isolated rat brain mitochondria and SH-SY5Y cells. *Neurobiology of disease* 2009; **34**(3): 487-500.
90. Mosharov EV, Larsen KE, Kanter E, et al. Interplay between cytosolic dopamine, calcium, and alpha-synuclein causes selective death of substantia nigra neurons. *Neuron* 2009; **62**(2): 218-29.
91. Haacke EM, Miao Y, Liu M, et al. Correlation of putative iron content as represented by changes in R2* and phase with age in deep gray matter of healthy adults. *Journal of magnetic resonance imaging : JMRI* 2010; **32**(3): 561-76.
92. Bilgic B, Pfefferbaum A, Rohlfing T, Sullivan EV, Adalsteinsson E. MRI estimates of brain iron concentration in normal aging using quantitative susceptibility mapping. *NeuroImage* 2012; **59**(3): 2625-35.
93. Bolam JP, Pissadaki EK. Living on the edge with too many mouths to feed: why dopamine neurons die. *Movement disorders : official journal of the Movement Disorder Society* 2012; **27**(12): 1478-83.
94. Pacelli C, Giguere N, Bourque MJ, Levesque M, Slack RS, Trudeau LE. Elevated Mitochondrial Bioenergetics and Axonal Arborization Size Are Key Contributors to the Vulnerability of Dopamine Neurons. *Current biology : CB* 2015; **25**(18): 2349-60.
95. Zucca FA, Bellei C, Giannelli S, et al. Neuromelanin and iron in human locus coeruleus and substantia nigra during aging: consequences for neuronal vulnerability. *Journal of neural transmission* 2006; **113**(6): 757-67.
96. Guzman JN, Sanchez-Padilla J, Wokosin D, et al. Oxidant stress evoked by pacemaking in dopaminergic neurons is attenuated by DJ-1. *Nature* 2010; **468**(7324): 696-700.
97. Goldberg JA, Guzman JN, Estep CM, et al. Calcium entry induces mitochondrial oxidant stress in vagal neurons at risk in Parkinson's disease. *Nature neuroscience* 2012; **15**(10): 1414-21.
98. Sanchez-Padilla J, Guzman JN, Ilijic E, et al. Mitochondrial oxidant stress in locus coeruleus is regulated by activity and nitric oxide synthase. *Nature neuroscience* 2014; **17**(6): 832-40.
99. Pearce RK, Owen A, Daniel S, Jenner P, Marsden CD. Alterations in the distribution of glutathione in the substantia nigra in Parkinson's disease. *Journal of neural transmission* 1997; **104**(6-7): 661-77.
100. Sofic E, Lange KW, Jellinger K, Riederer P. Reduced and oxidized glutathione in the substantia nigra of patients with Parkinson's disease. *Neuroscience letters* 1992; **142**(2): 128-30.
101. Surmeier DJ, Obeso JA, Halliday GM. Selective neuronal vulnerability in Parkinson disease. *Nature reviews Neuroscience* 2017; **18**(2): 101-13.
102. Burke RE, O'Malley K. Axon degeneration in Parkinson's disease. *Experimental neurology* 2013; **246**: 72-83.
103. Tagliaferro P, Burke RE. Retrograde Axonal Degeneration in Parkinson Disease. *Journal of Parkinson's disease* 2016; **6**(1): 1-15.
104. O'Malley KL. The role of axonopathy in Parkinson's disease. *Experimental neurobiology* 2010; **19**(3): 115-9.
105. Kuramoto L, Cragg J, Nandhagopal R, et al. The nature of progression in Parkinson's disease: an application of non-linear, multivariate, longitudinal random effects modelling. *PloS one* 2013; **8**(10): e76595.
106. Scherman D, Desnos C, Darchen F, Pollak P, Javoy-Agid F, Agid Y. Striatal dopamine deficiency in Parkinson's disease: role of aging. *Annals of neurology* 1989; **26**(4): 551-7.
107. Lee CS, Samii A, Sossi V, et al. In vivo positron emission tomographic evidence for compensatory changes in presynaptic dopaminergic nerve terminals in Parkinson's disease. *Annals of neurology* 2000; **47**(4): 493-503.
108. Jellinger KA, Logroscino G, Rizzo G, et al. Accuracy of clinical diagnosis of Parkinson disease: A systematic review and meta-analysis. *Neurology* 2016; **87**(2): 237-8.
109. Kalia LV, Lang AE. Parkinson's disease. *Lancet* 2015; **386**(9996): 896-912.

110. Chen H, Zhao EJ, Zhang W, et al. Meta-analyses on prevalence of selected Parkinson's nonmotor symptoms before and after diagnosis. *Translational neurodegeneration* 2015; **4**(1): 1.
111. Adams-Carr KL, Bestwick JP, Shribman S, Lees A, Schrag A, Noyce AJ. Constipation preceding Parkinson's disease: a systematic review and meta-analysis. *Journal of neurology, neurosurgery, and psychiatry* 2016; **87**(7): 710-6.
112. Stirpe P, Hoffman M, Badiali D, Colosimo C. Constipation: an emerging risk factor for Parkinson's disease? *European journal of neurology* 2016; **23**(11): 1606-13.
113. Higgins PD, Johanson JF. Epidemiology of constipation in North America: a systematic review. *The American journal of gastroenterology* 2004; **99**(4): 750-9.
114. Leentjens AF, Driessen G, Weber W, Drukker M, van Os J. Mental health care use in Parkinson's disease: a record linkage study. *Neuroepidemiology* 2008; **30**(2): 71-5.
115. Fang F, Xu Q, Park Y, et al. Depression and the subsequent risk of Parkinson's disease in the NIH-AARP Diet and Health Study. *Movement disorders : official journal of the Movement Disorder Society* 2010; **25**(9): 1157-62.
116. Schrag A, Horsfall L, Walters K, Noyce A, Petersen I. Prediagnostic presentations of Parkinson's disease in primary care: a case-control study. *The Lancet Neurology* 2015; **14**(1): 57-64.
117. Zhang X, Sun X, Wang J, Tang L, Xie A. Prevalence of rapid eye movement sleep behavior disorder (RBD) in Parkinson's disease: a meta and meta-regression analysis. *Neurological sciences : official journal of the Italian Neurological Society and of the Italian Society of Clinical Neurophysiology* 2017; **38**(1): 163-70.
118. Sixel-Doring F, Trautmann E, Mollenhauer B, Trenkwalder C. Associated factors for REM sleep behavior disorder in Parkinson disease. *Neurology* 2011; **77**(11): 1048-54.
119. Postuma RB, Gagnon JF, Vendette M, Fantini ML, Massicotte-Marquez J, Montplaisir J. Quantifying the risk of neurodegenerative disease in idiopathic REM sleep behavior disorder. *Neurology* 2009; **72**(15): 1296-300.
120. Schenck CH, Boeve BF, Mahowald MW. Delayed emergence of a parkinsonian disorder or dementia in 81% of older men initially diagnosed with idiopathic rapid eye movement sleep behavior disorder: a 16-year update on a previously reported series. *Sleep medicine* 2013; **14**(8): 744-8.
121. Iranzo A, Fernandez-Arcos A, Tolosa E, et al. Neurodegenerative disorder risk in idiopathic REM sleep behavior disorder: study in 174 patients. *PloS one* 2014; **9**(2): e89741.
122. Ansari KA, Johnson A. Olfactory function in patients with Parkinson's disease. *Journal of chronic diseases* 1975; **28**(9): 493-7.
123. Firestein S. How the olfactory system makes sense of scents. *Nature* 2001; **413**(6852): 211-8.
124. Spehr M, Munger SD. Olfactory receptors: G protein-coupled receptors and beyond. *Journal of neurochemistry* 2009; **109**(6): 1570-83.
125. Bushdid C, Magnasco MO, Vosshall LB, Keller A. Humans can discriminate more than 1 trillion olfactory stimuli. *Science* 2014; **343**(6177): 1370-2.
126. Serizawa S, Miyamichi K, Sakano H. One neuron-one receptor rule in the mouse olfactory system. *Trends in genetics : TIG* 2004; **20**(12): 648-53.
127. Moon C, Jun Yoo S, Soo Han H. Smell. In: Aminoff MJ, Daroff RB, eds. Encyclopedia of the Neurological Sciences (Second Edition). Oxford: Academic Press; 2014: 216-20.
128. Nagayama S, Homma R, Imamura F. Neuronal organization of olfactory bulb circuits. *Frontiers in Neural Circuits* 2014; **8**(98).
129. Doty RL, Kamath V. The influences of age on olfaction: a review. *Frontiers in psychology* 2014; **5**: 20.
130. Pinching AJ, Powell TP. The neuron types of the glomerular layer of the olfactory bulb. *Journal of cell science* 1971; **9**(2): 305-45.
131. Shao Z, Puche AC, Kiyokage E, Szabo G, Shipley MT. Two GABAergic intraglomerular circuits differentially regulate tonic and phasic presynaptic inhibition of olfactory nerve terminals. *Journal of neurophysiology* 2009; **101**(4): 1988-2001.

132. Wachowiak M, Shipley MT. Coding and synaptic processing of sensory information in the glomerular layer of the olfactory bulb. *Seminars in cell & developmental biology* 2006; **17**(4): 411-23.
133. Matsumoto H, Kobayakawa K, Kobayakawa R, et al. Spatial arrangement of glomerular molecular-feature clusters in the odorant-receptor class domains of the mouse olfactory bulb. *Journal of neurophysiology* 2010; **103**(6): 3490-500.
134. Ennis M, Zhou FM, Ciombor KJ, et al. Dopamine D2 receptor-mediated presynaptic inhibition of olfactory nerve terminals. *Journal of neurophysiology* 2001; **86**(6): 2986-97.
135. Zatorre RJ, Jones-Gotman M, Evans AC, Meyer E. Functional localization and lateralization of human olfactory cortex. *Nature* 1992; **360**(6402): 339-40.
136. Karpa MJ, Gopinath B, Rochtchina E, et al. Prevalence and neurodegenerative or other associations with olfactory impairment in an older community. *Journal of aging and health* 2010; **22**(2): 154-68.
137. Huttenbrink KB, Hummel T, Berg D, Gasser T, Hahner A. Olfactory dysfunction: common in later life and early warning of neurodegenerative disease. *Deutsches Arzteblatt international* 2013; **110**(1-2): 1-7, e1.
138. Bramerson A, Johansson L, Ek L, Nordin S, Bende M. Prevalence of olfactory dysfunction: the skovde population-based study. *The Laryngoscope* 2004; **114**(4): 733-7.
139. Schubert CR, Cruickshanks KJ, Fischer ME, et al. Olfactory impairment in an adult population: the Beaver Dam Offspring Study. *Chemical senses* 2012; **37**(4): 325-34.
140. Lafreniere D, Mann N. Anosmia: loss of smell in the elderly. *Otolaryngologic clinics of North America* 2009; **42**(1): 123-31, x.
141. Liu B, Luo Z, Pinto JM, et al. Relationship Between Poor Olfaction and Mortality Among Community-Dwelling Older Adults: A Cohort Study. *Annals of internal medicine* 2019; **170**(10): 673-81.
142. Arendt T, Bigl V, Arendt A, Tennstedt A. Loss of neurons in the nucleus basalis of Meynert in Alzheimer's disease, paralysis agitans and Korsakoff's Disease. *Acta neuropathologica* 1983; **61**(2): 101-8.
143. Nakano I, Hirano A. Parkinson's disease: neuron loss in the nucleus basalis without concomitant Alzheimer's disease. *Annals of neurology* 1984; **15**(5): 415-8.
144. Bohnen NI, Muller ML, Kotagal V, et al. Olfactory dysfunction, central cholinergic integrity and cognitive impairment in Parkinson's disease. *Brain : a journal of neurology* 2010; **133**(Pt 6): 1747-54.
145. Zarow C, Lyness SA, Mortimer JA, Chui HC. Neuronal loss is greater in the locus coeruleus than nucleus basalis and substantia nigra in Alzheimer and Parkinson diseases. *Archives of neurology* 2003; **60**(3): 337-41.
146. Sullivan RM, Wilson DA, Lemon C, Gerhardt GA. Bilateral 6-OHDA lesions of the locus coeruleus impair associative olfactory learning in newborn rats. *Brain research* 1994; **643**(1-2): 306-9.
147. Doucette W, Milder J, Restrepo D. Adrenergic modulation of olfactory bulb circuitry affects odor discrimination. *Learning & memory* 2007; **14**(8): 539-47.
148. Garland EM, Raj SR, Peltier AC, Robertson D, Biaggioni I. A cross-sectional study contrasting olfactory function in autonomic disorders. *Neurology* 2011; **76**(5): 456-60.
149. Kovacs GG, Kloppel S, Fischer I, et al. Nucleus-specific alteration of raphe neurons in human neurodegenerative disorders. *Neuroreport* 2003; **14**(1): 73-6.
150. Petzold GC, Hagiwara A, Murthy VN. Serotonergic modulation of odor input to the mammalian olfactory bulb. *Nature neuroscience* 2009; **12**(6): 784-91.
151. Tong ZY, Kingsbury AE, Foster OJ. Up-regulation of tyrosine hydroxylase mRNA in a sub-population of A10 dopamine neurons in Parkinson's disease. *Brain research Molecular brain research* 2000; **79**(1-2): 45-54.

152. Doty RL, Stern MB, Pfeiffer C, Gollomp SM, Hurtig HI. Bilateral olfactory dysfunction in early stage treated and untreated idiopathic Parkinson's disease. *Journal of neurology, neurosurgery, and psychiatry* 1992; **55**(2): 138-42.
153. Quinn NP, Rossor MN, Marsden CD. Olfactory threshold in Parkinson's disease. *Journal of neurology, neurosurgery, and psychiatry* 1987; **50**(1): 88-9.
154. Roth J, Radil T, Ruzicka E, Jech R, Tichy J. Apomorphine does not influence olfactory thresholds in Parkinson's disease. *Functional neurology* 1998; **13**(2): 99-103.
155. Huisman E, Uylings HB, Hoogland PV. A 100% increase of dopaminergic cells in the olfactory bulb may explain hyposmia in Parkinson's disease. *Movement disorders : official journal of the Movement Disorder Society* 2004; **19**(6): 687-92.
156. Mundinano IC, Caballero MC, Ordonez C, et al. Increased dopaminergic cells and protein aggregates in the olfactory bulb of patients with neurodegenerative disorders. *Acta neuropathologica* 2011; **122**(1): 61-74.
157. Duda JE, Shah U, Arnold SE, Lee VM, Trojanowski JQ. The expression of alpha-, beta-, and gamma-synucleins in olfactory mucosa from patients with and without neurodegenerative diseases. *Experimental neurology* 1999; **160**(2): 515-22.
158. Sengoku R, Saito Y, Ikemura M, et al. Incidence and extent of Lewy body-related alpha-synucleinopathy in aging human olfactory bulb. *Journal of neuropathology and experimental neurology* 2008; **67**(11): 1072-83.
159. Daniel SE, Hawkes CH. Preliminary diagnosis of Parkinson's disease by olfactory bulb pathology. *Lancet* 1992; **340**(8812): 186.
160. Pearce RK, Hawkes CH, Daniel SE. The anterior olfactory nucleus in Parkinson's disease. *Movement disorders : official journal of the Movement Disorder Society* 1995; **10**(3): 283-7.
161. Tsuboi Y, Wszolek ZK, Graff-Radford NR, Cookson N, Dickson DW. Tau pathology in the olfactory bulb correlates with Braak stage, Lewy body pathology and apolipoprotein epsilon4. *Neuropathology and applied neurobiology* 2003; **29**(5): 503-10.
162. Doty RL. The olfactory vector hypothesis of neurodegenerative disease: is it viable? *Annals of neurology* 2008; **63**(1): 7-15.
163. Antunes MB, Bowler R, Doty RL. San Francisco/Oakland Bay Bridge Welder Study: olfactory function. *Neurology* 2007; **69**(12): 1278-84.
164. Abeliovich A, Schmitz Y, Farinas I, et al. Mice lacking alpha-synuclein display functional deficits in the nigrostriatal dopamine system. *Neuron* 2000; **25**(1): 239-52.
165. Masliah E, Rockenstein E, Veinbergs I, et al. Dopaminergic loss and inclusion body formation in alpha-synuclein mice: implications for neurodegenerative disorders. *Science* 2000; **287**(5456): 1265-9.
166. Richfield EK, Thiruchelvam MJ, Cory-Slechta DA, et al. Behavioral and neurochemical effects of wild-type and mutated human alpha-synuclein in transgenic mice. *Experimental neurology* 2002; **175**(1): 35-48.
167. Dawson TM, Ko HS, Dawson VL. Genetic animal models of Parkinson's disease. *Neuron* 2010; **66**(5): 646-61.
168. Li Y, Liu W, Oo TF, et al. Mutant LRRK2(R1441G) BAC transgenic mice recapitulate cardinal features of Parkinson's disease. *Nature neuroscience* 2009; **12**(7): 826-8.
169. Perez FA, Palmiter RD. Parkin-deficient mice are not a robust model of parkinsonism. *Proceedings of the National Academy of Sciences of the United States of America* 2005; **102**(6): 2174-9.
170. Gispert S, Ricciardi F, Kurz A, et al. Parkinson phenotype in aged PINK1-deficient mice is accompanied by progressive mitochondrial dysfunction in absence of neurodegeneration. *PloS one* 2009; **4**(6): e5777.
171. Goldberg MS, Pisani A, Haburcak M, et al. Nigrostriatal dopaminergic deficits and hypokinesia caused by inactivation of the familial Parkinsonism-linked gene DJ-1. *Neuron* 2005; **45**(4): 489-96.

172. Kurtenbach S, Wewering S, Hatt H, Neuhaus EM, Lubbert H. Olfaction in three genetic and two MPTP-induced Parkinson's disease mouse models. *PloS one* 2013; **8**(10): e77509.
173. Fleming SM, Tetreault NA, Mulligan CK, Hutson CB, Masliah E, Chesselet MF. Olfactory deficits in mice overexpressing human wildtype alpha-synuclein. *The European journal of neuroscience* 2008; **28**(2): 247-56.
174. Zhang S, Xiao Q, Le W. Olfactory dysfunction and neurotransmitter disturbance in olfactory bulb of transgenic mice expressing human A53T mutant alpha-synuclein. *PloS one* 2015; **10**(3): e0119928.
175. Kim YH, Lussier S, Rane A, Choi SW, Andersen JK. Inducible dopaminergic glutathione depletion in an α-synuclein transgenic mouse model results in age-related olfactory dysfunction. *Neuroscience* 2011; **172**: 379-86.
176. Dawson HN, Ferreira A, Eyster MV, Ghoshal N, Binder LI, Vitek MP. Inhibition of neuronal maturation in primary hippocampal neurons from tau deficient mice. *Journal of cell science* 2001; **114**(Pt 6): 1179-87.
177. Ramsden M, Kotilinek L, Forster C, et al. Age-dependent neurofibrillary tangle formation, neuron loss, and memory impairment in a mouse model of human tauopathy (P301L). *The Journal of neuroscience : the official journal of the Society for Neuroscience* 2005; **25**(46): 10637-47.
178. Santacruz K, Lewis J, Spires T, et al. Tau suppression in a neurodegenerative mouse model improves memory function. *Science* 2005; **309**(5733): 476-81.
179. Petit GH, Berkovich E, Hickery M, et al. Rasagiline ameliorates olfactory deficits in an alpha-synuclein mouse model of Parkinson's disease. *PloS one* 2013; **8**(4): e60691.
180. Deacon RM. Measuring motor coordination in mice. *Journal of visualized experiments : JoVE* 2013; (75): e2609.
181. Matsuura K, Kabuto H, Makino H, Ogawa N. Pole test is a useful method for evaluating the mouse movement disorder caused by striatal dopamine depletion. *Journal of neuroscience methods* 1997; **73**(1): 45-8.
182. Lei P, Ayton S, Appukuttan AT, et al. Clioquinol rescues Parkinsonism and dementia phenotypes of the tau knockout mouse. *Neurobiology of disease* 2015; **81**: 168-75.
183. Parish CL, Castelo-Branco G, Rawal N, et al. Wnt5a-treated midbrain neural stem cells improve dopamine cell replacement therapy in parkinsonian mice. *The Journal of clinical investigation* 2008; **118**(1): 149-60.
184. Siderowf A, Jennings D, Eberly S, et al. Impaired olfaction and other prodromal features in the Parkinson At-Risk Syndrome Study. *Movement disorders : official journal of the Movement Disorder Society* 2012; **27**(3): 406-12.
185. Eisensehr I, Linke R, Noachtar S, Schwarz J, Gildehaus FJ, Tatsch K. Reduced striatal dopamine transporters in idiopathic rapid eye movement sleep behaviour disorder. Comparison with Parkinson's disease and controls. *Brain : a journal of neurology* 2000; **123 (Pt 6)**: 1155-60.
186. Kim YK, Yoon IY, Kim JM, et al. The implication of nigrostriatal dopaminergic degeneration in the pathogenesis of REM sleep behavior disorder. *European journal of neurology* 2010; **17**(3): 487-92.
187. Iranzo A, Lomena F, Stockner H, et al. Decreased striatal dopamine transporter uptake and substantia nigra hyperechogenicity as risk markers of synucleinopathy in patients with idiopathic rapid-eye-movement sleep behaviour disorder: a prospective study [corrected]. *The Lancet Neurology* 2010; **9**(11): 1070-7.
188. Xu SS, Alexander PK, Lie Y, et al. Diagnostic accuracy of imaging brain vesicular monoamine transporter type 2 (VMAT2) in clinically uncertain parkinsonian syndrome (CUPS): a 3-year follow-up study in community patients. *BMJ open* 2018; **8**(11): e025533.
189. Boeve BF, Molano JR, Ferman TJ, et al. Validation of the Mayo Sleep Questionnaire to screen for REM sleep behavior disorder in a community-based sample. *Journal of clinical sleep medicine : JCSM : official publication of the American Academy of Sleep Medicine* 2013; **9**(5): 475-80.

190. Villemagne VL, Okamura N, Pejoska S, et al. In vivo assessment of vesicular monoamine transporter type 2 in dementia with lewy bodies and Alzheimer disease. *Archives of neurology* 2011; **68**(7): 905-12.
191. Okamura N, Villemagne VL, Drago J, et al. In vivo measurement of vesicular monoamine transporter type 2 density in Parkinson disease with (18)F-AV-133. *J Nucl Med* 2010; **51**(2): 223-8.
192. Bohnen NI, Albin RL, Koeppe RA, et al. Positron emission tomography of monoaminergic vesicular binding in aging and Parkinson disease. *Journal of cerebral blood flow and metabolism : official journal of the International Society of Cerebral Blood Flow and Metabolism* 2006; **26**(9): 1198-212.
193. Albin RL, Koeppe RA, Chervin RD, et al. Decreased striatal dopaminergic innervation in REM sleep behavior disorder. *Neurology* 2000; **55**(9): 1410-2.
194. Barber TR, Klein JC, Mackay CE, Hu MTM. Neuroimaging in pre-motor Parkinson's disease. *NeuroImage Clinical* 2017; **15**: 215-27.
195. Martin I, Dawson VL, Dawson TM. The impact of genetic research on our understanding of Parkinson's disease. *Progress in brain research* 2010; **183**: 21-41.
196. Hashimoto M, Masliah E. Cycles of aberrant synaptic sprouting and neurodegeneration in Alzheimer's and dementia with Lewy bodies. *Neurochemical research* 2003; **28**(11): 1743-56.
197. Finkelstein DI, Stanic D, Parish CL, Tomas D, Dickson K, Horne MK. Axonal sprouting following lesions of the rat substantia nigra. *Neuroscience* 2000; **97**(1): 99-112.
198. Dorsey ER, Sherer T, Okun MS, Bloem BR. The Emerging Evidence of the Parkinson Pandemic. *Journal of Parkinson's disease* 2018; **8**(s1): S3-s8.
199. Chinta SJ, Lieu CA, Demaria M, Laberge RM, Campisi J, Andersen JK. Environmental stress, ageing and glial cell senescence: a novel mechanistic link to Parkinson's disease? *Journal of internal medicine* 2013; **273**(5): 429-36.
200. Jankovic J, Poewe W. Therapies in Parkinson's disease. *Current opinion in neurology* 2012; **25**(4): 433-47.
201. Milber JM, Noorigian JV, Morley JF, et al. Lewy pathology is not the first sign of degeneration in vulnerable neurons in Parkinson disease. *Neurology* 2012; **79**(24): 2307-14.
202. Doty RL, Deems DA, Stellar S. Olfactory dysfunction in parkinsonism. *A general deficit unrelated to neurologic signs, disease stage, or disease duration* 1988; **38**(8): 1237-.
203. Doty RL. Olfactory dysfunction in Parkinson disease. *Nature reviews Neurology* 2012; **8**(6): 329-39.
204. Hawkes CH, Del Tredici K, Braak H. Parkinson's disease: a dual-hit hypothesis. *Neuropathology and applied neurobiology* 2007; **33**(6): 599-614.
205. Ashwell K. Chapter 26 - The Olfactory System. In: Watson C, Paxinos G, Puelles L, eds. The Mouse Nervous System. San Diego: Academic Press; 2012: 653-60.
206. Braak H, Del Tredici K, Rub U, de Vos RA, Jansen Steur EN, Braak E. Staging of brain pathology related to sporadic Parkinson's disease. *Neurobiology of aging* 2003; **24**(2): 197-211.
207. Hsia AY, Vincent JD, Lledo PM. Dopamine depresses synaptic inputs into the olfactory bulb. *Journal of neurophysiology* 1999; **82**(2): 1082-5.
208. Pignatelli A, Belluzzi O. Dopaminergic Neurones in the Main Olfactory Bulb: An Overview from an Electrophysiological Perspective. *Frontiers in neuroanatomy* 2017; **11**: 7.
209. Gardner B, Dieriks BV, Cameron S, et al. Metal concentrations and distributions in the human olfactory bulb in Parkinson's disease. *Scientific reports* 2017; **7**(1): 10454.
210. Waragai M, Wei J, Fujita M, et al. Increased level of DJ-1 in the cerebrospinal fluids of sporadic Parkinson's disease. *Biochemical and biophysical research communications* 2006; **345**(3): 967-72.
211. Mita Y, Kataoka Y, Saito Y, et al. Distribution of oxidized DJ-1 in Parkinson's disease-related sites in the brain and in the peripheral tissues: effects of aging and a neurotoxin. *Scientific reports* 2018; **8**(1): 12056.

212. Ichimura Y, Kominami E, Tanaka K, Komatsu M. Selective turnover of p62/A170/SQSTM1 by autophagy. *Autophagy* 2008; **4**(8): 1063-6.
213. Lynch-Day MA, Mao K, Wang K, Zhao M, Klionsky DJ. The role of autophagy in Parkinson's disease. *Cold Spring Harbor perspectives in medicine* 2012; **2**(4): a009357.
214. Liu Z, Martin LJ. Olfactory bulb core is a rich source of neural progenitor and stem cells in adult rodent and human. *The Journal of comparative neurology* 2003; **459**(4): 368-91.
215. Porritt MJ, Batchelor PE, Hughes AJ, Kalnins R, Donnan GA, Howells DW. New dopaminergic neurons in Parkinson's disease striatum. *Lancet* 2000; **356**(9223): 44-5.
216. Song DD, Haber SN. Striatal responses to partial dopaminergic lesion: evidence for compensatory sprouting. *The Journal of neuroscience : the official journal of the Society for Neuroscience* 2000; **20**(13): 5102-14.
217. Cockerham R, Liu S, Cachope R, et al. Subsecond Regulation of Synaptically Released Dopamine by COMT in the Olfactory Bulb. *The Journal of neuroscience : the official journal of the Society for Neuroscience* 2016; **36**(29): 7779-85.
218. Muller T, Woitalla D, Hauptmann B, Fowler B, Kuhn W. Decrease of methionine and S-adenosylmethionine and increase of homocysteine in treated patients with Parkinson's disease. *Neuroscience letters* 2001; **308**(1): 54-6.
219. Jones SR, Gainetdinov RR, Hu XT, et al. Loss of autoreceptor functions in mice lacking the dopamine transporter. *Nature neuroscience* 1999; **2**(7): 649-55.
220. Altamura S, Muckenthaler MU. Iron toxicity in diseases of aging: Alzheimer's disease, Parkinson's disease and atherosclerosis. *Journal of Alzheimer's disease : JAD* 2009; **16**(4): 879-95.
221. Vitvitsky VM, Garg SK, Keep RF, Albin RL, Banerjee R. Na+ and K+ ion imbalances in Alzheimer's disease. *Biochimica et biophysica acta* 2012; **1822**(11): 1671-81.
222. Mellon EA, Pilkinton DT, Clark CM, et al. Sodium MR imaging detection of mild Alzheimer disease: preliminary study. *AJNR American journal of neuroradiology* 2009; **30**(5): 978-84.
223. Korf J, Gramsbergen JB, Prenen GH, Go KG. Cation shifts and excitotoxins in Alzheimer and Huntington disease and experimental brain damage. *Progress in brain research* 1986; **70**: 213-26.
224. Rosas HD, Chen YI, Doros G, et al. Alterations in brain transition metals in Huntington disease: an evolving and intricate story. *Archives of neurology* 2012; **69**(7): 887-93.
225. Zaaraoui W, Konstandin S, Audoin B, et al. Distribution of brain sodium accumulation correlates with disability in multiple sclerosis: a cross-sectional 23Na MR imaging study. *Radiology* 2012; **264**(3): 859-67.
226. Haacke EM, Makki M, Ge Y, et al. Characterizing iron deposition in multiple sclerosis lesions using susceptibility weighted imaging. *Journal of magnetic resonance imaging : JMRI* 2009; **29**(3): 537-44.
227. Franco J, Prediger RD, Pandolfo P, Takahashi RN, Farina M, Dafre AL. Antioxidant responses and lipid peroxidation following intranasal 1-methyl-4-phenyl-1,2,3,6-tetrahydropyridine (MPTP) administration in rats: increased susceptibility of olfactory bulb. *Life Sci* 2007; **80**(20): 1906-14.
228. Block ML, Calderon-Garciduenas L. Air pollution: mechanisms of neuroinflammation and CNS disease. *Trends in neurosciences* 2009; **32**(9): 506-16.
229. Wang B, Feng WY, Wang M, et al. Transport of intranasally instilled fine Fe2O3 particles into the brain: micro-distribution, chemical states, and histopathological observation. *Biological trace element research* 2007; **118**(3): 233-43.
230. Liu Y, Gao Y, Zhang L, et al. Potential health impact on mice after nasal instillation of nano-sized copper particles and their translocation in mice. *Journal of nanoscience and nanotechnology* 2009; **9**(11): 6335-43.
231. Kao YY, Cheng TJ, Yang DM, Wang CT, Chiung YM, Liu PS. Demonstration of an olfactory bulb-brain translocation pathway for ZnO nanoparticles in rodent cells in vitro and in vivo. *Journal of molecular neuroscience : MN* 2012; **48**(2): 464-71.

232. Dziewulska D, Doi H, Fasano A, et al. Olfactory impairment and pathology in neurodegenerative disorders with brain iron accumulation. *Acta neuropathologica* 2013; **126**(1): 151-3.
233. Tisdall FF, Brown A, Defries RD. Persistent anosmia following zinc sulfate nasal spraying. *The Journal of Pediatrics* 1938; **13**(1): 60-2.
234. Jafek BW, Linschoten MR, Murrow BW. Anosmia after intranasal zinc gluconate use. *American journal of rhinology* 2004; **18**(3): 137-41.
235. Davidson TM, Smith WM. The Bradford Hill criteria and zinc-induced anosmia: a causality analysis. *Archives of otolaryngology--head & neck surgery* 2010; **136**(7): 673-6.
236. Alberts JR. Producing and interpreting experimental olfactory deficits. *Physiology & behavior* 1974; **12**(4): 657-70.
237. Weiss J, Pyrski M, Jacobi E, et al. Loss-of-function mutations in sodium channel Nav1.7 cause anosmia. *Nature* 2011; **472**(7342): 186-90.
238. White LD, Cory-Slechta DA, Gilbert ME, et al. New and evolving concepts in the neurotoxicology of lead. *Toxicology and applied pharmacology* 2007; **225**(1): 1-27.
239. Coon S, Stark A, Peterson E, et al. Whole-body lifetime occupational lead exposure and risk of Parkinson's disease. *Environmental health perspectives* 2006; **114**(12): 1872-6.
240. Weisskopf MG, Weuve J, Nie H, et al. Association of cumulative lead exposure with Parkinson's disease. *Environmental health perspectives* 2010; **118**(11): 1609-13.
241. Riederer P, Sofic E, Rausch WD, et al. Transition metals, ferritin, glutathione, and ascorbic acid in parkinsonian brains. *Journal of neurochemistry* 1989; **52**(2): 515-20.
242. Hawkes CH, Del Tredici K, Braak H. A timeline for Parkinson's disease. *Parkinsonism & related disorders* 2010; **16**(2): 79-84.
243. Kertelge L, Bruggemann N, Schmidt A, et al. Impaired sense of smell and color discrimination in monogenic and idiopathic Parkinson's disease. *Movement disorders : official journal of the Movement Disorder Society* 2010; **25**(15): 2665-9.
244. Doty RL, Deems DA, Stellar S. Olfactory dysfunction in parkinsonism: a general deficit unrelated to neurologic signs, disease stage, or disease duration. *Neurology* 1988; **38**(8): 1237-44.
245. Simon-Sanchez J, Schulte C, Bras JM, et al. Genome-wide association study reveals genetic risk underlying Parkinson's disease. *Nat Genet* 2009; **41**(12): 1308-U68.
246. Drubin DG, Kirschner MW. Tau protein function in living cells. *The Journal of cell biology* 1986; **103**(6 Pt 2): 2739-46.
247. Jeganathan S, von Bergen M, Mandelkow EM, Mandelkow E. The natively unfolded character of tau and its aggregation to Alzheimer-like paired helical filaments. *Biochemistry* 2008; **47**(40): 10526-39.
248. Spillantini MG, Goedert M. Tau and Parkinson disease. *Jama* 2001; **286**(18): 2324-6.
249. Harada A, Oguchi K, Okabe S, et al. Altered microtubule organization in small-calibre axons of mice lacking tau protein. *Nature* 1994; **369**(6480): 488-91.
250. Lei P, Ayton S, Moon S, et al. Motor and cognitive deficits in aged tau knockout mice in two background strains. *Molecular neurodegeneration* 2014; **9**: 29.
251. Dauer W, Przedborski S. Parkinson's disease: mechanisms and models. *Neuron* 2003; **39**(6): 889-909.
252. Lang AE, Lozano AM. Parkinson's disease. First of two parts. *The New England journal of medicine* 1998; **339**(15): 1044-53.
253. Tillerson JL, Caudle WM, Parent JM, Gong C, Schallert T, Miller GW. Olfactory discrimination deficits in mice lacking the dopamine transporter or the D2 dopamine receptor. *Behavioural brain research* 2006; **172**(1): 97-105.
254. Taylor TN, Caudle WM, Shepherd KR, et al. Nonmotor symptoms of Parkinson's disease revealed in an animal model with reduced monoamine storage capacity. *The Journal of neuroscience : the official journal of the Society for Neuroscience* 2009; **29**(25): 8103-13.

255. Petit GH, Berkovich E, Hickery M, et al. Rasagiline Ameliorates Olfactory Deficits in an Alpha-Synuclein Mouse Model of Parkinson's Disease. *PloS one* 2013; **8**(4).
256. Klionsky DJ, Ohsumi Y. Vacuolar import of proteins and organelles from the cytoplasm. *Annual review of cell and developmental biology* 1999; **15**: 1-32.
257. Fader CM, Sanchez D, Furlan M, Colombo MI. Induction of autophagy promotes fusion of multivesicular bodies with autophagic vacuoles in k562 cells. *Traffic* 2008; **9**(2): 230-50.
258. Fader CM, Colombo MI. Autophagy and multivesicular bodies: two closely related partners. *Cell death and differentiation* 2009; **16**(1): 70-8.
259. Lee HJ, Cho ED, Lee KW, Kim JH, Cho SG, Lee SJ. Autophagic failure promotes the exocytosis and intercellular transfer of alpha-synuclein. *Experimental & molecular medicine* 2013; **45**: e22.
260. Weingarten MD, Lockwood AH, Hwo SY, Kirschner MW. A protein factor essential for microtubule assembly. *Proceedings of the National Academy of Sciences of the United States of America* 1975; **72**(5): 1858-62.
261. Cleveland DW, Hwo SY, Kirschner MW. Purification of tau, a microtubule-associated protein that induces assembly of microtubules from purified tubulin. *Journal of molecular biology* 1977; **116**(2): 207-25.
262. Jiang P, Nishimura T, Sakamaki Y, et al. The HOPS complex mediates autophagosome-lysosome fusion through interaction with syntaxin 17. *Molecular biology of the cell* 2014; **25**(8): 1327-37.
263. Itakura E, Kishi-Itakura C, Mizushima N. The hairpin-type tail-anchored SNARE syntaxin 17 targets to autophagosomes for fusion with endosomes/lysosomes. *Cell* 2012; **151**(6): 1256-69.
264. Kabeya Y, Mizushima N, Ueno T, et al. LC3, a mammalian homologue of yeast Apg8p, is localized in autophagosome membranes after processing. *The EMBO journal* 2000; **19**(21): 5720-8.
265. Nakatogawa H, Ichimura Y, Ohsumi Y. Atg8, a ubiquitin-like protein required for autophagosome formation, mediates membrane tethering and hemifusion. *Cell* 2007; **130**(1): 165-78.
266. Nguyen TN, Padman BS, Usher J, Oorschot V, Ramm G, Lazarou M. Atg8 family LC3/GABARAP proteins are crucial for autophagosome-lysosome fusion but not autophagosome formation during PINK1/Parkin mitophagy and starvation. *The Journal of cell biology* 2016; **215**(6): 857-74.
267. Tanida I, Ueno T, Kominami E. LC3 conjugation system in mammalian autophagy. *The international journal of biochemistry & cell biology* 2004; **36**(12): 2503-18.
268. Kliosnky D. Guidelines for the Use and Interpretation of Assays for Monitoring Autophagy (3rd edition) (vol 12, pg 1, 2015). *Autophagy* 2016; **12**(2): 443-.
269. Tian Y, Chang JC, Greengard P, Flajolet M. The convergence of endosomal and autophagosomal pathways: implications for APP-CTF degradation. *Autophagy* 2014; **10**(4): 694-6.
270. Simons M, Raposo G. Exosomes--vesicular carriers for intercellular communication. *Current opinion in cell biology* 2009; **21**(4): 575-81.
271. Schneider A, Simons M. Exosomes: vesicular carriers for intercellular communication in neurodegenerative disorders. *Cell and tissue research* 2013; **352**(1): 33-47.
272. Fevrier B, Vilette D, Archer F, et al. Cells release prions in association with exosomes. *Proceedings of the National Academy of Sciences of the United States of America* 2004; **101**(26): 9683-8.
273. Vella LJ, Sharples RA, Nisbet RM, Cappai R, Hill AF. The role of exosomes in the processing of proteins associated with neurodegenerative diseases. *European biophysics journal : EBJ* 2008; **37**(3): 323-32.
274. Ikegami S, Harada A, Hirokawa N. Muscle weakness, hyperactivity, and impairment in fear conditioning in tau-deficient mice. *Neuroscience letters* 2000; **279**(3): 129-32.
275. Ahmed T, Van der Jeugd A, Blum D, et al. Cognition and hippocampal synaptic plasticity in mice with a homozygous tau deletion. *Neurobiology of aging* 2014; **35**(11): 2474-8.

276. Morris M, Hamto P, Adame A, Devidze N, Masliah E, Mucke L. Age-appropriate cognition and subtle dopamine-independent motor deficits in aged tau knockout mice. *Neurobiology of aging* 2013; **34**(6): 1523-9.
277. Watt AD, Crespi GA, Down RA, et al. Anti-Abeta antibody target engagement: a response to Siemers et al. *Acta neuropathologica* 2014; **128**(4): 611-4.
278. Macknin JB, Higuchi M, Lee VM, Trojanowski JQ, Doty RL. Olfactory dysfunction occurs in transgenic mice overexpressing human tau protein. *Brain research* 2004; **1000**(1-2): 174-8.
279. Yang S, Kuan WL, Spillantini MG. Progressive tauopathy in P301S tau transgenic mice is associated with a functional deficit of the olfactory system. *The European journal of neuroscience* 2016; **44**(6): 2396-403.
280. Olichney JM, Murphy C, Hofstetter CR, et al. Anosmia is very common in the Lewy body variant of Alzheimer's disease. *Journal of neurology, neurosurgery, and psychiatry* 2005; **76**(10): 1342-7.
281. McShane RH, Nagy Z, Esiri MM, et al. Anosmia in dementia is associated with Lewy bodies rather than Alzheimer's pathology. *Journal of neurology, neurosurgery, and psychiatry* 2001; **70**(6): 739-43.
282. Attems J, Jellinger KA. Olfactory tau pathology in Alzheimer disease and mild cognitive impairment. *Clinical neuropathology* 2006; **25**(6): 265-71.
283. Ciechanover A. Proteolysis: from the lysosome to ubiquitin and the proteasome. *Nature reviews Molecular cell biology* 2005; **6**(1): 79-87.
284. Rubinsztein DC. The roles of intracellular protein-degradation pathways in neurodegeneration. *Nature* 2006; **443**(7113): 780-6.
285. Pan T, Kondo S, Le W, Jankovic J. The role of autophagy-lysosome pathway in neurodegeneration associated with Parkinson's disease. *Brain : a journal of neurology* 2008; **131**(Pt 8): 1969-78.
286. Cheung ZH, Ip NY. The emerging role of autophagy in Parkinson's disease. *Molecular brain* 2009; **2**: 29.
287. Wong E, Cuervo AM. Autophagy gone awry in neurodegenerative diseases. *Nature neuroscience* 2010; **13**(7): 805-11.
288. Banerjee R, Beal MF, Thomas B. Autophagy in neurodegenerative disorders: pathogenic roles and therapeutic implications. *Trends in neurosciences* 2010; **33**(12): 541-9.
289. Bandyopadhyay U, Cuervo AM. Chaperone-mediated autophagy in aging and neurodegeneration: lessons from alpha-synuclein. *Experimental gerontology* 2007; **42**(1-2): 120-8.
290. Alegre-Abarrategui J, Wade-Martins R. Parkinson disease, LRRK2 and the endocytic-autophagic pathway. *Autophagy* 2009; **5**(8): 1208-10.
291. Sahani MH, Itakura E, Mizushima N. Expression of the autophagy substrate SQSTM1/p62 is restored during prolonged starvation depending on transcriptional upregulation and autophagy-derived amino acids. *Autophagy* 2014; **10**(3): 431-41.
292. Kochl R, Hu XW, Chan EY, Tooze SA. Microtubules facilitate autophagosome formation and fusion of autophagosomes with endosomes. *Traffic* 2006; **7**(2): 129-45.
293. Yamamoto M, Suzuki SO, Himeno M. The effects of dynein inhibition on the autophagic pathway in glioma cells. *Neuropathology : official journal of the Japanese Society of Neuropathology* 2010; **30**(1): 1-6.
294. Shimozawa A, Ono M, Takahara D, et al. Propagation of pathological alpha-synuclein in marmoset brain. *Acta neuropathologica communications* 2017; **5**(1): 12.
295. Luk KC, Kehm V, Carroll J, et al. Pathological alpha-synuclein transmission initiates Parkinson-like neurodegeneration in nontransgenic mice. *Science* 2012; **338**(6109): 949-53.
296. Lee HJ, Bae EJ, Lee SJ. Extracellular alpha--synuclein-a novel and crucial factor in Lewy body diseases. *Nat Rev Neurol* 2014; **10**(2): 92-8.
297. Alvarez-Erviti L, Seow Y, Schapira AH, et al. Lysosomal dysfunction increases exosome-mediated alpha-synuclein release and transmission. *Neurobiology of disease* 2011; **42**(3): 360-7.

298. Emmanouilidou E, Melachroinou K, Roumeliotis T, et al. Cell-produced alpha-synuclein is secreted in a calcium-dependent manner by exosomes and impacts neuronal survival. *The Journal of neuroscience : the official journal of the Society for Neuroscience* 2010; **30**(20): 6838-51.
299. Danzer KM, Kranich LR, Ruf WP, et al. Exosomal cell-to-cell transmission of alpha synuclein oligomers. *Molecular neurodegeneration* 2012; **7**: 42.
300. Hasegawa T, Konno M, Baba T, et al. The AAA-ATPase VPS4 regulates extracellular secretion and lysosomal targeting of alpha-synuclein. *PloS one* 2011; **6**(12): e29460.
301. Bellingham SA, Guo BB, Coleman BM, Hill AF. Exosomes: vehicles for the transfer of toxic proteins associated with neurodegenerative diseases? *Frontiers in physiology* 2012; **3**: 124.
302. Ejlerskov P, Rasmussen I, Nielsen TT, et al. Tubulin polymerization-promoting protein (TPPP/p25alpha) promotes unconventional secretion of alpha-synuclein through exophagy by impairing autophagosome-lysosome fusion. *The Journal of biological chemistry* 2013; **288**(24): 17313-35.
303. Beauchamp LC, Chan J, Hung LW, et al. Ablation of tau causes an olfactory deficit in a murine model of Parkinson's disease. *Acta neuropathologica communications* 2018; **6**(1): 57.
304. Elsworth JD, Roth RH. Dopamine synthesis, uptake, metabolism, and receptors: relevance to gene therapy of Parkinson's disease. *Experimental neurology* 1997; **144**(1): 4-9.
305. Halasz N, Ljungdahl A, Hokfelt T, et al. Transmitter histochemistry of the rat olfactory bulb. I. Immunohistochemical localization of monoamine synthesizing enzymes. Support for intrabulbar, periglomerular dopamine neurons. *Brain research* 1977; **126**(3): 455-74.
306. Nappi AJ, Vass E. Hydroxyl radical formation via iron-mediated Fenton chemistry is inhibited by methylated catechols. *Biochimica et biophysica acta* 1998; **1425**(1): 159-67.
307. Taylor TN, Caudle WM, Miller GW. VMAT2-Deficient Mice Display Nigral and Extranigral Pathology and Motor and Nonmotor Symptoms of Parkinson's Disease. *Parkinson's disease* 2011; **2011**: 124165.
308. Costall B, Naylor RJ. The behavioural effects of dopamine applied intracerebrally to areas of the mesolimbic system. *European journal of pharmacology* 1975; **32**(1): 87-92.
309. Jackson DM, Anden NE, Dahlstrom A. A functional effect of dopamine in the nucleus accumbens and in some other dopamine-rich parts of the rat brain. *Psychopharmacologia* 1975; **45**(2): 139-49.
310. Wachtel H, Ahlenius S, Anden NE. Effects of locally applied dopamine to the nucleus accumbens on the motor activity of normal rats and following alpha-methyltyrosine or reserpine. *Psychopharmacology* 1979; **63**(3): 203-6.
311. Berkowicz DA, Trombley PQ. Dopaminergic modulation at the olfactory nerve synapse. *Brain research* 2000; **855**(1): 90-9.
312. Anden NE, Butcher SG, Corrodi H, Fuxe K, Ungerstedt U. Receptor activity and turnover of dopamine and noradrenaline after neuroleptics. *European journal of pharmacology* 1970; **11**(3): 303-14.
313. Carlsson A, Lindqvist M, Magnusson T, Waldeck B. On the presence of 3-hydroxytyramine in brain. *Science* 1958; **127**(3296): 471.
314. Ungerstedt U. Central Dopamine Mechanisms and Behaviour. In: A.S. Horn JK, and B.H.C. Westerink, ed. The Neurobiology of Dopamine. London: Academic Press; 1979: 577-96.
315. Fray PJ, Sahakian BJ, Robbins TW, Koob GF, Iversen SD. An observational method for quantifying the behavioural effects of dopamine agonists: contrasting effects of d-amphetamine and apomorphine. *Psychopharmacology* 1980; **69**(3): 253-9.
316. Lyon MaR, T. W. The action of central nervous system drugs: A general theory concerning amphetamine affects. In: W. B. Esssman aLV, ed. Current Developments in Psychopharmacology. New York: Spectrum; 1975: 79-163.
317. Cole SO. Brain mechanisms of amphetamine-induced anorexia, locomotion, and stereotypy: A review. *Neuroscience and Biobehavioral Reviews* 1978; **2**(2): 89-100.

318. Costa E, Garattini S. International Symposium on Amphetamines and Related Compounds: Raven Press; 1970.
319. Isaacson RL, Yongue B, McClearn D. Dopamine agonists: their effect on locomotion and exploration. *Behavioral biology* 1978; **23**(2): 163-79.
320. Marshall JF, Richardson JS, Teitelbaum P. Nigrostriatal bundle damage and the lateral hypothalamic syndrome. *Journal of comparative and physiological psychology* 1974; **87**(5): 808-30.
321. Iversen SD, Koob GF. Behavioral implications of dopaminergic neurons in the mesolimbic system. *Advances in biochemical psychopharmacology* 1977; **16**: 209-14.
322. Koob GF, Riley SJ, Smith SC, Robbins TW. Effects of 6-hydroxydopamine lesions of the nucleus accumbens septi and olfactory tubercle on feeding, locomotor activity, and amphetamine anorexia in the rat. *Journal of comparative and physiological psychology* 1978; **92**(5): 917-27.
323. Carter CJ, Pycock CJ. Behavioural and biochemical effects of dopamine and noradrenaline depletion within the medial prefrontal cortex of the rat. *Brain research* 1980; **192**(1): 163-76.
324. Arnt J. Hyperactivity following injection of a glutamate agonist and 6,7-ADTN into rat nucleus accumbens and its inhibition by THIP. *Life Sci* 1981; **28**(14): 1597-603.
325. Costall B, Naylor RJ, Cannon JG, Lee T. Differentiation of the dopamine mechanisms mediating stereotyped behaviour and hyperactivity in the nucleus accumbens and caudate-putamen. *The Journal of pharmacy and pharmacology* 1977; **29**(6): 337-42.
326. Dill RE, Jones DL, Gillin JC, Murphy G. Comparison of behavioral effects of systemic L-DOPA and intracranial dopamine in mesolimbic forebrain of nonhuman primates. *Pharmacology, biochemistry, and behavior* 1979; **10**(5): 711-6.
327. Pijnenburg AJ, Honig WM, Van der Heyden JA, Van Rossum JM. Effects of chemical stimulation of the mesolimbic dopamine system upon locomotor activity. *European journal of pharmacology* 1976; **35**(1): 45-58.
328. Pijnenburg AJ, Honig WM, Van Rossum JM. Inhibition of d-amphetamine-induced locomotor activity by injection of haloperidol into the nucleus accumbens of the rat. *Psychopharmacologia* 1975; **41**(2): 87-95.
329. Jul P, Volbracht C, de Jong IE, Helboe L, Elvang AB, Pedersen JT. Hyperactivity with Agitative-Like Behavior in a Mouse Tauopathy Model. *Journal of Alzheimer's disease : JAD* 2016; **49**(3): 783-95.
330. Pennanen L, Wolfer DP, Nitsch RM, Gotz J. Impaired spatial reference memory and increased exploratory behavior in P301L tau transgenic mice. *Genes, brain, and behavior* 2006; **5**(5): 369-79.
331. Gilley J, Seereeram A, Ando K, et al. Age-dependent axonal transport and locomotor changes and tau hypophosphorylation in a "P301L" tau knockin mouse. *Neurobiology of aging* 2012; **33**(3): 621 e1- e15.
332. Davila NG, Blakemore LJ, Trombley PQ. Dopamine modulates synaptic transmission between rat olfactory bulb neurons in culture. *Journal of neurophysiology* 2003; **90**(1): 395-404.
333. Puopolo M, Bean BP, Raviola E. Spontaneous activity of isolated dopaminergic periglomerular cells of the main olfactory bulb. *Journal of neurophysiology* 2005; **94**(5): 3618-27.
334. McGann JP, Pirez N, Gainey MA, Muratore C, Elias AS, Wachowiak M. Odorant representations are modulated by intra- but not interglomerular presynaptic inhibition of olfactory sensory neurons. *Neuron* 2005; **48**(6): 1039-53.
335. Ritz MC, Lamb RJ, Goldberg SR, Kuhar MJ. Cocaine receptors on dopamine transporters are related to self-administration of cocaine. *Science* 1987; **237**(4819): 1219-23.
336. Iversen LL. Role of transmitter uptake mechanisms in synaptic neurotransmission. *British journal of pharmacology* 1971; **41**(4): 571-91.
337. Giros B, Caron MG. Molecular characterization of the dopamine transporter. *Trends in pharmacological sciences* 1993; **14**(2): 43-9.
338. Hitri A, Hurd YL, Wyatt RJ, Deutsch SI. Molecular, functional and biochemical characteristics of the dopamine transporter: regional differences and clinical relevance. *Clinical neuropharmacology* 1994; **17**(1): 1-22.

339. Zilstorff K. Sense of Smell Alterations by Cocaine and Tetracaine. *Archives of otolaryngology* 1965; **82**: 53-5.
340. Doty RL, Risser JM. Influence of the D-2 dopamine receptor agonist quinpirole on the odor detection performance of rats before and after spiperone administration. *Psychopharmacology* 1989; **98**(3): 310-5.
341. Serguera C, Triaca V, Kelly-Barrett J, Banchaabouchi MA, Minichiello L. Increased dopamine after mating impairs olfaction and prevents odor interference with pregnancy. *Nature neuroscience* 2008; **11**(8): 949-56.
342. Carlsson A, Lindqvist M. Effect of Chlorpromazine or Haloperidol on Formation of 3methoxytyramine and Normetanephrine in Mouse Brain. *Acta pharmacologica et toxicologica* 1963; **20**: 140-4.
343. Nyback H, Sedvall G. Effect of chlorpromazine on accumulation and disappearance of catecholamines formed from tyrosine-C14 in brain. *The Journal of pharmacology and experimental therapeutics* 1968; **162**(2): 294-301.
344. Andén N-E, Roos B-E, Werdinius B. Effects of chlorpromazine, haloperidol and reserpine on the levels of phenolic acids in rabbit corpus striatum. *Life Sciences* 1964; **3**(2): 149-58.
345. Yue EL, Cleland TA, Pavlis M, Linster C. Opposing effects of D1 and D2 receptor activation on odor discrimination learning. *Behavioral neuroscience* 2004; **118**(1): 184-90.
346. Murphy KC. Schizophrenia and velo-cardio-facial syndrome. *Lancet* 2002; **359**(9304): 426-30.
347. Kaenmaki M, Tammimaki A, Myohanen T, et al. Quantitative role of COMT in dopamine clearance in the prefrontal cortex of freely moving mice. *Journal of neurochemistry* 2010; **114**(6): 1745-55.
348. Chen J, Song J, Yuan P, et al. Orientation and cellular distribution of membrane-bound catechol-O-methyltransferase in cortical neurons: implications for drug development. *The Journal of biological chemistry* 2011; **286**(40): 34752-60.
349. Guldberg HC, Marsden CA. Catechol-O-methyl transferase: pharmacological aspects and physiological role. *Pharmacological reviews* 1975; **27**(2): 135-206.
350. Li YJ, Zhang GL, Suzuki H, Kuriyama H. Actions of dipyridamole on endogenous and exogenous noradrenaline in the dog mesenteric vein. *British journal of pharmacology* 1991; **102**(1): 51-6.
351. Lam LK. Effects of butylated hydroxyanisole on glutathione S-transferase and catechol O-methyltransferase activities in Syrian golden hamsters. *Biochemical pharmacology* 1988; **37**(15): 3011-6.
352. Baldessarini RJ. Neuropharmacology of S-adenosyl-L-methionine. *The American journal of medicine* 1987; **83**(5A): 95-103.
353. Phipps D. The Biological Role of Metals. Cambridge University Press; 2002.
354. Fraga CG. Relevance, essentiality and toxicity of trace elements in human health. *Molecular aspects of medicine* 2005; **26**(4-5): 235-44.
355. Williams RJP. Zinc: what is its role in biology? *Endeavour* 1984; **8**(2): 65-70.
356. Bao B, Ahmad A, Azmi A, Li Y, Prasad A, Sarkar FH. Chapter 2 - The Biological Significance of Zinc in Inflammation and Aging. In: Rahman I, Bagchi D, eds. Inflammation, Advancing Age and Nutrition. San Diego: Academic Press; 2014: 15-27.
357. Festa RA, Thiele DJ. Copper: an essential metal in biology. *Current biology : CB* 2011; **21**(21): R877-83.
358. Kodama H, Fujisawa C, Bhadhprasit W. Inherited copper transport disorders: biochemical mechanisms, diagnosis, and treatment. *Current drug metabolism* 2012; **13**(3): 237-50.
359. Roberts RL, Fine RE, Sandra A. Receptor-mediated endocytosis of transferrin at the blood-brain barrier. *Journal of cell science* 1993; **104 (Pt 2)**: 521-32.
360. Crowe A, Morgan EH. Iron and transferrin uptake by brain and cerebrospinal fluid in the rat. *Brain research* 1992; **592**(1-2): 8-16.

361. Glinka Y GM, Youdim MBH. Iron and neurotransmitter function in the brain. In: JR C, ed. Metals and oxidative damage in neurological disorders. New York: Plenum; 1997: 1-22.
362. Waldmeier PC, Buchle AM, Steulet AF. Inhibition of catechol-O-methyltransferase (COMT) as well as tyrosine and tryptophan hydroxylase by the orally active iron chelator, 1,2-dimethyl-3-hydroxypyridin-4-one (L1, CP20), in rat brain in vivo. *Biochemical pharmacology* 1993; **45**(12): 2417-24.
363. Larkin EC RG. Importance of fetal and neonatal iron: adequacy for normal development of central nervous system. In: J D, ed. Brain, behaviour and iron in the infant diet. London: Springer-Verlag; 1990: 43-63.
364. Lane DJR, Ayton S, Bush AI. Iron and Alzheimer's Disease: An Update on Emerging Mechanisms. *Journal of Alzheimer's disease : JAD* 2018; **64**(s1): S379-S95.
365. van Rensburg SJ, Kotze MJ, van Toorn R. The conundrum of iron in multiple sclerosis--time for an individualised approach. *Metabolic brain disease* 2012; **27**(3): 239-53.
366. Llorens JV, Soriano S, Calap-Quintana P, Gonzalez-Cabo P, Moltó MD. The Role of Iron in Friedreich's Ataxia: Insights From Studies in Human Tissues and Cellular and Animal Models. *Frontiers in Neuroscience* 2019; **13**(75).
367. Muller M, Leavitt BR. Iron dysregulation in Huntington's disease. *Journal of neurochemistry* 2014; **130**(3): 328-50.
368. Bharath S, Hsu M, Kaur D, Rajagopalan S, Andersen JK. Glutathione, iron and Parkinson's disease. *Biochemical pharmacology* 2002; **64**(5-6): 1037-48.
369. Barnham KJ, Bush AI. Metals in Alzheimer's and Parkinson's diseases. *Current opinion in chemical biology* 2008; **12**(2): 222-8.
370. Dexter DT, Wells FR, Lees AJ, et al. Increased nigral iron content and alterations in other metal ions occurring in brain in Parkinson's disease. *Journal of neurochemistry* 1989; **52**(6): 1830-6.
371. Kaur D, Yantiri F, Rajagopalan S, et al. Genetic or pharmacological iron chelation prevents MPTP-induced neurotoxicity in vivo: a novel therapy for Parkinson's disease. *Neuron* 2003; **37**(6): 899-909.
372. Youdim MB, Fridkin M, Zheng H. Novel bifunctional drugs targeting monoamine oxidase inhibition and iron chelation as an approach to neuroprotection in Parkinson's disease and other neurodegenerative diseases. *Journal of neural transmission* 2004; **111**(10-11): 1455-71.
373. Youdim MB, Fridkin M, Zheng H. Bifunctional drug derivatives of MAO-B inhibitor rasagiline and iron chelator VK-28 as a more effective approach to treatment of brain ageing and ageing neurodegenerative diseases. *Mechanisms of ageing and development* 2005; **126**(2): 317-26.
374. Gal S, Fridkin M, Amit T, Zheng H, Youdim MB. M30, a novel multifunctional neuroprotective drug with potent iron chelating and brain selective monoamine oxidase-ab inhibitory activity for Parkinson's disease. *Journal of neural transmission Supplementum* 2006; (70): 447-56.
375. Zhu W, Xie W, Pan T, et al. Prevention and restoration of lactacystin-induced nigrostriatal dopamine neuron degeneration by novel brain-permeable iron chelators. *FASEB journal : official publication of the Federation of American Societies for Experimental Biology* 2007; **21**(14): 3835-44.
376. Grolez G, Moreau C, Sablonniere B, et al. Ceruloplasmin activity and iron chelation treatment of patients with Parkinson's disease. *BMC neurology* 2015; **15**: 74.
377. Klimek L, Muttray A, Moll B, Konietzko J, Mann W. [Anosmia caused by inhaled hazardous substances. Significance for expert assessment general practice]. *Laryngo- rhino- otologie* 1999; **78**(11): 620-6.
378. Mezzaroba L, Alfieri DF, Colado Simao AN, Vissoci Reiche EM. The role of zinc, copper, manganese and iron in neurodegenerative diseases. *Neurotoxicology* 2019; **74**: 230-41.
379. McKenzie-Nickson S, Chan J, Perez K, et al. Modulating Protein Phosphatase 2A Rescues Disease Phenotype in Neurodegenerative Tauopathies. *ACS chemical neuroscience* 2018; **9**(11): 2731-40.

380. Brewer GJ, Kanzer SH, Zimmerman EA, et al. Subclinical zinc deficiency in Alzheimer's disease and Parkinson's disease. *American journal of Alzheimer's disease and other dementias* 2010; **25**(7): 572-5.
381. Ahmed SS, Santosh W. Metallomic profiling and linkage map analysis of early Parkinson's disease: a new insight to aluminum marker for the possible diagnosis. *PloS one* 2010; **5**(6): e11252.
382. Squitti R, Gorgone G, Binetti G, et al. [Metals and oxidative stress in Parkinson's disease from industrial areas with exposition to environmental toxins or metal pollution]. *Giornale italiano di medicina del lavoro ed ergonomia* 2007; **29**(3 Suppl): 294-6.
383. Hozumi I, Hasegawa T, Honda A, et al. Patterns of levels of biological metals in CSF differ among neurodegenerative diseases. *Journal of the neurological sciences* 2011; **303**(1-2): 95-9.
384. Sheline CT, Zhu J, Zhang W, Shi C, Cai AL. Mitochondrial inhibitor models of Huntington's disease and Parkinson's disease induce zinc accumulation and are attenuated by inhibition of zinc neurotoxicity in vitro or in vivo. *Neuro-degenerative diseases* 2013; **11**(1): 49-58.
385. Uversky VN, Li J, Fink AL. Metal-triggered structural transformations, aggregation, and fibrillation of human alpha-synuclein. A possible molecular NK between Parkinson's disease and heavy metal exposure. *The Journal of biological chemistry* 2001; **276**(47): 44284-96.
386. Bharucha KJ, Friedman JK, Vincent AS, Ross ED. Lower serum ceruloplasmin levels correlate with younger age of onset in Parkinson's disease. *Journal of neurology* 2008; **255**(12): 1957-62.
387. Torsdottir G, Kristinsson J, Sveinbjornsdottir S, Snaedal J, Johannesson T. Copper, ceruloplasmin, superoxide dismutase and iron parameters in Parkinson's disease. *Pharmacology & toxicology* 1999; **85**(5): 239-43.
388. Boll MC, Alcaraz-Zubeldia M, Montes S, Rios C. Free copper, ferroxidase and SOD1 activities, lipid peroxidation and NO(x) content in the CSF. A different marker profile in four neurodegenerative diseases. *Neurochemical research* 2008; **33**(9): 1717-23.
389. Boll MC, Sotelo J, Otero E, Alcaraz-Zubeldia M, Rios C. Reduced ferroxidase activity in the cerebrospinal fluid from patients with Parkinson's disease. *Neuroscience letters* 1999; **265**(3): 155-8.
390. Ayton S, Lei P, Duce JA, et al. Ceruloplasmin dysfunction and therapeutic potential for Parkinson disease. *Annals of neurology* 2013; **73**(4): 554-9.
391. Ihara Y, Chuda M, Kuroda S, Hayabara T. Hydroxyl radical and superoxide dismutase in blood of patients with Parkinson's disease: relationship to clinical data. *Journal of the neurological sciences* 1999; **170**(2): 90-5.
392. Earle KM. Studies on Parkinson's disease including x-ray fluorescent spectroscopy of formalin fixed brain tissue. *Journal of neuropathology and experimental neurology* 1968; **27**(1): 1-14.
393. Sofic E, Riederer P, Heinsen H, et al. Increased iron (III) and total iron content in post mortem substantia nigra of parkinsonian brain. *J Neural Transm* 1988; **74**(3): 199-205.
394. Dexter DT, Carayon A, Javoy-Agid F, et al. Alterations in the levels of iron, ferritin and other trace metals in Parkinson's disease and other neurodegenerative diseases affecting the basal ganglia. *Brain : a journal of neurology* 1991; **114 (Pt 4)**: 1953-75.
395. Loeffler DA, Connor JR, Juneau PL, et al. Transferrin and iron in normal, Alzheimer's disease, and Parkinson's disease brain regions. *Journal of neurochemistry* 1995; **65**(2): 710-24.
396. Dexter DT, Carayon A, Vidailhet M, et al. Decreased ferritin levels in brain in Parkinson's disease. *Journal of neurochemistry* 1990; **55**(1): 16-20.
397. Connor JR, Snyder BS, Arosio P, Loeffler DA, LeWitt P. A quantitative analysis of isoferritins in select regions of aged, parkinsonian, and Alzheimer's diseased brains. *Journal of neurochemistry* 1995; **65**(2): 717-24.
398. Rybicki BA, Johnson CC, Uman J, Gorell JM. Parkinson's disease mortality and the industrial use of heavy metals in Michigan. *Movement disorders : official journal of the Movement Disorder Society* 1993; **8**(1): 87-92.
399. Beyers DW, Farmer MS. Effects of copper on olfaction of Colorado pikeminnow. *Environmental toxicology and chemistry* 2001; **20**(4): 907-12.

400. Rehnberg BC, Schreck CB. Acute metal toxicology of olfaction in coho salmon: behavior, receptors, and odor-metal complexation. *Bulletin of environmental contamination and toxicology* 1986; **36**(4): 579-86.
401. Hara TJ, Law YMC, Macdonald S. Effects of Mercury and Copper on the Olfactory Response in Rainbow Trout, Salmo gairdneri. *Journal of the Fisheries Research Board of Canada* 1976; **33**(7): 1568-73.
402. Finkelstein DI, Billings JL, Adlard PA, et al. The novel compound PBT434 prevents iron mediated neurodegeneration and alpha-synuclein toxicity in multiple models of Parkinson's disease. *Acta neuropathologica communications* 2017; **5**(1): 53.
403. Grunblatt E, Mandel S, Berkuzki T, Youdim MB. Apomorphine protects against MPTP-induced neurotoxicity in mice. *Movement disorders : official journal of the Movement Disorder Society* 1999; **14**(4): 612-8.
404. Grunblatt E, Mandel S, Gassen M, Youdim MB. Potent neuroprotective and antioxidant activity of apomorphine in MPTP and 6-hydroxydopamine induced neurotoxicity. *Journal of neural transmission Supplementum* 1999; **55**: 57-70.
405. Zhang X, Xie W, Qu S, Pan T, Wang X, Le W. Neuroprotection by iron chelator against proteasome inhibitor-induced nigral degeneration. *Biochemical and biophysical research communications* 2005; **333**(2): 544-9.
406. Green MA, Klippenstein DL, Tennison JR. Copper(II) bis(thiosemicarbazone) complexes as potential tracers for evaluation of cerebral and myocardial blood flow with PET. *Journal of nuclear medicine : official publication, Society of Nuclear Medicine* 1988; **29**(9): 1549-57.
407. Lewis J, Laforest R, Buettner T, et al. Copper-64-diacetyl-bis(N4-methylthiosemicarbazone): An agent for radiotherapy. *Proceedings of the National Academy of Sciences of the United States of America* 2001; **98**(3): 1206-11.
408. Xiao Z, Donnelly PS, Zimmermann M, Wedd AG. Transfer of copper between bis(thiosemicarbazone) ligands and intracellular copper-binding proteins. insights into mechanisms of copper uptake and hypoxia selectivity. *Inorganic chemistry* 2008; **47**(10): 4338-47.
409. Torres JB, Andreozzi EM, Dunn JT, et al. PET Imaging of Copper Trafficking in a Mouse Model of Alzheimer Disease. *Journal of nuclear medicine : official publication, Society of Nuclear Medicine* 2016; **57**(1): 109-14.
410. Ma D LY, Huang R, Zhao Z, Wang Q, Li L, Zhang L. Cornel Iridoid Glycoside Suppresses Tau Hyperphosphorylation and Aggregation in a Mouse Model of Tauopathy through Increasing Activity of PP2A. *Current Alzheimer's Research* 2020; **16**(14): 1316-31.
411. Doty RL, Singh A, Tetrud J, Langston JW. Lack of major olfactory dysfunction in MPTP-induced parkinsonism. *Annals of neurology* 1992; **32**(1): 97-100.
412. Kadavath H, Hofele RV, Biernat J, et al. Tau stabilizes microtubules by binding at the interface between tubulin heterodimers. *Proceedings of the National Academy of Sciences of the United States of America* 2015; **112**(24): 7501-6.
413. Gao YL, Wang N, Sun FR, Cao XP, Zhang W, Yu JT. Tau in neurodegenerative disease. *Annals of translational medicine* 2018; **6**(10): 175.
414. Hutton M, Lendon CL, Rizzu P, et al. Association of missense and 5'-splice-site mutations in tau with the inherited dementia FTDP-17. *Nature* 1998; **393**(6686): 702-5.
415. Ksiezak-Reding H, Liu WK, Yen SH. Phosphate analysis and dephosphorylation of modified tau associated with paired helical filaments. *Brain research* 1992; **597**(2): 209-19.
416. Kopke E, Tung YC, Shaikh S, Alonso AC, Iqbal K, Grundke-Iqbal I. Microtubule-associated protein tau. Abnormal phosphorylation of a non-paired helical filament pool in Alzheimer disease. *The Journal of biological chemistry* 1993; **268**(32): 24374-84.
417. Alonso A, Zaidi T, Novak M, Grundke-Iqbal I, Iqbal K. Hyperphosphorylation induces self-assembly of tau into tangles of paired helical filaments/straight filaments. *Proceedings of the National Academy of Sciences of the United States of America* 2001; **98**(12): 6923-8.

418. Li B, Chohan MO, Grundke-Iqbal I, Iqbal K. Disruption of microtubule network by Alzheimer abnormally hyperphosphorylated tau. *Acta neuropathologica* 2007; **113**(5): 501-11.
419. Qian W, Shi J, Yin X, et al. PP2A regulates tau phosphorylation directly and also indirectly via activating GSK-3beta. *Journal of Alzheimer's disease : JAD* 2010; **19**(4): 1221-9.
420. Liu F, Grundke-Iqbal I, Iqbal K, Gong CX. Contributions of protein phosphatases PP1, PP2A, PP2B and PP5 to the regulation of tau phosphorylation. *The European journal of neuroscience* 2005; **22**(8): 1942-50.
421. Sents W, Ivanova E, Lambrecht C, Haesen D, Janssens V. The biogenesis of active protein phosphatase 2A holoenzymes: a tightly regulated process creating phosphatase specificity. *The FEBS journal* 2013; **280**(2): 644-61.
422. Lee J, Stock J. Protein phosphatase 2A catalytic subunit is methyl-esterified at its carboxyl terminus by a novel methyltransferase. *The Journal of biological chemistry* 1993; **268**(26): 19192-5.
423. Bottiglieri T, Godfrey P, Flynn T, Carney MW, Toone BK, Reynolds EH. Cerebrospinal fluid S-adenosylmethionine in depression and dementia: effects of treatment with parenteral and oral S-adenosylmethionine. *Journal of neurology, neurosurgery, and psychiatry* 1990; **53**(12): 1096-8.
424. Morrison LD, Smith DD, Kish SJ. Brain S-adenosylmethionine levels are severely decreased in Alzheimer's disease. *Journal of neurochemistry* 1996; **67**(3): 1328-31.
425. G. Stramentinoli EC, A. Algeri. Concentrations of S-Adenosyl-L-Methionine in the CNS of Rats After Intramuscular and Intravenous Administration. In: V.M. Andreoli AA, C. Fazio, ed. Transmethylations and the Central Nervous System. Heidelberg: Springer-Verlag Berlin; 2013: 111-3.
426. Crouch PJ, Hung LW, Adlard PA, et al. Increasing Cu bioavailability inhibits Abeta oligomers and tau phosphorylation. *Proceedings of the National Academy of Sciences of the United States of America* 2009; **106**(2): 381-6.
427. Blackmore T, Meftah S, Murray TK, et al. Tracking progressive pathological and functional decline in the rTg4510 mouse model of tauopathy. *Alzheimer's research & therapy* 2017; **9**(1): 77.
428. Sontag E, Nunbhakdi-Craig V, Lee G, Bloom GS, Mumby MC. Regulation of the phosphorylation state and microtubule-binding activity of Tau by protein phosphatase 2A. *Neuron* 1996; **17**(6): 1201-7.
429. Vafai SB, Stock JB. Protein phosphatase 2A methylation: a link between elevated plasma homocysteine and Alzheimer's Disease. *FEBS letters* 2002; **518**(1-3): 1-4.
430. Sedjahtera A, Gunawan L, Bray L, et al. Targeting metals rescues the phenotype in an animal model of tauopathy. *Metallomics : integrated biometal science* 2018; **10**(9): 1339-47.
431. Tolstykh T, Lee J, Vafai S, Stock JB. Carboxyl methylation regulates phosphoprotein phosphatase 2A by controlling the association of regulatory B subunits. *The EMBO journal* 2000; **19**(21): 5682-91.
432. De Baere I, Derua R, Janssens V, et al. Purification of porcine brain protein phosphatase 2A leucine carboxyl methyltransferase and cloning of the human homologue. *Biochemistry* 1999; **38**(50): 16539-47.
433. Mudd SH LH, Kraus JP. Disorders of transsulfuration. In: Scriver CR BA, Sly WS, Valle D, Childs B, Kinzler K, Vogelstein B, ed. The Metabolic and Molecular Bases of Inherited Disease. New York: McGraw-Hill; 2001: 2007-56.
434. Surtees R, Leonard J, Austin S. Association of demyelination with deficiency of cerebrospinal-fluid S-adenosylmethionine in inborn errors of methyl-transfer pathway. *Lancet* 1991; **338**(8782-8783): 1550-4.
435. Linnebank M, Popp J, Smulders Y, et al. S-adenosylmethionine is decreased in the cerebrospinal fluid of patients with Alzheimer's disease. *Neuro-degenerative diseases* 2010; **7**(6): 373-8.
436. Schatz RA, Wilens TE, Sellinger OZ. Decreased in vivo protein and phospholipid methylation after in vivo elevation of brain S-adenosyl-homocysteine. *Biochemical and biophysical research communications* 1981; **98**(4): 1097-107.

437. Chan A, Tchantchou F, Graves V, Rozen R, Shea TB. Dietary and genetic compromise in folate availability reduces acetylcholine, cognitive performance and increases aggression: critical role of S-adenosyl methionine. *The journal of nutrition, health & aging* 2008; **12**(4): 252-61.
438. Herrmann W, Knapp JP. Hyperhomocysteinemia: a new risk factor for degenerative diseases. *Clinical laboratory* 2002; **48**(9-10): 471-81.
439. Seshadri S, Beiser A, Selhub J, et al. Plasma homocysteine as a risk factor for dementia and Alzheimer's disease. *The New England journal of medicine* 2002; **346**(7): 476-83.
440. Morris MS. Homocysteine and Alzheimer's disease. *The Lancet Neurology* 2003; **2**(7): 425-8.
441. Sontag E, Nunbhakdi-Craig V, Sontag JM, et al. Protein phosphatase 2A methyltransferase links homocysteine metabolism with tau and amyloid precursor protein regulation. *The Journal of neuroscience : the official journal of the Society for Neuroscience* 2007; **27**(11): 2751-9.
442. Louis JV, Martens E, Borghgraef P, et al. Mice lacking phosphatase PP2A subunit PR61/B'delta (Ppp2r5d) develop spatially restricted tauopathy by deregulation of CDK5 and GSK3beta. *Proceedings of the National Academy of Sciences of the United States of America* 2011; **108**(17): 6957-62.
443. Sontag E, Hladik C, Montgomery L, et al. Downregulation of protein phosphatase 2A carboxyl methylation and methyltransferase may contribute to Alzheimer disease pathogenesis. *Journal of neuropathology and experimental neurology* 2004; **63**(10): 1080-91.
444. Lee S, Lemere CA, Frost JL, Shea TB. Dietary supplementation with S-adenosyl methionine delayed amyloid-beta and tau pathology in 3xTg-AD mice. *Journal of Alzheimer's disease : JAD* 2012; **28**(2): 423-31.
445. Chan A, Paskavitz J, Remington R, Rasmussen S, Shea TB. Efficacy of a vitamin/nutriceutical formulation for early-stage Alzheimer's disease: a 1-year, open-label pilot study with an 16-month caregiver extension. *American journal of Alzheimer's disease and other dementias* 2008; **23**(6): 571-85.
446. Remington R, Chan A, Paskavitz J, Shea TB. Efficacy of a vitamin/nutriceutical formulation for moderate-stage to later-stage Alzheimer's disease: a placebo-controlled pilot study. *American journal of Alzheimer's disease and other dementias* 2009; **24**(1): 27-33.
447. Remington R, Bechtel C, Larsen D, et al. A Phase II Randomized Clinical Trial of a Nutritional Formulation for Cognition and Mood in Alzheimer's Disease. *Journal of Alzheimer's disease : JAD* 2015; **45**(2): 395-405.
448. Remington R, Lortie JJ, Hoffmann H, Page R, Morrell C, Shea TB. A Nutritional Formulation for Cognitive Performance in Mild Cognitive Impairment: A Placebo-Controlled Trial with an Open-Label Extension. *Journal of Alzheimer's disease : JAD* 2015; **48**(3): 591-5.
449. Chan A, Remington R, Kotyla E, Lepore A, Zemianek J, Shea TB. A vitamin/nutriceutical formulation improves memory and cognitive performance in community-dwelling adults without dementia. *The journal of nutrition, health & aging* 2010; **14**(3): 224-30.
450. Tobin JE, Latourelle JC, Lew MF, et al. Haplotypes and gene expression implicate the MAPT region for Parkinson disease: the GenePD Study. *Neurology* 2008; **71**(1): 28-34.
451. Edwards TL, Scott WK, Almonte C, et al. Genome-wide association study confirms SNPs in SNCA and the MAPT region as common risk factors for Parkinson disease. *Annals of human genetics* 2010; **74**(2): 97-109.
452. Muntane G, Dalfo E, Martinez A, Ferrer I. Phosphorylation of tau and alpha-synuclein in synaptic-enriched fractions of the frontal cortex in Alzheimer's disease, and in Parkinson's disease and related alpha-synucleinopathies. *Neuroscience* 2008; **152**(4): 913-23.
453. Lovestone S, Hartley CL, Pearce J, Anderton BH. Phosphorylation of tau by glycogen synthase kinase-3 beta in intact mammalian cells: the effects on the organization and stability of microtubules. *Neuroscience* 1996; **73**(4): 1145-57.
454. Lee VM, Goedert M, Trojanowski JQ. Neurodegenerative tauopathies. *Annual review of neuroscience* 2001; **24**: 1121-59.

455. Ittner LM, Fath T, Ke YD, et al. Parkinsonism and impaired axonal transport in a mouse model of frontotemporal dementia. *Proceedings of the National Academy of Sciences of the United States of America* 2008; **105**(41): 15997-6002.
456. Wang X, Smith K, Pearson M, et al. Early intervention of tau pathology prevents behavioral changes in the rTg4510 mouse model of tauopathy. *PloS one* 2018; **13**(4): e0195486.
457. Terwel D, Dewachter I, Van Leuven F. Axonal transport, tau protein, and neurodegeneration in Alzheimer's disease. *Neuromolecular medicine* 2002; **2**(2): 151-65.
458. Hawkes C. Olfaction in neurodegenerative disorder. *Advances in oto-rhino-laryngology* 2006; **63**: 133-51.
459. Hu Y, Ding W, Zhu X, Chen R, Wang X. Olfactory Dysfunctions and Decreased Nitric Oxide Production in the Brain of Human P301L Tau Transgenic Mice. *Neurochemical research* 2016; **41**(4): 722-30.
460. Deeb J, Shah M, Muhammed N, et al. A basic smell test is as sensitive as a dopamine transporter scan: comparison of olfaction, taste and DaTSCAN in the diagnosis of Parkinson's disease. *QJM : monthly journal of the Association of Physicians* 2010; **103**(12): 941-52.
461. Bohnen NI, Studenski SA, Constantine GM, Moore RY. Diagnostic performance of clinical motor and non-motor tests of Parkinson disease: a matched case-control study. *European journal of neurology* 2008; **15**(7): 685-91.
462. Ross GW, Petrovitch H, Abbott RD, et al. Association of olfactory dysfunction with risk for future Parkinson's disease. *Annals of neurology* 2008; **63**(2): 167-73.
463. Ponsen MM, Stoffers D, Booij J, van Eck-Smit BL, Wolters E, Berendse HW. Idiopathic hyposmia as a preclinical sign of Parkinson's disease. *Annals of neurology* 2004; **56**(2): 173-81.
464. Doty RL, Perl DP, Steele JC, et al. Odor identification deficit of the parkinsonism-dementia complex of Guam: equivalence to that of Alzheimer's and idiopathic Parkinson's disease. *Neurology* 1991; **41**(5 Suppl 2): 77-80; discussion -1.
465. Boyce JM, Shone GR. Effects of ageing on smell and taste. *Postgraduate medical journal* 2006; **82**(966): 239-41.
466. Beard JL, Connor JR, Jones BC. Iron in the brain. *Nutrition reviews* 1993; **51**(6): 157-70.
467. Beard JL, Chen Q, Connor J, Jones BC. Altered monamine metabolism in caudate-putamen of iron-deficient rats. *Pharmacology, biochemistry, and behavior* 1994; **48**(3): 621-4.
468. Youdim MB, Ben-Shachar D, Ashkenazi R, Yehuda S. Brain iron and dopamine receptor function. *Advances in biochemical psychopharmacology* 1983; **37**: 309-21.
469. Benarroch EE. Olfactory system: functional organization and involvement in neurodegenerative disease. *Neurology* 2010; **75**(12): 1104-9.
470. Postuma RB, Gagnon JF, Vendette M, Montplaisir JY. Markers of neurodegeneration in idiopathic rapid eye movement sleep behaviour disorder and Parkinson's disease. *Brain : a journal of neurology* 2009; **132**(Pt 12): 3298-307.
471. Fereshtehnejad SM, Romenets SR, Anang JB, Latreille V, Gagnon JF, Postuma RB. New Clinical Subtypes of Parkinson Disease and Their Longitudinal Progression: A Prospective Cohort Comparison With Other Phenotypes. *JAMA neurology* 2015; **72**(8): 863-73.
472. Postuma RB, Gagnon JF, Vendette M, Charland K, Montplaisir J. Manifestations of Parkinson disease differ in association with REM sleep behavior disorder. *Movement disorders : official journal of the Movement Disorder Society* 2008; **23**(12): 1665-72.
473. Rolinski M, Szewczyk-Krolikowski K, Tomlinson PR, et al. REM sleep behaviour disorder is associated with worse quality of life and other non-motor features in early Parkinson's disease. *Journal of neurology, neurosurgery, and psychiatry* 2014; **85**(5): 560-6.
474. Mullol J, Alobid I, Marino-Sanchez F, et al. Furthering the understanding of olfaction, prevalence of loss of smell and risk factors: a population-based survey (OLFACAT study). *BMJ open* 2012; **2**(6).
475. Serby M. Olfaction and Alzheimer's disease. *Progress in neuro-psychopharmacology & biological psychiatry* 1986; **10**(3-5): 579-86.

476. Nordin S, Paulsen JS, Murphy C. Sensory- and memory-mediated olfactory dysfunction in Huntington's disease. *Journal of the International Neuropsychological Society : JINS* 1995; **1**(3): 281-90.
477. Howell J, Costanzo RM, Reiter ER. Head trauma and olfactory function. *World journal of otorhinolaryngology - head and neck surgery* 2018; **4**(1): 39-45.
478. Abbott RD, Ross GW, White LR, et al. Environmental, life-style, and physical precursors of clinical Parkinson's disease: recent findings from the Honolulu-Asia Aging Study. *Journal of neurology* 2003; **250 Suppl 3**: III30-9.
479. Stewart WF, Liberman JN, Sandler RS, et al. Epidemiology of constipation (EPOC) study in the United States: relation of clinical subtypes to sociodemographic features. *The American journal of gastroenterology* 1999; **94**(12): 3530-40.
480. Glick ME, Meshkinpour H, Haldeman S, Bhatia NN, Bradley WE. Colonic dysfunction in multiple sclerosis. *Gastroenterology* 1982; **83**(5): 1002-7.
481. Ullman T, Reding M. Gastrointestinal dysfunction in stroke. *Seminars in neurology* 1996; **16**(3): 269-75.
482. Lee MA, Prentice WM, Hildreth AJ, Walker RW. Measuring symptom load in Idiopathic Parkinson's disease. *Parkinsonism & related disorders* 2007; **13**(5): 284-9.
483. Somers JM, Goldner EM, Waraich P, Hsu L. Prevalence and incidence studies of anxiety disorders: a systematic review of the literature. *Canadian journal of psychiatry Revue canadienne de psychiatrie* 2006; **51**(2): 100-13.
484. Beiske AG, Svensson E, Sandanger I, et al. Depression and anxiety amongst multiple sclerosis patients. *European journal of neurology* 2008; **15**(3): 239-45.
485. Dale M, van Duijn E. Anxiety in Huntington's Disease. *The Journal of neuropsychiatry and clinical neurosciences* 2015; **27**(4): 262-71.
486. Seignourel PJ, Kunik ME, Snow L, Wilson N, Stanley M. Anxiety in dementia: a critical review. *Clinical psychology review* 2008; **28**(7): 1071-82.
487. Wall CA, Rummans TA, Aksamit AJ, Krahn LE, Pankratz VS. Psychiatric manifestations of Creutzfeldt-Jakob disease: a 25-year analysis. *The Journal of neuropsychiatry and clinical neurosciences* 2005; **17**(4): 489-95.
488. Haba-Rubio J, Frauscher B, Marques-Vidal P, et al. Prevalence and determinants of rapid eye movement sleep behavior disorder in the general population. *Sleep* 2018; **41**(2).
489. Turner RS, D'Amato CJ, Chervin RD, Blaivas M. The pathology of REM sleep behavior disorder with comorbid Lewy body dementia. *Neurology* 2000; **55**(11): 1730-2.
490. Wang P, Wing YK, Xing J, et al. Rapid eye movement sleep behavior disorder in patients with probable Alzheimer's disease. *Aging clinical and experimental research* 2016; **28**(5): 951-7.
491. Plazzi G, Corsini R, Provini F, et al. REM sleep behavior disorders in multiple system atrophy. *Neurology* 1997; **48**(4): 1094-7.
492. Reijnders JS, Ehrt U, Weber WE, Aarsland D, Leentjens AF. A systematic review of prevalence studies of depression in Parkinson's disease. *Movement disorders : official journal of the Movement Disorder Society* 2008; **23**(2): 183-9; quiz 313.
493. Kroenke K, Strine TW, Spitzer RL, Williams JB, Berry JT, Mokdad AH. The PHQ-8 as a measure of current depression in the general population. *Journal of affective disorders* 2009; **114**(1-3): 163-73.
494. Whyte EM, Mulsant BH. Post stroke depression: epidemiology, pathophysiology, and biological treatment. *Biological psychiatry* 2002; **52**(3): 253-64.
495. Byers AL, Yaffe K. Depression and risk of developing dementia. *Nature reviews Neurology* 2011; **7**(6): 323-31.
496. Pilotto A, Heinzel S, Suenkel U, et al. Application of the movement disorder society prodromal Parkinson's disease research criteria in 2 independent prospective cohorts. *Movement disorders : official journal of the Movement Disorder Society* 2017; **32**(7): 1025-34.

497. Mahlknecht P, Gasperi A, Djamshidian A, et al. Performance of the Movement Disorders Society criteria for prodromal Parkinson's disease: A population-based 10-year study. *Movement disorders : official journal of the Movement Disorder Society* 2018; **33**(3): 405-13.
498. Fereshtehnejad SM, Montplaisir JY, Pelletier A, Gagnon JF, Berg D, Postuma RB. Validation of the MDS research criteria for prodromal Parkinson's disease: Longitudinal assessment in a REM sleep behavior disorder (RBD) cohort. *Movement disorders : official journal of the Movement Disorder Society* 2017; **32**(6): 865-73.
499. Kalra H, Drummen GP, Mathivanan S. Focus on Extracellular Vesicles: Introducing the Next Small Big Thing. *International journal of molecular sciences* 2016; **17**(2): 170.